UNIVERSITAT DE BARCELONA

Cuantificación y modelización de parámetros de interacción de radionucleidos en suelos

Carlos Javier Gil García

Tesis Doctoral

CUANTIFICACION Y MODELIZACION DE PARAMETROS DE INTERACCION DE RADIONUCLEIDOS EN SUELOS

CARLOS JAVIER GIL GARCIA

UNIVERSITAT DE BARCELONA

MARZO 2011

TESIS DOCTORAL

CUANTIFICACIÓN Y MODELIZACIÓN DE PARÁMETROS DE INTERACCIÓN DE RADIONUCLEIDOS EN SUELOS

Carlos Javier Gil García

UNIVERSITAT DE BARCELONA

Departament de Química Analítica

Facultat de Química

Universitat de Barcelona

Marzo, 2011

Programa de Doctorado
QUÍMICA ANALÍTICA DEL MEDI AMBIENT I LA POL.LUCIÓ
(Bienni 2003-2005)

CUANTIFICACIÓN Y MODELIZACIÓN DE PARÁMETROS DE INTERACCIÓN DE RADIONUCLEIDOS EN SUELOS

Memoria presentada por Carlos Javier Gil García para optar al grado de Doctor por la Universitat de Barcelona

Miquel Vidal Espinar y Anna Rigol Parera, Profesores Titulares del Departamento de Química Analítica de la Universitat de Barcelona,

CERTIFICAN

que el presente trabajo de investigación ha sido realizado por el Sr. Carlos Javier Gil García en el Departamento de Química Analítica de la Universitat de Barcelona bajo su dirección.

Barcelona, 8 de marzo de 2011

Anna Rigol	**Miquel Vidal**	**Carlos Javier Gil García**
Codirectora	Codirector	Autor

Tranqui, hay que mostrarse, sin complicarse,
sin enfadarse, dando margen a equivocarse,
comportarse, tipos no pueden superarse sin esforzarse,
prefieren conformarse y eso es engañarse.

Tranqui, si puede hacerse no hay que pararse,
es conocerse, jamás rendirse, no limitarse,
muchos para ganarse el respeto juegan a odiarse y a esconderse,
y eso es engañarse

Fragmento de la canción "**Ser o no ser**", de Nach Scratch

No era el hombre más honesto ni el más piadoso, pero era un hombre valiente. Se llamaba Diego Alatriste y Tenorio, y había luchado como soldado de los tercios viejos y en las guerras de Flandes.

Primeras líneas del libro **El Capitán Alatriste**, de Arturo Pérez-Reverte

Aunque aparecen los primeros, los agradecimientos siempre es la parte que se escribe lo último, y no lo digo yo sólo, sino que está reflejado en unas cuantas Tesis.

Primero de todo me gustaría agradecer a la Dra. Anna Rigol y Dr. Miquel Vidal su ayuda y sus consejos, pero sobre todo su esfuerzo profesional y personal, para que esta tesis pasase de ser un proyecto a ser una realidad.

A todos aquellos que hemos caminado juntos durante un tiempo dentro del grupo Qüestram, tanto metálicos (Amaia, Àngels, Dolo, Jaume, Jorge, Mª José, Mar, Mónica, Riqui, Rosa, Yaiza) como radioactivos (Àlex Damià, Dani, David, Eva, Héctor, Joana, Joan). Han sido casi cuatro años de convivencia diaria, de buenos y no tan buenos momentos, de risas y de enfados, pero sobretodo de crecimiento profesional y personal. Así como, a los integrantes de otros grupos de investigación del departamento.

Agradecer también al Dr. Jordi Sastre sus ánimos, sus consejos profesionales, ayuda y facilidades para poder acabar esta Tesis.

También quiero dar las gracias a Antonia y Ciriaco, por dejarme ocupar la mesa del salón de su casa con el ordenador y toda la documentación asociada a la escritura de la Tesis, cada vez que hemos ido a verlos. Ahora la ocuparé con otra cosa, ya veremos que será, pero seguro que la volveré a ocupar.

Agradecer y dedicar esta Tesis a mis abuelos, tanto a los siguen aquí, como los que son estrellas en el cielo (como dice Meritxell), es un honor por el Dr. delante de sus apellidos. Como no, a mis padres, que han luchado y creído en mi.

Por último, esta Tesis no se podría haber escrito sin la ayuda, pero sobre todo la compresión y paciencia de Inma, que realmente ha soportado las manías de un escritor y los nervios de un doctorando.

ÍNDICE

1. INTRODUCCIÓN

1.1

Los radionucleidos en el medio

La energía nuclear es una de las principales fuentes de producción de electricidad de que dispone nuestra sociedad a día de hoy. Además de su uso energético, las actividades radioactivas han conllevado la introducción de un gran número de radionucleidos con fines diagnósticos en el campo de la medicina o con fines científicos en campos como la biología o la química. Desgraciadamente, la energía nuclear también ha constituido a lo largo de los años un motivo de preocupación para el hombre debido especialmente a las consecuencias negativas que se pueden derivar de su uso. Además, hay que sumar a esta preocupación la gestión de los residuos radioactivos generados, siendo éste el tema que en la actualidad más interés y polémica suscita a todos los niveles de la sociedad.

Ya desde finales de los años cincuenta y principios de los sesenta, y debido a las múltiples pruebas nucleares que se realizaron en la atmósfera, la comunidad científica consideró los radionucleidos como contaminantes ambientales de alto riesgo y la radioactividad ambiental como un tema de especial interés, creándose organismos internacionales como el Organismo Internacional de la Energía Atómica (*International Atomic Energy Agency* –IAEA-, fundada en 1957) o la Comisión Internacional de la Protección Radiológica (*International Comission on Radiological Protection* –ICRP-, fundada en 1950) con el objetivo de liderar los estudios y regulaciones internacionales en el campo de las actividades con radionucleidos.

Aunque las pruebas nucleares ya demostraron el impacto que las emisiones radioactivas podían tener en el medio, los accidentes sucedidos en instalaciones nucleares han sido los que más impacto medioambiental han provocado. Sin duda, el accidente más importante que ha puesto de manifiesto todas las consecuencias negativas de la energía nuclear fue el ocurrido en abril de 1986 en la central nuclear de Chernóbil (Ucrania), con graves implicaciones sanitarias, sociales y económicas, incluso en países lejanos de la zona del accidente.

1.1.1. Presencia de la radioactividad de origen natural en el medio ambiente

La existencia de la radioactividad es inherente a la creación de la tierra, ya que las radiaciones ionizantes están presentes en el medio natural incluso sin la acción del hombre. La radioactividad que se encuentra en la naturaleza se denomina radioactividad natural y tiene dos orígenes principales: a) radiación cósmica y radionucleidos cosmogénicos, y b) radionucleidos primordiales.

1.1.1.1 Radiación cósmica y radionucleidos cosmogénicos

La radiación cósmica está constituida por partículas subatómicas que se originan en el espacio exterior, dotadas con una gran energía y que al interaccionar con determinados elementos presentes en la atmósfera terrestre los transforman en especies radioactivas, que son los denominados radionucleidos cosmogénicos, tras reacciones de espalación con núcleos más pesados (Figura 1.1). La producción y concentración de los radionucleidos cosmogénicos varía de forma ostensible con la altitud y la latitud, siendo los más importantes: ^{3}H, ^{7}Be, ^{10}Be, ^{14}C, ^{22}Na, ^{26}Al, ^{36}Cl y ^{41}Ca (Ortega et al., 1996).

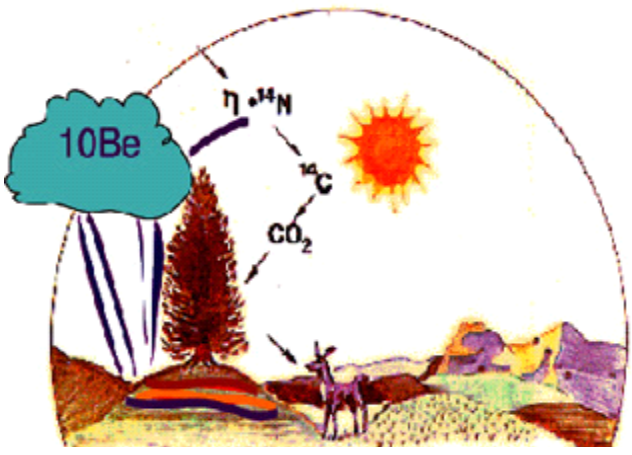

Figura 1.1. Producción atmosférica de ^{10}Be.

Los radionucleidos cosmogénicos pueden asociarse con aerosoles atmosféricos y acabar acumulándose en la superficie del suelo tras episodios de lluvia. El seguimiento

de las variaciones de la concentración de radionucleidos cosmogénicos puede ser útil para entender procesos geoquímicos, tales como la erosión de los suelos.

1.1.1.2. Radionucleidos primordiales

Los radionucleidos primordiales (*Naturally Occurring Radioactive Material* –NORM-) existen en la corteza terrestre desde su origen. La mayoría de los NORM provienen de las series o cadenas naturales de desintegración encabezadas por el ^{235}U (Uranio-actinio), ^{232}Th, ^{237}Np y ^{238}U (Uranio-radio). Los radionucleidos presentes en la cadena del ^{235}U apenas contribuyen al fondo radioactivo natural, ya que éste está presente en la corteza terrestre con una abundancia isotópica del 0,007%, mientras que los radionucleidos de la cadena de desintegración del ^{238}U contribuyen al fondo de forma mucho más significativa, ya que la abundancia natural del ^{238}U es del 0,993%. Además de las series radioactivas, también se incluyen en este grupo otros radionucleidos, como el ^{40}K y el ^{87}Rb.

La concentración de los radionucleidos primordiales depende del material considerado, siendo las rocas ígneas (entre las que se encuentran los granitos) las que presentan una mayor concentración, tal como muestra la Tabla 1.1. Por el contrario, las rocas sedimentarias contienen niveles más bajos de NORM, aunque existen algunas pizarras y fosforitas con importantes concentraciones de estos radionucleidos.

Tabla 1.1. Concentraciones de los principales NORM en diferentes tipos de rocas y suelos (IAEA, 2003).

Tipo de roca	**^{40}K**	**^{87}Rb**	**^{232}Th**	**^{238}U**
	Bq/kg	**Bq/kg**	**Bq/kg**	**Bq/kg**
Rocas ígneas				
Basalto	70 - 1500	1-180	7-83	7-60
Granito	>1000	150-180	70	40
Rocas sedimentarias				
Pizarra	800	110	50	40
Cuarzo	<300	<40	<8	<10
Arena playa	<300*	<40*	25	40
Rocas carbonatadas	70	8	8	25
Capa superficial terrestre (valor medio)	850	100	44	36
Suelos	400	50	37	66

*Valor estimado

Dentro de los NORM, es necesario destacar el radón, ya que es uno de los elementos que más contribuye a la radioactividad ambiental y que en consecuencia más puede afectar a la salud de la población no expuesta profesionalmente y en ausencia de situaciones accidentales. Su formación se produce a partir de las cadenas radioactivas naturales ($^{232}Th \rightarrow {}^{220}Rn$, $^{235}U \rightarrow {}^{219}Rn$ y $^{238}U \rightarrow {}^{222}Rn$) y está presente en los materiales que se utilizan para edificación (granito, cemento, etc), tal y como se puede observar en la Figura 1.2. Su naturaleza gaseosa provoca que pueda acumularse en el aire en espacios cerrados, lo que obliga a realizar controles de su concentración en lugares en los que se pueda suponer que se excederán los niveles permitidos de radioactividad en el aire (Quindós Poncela, 1995).

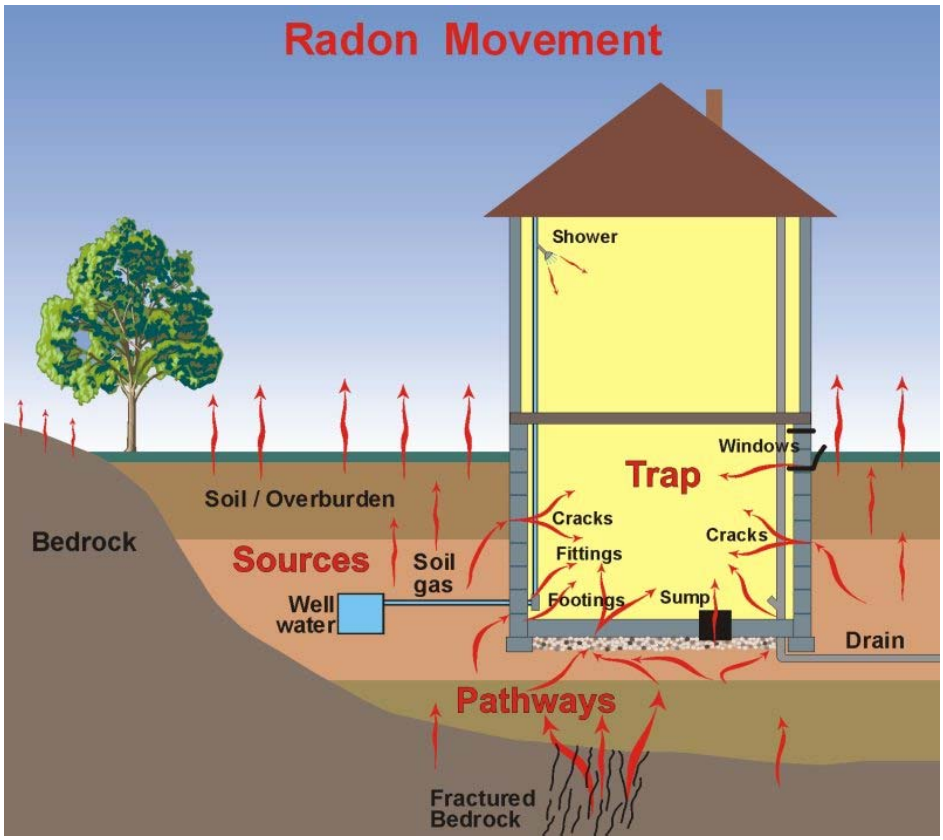

Figura 1.2. Vías potenciales de formación y transporte del radón.

El procesamiento industrial de materiales que contienen NORM puede provocar un aumento de la concentración de los radionucleidos de origen natural. Estos materiales enriquecidos se agrupan en el grupo de los TENORM (*Technologically Enhanced Naturally Occurring Radioactive Material*) (Gesell y Prichard, 1975). Los TENORM se pueden encontrar en los residuos generados por industrias relacionadas con la

producción de fertilizantes, minas de carbón, refinerías de petróleo y gas, minería, producción de papel, energía geotérmica o plantas potabilizadoras de agua. A pesar de que el contenido de radionucleidos en estos residuos puede considerarse pequeño, su continua deposición en los lugares destinados a los residuos puede provocar un aumento del fondo radioactivo característico de la zona. Como los TENORM provienen de materiales radioactivos de origen natural, los radioisótopos que se encontrarán concentrados en los residuos generados por estas actividades industriales serán los productos de desintegración de las series del uranio y del torio. Por ejemplo, en la industria del gas y del petróleo, los radionucleidos más importantes a tener en cuenta son el ^{226}Ra, de la serie de desintegración del ^{238}U, y en menor grado el ^{228}Ra perteneciente a la serie de desintegración del ^{232}Th (Canoba y Gnoni, 2006).

Tabla 1.2. Intervalos de concentración de actividad de diversos radionucleidos obtenidos en residuos procedentes de la producción de petróleo y gas (OGP, 2008).

Radionucleido	Fangos (Bq/g)	Residuos de tuberías (Bq/g)
^{226}Ra	0,05 - 800	0,01 -75
^{228}Ra	0,5 - 50	0,01 -10
^{210}Pb	0,1 -1300	0,05 - 50
^{210}Po	0,004 - 160	0,1 - 4

Otro ejemplo más cercano y significativo de esta concentración de residuos derivados de procesos industriales, es el que se ha hecho público recientemente en el lecho del río Ebro, a su paso por Flix (Tarragona). En esta localidad, la empresa Ercros posee una fábrica que produce diversos compuestos, entre ellos el fosfato bicálcico. Su producción se realiza a partir de la fosforita, un fosfoyeso de origen natural, el cual en su formación tiene gran capacidad de incorporar radionucleidos de origen natural a su estructura cristalina. Al realizarse la reacción de la fosforita con sales de calcio en presencia de ácido clorhídrico, los radionucleidos son desplazados de la estructura y pasan a formar parte de los residuos de la reacción. Estos residuos de reacción son los que se han ido vertiendo durante años en la zona llamada “Racó de la Pubilla”, provocando un aumento de la concentración de radionucleidos procedentes de las cadenas de desintegración de ^{235}U, ^{238}U y ^{232}Th (Ortega et al., 2008).

1.1.2. Presencia en el medio ambiente de radioactividad de origen artificial

Además de la radioactividad de origen natural, existe también la radioactividad de origen artificial, debido a radioisótopos que no se encuentran de forma natural en el medio ambiente, sino que se han introducido debido a la actividad humana. Su paso al medio ambiente se ha debido mayoritariamente a pruebas con armas atómicas realizadas en la atmósfera, accidentes nucleares acaecidos en instalaciones nucleares y a la gestión incorrecta de los residuos generados en actividades industriales.

1.1.2.1. Pruebas atómicas

Las primeras actividades que provocaron la introducción de radionucleidos artificiales en el medio ambiente de forma masiva fue la deposición radioactiva (*fallout*) subsiguiente a los numerosos ensayos nucleares que se realizaron en la atmósfera en diferentes períodos en los años 50 y 60 (principalmente, entre los años 1954 y 1958, y 1961 y 1962). Tras la explosión nuclear, se generan diversos tipos de partículas: las de mayor tamaño y que son intensamente radioactivas, que se depositan preferentemente en áreas cercanas al lugar de la explosión en cuestión de horas, y partículas más pequeñas que permanecen en la troposfera, hecho que provoca que con la ayuda de los vientos se transporten a grandes distancias antes de depositarse lentamente. Los radioisótopos que tienen un mayor impacto ambiental a medio y largo plazo debido a estas pruebas son ^{90}Sr, ^{137}Cs, ^{14}C, ^{238,239}Pu, ^{241}Am, y ^{131}I (Ortega y Jorba, 1996).

1.1.2.2. Accidentes nucleares

Los episodios accidentales en centrales nucleares, centros de producción de armas y procesamiento de combustible nuclear, han tenido lugar en diversos países y en varias ocasiones a lo largo de las últimas décadas, dando lugar a importantes liberaciones de radionucleidos al medio ambiente. A continuación se destacan aquellas situaciones accidentales que han provocado un mayor impacto radioactivo.

1.1.2.2.1. Sucesos accidentales destacables entre 1950 y 2000

Además de los accidentes de Chernóbil y de Mayak, de los que se hablará más adelante, a lo largo de las últimas décadas se han ido sucediendo otros accidentes que han provocado episodios de contaminación radioactiva. Sanderson et al. (1997) identifica hasta 150 accidentes entre 1945 y 1996 (Figura 1.3), produciéndose el máximo número de situaciones accidentales entre finales de los años sesenta y principios de los años setenta. En 38 de ellos se produjo emisión de radioactividad al medio.

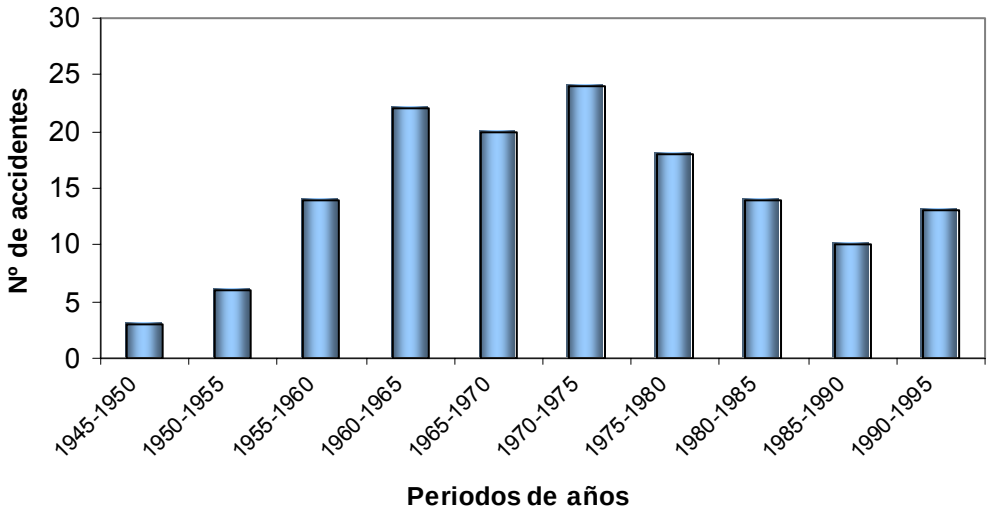

Figura 1.3. Número de accidentes ocurridos en instalaciones nucleares distribuidos en periodos de 5 años entre 1945 y 1995 (Sanderson et al., 1997).

La Tabla 1.3 resume los accidentes nucleares más importantes junto con los ya citados de Chernóbil y Mayak. Como puede observarse en la lista de sucesos accidentales descritos, tanto los radionucleidos como la actividad emitida presentan una gran variabilidad.

Tabla 1.3. Descripción de los accidentes más importantes sucedidos entre 1950 y 1999 (Sanderson et al., 1997; IAEA, 1999).

Lugar y fecha	Descripción del accidente	Radionucleidos emitidos
Windscale, UK Octubre 1957	Incendio del núcleo durante una reparación en una planta de producción de plutonio para uso militar	^{131}I (740 TBq) ^{137}Cs (22 TBq) ^{106}Ru (3 TBq) ^{133}Xe (1,2 TBq) ^{210}Po (8,8 TBq)
Atmósfera Océano Índico Abril 1964	Un satélite americano se quema en la estratosfera conteniendo una fuente de ^{238}Pu	^{238}Pu (629 TBq)
Palomares, España Enero 1966	Rotura de bombas con cabeza nuclear al impactar contra el suelo	^{239}Pu ^{240}Pu
Thule, EEUU 1968	Rotura de bombas con cabeza nuclear al impactar contra el suelo	$^{239, 240}$Pu (11 TBq)
Norte de Canadá Enero 1978	Impacto de un satélite ruso contra el suelo, contaminando un área ~ 50 x 800 km	20 kg U enriquecido ^{90}Sr (3,11 TBq) ^{131}I (181 TBq) ^{137}Cs (3,18 TBq)
Three Mile Island, EEUU Marzo 1979	Eliminación por error de parte del refrigerante del núcleo. Contaminación del edificio del reactor, con poca descarga al medio ambiente	Gases nobles, mayoritariamente de ^{133}Xe (~370 PBq) ^{131}I (550 GBq)
Tokaimura, Japón Septiembre 1999	Durante el proceso de enriquecimiento de uranio se alcanzó el estado de masa crítica, provocando la explosión del reactor y el descontrol de la reacción nuclear	2,5 EBq Radionucleidos más importantes: ^{24}Na, ^{56}Mn, ^{131}I, ^{133}I, ^{135}I y ^{137}Cs

1.1.2.2.2. El accidente de Chernóbil

El accidente de la central nuclear de Chernóbil (Ucrania) está considerado el accidente más importante de la historia de la energía nuclear, tanto por la cantidad de radiactividad que se emitió como por la gran extensión de terrero que fue afectada.

El accidente se produjo en el complejo nuclear de Chernóbil, durante la realización de un test de los sistemas de seguridad del reactor nº 4. A causa de la desconexión de diversos sistemas de seguridad del reactor, éste generó tal cantidad de energía que condujo a la ebullición del refrigerante hasta el punto de que el vapor generado provocó la explosión del reactor.

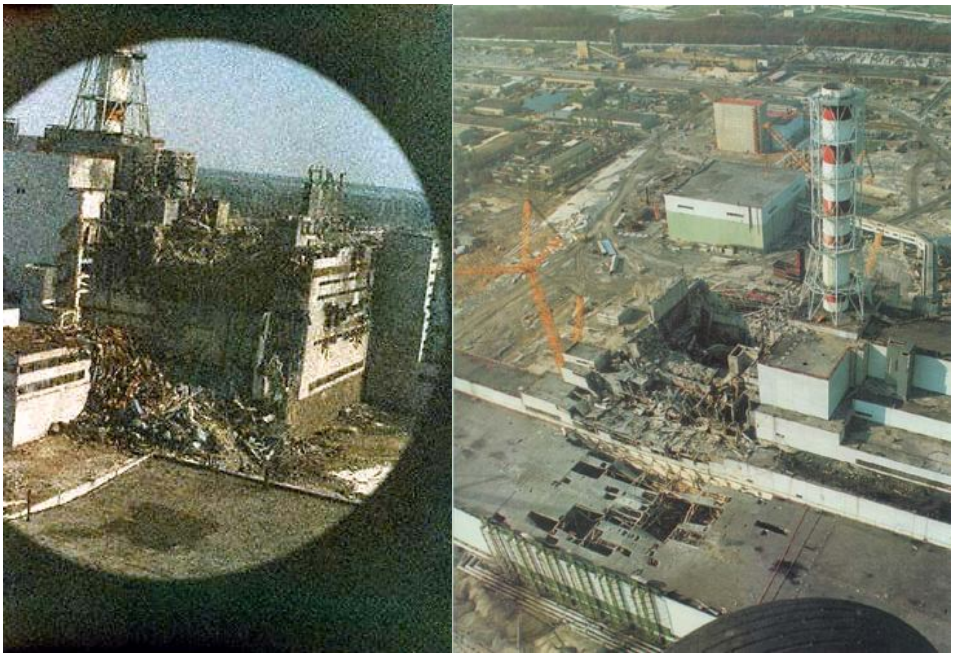

Figura 1.4. Vista aérea de la central de Chernóbil, el 26 de abril de 1986. El aspecto granulado de la primera foto es debido al alto nivel de radiación, ya que fue tomada por Igor Kostin pocas horas después de la explosión.

Las acciones inmediatas que se tomaron fueron la extinción de los incendios y el lanzamiento por vía aérea de unas 5000 toneladas de varios materiales: arena y arcilla para retener los radionucleidos liberados, carburo de boro para la absorción de neutrones, plomo como líquido sellador y dolomita para generar CO_2 y de esa forma absorber la energía del grafito incendiado, así como la inyección de nitrógeno líquido para reducir la temperatura del reactor e impedir la entrada de oxígeno para evitar que siguiese el incendio. Aproximadamente 135 toneladas de combustible (alrededor del

71% del total de combustible presente en el reactor) se fundieron, quedando posteriormente solidificadas en las partes inferiores del núcleo. La contención final se realizó construyendo un sarcófago de cemento armado alrededor del núcleo (Sanderson et al., 1997).

A consecuencia del accidente se emitieron el 100 % de los gases nobles, alrededor del 10-20% de los radionucleidos volátiles y aproximadamente el 3-6% de los radionucleidos no volátiles presentes en el núcleo del reactor, liberándose una actividad total aproximada de 12 x 10^{18} Bq (30000 veces más que las emisiones radioactivas de todas las instalaciones nucleares del mundo en un año).

Debido a las condiciones climatológicas adversas y cambiantes, además del largo período en que el reactor estuvo en llamas y expuesto a la atmósfera, la nube radioactiva compuesta por materiales radioactivos volátiles o asociados a aerosoles atmosféricos se extendió por una extensa área, a lo largo de toda Europa, tal y como se puede ver en la Figura 1.5. En primer lugar, las masas de aire contaminado se movieron hacia el oeste, noroeste y posteriormente hacia el noreste, hecho que se tradujo en una elevada contaminación de Bielorrusia, la parte europea de Rusia y Ucrania, y en menor extensión, Escandinavia. A continuación, la dirección del viento cambió hacia el sureste, transportando la nube radioactiva por encima de los Balcanes y los Alpes. Algunos días más tarde del accidente, las masas de aire con partículas radioactivas ya habían atravesado la mayor parte de los países europeos (Eisenbud y Gessell, 1997).

La emisión total que se depositó en territorio europeo fue del 4% de la radioactividad total acumulada en el reactor, de la cual ≈7,8 x 10^{16} Bq fueron de ^{137}Cs. La Figura 1.6 y 1.7 muestran, respectivamente, la deposición de ^{137}Cs en toda Europa y la clasificación de las zonas controladas según su nivel de contaminación. La contribución más importante de la deposición de radiocesio tuvo lugar en tres repúblicas de la antigua Unión Soviética: Bielorrusia con un 33%, Rusia con un 24% y Ucrania con un 20%. En estas repúblicas los niveles de deposición oscilaron entre 40 a 1480 kBq m^{-2}. Otros países, como Suecia, Finlandia, Austria, Noruega, Rumania y Alemania, también recibieron deposiciones importantes, entre el 1 y el 4%. En el resto de países europeos la deposición fue bastante inferior (Izrael et al., 1996).

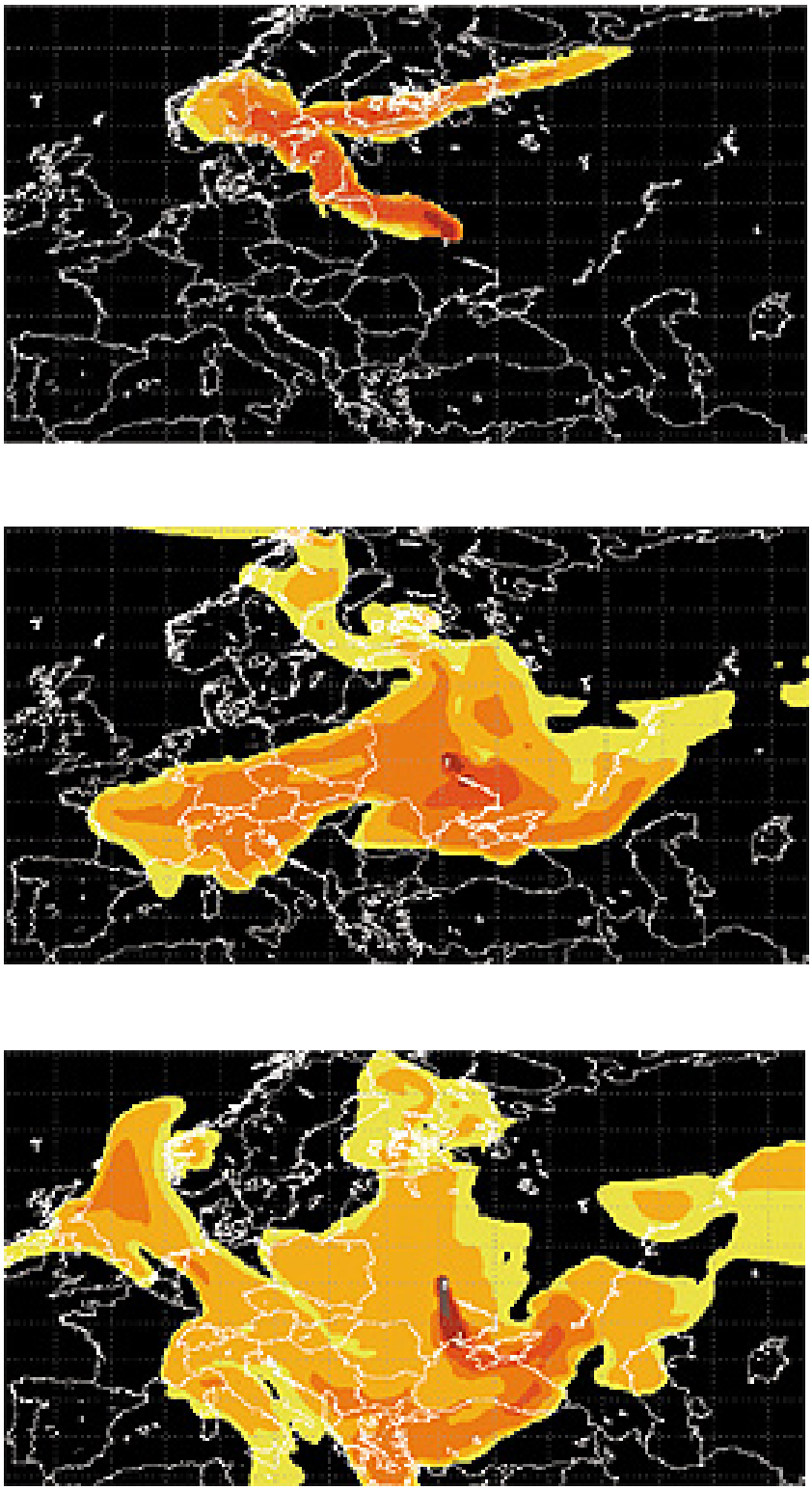

Figura 1.5. Movimiento de la nube radioactiva. Cambios de concentración de ^{137}Cs en la atmosfera.

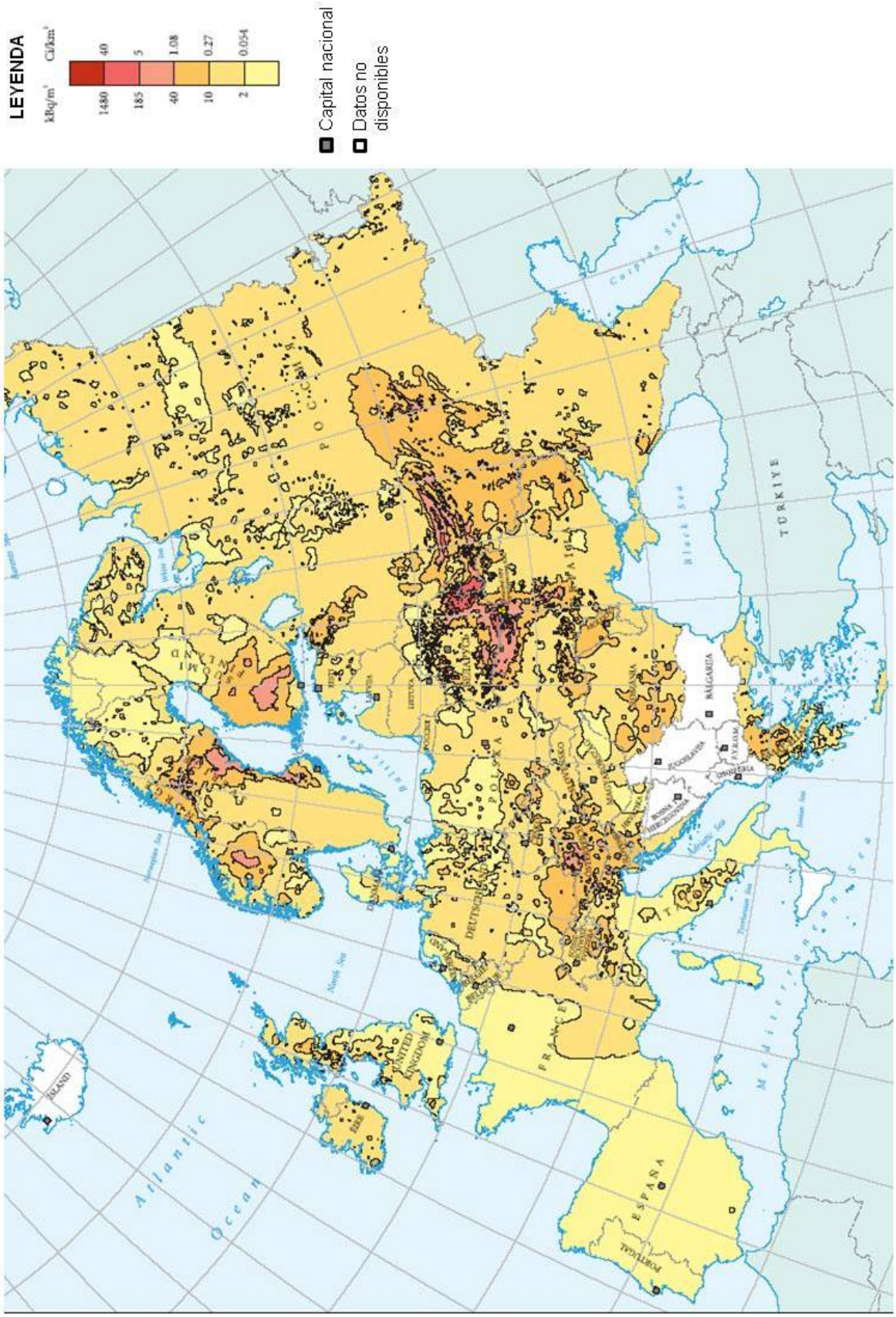

Figura 1.6. Deposición total de ^{137}Cs en Europa determinada entre 1995 y 1998. (De Cort et al., 1998).

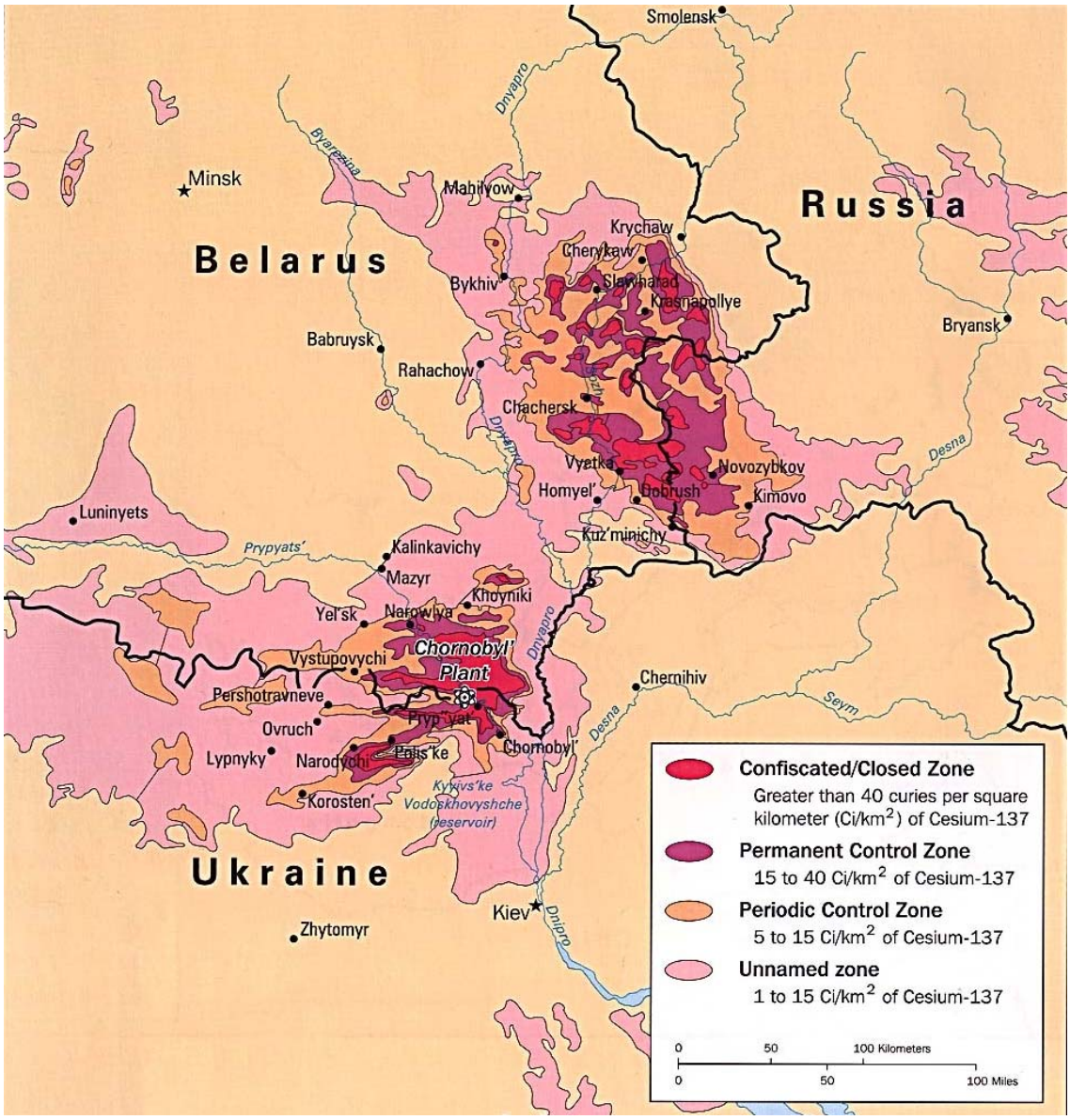

Figura 1.7. Clasificación de las diversas zonas controladas en función de la contaminación existente de ^{137}Cs en 1998 (De Cort et al., 1998).

De los productos de fisión liberados, los isótopos de radiocesio y de radioestroncio son los que tuvieron un mayor impacto medioambiental, a pesar de que fueron emitidos en una proporción inferior a otros presentes en el reactor (Tabla 1.4). No obstante, el relativamente largo periodo de semidesintegración de algunos de sus isótopos (el ^{137}Cs con $t_{1/2}$ de 30,2 años y el ^{90}Sr con un $t_{1/2}$ de 28,5 años), su elevada disponibilidad biológica, y su alta solubilidad y movilidad en el medio hicieron que se convirtieran en los radionucleidos claves en el seguimiento del impacto del accidente, incluso décadas después del suceso.

Tabla 1.4. Proporción de radionucleidos emitidos en función del periodo de semidesintegración ($t_{1/2}$) (IAEA, 2006).

$t_{1/2}$	% respecto al total emitido	Ejemplos
Menos de 1 mes	84	^{131}I; ^{133}Xe; ^{140}Ba
Entre 1 mes y 25 años	15	^{134}Cs; ^{106}Ru; ^{95}Zr
Entre 25 y 50 años	1	^{137}Cs; ^{90}Sr
Más de 50 años	0,001	^{239}Pu

Más de dos décadas después del accidente, hay aún centenares de emplazamientos rurales habitados en Rusia, Bielorusia y Ucrania con dosis anuales superiores a 1 mSv, debido principalmente, a las altas concentraciones de radiocesio en suelos (tanto agrícolas como forestales) en zonas en las que la población local decidió seguir viviendo. Las altas dosis, superiores a las permitidas por las respectivas legislaciones nacionales, se deben especialmente a la ingesta de alimentos contaminados. En 2004, el número de poblaciones afectadas en las tres repúblicas era un total de 290 (afectando directamente a unas 80000 personas) (Jacob et al., 2009). Debido a los procesos de desintegración natural del ^{137}Cs, este número se predice que habrá disminuido a 250 en 2010 (afectando a 70000 personas) y a 120 (afectando a 35000 personas) en 2020, tal como muestra la Figura 1.8.

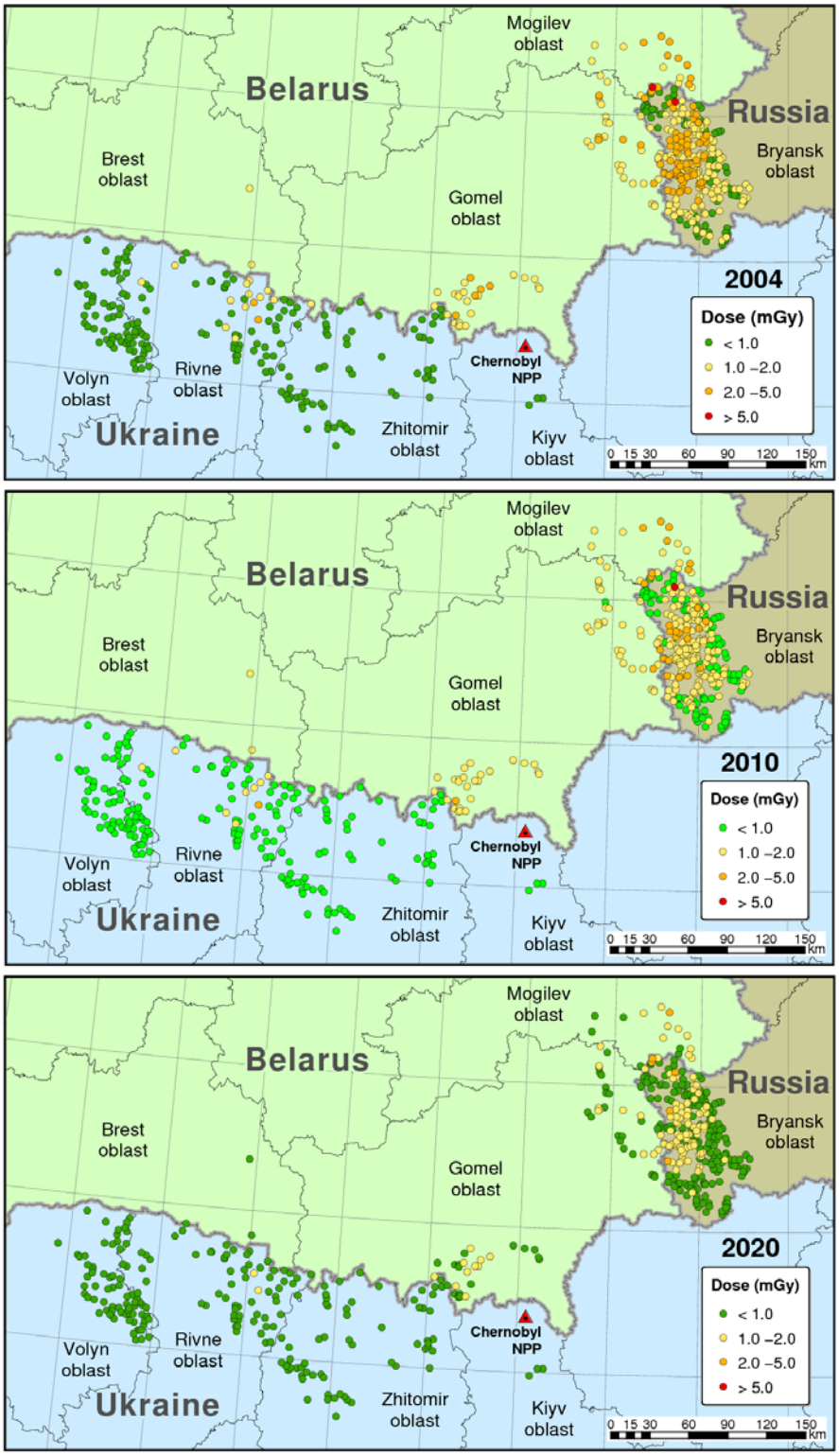

Figura 1.8. Evolución temporal del número de emplazamientos rurales con dosis superiores a las permitidas en Rusia, Bielorusia y Ucrania, en función del contenido de ^{137}Cs en los suelos a) en 2004, b) en 2010 c) en 2020 (Jacob et al., 2009).

1.1.2.2.3. Emisión de partículas radioactivas al medio ambiente en la Central Nuclear de Ascó

Durante uno de los exámenes incluidos en el plan de la vigilancia radiológica de la central nuclear, se encontraron partículas en zonas próximas al edificio de contención, en terrazas de diversos edificios de la central y terrenos situados dentro del doble vallado de seguridad que rodea la central. Este incidente se produjo el 26 de noviembre de 2007, durante una parada para la recarga del reactor, en la que una pequeña cantidad del agua proveniente de la limpieza de los canales de trasvase del combustible del núcleo a la piscina de almacenaje, fue aspirada por el sistema de ventilación. Este sistema de ventilación está dividido de dos líneas: una de emergencia (con sistema de filtrado de alta eficiencia previo a la salida por la chimenea de descarga) y otro de operación normal con salida directa (sin filtración) a la chimenea. Durante la recarga, el sistema que funcionó fue el de emergencia, filtrando y reteniendo todas las partículas, pero al darse por acabada la operación de recarga, se activó el sistema de ventilación normal, provocando que las partículas todavía presentes en los conductos de ventilación del edificio fuesen expulsados por la chimenea de descarga, depositándose mayoritariamente dentro del recinto de seguridad de la central, tal y como muestra la Figura 1.9.

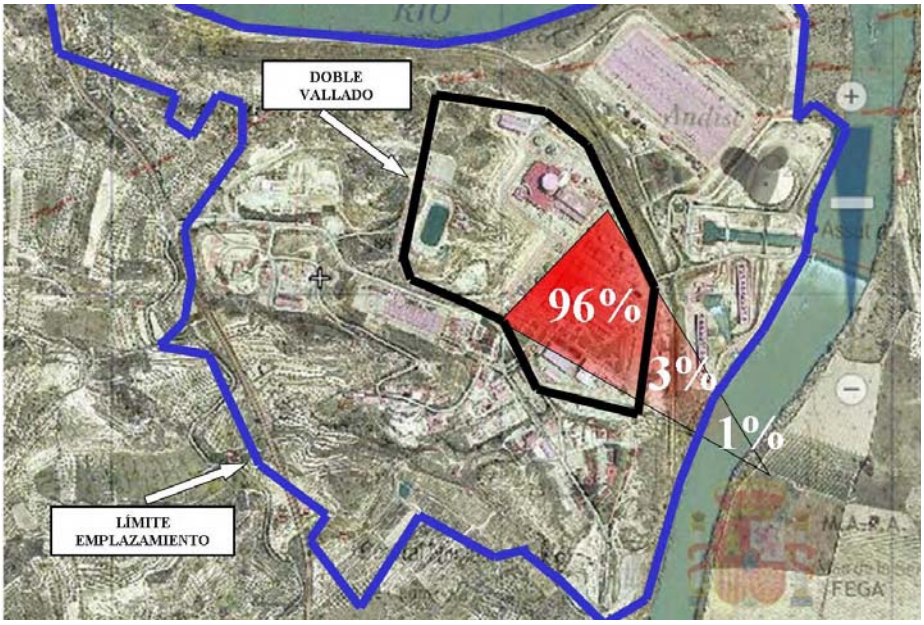

Figura 1.9. Distribución de las partículas radioactivas emitidas por la chimenea de descarga.

La actividad que pasó accidentalmente al sistema de ventilación fue de alrededor de 260 MBq. Los isótopos radiactivos presentes en las partículas y sus proporciones relativas aproximadas fueron: 45% de ^{60}Co, 15% de ^{58}Co, 25% de ^{54}Mn, 8% de ^{51}Cr y cantidades menores de ^{59}Fe, ^{95}Nb y ^{95}Zr (CSN, 2008).

1.1.2.3. Gestión de residuos

Al terminar el ciclo de vida útil del combustible nuclear o de los radionucleidos utilizados con fines científicos, médicos o industriales, éstos pasan a considerarse residuos radioactivos, siendo su gestión y almacenaje, uno de los puntos que mayor controversia científica y social provoca.

Los residuos nucleares se pueden clasificar en residuos de alta, media o baja actividad. Son considerados residuos de alta actividad el combustible nuclear gastado, los residuos líquidos y sólidos del reprocesamiento de combustible gastado y determinadas partes de una central nuclear derivadas de su desmantelamiento. Actualmente su almacenaje temporal se realiza dentro de las mismas centrales nucleares o en industrias de reprocesamiento de combustible. Para su almacenamiento definitivo a largo plazo, la opción más aceptada es el uso de *almacenamientos* en formaciones *geológicas profundas* (AGP) y que ya ha sido aprobado en países como Bélgica, Canadá, Finlandia, Francia, Japón, Suecia, Suiza y Estados Unidos (NEA, 1989). Otros países, entre los que se encuentran España, han optado por un *almacén temporal centralizado* (ATC), mientras acaban de tomar una decisión sobre la conveniencia o no de disponer de un AGP en su territorio, o de forma preliminar a la construcción del AGP. Ejemplos de estos emplazamientos se encuentran en Japón (Rokkasho), Francia (La Hague y Cascad), Suiza (Zwilag), Suecia (Clab), Bélgica (Dessel), Alemania (Ahaus y Gorleben), Reino Unido (Sellafield), Holanda (Habog) y Rusia (Mayak y Krasnoyarsk) (WNA, 2009).

El ATC es una instalación industrial diseñada para guardar en un único lugar el combustible gastado y los residuos radioactivos de alta actividad por un periodo limitado, del orden de unos sesenta años. Es una instalación en superficie para el almacenamiento en seco (ver Figura 1.10, donde se muestra el proyecto para el ATC español que está inspirado en la instalación en Habog, Holanda) del combustible gastado y los residuos vitrificados de alta actividad mediante un sistema de bóvedas y

naves de hormigón. En esta instalación se centralizarán los procesos de gestión de estos materiales para su tratamiento, almacenamiento controlado, reprocesamiento y reducción. En este almacén, los residuos están acondicionados y aislados con las barreras de ingeniería oportunas, siendo por tanto una instalación pasiva, que no produce energía, ni se dan en ella reacciones nucleares (ENRESA, 2010a).

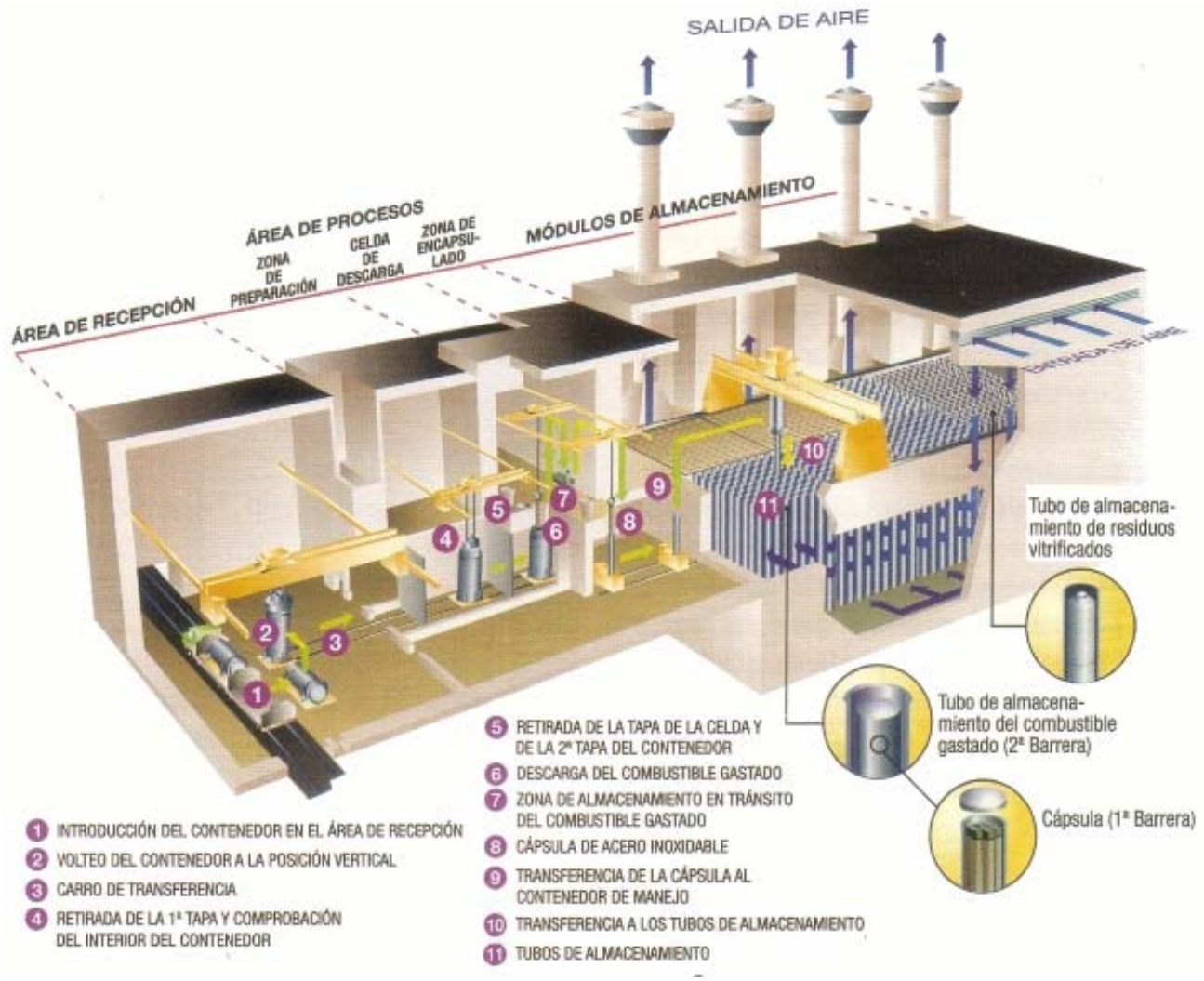

Figura 1.10. Descripción de las instalaciones del futuro ATC (ENRESA, 2010a).

A su vez, existen otros residuos que no se consideran de alta actividad. Pueden provenir de las centrales nucleares y su desmantelamiento, pero también son los generados en aplicaciones sanitarias, industriales y en centros de investigación y docencia, siendo los radionucleidos mayoritariamente presentes: ^{3}H, ^{14}C, ^{32}P, ^{51}Cr, ^{59}Fe, $^{57,60}Co$, ^{67}Ga, ^{75}Se, ^{81m}Kr, ^{99m}Tc, ^{110}In, $^{123,125,131}I$, ^{133}Xe, $^{134,137}Cs$, ^{192}Ir, ^{198}Au, ^{200}Tl y

^{226}Ra. Estos residuos se introducen en bidones que se colocan en módulos de hormigón armado situados en la superficie o a pequeñas profundidades bajo tierra. En España, los residuos de media y baja actividad se concentran en una única instalación llamada “El Cabril”, situada en Córdoba (ENRESA, 2010b).

Figura 1.11. Foto aérea de las instalaciones de “El Cabril”.

1.1.2.4. Gestión incorrecta de residuos

Además de los accidentes nucleares, la gestión incorrecta de los residuos de ciertas actividades industriales también ha supuesto una fuente de liberación de radionucleidos al medioambiente, como el ocurrido en el centro de producción de armas nucleares “Mayak” (antigua URSS).

El programa soviético de desarrollo de armas nucleares se emprendió a finales de los años 40, siendo su núcleo neurálgico el complejo de producción de armas nucleares de Mayak, construido entre 1945 y 1948 en la vertiente oriental de los Urales. La actividad principal del complejo era la de extraer, refinar y preparar plutonio para su uso en armas. Más tarde el complejo se especializó en el reprocesamiento de armas decomisadas y desechos de reactores nucleares. Actualmente se dedica al reprocesamiento de combustible nuclear, al almacenamiento de residuos radioactivos y a la producción de tritio (^{3}H) y radionucleidos de uso civil.

La historia del complejo Mayak está llena de episodios de liberación de radionucleidos al medio ambiente por una mala gestión de los residuos y por accidentes nucleares. Durante los primeros años de funcionamiento, el complejo fue vertiendo residuos líquidos en diversos lagos cercanos a la planta y en el río Techa, estimándose que desde 1949 a 1956, se vertieron unos 2,7 MCi de radionucleidos con diversos periodos de desintegración (Eisenbud y Gessell, 1997).

Figura 1.12. Foto de satélite del complejo nuclear de Mayak.

En septiembre de 1957, un tanque de almacenamiento que contenía 300 m³ de residuos de alto nivel radioactivo, explotó liberando casi la mitad de radiación que en Chernóbil, esparciendo 2 MCi de radioactividad sobre un área de 23.000 km² y afectando a 272.000 personas. Los radionucleidos emitidos en este accidente fueron principalmente ^{144}Ce + ^{144}Pr (66%), ^{95}Zr + ^{95}Nb (24,9%), ^{90}Sr + ^{90}Y (5,4%) y ^{106}Ru + ^{106}Rh (3,7%). Este accidente nuclear es conocido como el accidente de Kyshtym. Posteriormente, en 1967, el lago Karachay, que contenía grandes cantidades de residuos radioactivos líquidos, se secó debido a un período sin lluvias. Debido a esto, grandes cantidades de polvo radioactivo se esparcieron a lo largo de 2.700 km², afectando a 41.500 personas.

1.2

Conceptos básicos para la descripción del suelo

El compartimento medioambiental que acumula la mayor carga de contaminantes es el ecosistema terrestre, siendo el suelo la principal vía de entrada de los contaminantes en la cadena trófica. Por lo tanto, para poder evaluar el posible impacto de una contaminación radioactiva, es necesario tener la máxima información sobre los procesos de interacción radionucleido-suelo.

Como etapa previa al estudio de los mecanismos de interacción de radionucleidos en suelos, es necesario conocer las fases que forman un suelo, así como conocer los parámetros descriptivos o propiedades edáficas básicas necesarias para realizar la caracterización general de un suelo.

1.2.1. Características de las fases del suelo

Los suelos se pueden considerar sistemas heterogéneos y dinámicos compuestos por tres fases: sólida, líquida y gaseosa.

La fase sólida suele representar aproximadamente el 50% en volumen, mientras que las fases líquida y gaseosa ocupan el resto del volumen (Sposito, 1986). Las proporciones entre sí pueden depender tanto de las características morfológicas del suelo o variar rápidamente dependiendo de las condiciones climatológicas e hídricas de cada momento, ya que en condiciones de mayor humedad o bajo situaciones de lluvia, la fase líquida irá desplazando a la fase gaseosa (Porta et al., 1994). Dentro de la fase sólida se pueden distinguir las fracciones orgánica y mineral (o inorgánica), entre las cuales existen espacios intersticiales o huecos. Estos huecos están parcialmente ocupados por agua (porosidad fina o capilar, < 10 μm), que es el componente mayoritario de la fase líquida o solución de suelo, y por aire, que constituye la fase gaseosa o atmósfera del suelo (porosidad gruesa, > 10 μm).

1.2.2. Fase sólida

1.2.2.1. Fracción mineral

La fracción mineral es uno de los componentes básicos de la fase sólida de un suelo, pudiéndose clasificar en diferentes texturas dependiendo de la proporción de los diferentes tamaños de partícula presentes. La textura describe los suelos en función de tres grupos básicos con distinto tamaño de partícula: arena (entre 50 μm y 2 mm), limo (entre 2 y 50 μm) y arcilla (< 2 μm) (Brady, 2008). La fracción de arena y la fracción de limo están formadas mayoritariamente por silicatos (cuarzo, feldespatos, etc) y óxidos metálicos (goetita, hematita, etc.), mientras que la fracción de arcilla está formada mayoritariamente por aluminosilicatos.

A continuación se comentan algunos de los minerales que se pueden encontrar en la fracción mineral:

- *Óxidos metálicos*: Este término general se refiere a los óxidos, hidróxidos y oxihidróxidos de Fe^{2+}/Fe^{3+} (goetita [FeOOH], hematita [Fe_2O_3]), Mn^{2+}/Mn^{4+} (birnessita

[$(Na,Ca)_{0,5}(Mn^{4+},Mn^{3+})_2O_4 \cdot 1,5H_2O$]) y Al^{3+} (gibbsita [$Al(OH)_3$]) presentes en la fase sólida de los suelos. Dichos óxidos se presentan en los suelos en formas cristalinas puras o coprecipitados con aluminosilicatos y materia orgánica. Tienen gran influencia en el comportamiento de los suelos debido a que tienen una elevada área superficial específica y presentan gran reactividad (Martínez y McBride, 1998). Los óxidos metálicos tienen una elevada capacidad de sorción de elementos traza mediante sustituciones isomórficas de cationes divalentes o trivalentes, o mediante procesos de oxidación superficial.

- *Carbonatos*: Los carbonatos típicamente presentes en la fase sólida de un suelo son la calcita ($CaCO_3$) y la dolomita ($CaMg(CO_3)_2$). Dichos minerales presentan gran capacidad de intercambio catiónico debido a sus enlaces predominantemente iónicos con Ca^{2+} y Mg^{2+}. Existen también procesos de coprecipitación de los carbonatos con otros minerales de Fe y Mn, cuya formación y solubilización viene controlada por las condiciones de pH y régimen hídrico (Porta et al., 1994).

- *Otros minerales*: Las formas cristalinas de los fosfatos raramente se encuentran en los suelos, aunque sí se encuentran mezclas amorfas de fosfatos de Ca^{2+}, Fe^{2+} y Al^{3+} (Kabata-Pendias y Pendias, 2001). Los sulfuros (pirita: FeS_2), sulfatos (yeso: $CaSO_4 \cdot 2H_2O$) y cloruros (NaCl) son compuestos cuya presencia sólo suele ser significativa en suelos con características específicas, como es el caso de suelos con baja hidratación o alta salinidad.

- *Aluminosilicatos*: Son minerales secundarios, derivados de los procesos de envejecimiento (alteración de la estructura, disolución y reprecipitación) de minerales primarios provenientes directamente de la roca madre. Los aluminosilicatos tienen un reducido tamaño de partícula, y son los minerales de mayor presencia en la composición de los suelos (Moore Y Reynolds, 1989).

Los aluminosilicatos son clasificados usualmente en dos grupos principales: los estructurados y los amorfos. Los aluminosilicatos estructurados están formados por dos unidades estructurales: un tetraedro con cuatro átomos de oxígeno alrededor de un catión central, normalmente Si^{4+}, y un octaedro de seis átomos de oxígeno o iones hidroxilo alrededor de un catión de menor valencia, normalmente Al^{3+} o Mg^{2+}. Los tetraedros están unidos por sus esquinas basales, a través de los átomos de oxígeno, y forman una red hexagonal en forma de láminas. Los octaedros se unen de forma

similar por sus extremos y forman también estructuras laminares (Hillel, 1998).

En función de la relación entre las capas tetraédricas y octaédricas, los aluminosilicatos se clasifican en dos tipos denominados 1:1 o 2:1. En los minerales 1:1, como la caolinita [$Al_2Si_2O_5(OH)_4$], una capa de octaedros está unida por los oxígenos a los átomos de silicio de una capa tetraédrica. En los minerales de tipo 2:1, como por ejemplo las esmectitas, la capa de octaedros se une a dos capas tetraédricas, una por cada banda, produciéndose normalmente sustituciones por iones de radio aproximadamente igual, denominadas sustituciones isomórficas. En las capas tetraédricas el Al^{3+} puede sustituir al Si^{4+}, y en las octaédricas el Mg^{2+} puede sustituir al Al^{3+}. Como consecuencia, se produce un aumento de carga negativa en diferentes partes de las láminas, que puede ser externamente compensada por la sorción de cationes que se concentran en la superficie de la partícula de arcilla, pudiendo penetrar ocasionalmente en los espacios interlaminares, tal y como se puede observar en la Figura 1.13.

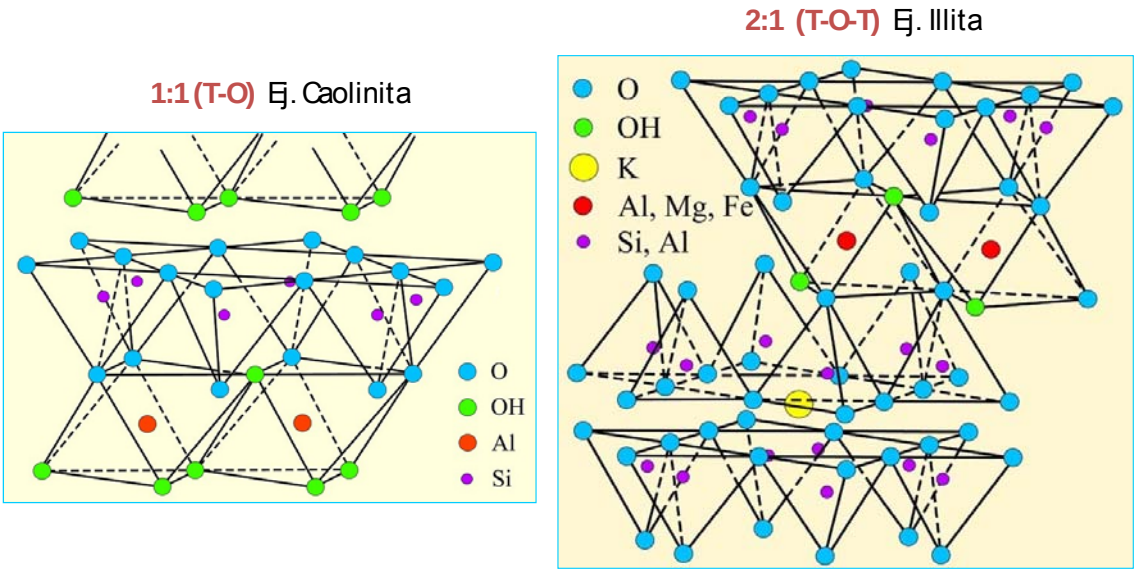

Figura 1.13. Representaciones tridimensionales de la estructura en capas de los aluminosilicato 1:1 y 2:1.

Los cationes sorbidos, como Na^+, K^+, Mg^{2+}, Ca^{2+}, NH_4^+ y Al^{3+}, no forman parte de la estructura de capas y pueden ser substituidos, o intercambiados, por otros cationes en la solución de suelo.

Desde el punto de vista de la interacción con algunos radionucleidos, los minerales arcillosos del tipo 2:1 son los más importantes. Tal y como se puede observar en la Tabla 1.5, la vermiculita y la esmectita son arcillas que presentan esta estructura 2:1, además de la illita. En el caso de la vermiculita y la esmectita, el agua y los iones

presentes en espacios interlaminares hacen que la estructura se expanda y que se puedan separar en diversas unidades. De esta forma, las superficies internas pasan a tener un papel activo y aumenta su superficie específica. La illita presenta sustituciones isomórficas de silicio por aluminio en las capas tetraédricas, hasta un total del 15%, que hace que aumente en gran medida la densidad negativa de estas láminas (Hillel, 1998). Si este aumento de carga es compensado por la atracción de cationes con una baja energía de hidratación, como el potasio, el rubidio, el amonio y el cesio, estos pueden perder su agua de hidratación e inducir al colapso de las dos láminas adyacentes. De esa forma se crea una estructura muy estable de láminas separadas por una distancia basal (distancia entre el plano de una lámina y el plano de la otra lámina) de 10 Å, donde los cationes deshidratados se adaptan perfectamente (Sposito, 1986; Porta, 1994). La caracterización cualitativa y cuantitativa de la fracción mineral, especialmente de las arcillas, necesita de técnicas de análisis estructural, siendo la difracción de rayos X (XRD) la más utilizada.

Tabla 1.5. Propiedades generales de determinados minerales (Brady y Weil, 2008).

Mineral	Tipo	Tamaño (µm)	Área superficial (m^2/g)		Distancia interlaminar[a] (nm)	Carga neta[b] ($cmol_c/kg$)
			Externa	Interna		
Esmectita	Silicato 2:1	0,01 – 1,0	80 – 150	550 – 650	1,0 – 2,0	-80 a -150
Vermiculita	Silicato 2:1	0,1 – 0,5	70 – 120	600 – 700	1,0 – 1,5	-100 a -200
Illita	Silicato 2:1	0,2 – 2,0	70 – 175	-	1,0	-10 a -40
Clorita	Silicato 2:1/2:1:1	0,1 – 2,0	70 – 100	-	1,41	-10 a -40
Caolinita	Silicato 1:1	0,1 – 5,0	5 - 30	-	0,72	-1 a -15
Gibsita	Óxido de Al	< 0,1	80 - 200	-	0,48	+10 a -5
Goetita	Óxido de Fe	< 0,1	100 – 300	-	0,42	+20 a -5

[a] Desde la parte superior de una capa a la capa similar más cercana, 1 nm = 10 Å. [b] Centimoles de carga neta por kilogramo de mineral (estimación de la capacidad de intercambio iónico).

1.2.2.2. Fracción orgánica

La fracción orgánica en suelos se forma a partir de los restos de plantas y animales, como resultado de las transformaciones ocasionadas por los microorganismos.

La materia orgánica del suelo está formada por dos grandes grupos de sustancias: las sustancias no húmicas que pertenecen a grupos conocidos de la bioquímica

(carbohidratos, proteínas, péptidos, aminoácidos y ácidos grasos de bajo peso molecular) y las sustancias húmicas, que son todos aquellos compuestos orgánicos que se encuentran en el medio y que no pueden ser clasificados en ningún otro grupo de compuestos químicos. Estas sustancias son compuestos poliméricos tridimensionales de elevado peso molecular, de colores oscuros y formados a partir de reacciones de degradación microbiana de otros compuestos orgánicos como la lignina o la celulosa. Dentro de las sustancias húmicas, se pueden definir, en función de su solubilidad y el pH, tres tipos de compuestos: ácidos húmicos, ácidos fúlvicos y humina. Los ácidos fúlvicos son solubles a cualquier pH, los ácidos húmicos son insolubles en medio ácido (pH < 2) pero solubles a pH elevados, y finalmente, la humina es la fracción insoluble en todo el intervalo de pH (Stevenson, 1982). La gran cantidad de grupos funcionales presentes en las sustancias húmicas es responsable de muchas de las propiedades y reactividad de la fracción orgánica de los suelos.

La materia orgánica, además de aportar sitios de sorción, también puede participar de forma competitiva en los procesos de sorción, ya que la materia orgánica disuelta (*Dissolved Organic Matter*, DOC) compite en los procesos de sorción en sitios de la fase sólida del suelo. Diversos estudios han demostrado que la sorción de la materia orgánica disuelta en los suelos se produce principalmente en los óxidos/hidróxidos de Al y/o Fe, además de minerales arcillosos como la caolinita o montmorillonita (Baham y Sposito, 1994; Kaiser y Zech, 2000).

1.2.3. Fase líquida o solución de suelo

La solución de suelo está constituida por el agua contenida en los poros y diferentes compuestos en solución, tanto iones libres como formando complejos con ligandos orgánicos e inorgánicos, así como materia en suspensión (Porta et al., 1994). Entre los iones típicamente presentes en la solución de suelo se encuentran diferentes cationes (Ca^{2+}, Mg^{2+}, Na^{+} y K^{+}) y aniones (HCO_3^-, SO_4^{2-} y Cl^-) provenientes de sales disueltas. Dependiendo de la cantidad de agua retenida que presenta un suelo, se pueden definir tres estados de humedad: capacidad máxima de retención o *pasta saturada* (el agua llena todos los espacios porosos y la presión adicional que se necesitaría aplicar para extraerla es prácticamente nula), capacidad de campo (el agua que queda retenida después de un drenaje rápido tras lluvia o riego y la presión necesaria para su extracción es de ~ 0,3 atm) y punto de marchitamiento (la proporción de aire es muy

superior a la de agua y la presión que se necesitaría aplicar para su extracción es de ~ 15 atm). La cantidad de agua que puede retener un suelo depende de las características de éste, principalmente la textura y el contenido en materia orgánica: un suelo orgánico admite más agua que un suelo mineral (hasta cuatro veces su peso), mientras que entre los suelos minerales, la retención de agua es mayor cuanto más pequeño sea el tamaño de partícula.

Como la solución de suelo actúa como vehículo de transporte de los nutrientes y los contaminantes a través del perfil del suelo, así como de interfase en los equilibrios suelo-planta (Lawrence y David, 1996), conocer su composición es un importante factor a tener en cuenta a la hora de estudiar los procesos de intercambio suelo-planta y en la distribución de contaminantes entre la fase sólida y fase líquida. A causa de la fácil modificación de los equilibrios entre la fase sólida y la solución de suelo, no existe ningún método simple que al ser aplicado permita obtener una solución de suelo absolutamente representativa (Iggy, 1988). En general, se considera que para obtener la composición in situ de la solución de suelo, ésta se ha de determinar de forma inmediata a su toma de la muestra, hecho que comporta problemas metodológicos complejos. Por ello, la solución de suelo se determina generalmente en suelos previamente secados y a los cuáles se les ha añadido agua.

1.2.4. Propiedades edáficas

Una vez se han estudiado las diferentes fases de las que está formado el suelo, el siguiente paso para poder explicar y predecir los mecanismos de interacción radionucleido-suelo que se establecen entre las diferentes fases, es realizar una caracterización de las propiedades del suelo.

Habitualmente, los parámetros que describen de forma general un suelo son el pH, el contenido en materia orgánica, la textura, la capacidad de intercambio catiónico (CIC), las bases de intercambio, la capacidad de campo, la conductividad eléctrica y el porcentaje de carbonatos. Estos parámetros se suelen determinar habitualmente y, con algunas excepciones, su determinación se basa en la aplicación de métodos normalizados. Además de estas propiedades generales, para poder explicar y entender los mecanismos sorción es necesario realizar una caracterización más detallada y especifica. Esta caracterización específica viene determinada por el

analito/radionucleido que se quiera estudiar. Algunas de las propiedades específicas que se deben determinar son la composición catiónica y aniónica de la solución de suelo, el análisis cualitativo y cuantitativo de la fracción de arcillas y la materia orgánica disuelta.

La acidez de un suelo viene expresada por el valor de pH. El pH del suelo se mide a partir de la concentración de protones en una solución obtenida a partir del suelo o acidez activa, los cuales son una pequeña parte de los protones presentes en el suelo o acidez reserva. Esta acidez reserva está inversamente relacionada con el porcentaje de saturación de bases, y es capaz de contrarrestar por intercambio cualquier cambio de pH en la solución de suelo, definiendo de esta forma la capacidad amortiguadora del suelo a posibles cambios de pH. La presencia de materia orgánica es muy importante en la acidez de un suelo, hasta el punto de que los suelos orgánicos presentan una acidez superior a los suelos inorgánicos, llegando a valores inferiores a pH 5. En el otro extremo, se encuentran los suelos con un alto contenido en carbonatos caracterizados por un elevado valor de pH, con valores superiores a pH 8.

En relación al contenido de materia orgánica, éste se puede expresar como porcentaje de materia orgánica o de carbono orgánico. Se considera que un suelo es orgánico cuando su porcentaje de materia orgánica supera el 30% o, lo que es equivalente, su contenido en carbono orgánico es superior al 18%.

La textura de un suelo se define a partir de la distribución de tamaño de las partículas de la fracción mineral del suelo. A partir de los porcentajes de arena, limo y arcilla que presente un suelo, se puede obtener su textura utilizando un triángulo de textura establecido por la Sociedad Internacional de la Ciencia del Suelo (*International Society of Soil Science*, ISSS), el cuál esta divido en zonas que representan una textura diferente (franco-arenosa, franco-limosa, etc.). Para los suelos que presentan un alto contenido en materia orgánica, esta clasificación por texturas no es del todo aplicable.

La Capacidad de Intercambio Catiónico (CIC) de un suelo es la medida cuantitativa de la capacidad de un suelo para intercambiar cationes e indica la carga negativa presente por unidad de masa de suelo. La unidad habitual de la CIC son los centimoles de carga por kilogramo de suelo ($cmol_c\ kg^{-1}$). Como se ha indicado anteriormente, la fase sólida del suelo presenta una carga negativa global, la cual es neutralizada por cationes depositados sobre la superficie de estas partículas.

Mayoritariamente, estos cationes no son retenidos irreversiblemente, sino que están en equilibrio con la solución de suelo y pueden ser intercambiados. Estos cationes reciben el nombre de cationes de intercambio, los cuáles son reducidos en número y se pueden separar en dos grupos: los cationes básicos o bases que son Na^+, K^+, Mg^{2+} y Ca^{2+}, y los cationes ácidos, que son H^+ y Al^{3+}. El suelo también contiene otros cationes como NH_4^+, más abundantes en los suelos ácidos que han sido sometidos a condiciones anóxicas. La proporción de la CIC que está ocupada por bases es lo que se denomina porcentaje de saturación de bases. La materia orgánica es el componente del suelo con un mayor valor de la CIC, de 100 a 300 $cmol_c\ kg^{-1}$, mientras que en las arcillas el valor de CIC es muy variable, presentando la siguiente secuencia: vermiculita (100-200 $cmol_c\ kg^{-1}$) > esmectita (80-150 $cmol_c\ kg^{-1}$) > illita (10-40 $cmol_c\ kg^{-1}$) > caolinita (1-15 $cmol_c\ kg^{-1}$) (Mclaren y Cameron, 1996).

Como la CIC indica la capacidad de un suelo de intercambiar cationes y al estar estos en equilibro con los presentes en la solución de suelo, es necesario determinar la composición catiónica de la solución de suelo, con la finalidad de poder estudiar y cuantificar ese equilibrio. A la hora de determinar la composición de la solución de suelo, hay que tener en cuenta que la concentración de los cationes dependerá de la relación masa de suelo y el volumen de agua (masa de suelo/volumen de agua). Habitualmente, esta determinación se realiza en soluciones de suelo que han sido obtenidas de suelos a los que se les ha añadido agua hasta obtener el nivel de contenido de agua de capacidad de campo.

Las propiedades edáficas generales, así como las específicas, son utilizadas como datos de entrada en modelos o códigos geoquímicos existentes y que se utilizan para describir las interacciones contaminante-suelo o predecir su movilidad. El desarrollo de estos modelos es dispar según el analito o contaminante que se estudie, siendo los más desarrollados aquellos que estudian metales pesados, como pueden ser los códigos ORCHESTRA (*Objects Representing CHEmical Speciation and TRAnsport*) (Meeussen, 2003) o MINTEQA2 (EPA, 1998). Estos modelos utilizan propiedades generales para calcular la distribución de las diferentes especies químicas sobre las diferentes fases o formas fisicoquímicas existentes en un equilibrio químico. En el caso de los radionucleidos, estos códigos geoquímicos están mucho menos desarrollados, aunque existen ya algunos desarrollados para predecir la especiación de radionucleidos del grupo de los NORM (PHREEQC, WHAM-VI MINITAB), que en algunos casos son ampliaciones de los programas de cálculo utilizados para metales

pesados (Di Bonito, 2005). Para el caso de otros radionucleidos de gran impacto ambiental, como por ejemplo radiocesio y radioestroncio, no existen propiamente modelos establecidos y en los modelos matemáticos para la toma de decisiones (*Environmental Decision Suport Systems*, EDSS) (CIEMAT, 2000) se intenta incluir correlaciones entre propiedades generales y específicas de los suelos con la constante de distribución sólido-líquido de los radionucleidos (K_d), parámetro clave para la descripción y predicción del comportamiento de radionucleidos en suelos, siendo éste un campo de investigación muy activo en la actualidad.

1.3

Interacción radionucleido-suelo

Al incorporarse al suelo, un contaminante radioactivo interacciona de forma diversa con los componentes de las fracciones mineral y orgánica de la fase sólida del suelo. La fracción de contaminante sorbida dependerá del coeficiente de distribución sólido-líquido (K_d), que también controlará la tendencia del suelo a permitir que los contaminantes puedan pasar de nuevo a la solución de suelo y ser movilizados en la cadena trófica.

La interacción radionucleido-suelo depende del tipo de radionucleido y de suelo. Los radionucleidos de más impacto medioambiental (isótopos de radiocesio y radioestroncio; actínidos) presentan una interacción muy diferente en suelos. Esto obliga a no poder extrapolar el comportamiento de un radionucleido a otro, y por lo tanto, que sea necesario identificar los mecanismos responsables de la interacción de un radionucleido en un suelo determinado. Mientras que los mecanismos para ciertos radionucleidos (radiocesio, radioestroncio) comienzan a ser conocidos y cuantificables en algunos escenarios, la naturaleza química de los actínidos, más compleja, (especialmente Pu, U y Am) ha dificultado una sistematización en su estudio, existiendo aún abundantes lagunas en la predicción de su comportamiento, especialmente a largo plazo.

1.3.1. Introducción a la interacción radionucleido-suelo

Es necesario conocer los diferentes procesos que pueden afectar la interacción de los radionucleidos para poder predecir su comportamiento y movilidad en un suelo. La Figura 1.14 resume de forma esquemática los principales procesos que describen la interacción de los radionucleidos con el suelo.

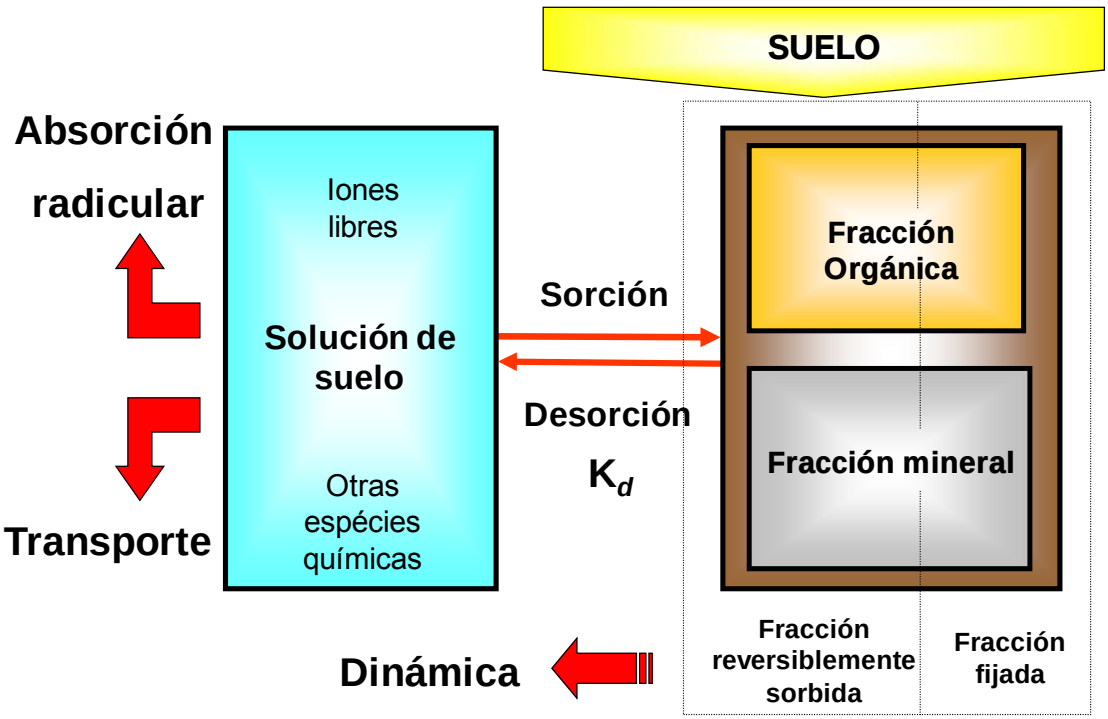

Figura 1.14. Procesos implicados en la interacción de radionucleidos con el suelo.

Una vez que el radionucleido entra en contacto con el suelo, normalmente a través de su fase líquida o solución de suelo, se origina un proceso de sorción, en el que se produce una distribución del radionucleido entre la fase sólida y la fase líquida (coeficiente de distribución sólido-líquido, K_d) (Hiton y Comans, 2001). La sorción es un concepto que engloba la incorporación de un soluto a la fase sólida del suelo mediante diferentes mecanismos, tales como adsorción, intercambio catiónico y precipitación. Entre ellos, el mecanismo más complejo es la adsorción, ya que engloba reacciones químicas entre el soluto y sitios en la superficie de fase sólida. En función de los ligandos disponibles en estos sitios y la naturaleza de la interacción los procesos se basarán en complejación superficial, intercambio de ligandos, formación de puentes de hidrógeno, interacciones eléctricas (electrostáticas y por polarización) e interacciones con los solventes (expulsión hidrofóbica) (Stumm y Morgan, 1981).

En una segunda etapa, el radionucleido incorporado a la fase sólida se reparte entre una fracción fijada, enlazada de forma estable con los componentes de la fase sólida, y una fracción sorbida reversiblemente, la cual puede removilizarse y volver a participar en los equilibrios de distribución entre la fase sólida y la solución de suelo y que será clave en la predicción de la disponibilidad de un determinado radionucleido. Así, la fracción de radionucleido resolubilizada quedará en la solución de suelo disponible para ser transportada hacia zonas no contaminadas o aguas subterráneas y superficiales, o para ser absorbido por las raíces de las plantas.

En tercer lugar, se ha de considerar el concepto de la dinámica de la interacción entre los radionucleidos y el suelo. Los procesos que controlan la sorción pueden no ser constantes a lo largo del tiempo, debido a que el comportamiento activo de la fase sólida del suelo puede hacer variar la distribución del radionucleido entre la fracción fijada y la fracción sorbida reversiblemente, que suele disminuir con el tiempo. La consideración de los aspectos dinámicos será clave para extender la predicción de riesgo a medio o largo plazo.

1.3.2. Concepto de coeficiente de distribución sólido-líquido (K_d)

Tal como se ha descrito en el apartado anterior, los radionucleidos se pueden unir a sitios en la superficie de la fase sólida de los suelos por diversos procesos clasificados habitualmente bajo el término general de sorción. Aunque se han realizado importantes progresos a la hora de describir la sorción en sólidos heterogéneos partiendo de los resultados obtenidos de estudios de sorción sobre fases sólidas puras, muchos modelos que miden la sorción de los radionucleidos están aún basados en una aproximación empírica, como es el caso de utilizar los valores del coeficiente de distribución sólido-líquido, K_d. Esta aproximación es el modelo de sorción más simple disponible y se define como la relación entre las concentraciones en equilibrio del radionucleido en la fase sólida y en la fase líquida (Hilton y Comans, 2001):

$$K_d(\mathrm{RN})\,(\mathrm{L/kg}) = \frac{[\mathrm{RN}]_S\ (\mathrm{Bq/kg})}{[\mathrm{RN}]_L\ (\mathrm{Bq/L})} \qquad \textbf{[Ec. 1.1]}$$

La K_d no informa sobre los mecanismos de sorción, con lo que no permite de forma directa la identificación y cuantificación de la capacidad o la selectividad de los sitios

de sorción, ni la descripción de la posible competición entre varios solutos para ocupar esos sitios de sorción.

El modelo simple de la K_d está basado en la hipótesis de que todo el radionucleido en la fase sólida está en equilibrio con el radionucleido en solución, por lo tanto, puede existir un intercambio entre las dos fases. Sin embargo, está demostrado que la cuantificación del valor de la K_d depende del tiempo de contacto, ya que una fracción del radionucleido puede fijarse de forma irreversible por la fase sólida y ésta puede aumentar con el tiempo, lo que está relacionado con aspectos de la dinámica de sorción (Gillet et al., 2001; Sánchez et al., 2002). La significación de este proceso aconseja definir la existencia de diferentes K_d en función de si se refieren únicamente a la fracción de radionucleido sorbido reversiblemente (K_d *lábil* o *intercambiable*) o si incluyen todo el radionucleido sorbido, independientemente de la reversibilidad de su sorción.

Los ensayos de laboratorio diseñados con tiempos de contacto cortos permiten principalmente obtener la K_d *intercambiable* (K_d^{exch}), que en algún caso puede predecirse a partir de propiedades edáficas que midan la capacidad de sorción del suelo (cantidad y selectividad de los sitios de sorción) y la composición de la solución de suelo (concentración de los iones competitivos en la sorción presentes en la solución).

1.3.3. Métodos experimentales para la determinación de la K_d

Los valores experimentales de K_d pueden obtenerse a partir de suelos contaminados, o a partir de experimentos a escala de laboratorio a partir de suelos no contaminados

1.3.3.1. Determinación de K_d a partir de suelos contaminados

La K_d se puede cuantificar a partir de la concentración de radionucleido en la fase sólida del suelo dividida por la concentración del radionucleido en la solución de suelo obtenida a partir de suelo contaminado (Goody et al., 1995). Esta aproximación es correcta cuando el nivel de contaminación es suficientemente alto para despreciar la posible incertidumbre a la hora de obtener y medir una muestra representativa de la solución de suelo.

Esta aproximación puede conducir a obtener valores de K_d superiores a aquellos que se obtienen a partir de experimentos de sorción, ya que el radionucleido cuantificado en la fase sólida del suelo contaminado puede incluir radionucleido sorbido no disponible para el equilibrio que se establece con la solución de suelo, debido al tiempo transcurrido desde la incorporación del radionucleido. Este método no está recomendado para la determinación de la K_d *intercambiable* (K_d^{exch}).

1.3.3.2. Experimentos de sorción en *batch* a escala de laboratorio

De entre todos los estudios de laboratorio, la aproximación más habitual es realizar experimentos de sorción con suelos no contaminados, principalmente usando métodos en *batch* en que la muestra se dispersa en una solución de composición determinada, tal y como se muestra en la Figura 1.15. Aún no se ha establecido ningún método como estándar, aunque diversas organizaciones han recomendado algunos detalles en los procedimientos a aplicar (OECD, 2000; ASTM, 2001).

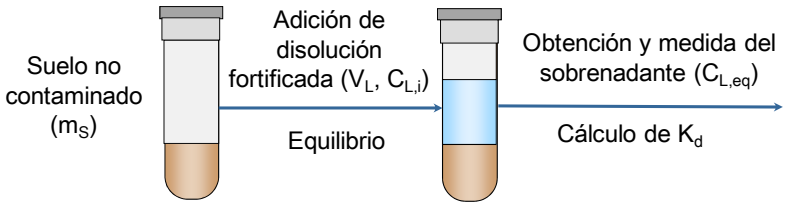

$$K_d = \frac{C_{S,sor}}{C_{L,eq}} = \frac{(C_{L,i} - C_{L,eq})V_L / m_S}{C_{L,eq}}$$

Figura 1.15. Diagrama descriptivo del método en *batch* para la determinación de la K_d de sorción.

Los experimentos de sorción se realizan a varios niveles de actividad del radionucleido y en diferentes contextos, tanto mineralógicos como hidroquímicos. Las condiciones experimentales, tales como la composición de la solución de contacto, tiempo de contacto, relación masa/volumen, y la filtración de la solución resultante, pueden variar ampliamente en los experimentos en *batch*. Se recomienda que los experimentos de sorción se realicen de forma que simulen lo más posible las condiciones de campo que se quieran estudiar, como por ejemplo reproduciendo el pH y la composición iónica de la solución en el medio de sorción (Staunton, 2004).

Los experimentos de sorción en *batch* suelen venir acompañados por experimentos de desorción, usualmente basados en técnicas de extracción, que tienen como objetivo estimar la fracción sorbida reversiblemente, lo que permite distinguir entre la fracción de radionucleidos intercambiable de la fijada irreversiblemente (Kennedy et al., 1997; Roig et al., 1998). Como muestra la Figura 1.16 estos experimentos pueden realizarse a partir tanto de suelos ya contaminados, como a partir de los suelos fortificados tras experimentos de sorción. En ambos casos, tras la adición de un agente extractante adecuado es posible el cálculo del porcentaje de extracción y de la K_d de desorción.

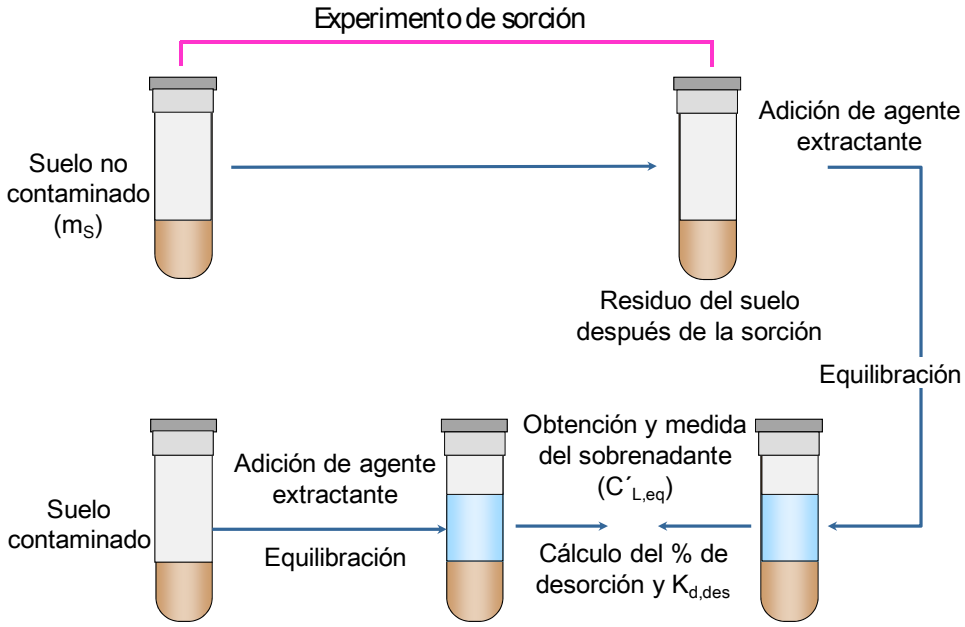

Figura 1.16. Diagrama descriptivo de experimentos de desorción.

1.3.3.3. Experimentos de difusión a escala de laboratorio

Otra aproximación experimental es determinar la K_d a partir de la difusión de un radionucleido en un suelo compactado, en columna o en celdas de difusión (García-Gutiérrez et al., 2004). En un medio poroso como son los suelos, el proceso de difusión del radionucleido es diferente del que presenta en agua. En general, el comportamiento de los radionucleidos en los poros es un proceso complejo afectado por muchos parámetros como la temperatura, las propiedades de difusión de las especies y las propiedades intrínsecas del suelo, tales como la estructura de poros, el nivel de compactación y su capacidad de sorción. En el caso de solutos que presentan

una sorción en el suelo, se puede definir un coeficiente de difusión aparente, D_a [m^2 s^{-1}], que considera implícitamente el retraso del soluto debido a las interacciones con el material poroso:

$$D_a = \frac{D_w}{\tau \ R_f} \qquad \textbf{[Ec.1.2]}$$

donde D_w es el coeficiente de difusión en agua [m^2 s^{-1}], τ es la tortuosidad [adimensional], y R_f es el factor de retraso [adimensional]. Este factor se relaciona con la K_d mediante la siguiente expresión (Bégin et al., 2003):

$$R_f = 1 + \frac{K_d \ \rho_{seco}}{\varepsilon \ RS} \qquad \textbf{[Ec. 1.3]}$$

donde ρ_{seco} [kg m^{-3}] es la densidad aparente del suelo en función de su peso seco, ε es la porosidad y RS es la saturación relativa del suelo.

A día de hoy, son escasos los estudios que intentan comparar los valores obtenidos de K_d a partir de experimentos de *batch* y de difusión. Las conclusiones son contradictorias, y aunque se han descrito trabajos en los que se concluye que los valores obtenidos a partir de los métodos de *batch*, subestiman o sobreestiman los valores de K_d medidos a partir de los experimentos de difusión (Ochset al., 1998; Ochs et al., 2001), de forma mayoritaria se postula que los valores de K_d obtenidos a partir de experimentos de difusión son inferiores a los obtenidos a partir de experimentos en *batch* (Okamoto et al., 1991; Fernández-Torrent et al., 2005), generalmente debido a las condiciones experimentales utilizadas en los experimentos de *batch*, como la relación volumen/masa o el tiempo de contacto (Aldaba et al., 2010).

1.3.4. Cambios de la interacción radionucleido-suelo con el tiempo

Con el paso del tiempo, el escenario después de la etapa de sorción puede evolucionar hacia una situación de mayor o menor riesgo ambiental, en función de si los radionucleidos incrementan su movilidad o su fijación en las fases del suelo respecto a la situación inicial tras el episodio de contaminación (McDonald, 2000). En el segundo caso, los diferentes procesos que influencian la dinámica de la interacción

se engloban bajo el concepto de *atenuación natural*. Entre dichos procesos destaca el incremento del pH del suelo, que induce la precipitación de óxidos e hidróxidos de los compuestos contaminantes, y la difusión de los radionucleidos a sitios de mayor afinidad en la estructura de los aluminosilicatos u óxidos de hierro que componen el suelo (McDonald et al., 2000). La incidencia de estos procesos puede incrementarse debido a ciertos factores ambientales y climáticos, tales como cambios bruscos de la temperatura y de régimen hídrico, ya que tienen gran influencia en todos los procesos físicos, químicos y biológicos que tienen lugar en un suelo.

Los estudios de dinámica se basan en la monitorización a lo largo del tiempo de los procesos de sorción mediante el seguimiento de la K_d, o los cambios en la reversibilidad de dicha sorción mediante experimentos de desorción, principalmente a escala de laboratorio (Vidal et al., 1995; Absalom et al., 1995; Roig et al., 2007). Los estudios de dinámica de la interacción a nivel de campo se realizan con suelos contaminados, mediante el control de los cambios con el tiempo de los valores de K_d *in situ*. Esta aproximación no aporta información mecanística detallada y presenta grandes problemas debido a la gran variabilidad y dificultad de cuantificación de la K_d *in situ*, hecho que limita la comparación de datos. En cambio, y aún cuando los ensayos de laboratorio sean operacionales, a escala de laboratorio los ensayos tienen menos variabilidad y pueden diseñarse para evidenciar el peso relativo de diferentes variables y mecanismos que puedan afectar a la dinámica de la interacción. Otro aspecto positivo de los ensayos a escala de laboratorio es que permiten acelerar la dinámica que se observaría a escala de campo, por ejemplo por medio de la inducción de los procesos ambientales de envejecimiento del suelo, mediante la aplicación sucesiva de ciclos de secado y mojado a una temperatura dada (Degryse et al., 2004). En dichos casos se pueden comparar los cambios detectados en la interacción, a través de los valores de K_d y las características de reversibilidad o extractabilidad (Roig et al., 2007), entre las muestras iniciales no alteradas y aquellas a las que se han aplicado los ciclos de envejecimiento.

1.3.5. Factores que gobiernan la interacción en suelos de los radionucleidos de mayor interés medioambiental

1.3.5.1 Radioestroncio

El estroncio es un elemento alcalinotérreo, con un elevado carácter electropositivo y de una gran reactividad química. Este catión muestra una gran tendencia a formar compuestos de naturaleza iónica, la mayoría solubles en agua, aunque algunas de sus sales formadas con fluoruros, carbonatos y sulfatos son bastante insolubles (Cotton y Wilkinson, 1986).

Además del ^{90}Sr (emisor beta), que es el radioisótopo más estudiado, con un periodo de semidesintegración ($t_{1/2}$) de 28 años, existen el ^{85}Sr y el ^{89}Sr, que se generan también como productos de fisión, pero su interés es menor ya que tiene $t_{1/2}$ cortos (64,85 y 50,55 días, respectivamente) (Kocher, 1981). A causa de su corto periodo de semidesintegración y de ser emisor gamma, el ^{85}Sr es muy utilizado en experimentos de laboratorio con la finalidad de estudiar el comportamiento del ^{90}Sr.

El coeficiente de distribución sólido-líquido de un radionucleido (RN) como el radioestroncio, puede ser mejor entendido utilizando como referencia la sorción de un ión análogo (AN) competitivo, caracterizado por un comportamiento similar de sorción y que esté presente en concentraciones significativas en la solución de suelo. Según esta aproximación:

$$K_d(RN) = K_d(AN) \cdot K_C(RN/AN) \qquad \textbf{[Ec. 1.4]}$$

donde $K_d(RN)$ se calcula por una amplificación lineal de la $K_d(AN)$ por un factor igual al coeficiente de selectividad RN-AN en los sitios de sorción, $K_C(RN/AN)$.
La sorción de radioestroncio está controlada por la existencia de sitios de intercambio regular en la materia orgánica y en las arcillas (*Regular Exchangeable Sites*, RES), que son los responsables de la capacidad de intercambio catiónico de un suelo (Rauret y Firsakova, 1996; Hilton y Comans, 2001), siendo el Ca y Mg los elementos que presentan comportamientos análogos al radioestroncio. Como las diferencias de selectividad entre los cationes alcalinotérreos son poco importantes (Juo y Barber, 1969; Valcke, 1993; Sysoeva et al., 2005), se puede expresar el coeficiente de distribución sólido-líquido del radioestroncio según la siguiente expresión:

$$K_d(Sr) = K_d(Ca,Mg) \cdot K_C(Sr/Ca,Mg) = \frac{Z_{Ca+Mg} \cdot [CIC]}{m_{Ca+Mg}} \cdot K_C(Sr/Ca,Mg) \qquad \textbf{[Ec.1.5]}$$

donde Z_{Ca+Mg} expresa la proporción relativa de Ca y Mg en el complejo de intercambio (es decir, el nivel de Ca y Mg intercambiables) y m es la suma de las concentraciones de Ca y Mg en la solución de contacto. Como que en el caso del radioestroncio, el coeficiente de selectividad K_c(Sr/Ca,Mg) es prácticamente la unidad, los parámetros clave en la interacción de radioestroncio en un suelo son la CIC y el nivel de especies divalentes en la fase sólida y en la solución de suelo.

1.3.5.2. Radiocesio

El cesio es un elemento alcalino, fuertemente electropositivo y con un bajo potencial de ionización. Los compuestos que forman son mayoritariamente de naturaleza iónica y no muestra casi tendencia a formar enlaces covalentes ni complejos de estabilidad apreciable (Cotton y Wilkinson, 1986).

El interés del estudio del cesio se debe a la existencia de tres radioisótopos, ^{134}Cs, ^{135}Cs y ^{137}Cs. Mientras que el ^{134}Cs y ^{137}Cs son productos de fisión, con $t_{1/2}$ de 2,06 y 30,1 años, respectivamente, el ^{135}Cs forma parte del combustible gastado, con un período de semidesintegración de millones de años (2,3x10^6 años).

En la sorción de radiocesio, los sitios de intercambio regular no tienen un papel tan significativo en su sorción. En cambio, los sitios interlaminares de las arcillas, en especial en los extremos expandidos (*Frayed Edge Sites*, FES), son los que rigen la sorción de radiocesio. Tal como muestra la Figura 1.17, los sitios FES están compuestos de sitios interlaminares en los extremos expandidos de las arcillas, que discriminan poco entre Cs y otros cationes monovalentes (NH_4, K, Rb), pero discriminan considerablemente entre cationes monovalentes y divalentes, y los sitios interlaminares más interiores y próximos al centro colapsado de las láminas de las arcillas, que sí son claves para entender la sorción de radiocesio (Cremers et al., 1988). De hecho, los sitios internos son muy específicos para cesio y el intercambio catiónico con los cationes monovalentes similares se realiza por difusión y de manera muy lenta, ya que el radio hidratado de cesio se adapta al espacio interlaminar que tras deshidratación de la arcilla puede provocar el colapso del espacio interlaminar.

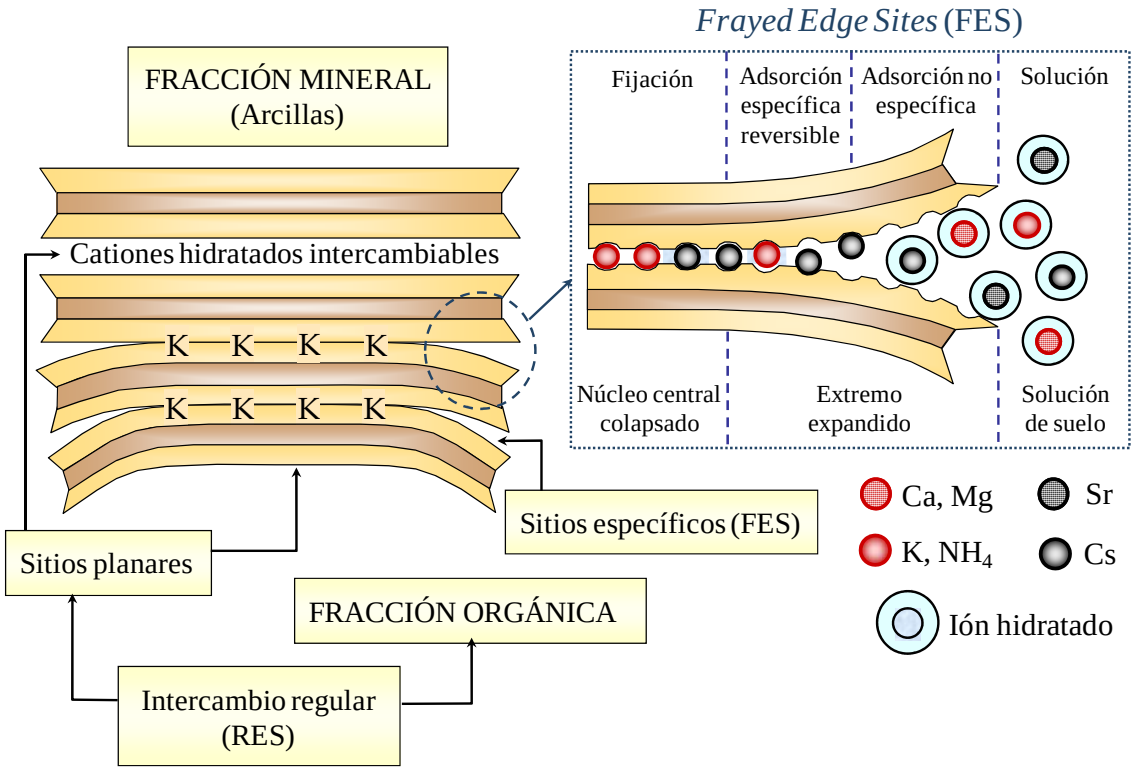

Figura 1.17. Sitios de interacción de radionucleidos con el suelo

Las diferencias de selectividad entre el radiocesio y otros cationes monovalentes homólogos, como son el K y el NH_4, son muy diversas dependiendo del sitio de sorción implicado en la interacción, lo que aconseja separar la sorción que se produce en los RES de la que tiene lugar en los FES:

$$K_d^T(Cs) = K_d^{RES}(Cs) + K_d^{FES}(Cs) \qquad \textbf{[Ec. 1.6]}$$

1.3.5.2.1. Sorción de radiocesio en los RES

En los suelos con un alto contenido en materia orgánica y con un contenido virtualmente negligible de arcillas, la sorción de radiocesio puede tener lugar en los sitios de intercambio regular (RES). En estos sitios, los coeficientes de selectividad Cs/K y Cs/NH_4 tienen valores muy próximos a la unidad (Stevenson, 1982; Sweeck et al., 1990), de manera que Cs, K y NH_4 se pueden considerar una única especie. Como la CIC es una buena estimación de la capacidad de los RES, de forma análoga a la

[Ec. 1.5], el coeficiente de distribución de radiocesio en los RES se puede expresar como:

$$K_d^{RES}(Cs) = \frac{Z_{K+NH_4}^{RES} \cdot [CIC]}{m_{K+NH_4}} \cdot K_C^{RES}(Cs/K,NH_4) \qquad \textbf{[Ec. 1.7]}$$

donde Z^{RES}_{K+NH4} expresa la proporción relativa de K y NH_4 en el los sitios de intercambio regular, m es la suma de las concentraciones de K y NH_4 en la solución de contacto y $K^{RES}_c(Cs/K,NH_4)$ es el coeficiente de selectividad RN-AN en los sitios de intercambio regular.

1.3.5.2.2. Sorción de radiocesio en los FES

La K_d (Cs) en los FES se puede definir de forma análoga a la de los RES, pero con dos diferencias sustanciales: la capacidad de los FES no es asimilable a ninguna de las propiedades edáficas que se determinan de forma rutinaria, y los K_C (Cs/K) y $K_C(Cs/NH_4)$ son diferentes en estos sitios, ya que presentan valores diferentes (lnK_C(Cs/K) entre 4,7-6,2 y $lnK_C(Cs/NH_4)$ entre 3,5-4,5), y por lo tanto hay que considerarlos de forma individual (Sweeck, 1996). Teniendo en cuenta estas consideraciones, la K_d(Cs) en los FES se puede expresar tal como se muestra en la siguiente ecuación, donde X representa los iones K y NH_4:

$$K_d^{FES}(Cs) = \frac{Z_X^{FES} \cdot [FES]}{m_X} \cdot K_C^{FES}(Cs/X) \qquad \textbf{[Ec. 1.8]}$$

De esta expresión se puede deducir que la interacción específica del radiocesio en los FES depende esencialmente de la capacidad total de los FES ([FES]), de la selectividad del Cs frente a los iones competitivos K y NH_4 (K_C (Cs/X)) y de la concentración de estos iones en los FES (Z_x^{FES}) y en la solución de suelo (m_x).

Debido al hecho de que la capacidad de los FES no se estima a partir de ningún parámetro de suelo general, una de las aproximaciones para su estimación y para el consiguiente cálculo de la K_d (Cs) está basada en la aplicación del concepto denominado Potencial de Intercepción de Radiocesio *(Radiocaesium Interception Potential, RIP*), que estima la capacidad que tiene un suelo para sorber de forma específica el radiocesio. Su cuantificación se estima en un suelo saturado homoiónicamente con alguno de los cationes competitivos ($Z_X^{FES} \rightarrow 1$), de forma que la

concentración de radiocesio se puede considerar infinitesimal y representativa de una contaminación radioactiva. En estas condiciones, la [Ec. 1.8] toma la siguiente forma:

$$\left[K_d^{FES}(Cs)\cdot m_x\right] = K_C^{FES}(Cs/X)\cdot[FES] = RIP_X \qquad \textbf{[Ec. 1.9]}$$

El protocolo más común utilizado para determinar el RIP está basado en pre-equilibrar las muestras con una solución que contiene 100 mmol/L de Ca y 0,5 mmol/L de K (m_K). Después de pre-equilibrar las muestras, estás se equilibran de nuevo con la misma solución pero esta vez marcada con radiocesio. El coeficiente de distribución sólido-líquido (K_d (Cs)) se determina por la relación de actividad de radiocesio en el sobrenadante antes y después de realizar el equilibrio (Wauters et al., 1996a).

El valor de RIP se puede determinar tanto en un escenario de K (RIP_K) como de amonio (RIP_{NH4}) (Sweeck et al., 1990). Como la presencia de amonio influye de forma diferente en la sorción de radiocesio, ya que el ión NH_4 es más competitivo que el K en la sorción de Cs en los FES (Evans et al., 1983; Comans et al., 1989), los valores obtenidos en escenario de amonio son ligeramente inferiores a los obtenidos en escenario de potasio. En términos cuantitativos, este efecto se puede expresar mediante la relación:

$$\frac{RIP_K}{RIP_{NH_4}} = \frac{\left[K_d^{FES}(Cs)\cdot m_K\right]}{\left[K_d^{FES}(Cs)\cdot m_{NH_4}\right]} = \frac{K_C^{FES}(Cs/K)\cdot[FES]}{K_C^{FES}(Cs/NH_4)\cdot[FES]} = K_C^{FES}(NH_4/K) \qquad \textbf{[Ec. 1.10]}$$

El K_C^{FES} (NH_4/K) es el coeficiente de selectividad amonio/potasio en los sitios específicos, el cual presenta un intervalo de valores que oscila entre 4 y 8 en suelos en los cuales los sitios específicos controlan la sorción de Cs de forma cuantitativa, y disminuye hasta valores entre 1 y 2 en aquellos suelos en los cuales la sorción se produce en los sitios de intercambio regular (Waters et al., 1996b; Rigol et al., 1998).

1.3.5.3. Radionucleidos del grupo NORM

Tal y como ya se ha definido en el primer capítulo, los radionucleidos primordiales también se pueden comportar como contaminantes ambientales debido al aumento de su concentración en el medio ambiente como consecuencia de actividades

antropogénicas. En este caso los radionucleidos primordiales en suelos más estudiados son el uranio (U), el radio (Ra) y el torio (Th).

1.3.5.3.1. Uranio

El uranio se puede encontrar en diferentes estados de oxidación: +3, +4, +5 y +6, siendo los estados +4 y +6 los que predominan en los suelos. El U (IV) tiene tendencia a formar fuertes uniones con la materia orgánica, llegando a formar especies insolubles. El U(VI) es el estado de oxidación más abundante. A pH 5 forma el ión uranilo UO_2^{2+}, pero a pH más alto se hidroliza de forma que puede formar hidróxidos y también carbonatos, sulfatos y fosfatos. Esta complejidad de compuestos y reacciones requiere la utilización de códigos geoquímicos y modelos de complejación para la predicción de las especies químicas existentes de uranio en función del valor de pH y de la concentración de otros aniones en la solución de suelo (Echevarria et al., 2001; Vandenhove et al., 2007a).

Como la K_d(U) está influenciada por muchos factores (pH, concentración de carbonato en la solución de suelo, contenido de Fe amorfo, mineralogía, CIC, contenido en materia orgánica), es difícil su predicción y presenta una gran variabilidad en suelos. En general, la sorción de U en los suelos es baja a pH por debajo de 3, aumenta rápidamente al pasar de 3 a 5, llegando a un máximo en el intervalo de pH de 5 a 7, y entonces decrece cuando el pH aumenta a partir de 7 (EPA, 1999).

1.3.5.3.2. Radio

El radio es un elemento alcalino que se encuentra en la naturaleza en el estado de oxidación +2. Todos los isótopos del radio (un total de 34) son radioactivos, de los cuales sólo 4 son de origen natural (^{226}Ra, ^{228}Ra, ^{224}Ra y ^{223}Ra). El Ra presenta una gran afinidad por los sitios de intercambio regular del suelo, ya que el Ra es sorbido 10 veces más en la materia orgánica que en las arcillas (Simon y Ibrahim, 1990). El Ra tiene tendencia a coprecipitar con el bario y el estroncio formando sulfatos insolubles.

En lo referente al estudio del coeficiente de distribución sólido-líquido (K_d(Ra)), no existen muchas referencias. Se suele utilizar el bario como especie análoga y se han buscado correlaciones entre la K_d(Ra) y la capacidad de intercambio catiónico o con el contenido de la materia orgánica del suelo (Vandenhove et al., 2007b).

1.3.5.3.3. Torio

El torio se encuentra en los suelos en el estado de oxidación +4. Se conocen 25 isótopos del torio con números másicos en el intervalo desde 212 a 236. Todos los isótopos del torio son inestables. El radioisótopo primordial es el ^{232}Th, con un periodo de semidesintegración de $1,4 \times 10^{10}$ años.

En función de la concentración de torio y de la solubilidad de su hidróxido, el pH del suelo afecta directamente la $K_d(Th)$, especialmente en el intervalo de pH entre 4 y 8 (Hunter et al., 1987; LaFlamme y Murray, 1987). Esta dependencia con el pH se puede explicar en parte considerando la especiación del torio en la solución de suelo, ya que en este intervalo de pH los complejos de torio son aniónicos o neutros, siendo atraídos electroestáticamente por la fase sólida, provocando en consecuencia un aumento de la $K_d(Th)$, lo que no sucedería a valores superiores de pH.

1.3.5.4. Radionucleidos pertenecientes al grupo de los metales pesados

De forma general, la sorción de los radionucleidos que, químicamente hablando, son metales pesados, viene regida por los mismos mecanismos que controlan la sorción de los isótopos estables, con la salvedad de que su concentración será inferior a la que se suele encontrar en escenarios con contaminación de metales pesados y que las K_d de los radioisótopos se moverán en los extremos superiores de los intervalos de valores válidos para los metales pesados (EPA, 1999). Así se predice que las K_d de radioisótopos de metales pesados aumentarán al aumentar el pH, y que se verá afectada por la presencia de especies aniónicas, tales como fosfatos y carbonatos, y por el contenido de materia orgánica, de óxidos de Fe/Mn y de arcilla (Gerritse et al., 1982; Rhoads et al, 1992).

1.3.5.5. Otros radionucleidos con relevancia ambiental

1.3.5.5.1. Plutonio

El plutonio se produce a partir de la fisión del combustible de uranio y es usado en la fabricación de armas nucleares. Su paso al medioambiente se ha debido principalmente a liberaciones accidentales, debido a la mala gestión de los residuos

surgidos durante la producción del combustible nuclear o de la producción y detonación de armas nucleares. Existen 15 isótopos de Pu, pero sólo 4 son de importancia ambiental debido a su abundancia o por sus largos periodos de semidesintegración: ^{238}Pu ($t_{1/2}$ = 86 años), ^{239}Pu ($t_{1/2}$ = 24400 años), ^{240}Pu ($t_{1/2}$ = 6580 años) y ^{241}Pu ($t_{1/2}$ = 13,2 años). En los intervalos de pH y las condiciones redox que se encuentran típicamente en el medioambiente, el Pu puede presentar 4 estados de oxidación: +3, +4, +5, y +6. Estos estados de oxidación vienen influenciados por factores como el pH, la presencia de agentes complejantes y/o reductores y la temperatura (EPA, 1999).

Los valores de K_d (Pu) que se encuentran en la literatura presentan valores que oscilan en un intervalo de hasta 4 órdenes de magnitud (Thibault et al., 1990). Los factores que afectan a la sorción de Pu, además del pH, son la concentración de materia orgánica disuelta en la solución de suelo, el contenido de arcillas y la concentración de carbonatos.

1.3.5.5.2. Yodo

Existen 37 isótopos del yodo, de los cuales únicamente es estable el ^{127}I, presentando diversos estados de oxidación: -1, +1, +3, +5 y +7. ^{129}I y ^{131}I son generados durante el funcionamiento de las centrales nucleares, el reprocesamiento del combustible nuclear y las pruebas de armas nucleares. Debido a su largo periodo de semidesintegración ($t_{1/2}$ = 1,57 x 10^7 años), el ^{129}I es el único isótopo del yodo que tiene interés ambiental en un medio o largo plazo después de su incorporación en el medio.

Los factores que afectan la sorción del yodo en suelos son principalmente el pH, el estado de oxidación, que marcará la especie química participante en el proceso de sorción, y el contenido de carbono orgánico del suelo (EPA, 2004).

2. OBJETIVOS Y PLAN DE TRABAJO

2.1

Objetivos

Después de producirse un episodio de contaminación radioactiva en un suelo no solamente es necesario conocer la concentración de los radionucleidos, sino que también es importante conocer su movilidad y disponibilidad, con la finalidad de predecir su impacto en el medio y el riesgo asociado. Como el tipo de interacción radionucleido-suelo marcará el comportamiento posterior de los contaminantes, es necesario una correcta cuantificación y/o estimación del coeficiente de distribución sólido-líquido (K_d) para predecir el impacto de una contaminación radioactiva en suelos. Es por esto que el objetivo general de esta tesis ha sido un estudio crítico sobre la cuantificación y la predicción del coeficiente de distribución sólido-líquido de radionucleidos en suelos.

El objetivo general de la presente Tesis Doctoral se ha desglosado en los siguientes objetivos específicos:

1. Estudio de los coeficientes de distribución de radioestroncio y radiocesio en suelos del territorio español.
2. Evaluación de los criterios adecuados para el agrupamiento de los valores de K_d en función de propiedades edáficas generales y de los factores clave que rigen la interacción-radionucleido en suelos.
3. Predicción de los valores de K_d de radioestroncio y radiocesio en suelos a partir de modelos mecanísticos y de modelos multivariantes blandos.

2.2

Plan de trabajo

2.2.1. Descripción del plan de trabajo

La mayoría de los datos referidos a los valores de K_d que se utilizan en los modelos de predicción de la movilidad de radionucleidos en sistemas de ayuda para la toma de decisiones, están construidos a partir de datos experimentales obtenidos en suelos próximos a la central nuclear de Chernóbil y en suelos pertenecientes a zonas de clima templado, los cuáles no presentan las mismas características que las que presentan los suelos del sur de Europa y, en concreto, del territorio español. Es por esto que, como primer objetivo específico de esta Tesis Doctoral, se obtuvieron los valores de los coeficientes de distribución de radioestroncio y radiocesio en suelos que presentan características edáficas representativas del territorio español, como son un mayor contenido de carbonatos y de arcillas, y un menor contenido de materia orgánica respecto a los suelos de clima templado. Se escogieron unos 30 suelos próximos a instalaciones radioactivas del territorio español, incluyendo centrales nucleares, y se obtuvieron los coeficientes de distribución de radioestroncio y radiocesio en medios con diferente composición catiónica, además de determinar propiedades edáficas generales y específicas, tales como la CIC y el Potencial de Intercepción de Radiocesio (RIP). Además se evaluó la reversibilidad de la sorción a medio y largo plazo con la aplicación de ensayos de desorción, con muestras sometidas a ciclos de secado-mojado, y finalmente se compararon los valores de K_d obtenidos con datos disponibles para suelos de climas templados.

Los resultados obtenidos en el marco del primer objetivo específico de la presente Tesis se recogieron en la siguiente publicación:

1. **Radionuclide sorption–desorption pattern in soils from Spain.**
C.J. Gil-García, A. Rigol, G. Rauret, M. Vidal.
Applied Radiation and Isotopes, 66, 126–138, 2008.
Corrigendum: *Applied Radiation and Isotopes*, 67, 367, 2009.

Los modelos de predicción del impacto de una contaminación radioactiva pueden utilizar como información de entrada datos individuales de K_d, o datos agrupados en función de unos parámetros predeterminados, que hasta la fecha suelen ser propiedades edáficas generales. La inadecuación de algunos de estos parámetros,

junto con el hecho de que los datos de K_d obtenidos proceden de la aplicación de métodos y procedimientos muy diferentes entre sí, ha provocado que las agrupaciones asocien K_d con intervalos de variabilidad de varios órdenes de magnitud, lo que repercute en la calidad de los ejercicios de predicción. Es por esto que en el segundo objetivo de esta tesis se propuso llevar a cabo un análisis crítico de la literatura y de los criterios previamente utilizados para agrupar los valores de K_d, e introducir como criterios clave para el agrupamiento aquellos factores que rigen la interacción de un radionucleido en los suelos. En este contexto, se creó una nueva base de datos de valores de K_d de radionucleidos en suelos, para un extenso número de radionucleidos, en la que, con el objeto de disminuir fuentes de variabilidad ajenas a la interacción radionucleido-suelo, se aplicaron ciertos filtros estrictos para la aceptación de datos, basados por ejemplo en excluir datos que no eran representativos de suelos contaminados (por ejemplo, se ha excluido datos con matrices ambientales diferentes de suelos), limitar la metodología utilizada para la obtención de los datos de K_d (en lo posible, a partir únicamente de experimentos en *batch*). La base de datos contempló la inclusión no sólo de datos de K_d sino también de propiedades edáficas generales y específicas de los suelos. Entre la información que se incluyó en la base de datos figuran los resultados obtenidos en el marco del objetivo anterior.

A partir de la información incluida en la base de datos, se revisaron los criterios para el agrupamiento de los valores de K_d. Primero, se aplicó el criterio basado en textura y contenido de materia orgánica, que era la aproximación utilizada hasta la fecha para agrupar los valores de K_d. Adicionalmente, y para un número alto de radionucleidos (por ejemplo, radiocesio, radioestroncio, radionucleidos del grupo de los NORM, radioisótopos de metales pesados, radioyodo, etc.), se evaluaron otros criterios para su agrupación, por medio de la inclusión de otros parámetros clave en la interacción radionucleido-suelo, tales como el pH, la CIC, el RIP y la composición catiónica de la solución de suelo. La revisión crítica y la evaluación de nuevas agrupaciones se completaron con una propuesta de los mejores valores de K_d estimados para diferentes tipos de suelo y de correlaciones entre los valores de las K_d y propiedades edáficas para cuantificar la variabilidad de los valores de K_d explicada por los parámetros elegidos.

Los resultados de estos estudios que, cómo se indicará posteriormente se realizaron en el marco de un proyecto internacional auspiciado por la IAEA, se resumieron en las siguientes publicaciones:

2. **New best estimates for radionuclide solid–liquid distribution coefficients in soils. Part 1: radiostrontium and radiocaesium.**
C. Gil-García, A. Rigol, M. Vidal
Journal of Environmental Radioactivity, 100, 690–696, 2009.

3. **New best estimates for radionuclide solid–liquid distribution coefficients in soils. Part 2. naturally occurring radionuclides.**
H. Vandenhove, C. J. Gil-García, A. Rigol, M. Vidal.
Journal of Environmental Radioactivity, 100, 697–703, 2009.

4. **New best estimates for radionuclide solid–liquid distribution coefficients in soils. Part 3: miscellany of radionuclides (Cd, Co, Ni, Zn, I, Se, Sb, Pu, Am, and others).**
C. J. Gil-García, K. Tagami, S. Uchida, A. Rigol, M. Vidal.
Journal of Environmental Radioactivity, 100, 704–715, 2009.

De los estudios anteriores realizados, se evidenció que las correlaciones entre las K_d de radioestroncio y radiocesio y ciertos parámetros escogidos podían describir un elevado porcentaje de la varianza encontrada, pero no permitían la predicción de valores individuales de K_d suficientemente satisfactorios. En este contexto se decidió llevar a cabo, en el marco del objetivo tercero de esta tesis, una serie de ejercicios de modelización para poder predecir los valores de K_d a partir de las propiedades de los suelos utilizando los datos de K_d obtenidos experimentalmente recopilados en la Publicación 1. Se aplicaron modelos mecanísticos, en los que las ecuaciones utilizadas se basaron en el conocimiento y uso de los mecanismos de interacción de radioestroncio y radiocesio en suelos, y modelos multivariantes blandos, en los que no se realizó ninguna asunción a priori de los parámetros clave para predecir los valores de K_d y se utilizaron herramientas quimiométricas robustas, tal como la Regresión por Mínimos Cuadrados Parciales (*Partial Least Squares Regression,* PLS). Las dos aproximaciones se compararon en términos de la bondad de las regresiones y de su capacidad de predicción.

Los resultados obtenidos en el marco del tercer objetivo de la Tesis dieron lugar a las dos publicaciones siguientes:

5. **The use of hard and soft modelling to predict radiostrontium solid-liquid distribution coefficient in soils.**
C. J. Gil-García, A. Rigol, M. Vidal.
Enviado a *Chemosphere* para su publicación.

6. **Comparison of mechanistic and PLS-based models to predict radiocaesium distribution coefficient in soils.**
C. J. Gil-García, A. Rigol, M. Vidal.
Enviado a *Journal of Hazardous Materials* para su publicación.

2.2.2. Participación en proyectos de investigación

El plan de trabajo de la presente Tesis Doctoral se ha realizado en el marco de diversos proyectos de investigación, tanto de ámbito nacional como internacional.

En el ámbito nacional, durante los años 2002-2005, se participó en un proyecto de investigación financiado por la Comisión Interministerial de Ciencia y Tecnología (CICYT), titulado “Herramientas para la estimación del riesgo derivado de la contaminación radioactiva de los suelos y efluentes líquidos, PPQ2002-00264”. En este proyecto, el plan de trabajo se enmarcó en la siguiente actividad: “Estudio de la movilidad de radiocesio y radioestroncio en suelos agrícolas españoles en función de sus mecanismos de interacción: estimación del riesgo y estrategias de remediación”.

A continuación, en el período 2005-2008, se participó en un proyecto de investigación financiado por el Ministerio de Educación y Ciencia, dentro del Programa Nacional de Ciencias y Tecnologías Medioambientales, titulado “Desarrollo y aplicación de métodos de laboratorio para evaluar el efecto de la incorporación de metales pesados y radionucleidos en muestras ambientales, CTM2005-03847/TECNO”. En este proyecto, el plan de trabajo de la presente Tesis se realizó en el contexto de la siguiente actividad: “Interacción de contaminantes inorgánicos en suelos agrícolas: mejora en el asesoramiento del riesgo derivado de un episodio de contaminación”.

Finalmente, en los años 2005-2006 también se participó en un proyecto de investigación financiado por la Secretaría General para la Prevención de la Contaminación y el Cambio Climático del Ministerio de Medio Ambiente, en concreto el proyecto “Aplicación y aseguramiento de la calidad de ensayos de sorción-desorción para la caracterización de suelos contaminados por metales pesados y radionucleidos, 1.2-193/2005/3-B y 240/2006/2-1.2”). En estos dos proyectos, el plan de trabajo se enmarcó en la siguiente actividad: “Desarrollo y aplicación de ensayos de sorción y desorción para la caracterización de suelos contaminados y posterior evaluación del comportamiento de metales pesados y radionucleidos en suelos, tanto en escenarios con contaminación simple como mixta”.

En el ámbito internacional, durante los años 2003-2007, se participó en el proyecto EMRAS (*Environmental Modelling for Radiation Safety*) auspiciado por la IAEA. Este proyecto fue la continuación de otros proyectos internacionales previos que se habían centrado en el campo de la modelización del comportamiento de radionucleidos en el medio ambiente. Las actividades del proyecto EMRAS se centraron en aquellas áreas en las cuales existían dudas sobre la capacidad predictiva de los modelos medioambientales, principalmente en las consecuencias de posibles liberaciones de radionucleidos en determinados sistemas (como por ejemplo, ambientes urbanos o acuáticos), en la rehabilitación de emplazamientos contaminados, así como en el comportamiento de ciertos radionucleidos, como los del grupo de los NORM.

Nuestra participación se centró en la revisión del documento de la IAEA “*Technical Report Series No. 364: Handbook of parameter values for the prediction of radionuclide transfer in temperate environments*”, publicado en 1994. Este documento se consideraba hasta la fecha la fuente de datos de referencia para la modelización de la movilidad de radionucleidos en diferentes compartimentos ambientales. Los numerosos estudios realizados con posterioridad a su edición inicial, que incluían la información disponible sobre la evolución de la contaminación causada por Chernóbil, provocó que la IAEA promoviese su revisión. En este contexto, nuestro grupo de investigación lideró la revisión del capítulo sobre la interacción de radionucleidos en suelos. Aunque no se incluye como publicación de la Tesis Doctoral, se incluye como Anexo la publicación resultante de la revisión del mencionado capítulo en forma de un documento técnico oficial de la IAEA (Vidal, 2009). Este documento se publicó de forma anticipada a la nueva edición del *Handbook* (IAEA, 2010).

3.RESULTADOS

3.1

Radionuclide sorption–desorption pattern in soils from Spain

C.J. Gil-García, A. Rigol, G. Rauret, M. Vidal.

Applied Radiation and Isotopes, 66, 126–138, 2008.

Corrigendum: *Applied Radiation and Isotopes*, 67, 367, 2009

Páginas 73-88

Available online at www.sciencedirect.com
ScienceDirect
Applied Radiation and Isotopes 66 (2008) 126–138
Applied Radiation and Isotopes
www.elsevier.com/locate/apradiso

Radionuclide sorption–desorption pattern in soils from Spain

C.J. Gil-García, A. Rigol, G. Rauret, M. Vidal*

Departament de Química Analítica, Universitat de Barcelona, Martí i Franqués 1-11, 3ª Planta, 08028 Barcelona, Spain

Received 5 September 2006; received in revised form 30 July 2007; accepted 31 July 2007

Abstract

The pattern of radiostrontium and radiocesium sorption–desorption was examined in 30 Spanish soils by the quantification of the distribution coefficients (K_d) with batch tests, the evaluation of sorption reversibility with a single extraction, the estimation of sorption dynamics by the application of drying–wetting cycles, and the calculation of $K_d^{adjusted}$ values as an input for risk assessment models. The data obtained overlapped with those found in soils from other climatic areas, suggesting identical interaction mechanisms and allowing the extrapolation of parameterisations and prediction models among different scenarios.

Keywords: Radiostrontium; Radiocesium; Soils; Sorption; Distribution coefficients; Radiocesium interception potential; Desorption; Single extraction; Aging

1. Introduction

When a radioactive contamination event occurs in soils, radionuclide mobility needs to be examined to predict the impact of the contamination and to assess the derived risk. Radionuclide transfer in the food chain is the result of a multifactorial process in which, from the soil standpoint, sorption at the solid phase and its reversibility govern the amount of radionuclide available for root uptake. Existing databases make it possible to parameterise interaction descriptors from soil characteristics (Smolders et al., 1997; Absalom et al., 1999). However, environmental decision support systems may become useless when extrapolated to conditions different from those used in their construction, because the quality of the parameterisation decreases when extrapolated to soils with different properties. Although relevant information is available for a few radionuclides in soils from temperate areas, including soils from Chernobyl-affected areas, there are gaps of data for scenarios such as those from Southern Europe, including the Mediterranean area. The potentially distinctive characteristics of the soils in this area (high carbonate and clay content; low organic matter content; dry seasons followed by potential flooding periods) justify further studies to verify conclusions and ranges of values for the most significant parameters.

The broad term of sorption includes a number of processes by means of which dissolved radionuclide ions can bind to solid surfaces. Models for the description of radionuclide sorption are still mostly based on empirical solid–liquid distribution coefficient (K_d) values. This is the ratio of the concentration of radionuclide sorbed on a specified solid, divided by its concentration in solution under steady-state conditions. The usual units of K_d are $L\,kg^{-1}$. The K_d-based model does not assume any knowledge of sorption mechanisms, nor does it contain a term to quantify the capacity and selectivity of the sorption sites or the competition with other ions to fill the sorption sites. Results from sorption tests at laboratory scale are highly operational. There are no standardised methods yet, although recommended procedures are increasingly being described (OECD, 2000; ASTM, 2001). The experimental approaches that can be applied for the estimation of solid–liquid distribution coefficient (K_d) values are various, and include methods using columns and mass transport experiments (Bachhuber et al., 1982; Dewiere et al., 2004), quantification of the in situ soil solution (Agapkina et al., 1995; Sanchez et al., 2002), or batch experiments (Elejalde et al., 2000; Tianwei et al., 2001). Batch experiments are usually conducted in a given electrolyte-background

*Corresponding author. Tel.: +34 934039276; fax: +34 934021233.
E-mail address: miquel.vidal@ub.edu (M. Vidal).

0969-8043/$ - see front matter © 2007 Elsevier Ltd. All rights reserved.
doi:10.1016/j.apradiso.2007.07.032

scenario formed by a single salt solution at various concentrations (Gutierrez and Fuentes, 1991; Twining et al., 2004). In these experiments, radionuclide sorption is altered with respect to the field situation, where sorption processes take place in the soil solution medium (Sauvé et al., 2000). This fact is especially relevant since major ions compete with radionuclides for sorption. It is thus recommended to carry out the batch sorption tests in a medium that simulates the composition of the soil solution (Yasuda et al., 1995; Camps et al., 2003). To date, a systematic comparison of all approaches and of the derived K_d values have not yet been performed. It is therefore necessary to examine the effect of changing the composition of the sorption medium on the subsequent risk assessment.

The estimation of the sorption process reversibility complements the K_d quantification. Usually, this is addressed by applying extraction tests (Wauters et al., 1994; Roig et al., 1998), an approach that makes it possible both to estimate the percentage of the radionuclide that may be remobilised when the environmental conditions change and to discuss on-going processes affecting the reversibility of the sorption, such as interaction aging (Rigol et al., 1999).

Here, we present radiostrontium and radiocesium sorption–desorption data gathered from 30 soils in areas representative of the Spanish territory, including soils from areas close to nuclear power plants and other radioactive facilities. Studies had been carried out in the past to qualitatively estimate the radiological vulnerability of Spanish soils (Trueba et al., 2000), or on radiocesium sorption in soils of specific plots (Elejalde et al., 2000). However, this is the first time that a database has been created with data on the parameter that estimates the soil capacity to specifically sorb radiocesium (the so-called radiocesium interception potential (RIP)) and the radiostrontium and radiocesium solid–liquid distribution coefficient—K_d (Sr) and K_d (Cs), respectively—for soils representative of the Spanish territory in its entirety. Two media were compared in sorption batch experiments: (1) a medium that simulated the cationic composition of the soil solution, and (2) a contact solution derived from the soil wash-off. The obtained sorption data were compared with values of sorption data gathered from the literature. Additional information about the reversibility of the sorption process, in both the short and medium term, was obtained in the target soils by applying a single extraction test and subsequent drying–wetting (DW) cycles to accelerate sorption dynamics and predict radionuclide aging at field level (Roig et al., 2006). The use of sorption and desorption data permitted the quantification of an adjusted K_d ($K_d^{adjusted}$) defined as the measured K_d corrected by the corresponding reversible fraction for the same soil quantified by the extraction yield. The comparison of the $K_d^{adjusted}$ values provided information on the relative scales of radionuclide mobility expected for the two radionuclides in the examined soils and at different times from the contamination event.

2. Material and methods

2.1. Soil samples

Thirty soil samples were collected throughout Spain, including locations close to radioactive facilities and nuclear power plants, as seen in Fig. 1. Samples were taken from the surface layer (0–5 and 0–10 cm depths), air-dried, sieved through a 2-mm mesh and homogenised with a roller table (1–5 kg in 5–10 L cylinders; shaking for 90 h) before analyses and experiments.

2.2. Analytical methods for sample characterisation

2.2.1. Main soil parameters

Main soil characteristics were determined by duplicate in all soil samples. The pH was measured in Milli-Q water, using a solution-to-soil ratio of 2.5 mL g^{-1}. The cation exchange capacity (CEC) was determined from the sum of extractable bases plus the extractable acidity obtained by displacement with $BaCl_2$–triethanolamine (TEA) solution buffered at pH 8.2 (Burt, 2004). Exchangeable K, Na, Ca, and Mg were determined from the $BaCl_2$–TEA extract, while exchangeable NH_4^+ was determined by displacement with K_2SO_4. Organic carbon (C_{org}) content was determined by elemental analysis using tin capsules and V_2O_5 as additive (ISO, 1995). Samples were pre-treated with 2 mol L^{-1} HCl before the organic carbon analysis in order to eliminate carbonates. The carbonate content was determined by using the calcimeter Bernard method (Mueller and Gastner, 1971). Particle size distribution was also determined in all soil samples by the pipet method (Burt, 2004). Mineralogical characterisation of soil samples was performed by X-ray diffraction in a Siemens D-500 $\theta/2\theta$ Bragg–Brentano powder diffractometer using Cu Kα radiation and a secondary graphite monochromator.

2.2.2. Determination of the soil solution cationic composition

The soil solution composition was determined following a method based on ultracentrifugation for the removal of the pore water, as recommended elsewhere (Adams et al., 1980; Sheppard et al., 1992). The method consisted of obtaining the soil solution by physical separation with centrifugation after determining the field capacity of the soils. Field capacity was determined by centrifuging the moist soils at 0.33 bar ($30 \times g$, 30 min, 10 °C, Beckman J2-HS centrifuge, with a rotor JA14) and drying the soils at 105 °C up to constant weight. To determine the concentration of major elements in the soil solution, soils were wetted at field capacity, left for 24 h, placed in the upper part of a cylinder with a porous plate, and subsequently centrifuged ($7\ 006 \times g$, 90 min, 10 °C). The solution separated and recovered in the base of the cylinder was then filtered through a 0.45 μm membrane, collected in polyethylene bottles, acidified and stored at 4 °C until the analysis of Ca, Mg, Na and K concentrations.

Fig. 1. Soil sampling points in Spain.

2.2.3. Determination of the radiocesium interception potential

There is a general consensus that the strong retention of cesium in geochemical substrates is controlled by the frayed edge sites (FES) of micaceous clay minerals. The characterisation of a system in terms of the number of FES and the ion selectivity pattern in these specific sites with respect to major analogues, as K (K_c(Cs/K)) allows predictions of K_d (Cs) in scenarios for which the FES are homoionically potassium saturated (Cremers et al., 1988; De Preter et al., 1991), as shown by the following equations:

$$K_c(\mathrm{Cs/K}) = \frac{Z_{\mathrm{Cs}} m_{\mathrm{K}}}{Z_{\mathrm{K}}(1) m_{\mathrm{Cs}}} = \frac{[\mathrm{Cs}]_{soil}/[\mathrm{FES}] m_{\mathrm{K}}}{m_{\mathrm{Cs}}} = \frac{K_d(\mathrm{Cs}) m_{\mathrm{K}}}{[\mathrm{FES}]}, \quad (1)$$

$$K_d(\mathrm{Cs}) = \frac{K_c(\mathrm{Cs/K})[\mathrm{FES}]}{m_{\mathrm{K}}}, \quad (2)$$

in which Z_i refers to the fractional occupancy of the species in the FES, m_i to the concentration of the species in the liquid phase (meq L^{-1}), [FES] to the capacity of the pool of frayed edge sites (meq kg^{-1}). Eq. (2) expresses the fact that K_d (Cs) equals the K_d (K) ($[\mathrm{FES}]_{\text{homoionically K saturated}}/m_{\mathrm{K}}$) amplified by some characteristic Cs/K selectivity coefficient. Following this equation, the K_d (Cs) m_{K} plateau value reached at a given potassium solution concentration can be identified with the product of [FES] and K_c(Cs/K), defined as the RIP, and expressed in meq kg^{-1} (or mmol kg^{-1}).

The RIP value was determined after pre-equilibrating the soil samples (approximately 1 g) with 50 mL of a solution containing 100 mmol L^{-1} in Ca and 0.5 mmol L^{-1} in K ($m_{\mathrm{K}} = 0.5$). After four pre-equilibrations, soils were equilibrated for 24 h with the same solution, but labelled with ^{137}Cs (CS137ELSB45, supplied by CERCA-LEA FRAMATOME). Trace radiocesium distribution coefficients (K_d) were quantified in this scenario by measuring radiocesium level in the supernatant before and after the equilibration. The calculated product K_d m_{K} defined the RIP value (Wauters et al., 1996).

2.3. Sorption–desorption experiments

2.3.1. Determination of radiocesium and radiostrontium solid–liquid distribution coefficients

The K_d (Sr) and K_d (Cs) were determined applying two batch sorption tests, differing in the composition of the contact solution.

Quantification of K_d (Sr) and K_d (Cs) in a medium simulating the soil solution: Batch sorption experiments were performed in 80 mL polypropylene centrifuge tubes, equilibrating for 16 h the soil samples (1 g) with 50 mL of a solution representing the cationic composition of the soil solution of each soil. The solutions were prepared by mixing and weighing known amounts of $CaCl_2 \cdot 2H_2O$, $Mg(NO_3)_2 \cdot 6H_2O$, NaCl, NH_4Cl, and KCl salts (Merck Pro-Analysi) to a final concentration of the cationic species equal to their concentration in soil solution for the corresponding soil (see Tables 1a and b). In order to avoid problems on the reliability of experimental determination of NH_4^+ in air-dried soils, the concentration of the NH_4^+ in the soil solution was derived from the NH_4^+ to K ratio in

Table 1a
Summary of soil characteristics

Soil sample	pH	C_{org} (%)	$CaCO_3$ (%)	CEC $cmol_c\ kg^{-1}$	Clay (%)	Sand (%)	Quartz	Calcite	Dolomite	Albite	K-Feldspar	Other
MALAGA	8.2	0.9	12	30.5	52.4	4.5	+ +	+ +	+			
TENF1	9.2	0.6	2	66.2	16.1	56.7	+			+ +	+ + +	
TENF2	6.1	2.3	2	77.8	41.2	14.0	+					iron minerals
AYUD	8.2	1.7	19	49.7	36.4	22.0	+ +	+	+	+		
CABRIL	6.4	1.4	2	21.3	21.2	61.2	+					iron minerals
BILBAO	6.8	4.1	3	43.6	22.5	45.4	+ +			+ + +	+	
VAN2	8.3	1.7	29	35.6	23.4	32.1	+ +	+ + +	+			
UIB	8.0	1.8	38	32.1	28.1	27.5	+ +	+ +	+	+	+	hematite
UPV	8.0	0.8	17	21.5	19.4	25.0	+	+	+ + +	+	+	gypsum
OVI01	4.6	9.4	3	46.3	23.6	51.7	+ + + +			+		hematite
TRILLO	8.3	1.9	43	32.4	25.7	24.4	+ +	+ +	+	+	+	
BAD2	8.3	0.6	4	26.3	27.8	46.7	+ + +			+	+	
ZORITA	8.6	1.0	40	29.1	21.9	43.3	+ +	+ +	+		+	
LEON	6.7	7.0	5	48.1	31.3	37.5	+ + + +			+	+	
GAROÑA	7.8	2.2	43	34.7	30.0	16.1	+ +	+ + +	+		+	
ASCO	8.0	0.2	38	42.8	17.2	18.9	+ +	+ +	+	+	+	gypsum
USAL	7.8	4.3	4	49.8	17.4	55.1	+ + +	+		+	+	
OVI03	5.3	7.4	2	44.6	30.6	49.3	+ + + +	+	+	+		hematite
BAD1	7.3	0.9	2	24.0	19.9	51.7	+ + + +			+	+	
GRACOR	5.4	0.8	2	30.6	20.5	36.7	+ + +			+ +		hornblende
ALM	5.9	1.6	2	23.4	10.9	56.4	+ + + +	+		+	+	
ENUSA	6.8	3.2	6	21.6	11.5	67.8	+ + + +	+		+	+	
GOLOSO	6.3	3.9	4	72.4	10.4	78.0	+ +			+ +	+ + +	
VAN1	9.2	0.3	5	27.3	6.3	86.8	+ + +	+	+	+ +	+	
ANDCOR	4.3	9.3	2	56.2	22.6	48.2	+					hornblende (major)
FONCOR	5.9	8.4	2	45.0	15.8	72.0	+ + +	+		+	+ +	
VILCOR	5.4	1.1	1	31.6	11.7	72.6	+ + +			+ +		gibsite
FROCOR	4.6	6.3	5	48.1	16.4	70.6	+ + +			+ +	+	hornblende
DELTA1	7.6	6.3	29	65.2	34.4	48.4	+ +	+ +		+	+	gypsum
DELTA2	7.9	7.7	51	89.3	43.6	15.8	+	+ +	+	+		hematite

Mineral phase predominance: + + + +, major; + + +, medium-high; + +, medium-low; +, minor.

Table 1b
Summary of soil characteristics

Soil sample	FC (%)	Exchangeable cations ($cmol_c\,kg^{-1}$)					Soil solution ($mmol\,L^{-1}$)				EC ($\mu S\,cm^{-1}$)	RIP ($mmol\,kg^{-1}$)
		Na	K	Ca	Mg	NH_4^+	Na	K	Ca	Mg		
MALAGA	43.3	0.76	2.0	12.8	3.6	0.14	0.69	0.42	0.63	1.7	327	5958 (120)
TENF1	29.4	19.6	10.2	10.2	2.8	0.17	27.2	1.5	0.35	1.2	523	6669 (422)
TENF2	42.4	1.4	1.6	12.1	14.1	0.34	8.2	0.84	6.4	4.1	477	6758 (304)
AYUD	31.7	0.33	1.0	13.7	4.4	0.14	1.3	0.98	6.8	10.3	404	4929 (355)
CABRIL	29.0	0.26	0.66	7.8	4.1	0.08	0.51	0.13	0.46	0.44	89	4852 (669)
BILBAO	30.1	0.40	1.7	15.4	1.4	0.17	0.82	0.95	0.57	3.8	220	4419 (474)
VAN2	27.2	0.71	0.76	13.4	1.1	0.19	1.9	0.13	0.59	5.5	271	4488 (111)
UIB	26.7	0.91	1.7	16.1	1.0	0.20	1.0	1.2	1.6	17.6	435	7000 (454)
UPV	19.2	1.0	0.74	9.2	0.45	0.16	0.39	0.90	0.60	17.3	2001	3213 (88)
OVI01	29.4	0.6	0.39	9.8	0.91	0.91	1.8	0.55	3.9	24.6	584	3221 (586)
TRILLO	26.6	0.12	0.79	13.8	1.7	0.11	0.18	0.96	1.6	7.6	231	2897 (205)
BAD2	22.6	0.59	0.77	9.9	1.5	0.15	1.4	0.48	1.1	6.6	235	2594 (110)
ZORITA	20.0	0.13	0.48	9.3	1.2	0.11	0.38	0.33	0.39	3.4	237	2371 (187)
LEON	32.9	0.83	0.40	24.5	2.3	0.27	2.9	0.16	4.1	26.3	580	2314 (189)
GAROÑA	32.1	0.84	1.4	11.9	1.5	0.21	0.60	2.7	3.1	18.7	486	2080 (256)
ASCO	24.2	0.44	0.84	22.7	1.6	0.12	0.69	1.0	2.5	15.8	1547	2034 (233)
USAL	33.2	0.45	1.7	12.4	3.0	0.30	0.51	1.4	1.7	5.0	318	1874 (238)
OVI03	26.3	0.67	0.40	11.9	0.94	0.72	1.7	0.43	3.2	20.4	413	1718 (94)
BAD1	17.0	0.48	0.62	5.5	1.7	0.18	2.0	0.63	2.2	4.3	297	1523 (162)
GRACOR	29.2	0.64	0.19	5.4	1.1	0.18	3.3	0.16	2.3	6.0	239	1017 (42)
ALM	21.0	0.60	0.41	4.1	0.76	0.21	0.69	0.42	0.63	1.7	283	1002 (23)
ENUSA	20.2	0.39	0.30	7.2	0.56	0.17	0.17	0.17	0.17	1.3	197	744 (76)

Table 1b (*continued*)

Soil sample	FC (%)	Exchangeable cations ($cmol_c\,kg^{-1}$)					Soil solution ($mmol\,L^{-1}$)				EC ($\mu S\,cm^{-1}$)	RIP ($mmol\,kg^{-1}$)
		Na	K	Ca	Mg	NH_4^+	Na	K	Ca	Mg		
GOLOSO	16.9	0.15	0.24	6.6	0.94	0.16	0.55	1.3	3.3	16.2	278	672 (30)
VAN1	6.2	0.77	0.34	12.5	0.93	0.15	3.4	0.34	4.6	14.0	397	660 (98)
ANDCOR	40.2	0.96	0.40	3.5	4.0	1.9	3.9	1.9	21.8	4.5	921	366 (28)
FONCOR	28.5	0.98	0.40	13.5	2.5	0.36	8.4	1.7	12.5	38.4	951	340 (24)
VILCOR	20.1	0.58	0.30	4.4	0.5	0.26	3.1	1.5	5.1	27.4	489	225 (6)
FROCOR	23.7	3.4	2.7	6.8	5.1	2.6	91.2	23.7	72.5	52.1	2300	179 (3)
DELTA1	28.9	1.9	2.9	33.9	7.2	0.16	58.2	5.6	19.9	30.6	3010	1186 (96)
DELTA2	56.1	2.2	3.5	52.0	8.6	0.06	128	2.0	20.4	43.5	3390	1463 (117)

FC: field capacity; EC: electrical conductivity; RIP: mean values (SD) for $n = 4$.

the exchangeable complex, multiplied by the K concentration in the soil solution.

After four pre-equilibrations, soils were equilibrated for 24 h with the same solution, but labelled with ^{137}Cs and ^{85}Sr (CS137ELSB45, SR85ELSB45; CERCA-LEA FRAMATOME). Trace radiocesium and radiostrontium distribution coefficients (K_d) were measured in this scenario by measuring ^{137}Cs and ^{85}Sr level in the supernatant before and after the equilibration.

Quantification of K_d (Sr) and K_d (Cs) in the soil wash-off solution: The soil wash-off solution was obtained by equilibrating soil samples in Milli-Q water ($30\,mL\,g^{-1}$), end-over-end shaking for 16 h, and subsequent centrifugation (12 880 × *g*, 30 min, 10 °C, Beckman J2-HS centrifuge, with a rotor JA14). The solution was then decanted off and stored at 4 °C in polyethylene vials before analyses. Soil samples (1 g) were shaken for 24 h with 30 mL aliquots of the wash-off solution labelled with almost carrier-free ^{137}Cs and ^{85}Sr solutions. The K_d (Cs) and K_d (Sr) values were calculated from ^{137}Cs and ^{85}Sr levels in the supernatant before and after equilibration. In parallel, aliquots of non-labelled wash-off solution were analysed for Na, Ca, Mg, K and NH_4^+ contents.

2.3.2. Estimation of radionuclide reversibly sorbed fraction

The radionuclide reversibly sorbed fraction was estimated by the application of a single extraction test to soil samples coming from the sorption step based on the use of wash-off solutions. After the sorption experiment, and before the addition of the extractant reagent for the desorption test the soil sample was submitted to one or 20 DW cycles. As the soil was dried, it incorporated the radionuclide present in the contact solution that was not possible to separate from the soil by centrifugation. Therefore, the desorption experiment was initiated considering the weight and radionuclide activity concentration of the soil at that moment. The application of one drying step to the soil sample simulated the situation immediately after the contamination event (short term), whereas the application of 20 DW cycles was representative of the situation few years after the contamination event (medium term).

DW cycles consisted of rewetting the soil residues at field capacity, maintaining them in closed vessels at 40 °C for 48 h, and then drying them in open vessels at 40 °C for 48 h. After a given number of cycles, the soils were submitted to a single extraction with 30 mL of NH_4Cl $1\,mol\,L^{-1}$, and soil suspensions were end-over-end shaken for 16 h at room temperature. After shaking, suspensions were centrifuged (3000 × g, 15 min) (Hettich Universal 30F, with a rotor E1174). The supernatants were collected in polyethylene bottles and stored at 4 °C until analysis.

2.4. Analytical measurements

Ca, Mg, K, and Na in wash-off and soil solutions were determined by inductively coupled plasma atomic emission spectroscopy (ICP-AES, Thermo-Jarrell Ash 25 and Perkin Elmer Optima 3200 RL). The following emission lines were used (nm): Ca: 315.887 and 317.933; Mg: 279.077 and 285.213; K: 766.490; Na: 330.237. NH_4^+ was determined in the wash-off solutions by UV–Vis (Unicam Helios Gamma) by colorimetric method based on the salicylate reaction (Krom, 1980). The ^{137}Cs and ^{85}Sr activity was measured in samples derived from the sorption–desorption experiments in 20 mL capacity polyethylene vials using a solid scintillation detector (PACKARD MINAXI 5000 Series), equipped with a 3-inch NaI (Tl activated) crystal, using a mathematical correction for the ^{137}Cs contribution in the ^{85}Sr channels. Measurement time was set to obtain RSD < 0.5%.

2.5. Exploratory analyses

The comparison of the K_d (Sr) and K_d (Cs) was carried out at two levels: comparison of the ranges of values obtained using the two experimental procedures, and comparison of the whole data set obtained for the Spanish soils with available data in the literature for soils of other climatic zones. Soil properties such as CEC, organic matter content, clay content and soil solution composition were considered for grouping the soils and establishing ranges of values for K_d. These parameters were selected since they are commonly used for soil characterisation and/or a suitable

number of data was available in the literature to do the exploratory analyses. pH was not used for the comparison because, in most cases, its value does not correspond to the real pH value of the soil, but to the value applied for the experimental conditions used for K_d determination. Carbonate content was neither considered since a few data were available in the literature.

The multiple sample comparisons were based on the construction and interpretation of box-and-whisker plots using Statgraphics Plus 5.1 (StatPoint INC., Virginia, EUA), a software package useful for exploratory data analysis.

2.6. Quality control

Intermediate activity solutions of ^{85}Sr and ^{137}Cs were prepared by diluting weighed amounts of commercial solutions with deionised water, and used as internal controls for measurements with the PACKARD MINAXI 5000 Series instrument. Additionally, blank experiments without soil sample but applying the same procedures for the sorption and extraction tests were carried out in parallel for each set of analysis.

Table 2
Radiostrontium and radiocesium distribution coefficient values ($L\,kg^{-1}$; mean values (SD); $n = 4$)

Soil sample	K_d (Sr)		K_d (Cs)	
	Soil solution	Wash-off	Soil solution	Wash-off
MALAGA	61 (1)	218 (9)	14616 (923)	34945 (4674)
TENF1	110 (1)	1764 (249)	9174 (663)	6679 (358)
TENF2	29 (2)	747 (129)	4720 (82)	6586 (1083)
AYUD	9 (1)	145 (7)	3313 (23)	12197 (254)
CABRIL	97 (1)	569 (29)	1943 (1292)	7016 (2292)
BILBAO	30 (1)	442 (20)	5829 (84)	9531 (419)
VAN2	25 (1)	249 (8)	6789 (202)	23878 (3446)
UIB	9 (1)	232 (4)	2422 (48)	20498 (1571)
UPV	3 (1)	11 (1)	1569 (25)	12540 (1824)
OVI01	5 (1)	162 (9)	754 (8)	5746 (380)
TRILLO	9 (1)	143 (2)	2230 (663)	11123 (1012)
BAD2	12 (1)	176 (7)	2373 (2)	13386 (1316)
ZORITA	12 (5)	95 (4)	3220 (68)	13167 (1117)
LEON	9 (1)	260 (12)	3252 (138)	10617 (660)
GAROÑA	5 (1)	111 (2)	887 (19)	8025 (347)
ASCO	3 (1)	14 (1)	1195 (99)	5792 (675)
USAL	27 (1)	209 (3)	2752 (477)	6659 (580)
OVI03	6 (1)	212 (6)	1017 (4)	5795 (1158)
BAD1	10 (1)	114 (6)	1419 (40)	6695 (531)
GRACOR	8 (1)	164 (30)	1206 (52)	4154 (1398)
ALM	14 (1)	249 (7)	1053 (10)	3024 (1010)
ENUSA	39 (2)	294 (10)	1776 (6)	2125 (327)
GOLOSO	5 (1)	241 (22)	139 (9)	1860 (251)
VAN1	4 (1)	106 (6)	1132 (35)	4859 (1196)
ANDCOR	7 (1)	228 (34)	39 (1)	628 (43)
FONCOR	4 (1)	199 (10)	115 (1)	1325 (177)
VILCOR	2 (1)	81 (2)	75 (2)	1358 (227)
FROCOR	1 (1)	77 (3)	10 (1)	153 (6)
DELTA1	8 (1)	91 (4)	202 (10)	2656 (159)
DELTA2	9 (1)	269 (4)	627 (1)	3083 (261)

Table 3
Concentration of major elements in the wash-off solution ($mmol\,L^{-1}$)

Soil sample	Na	K	Mg	Ca	NH_4^+
MALAGA	0.20	0.18	0.07	0.29	0.02
TENF1	1.9	0.11	0.02	0.01	0.03
TENF2	0.40	0.10	0.11	0.09	0.05
AYUD	0.04	0.10	0.16	0.34	0.03
CABRIL	0.17	0.03	0.03	0.03	0.02
BILBAO	n.d.	0.12	0.03	0.18	0.04
VAN2	0.04	0.04	0.03	0.38	0.02
UIB	0.26	0.12	0.03	0.46	0.03
UPV	0.03	0.10	0.04	6.6	0.03
OVI01	0.12	0.05	0.07	0.56	0.21
TRILLO	0.07	0.10	0.05	0.30	0.05
BAD2	0.10	0.07	0.04	0.27	0.03
ZORITA	0.17	0.08	0.02	0.37	0.02
LEON	0.02	0.03	0.11	0.76	0.06
GAROÑA	0.11	0.10	0.12	3.0	0.06
ASCO	n.d.	0.18	0.06	0.47	0.03
USAL	0.05	0.16	0.11	0.41	0.07
OVI03	0.11	0.04	0.07	0.48	0.12
BAD1	0.08	0.06	0.10	0.22	0.03
GRACOR	0.26	0.03	0.04	0.11	0.03
ALM	0.04	0.04	0.01	0.04	0.03
ENUSA	0.06	0.02	0.01	0.10	0.02
GOLOSO	n.d.	0.06	0.03	0.14	0.04
VAN1	0.21	0.02	0.03	0.28	0.02
ANDCOR	0.13	0.08	0.31	0.08	0.46
FONCOR	0.20	0.07	0.18	0.56	0.07
VILCOR	n.d.	0.06	0.04	0.27	0.04
FROCOR	0.99	0.35	0.56	0.43	0.96
DELTA1	1.1	0.23	0.76	2.7	0.06
DELTA2	3.6	0.12	0.47	1.2	0.05

Mean value; $n = 3$; n.d.: not detected.

3. Results and discussion

3.1. Characteristics of studied soils

Tables 1a and b summarises the main soil characteristics of the soils examined in this work. All soils studied here could be considered as mineral soils, with a maximum C_{org} content lower than 10%. Main soil parameters had wide ranges of variation, with the upper values within the highest found in the literature in studies dealing with soil–radionuclide interaction: pH values ranged from 4.3 to 9.2; CEC from 21.3–89.3 $cmol_c\,kg^{-1}$; $CaCO_3$ from 1 to over 51%, with a few soils having $CaCO_3$ contents higher than 20%. Most soils belonged to the loam textural class, and only a few could be grouped within the sandy (VAN1 soil) and clay categories (MALAGA, TENF2, and DELTA2 soils), according to the USDA criteria. The qualitative description of soil mineralogy indicated the predominance of quartz in most samples. Calcite and albite were found in relatively high amounts in many soils, whereas dolomite, microcline, and horblende only for a few of them. Moreover, both texture and mineralogical analysis showed a high percentage of clay in most soil samples, the two experimental approaches giving coincident values for each soil. Therefore, the fact that some soils have pH >8 and

$CaCO_3$ content $>25\%$, that all soils have clay content $>10\%$ and most of them $\geqslant 20\%$, and that there is a lack of organic matter soils in the Spanish territory, confirms their distinctive values of soil properties with respect to soils from temperate areas.

Although Na status in the exchangeable complex or in the soil solution is not usually considered in most studies with Sr and Cs radionuclides, here some soils had high concentrations of this element due to either a dry hydric regime or for being close to marshlands. In some soils, Na was the predominant cation in the exchangeable complex (see TENF1 soil) and in the soil solution (see TENF1, TENF2, FROCOR, DELTA1, and DELTA2 soils). A parameter deserving special attention is the RIP, which estimates the capacity of a soil to specifically sorb radiocesium (Sweeck et al., 1990). Here the RIP values ranged from 179 mmol kg^{-1} in the FROCOR soil to 7000 mmol kg^{-1} in the UIB soil. This range of values was of a similar order of magnitude to those reported in the literature, for instance, by Sweeck et al. (1990), with a range of values of 67–4890 mmol kg^{-1} ($n = 12$), by Valcke (1993), with a range of 7–3180 mmol kg^{-1} ($n = 32$), with an outstanding soil having an RIP value of 9199 mmol kg^{-1}, or by Sanchez et al. (2002), with a range of values derived from analysing 51 soils of 5–6545 mmol kg^{-1}. The high RIP values within the soils examined here, with values higher than 5000 mmol kg^{-1} for a few soils, confirmed that in these soils there was a significant number of specific sites governing radiocesium sorption, but the range of values obtained here cannot be considered as outstandingly higher than others obtained in soils from areas of Western Europe, although it is higher than ranges derived from soils of the Chernobyl area (Vidal et al., 1995; Camps et al., 2004).

3.2. Influence of the composition of the contact solution on the quantification of the radionuclide distribution coefficient

Table 2 shows the values obtained for K_d (Sr) and K_d (Cs) in all soils and applying the two experimental conditions. The values derived from the use of the wash-off solution were higher than those from the contact solution based on the soil solution cationic composition. This fact is consistent with the differences in the concentration of Ca and Mg in the two contact solutions, which affect K_d (Sr), and of K and NH_4^+, which in turn affect K_d (Cs). Thus, in general, Ca + Mg, K and NH_4^+ concentrations were higher in the soil solution than in the wash-off solution, as can be noticed by comparing data in Tables 1 and 3, thus leading to the quantification of lower K_d values. The $\log K_d$ (Sr) derived from the application of the two procedures were well correlated (Pearson coefficient of $r = 0.71$), while the log of the sum of Ca + Mg concentrations in the wash-off and soil solutions were also correlated ($r = 0.71$). Similarly, the $\log K_d$ (Cs) derived from the application of the two procedures were strongly correlated (Pearson coefficient of 0.87), in a similar way as the log of K concentrations in both solutions ($r = 0.79$), thus confirming that changes in the K_d (Cs) could also be mostly attributed to the changes in the composition of the contact solution. Both batch procedures were intended to simulate the scenario in which sorption takes place at field level, although the two are partially biased by the fact that batch tests use higher volume-to-mass ratios than at field, due to the difficulty of calculating the K_d values at the actual soil solution ratios. When the contact solution has the same cationic composition as the soil solution, the sorption takes place in the same cationic scenario as at field, but the various pre-equilibrations and the high load of major cations due to the high volume-to-mass ratios may lead to an increase in the levels of major cations in the exchangeable complex. On the contrary, the procedure based on the wash-off solution involves a dilution of the actual soil solution, although secondary effects on the exchangeable complex are expected to be lower.

3.3. Categorisation of K_d values with respect to soil parameters and comparison with data in the literature

Comparison of K_d (Sr) and K_d (Cs) values was carried out taking into account, on the one hand, the two experimental procedures used to determine K_d for the soils of the Spanish territory and, on the other, the values of K_d that can be found in the literature, which basically correspond to soils from temperate zones. For these comparisons several criteria of grouping soils were used based on some soil characteristics. Figs. 2–4 show the percentile distributions (box-and-whisker plots), including median and geometric means, for K_d (Sr) and K_d (Cs) values grouped according to ranges of values of CEC, OM content, clay content and soil solution composition.

As shown before, with respect to the comparison of the two experimental procedures, the use of a soil wash-off solution always led to higher values of K_d than simulating the cationic composition of the soil solution. However, a similar pattern for the K_d values was observed regardless the soil property used for classification, suggesting that the two procedures provide equivalent relative information. A problem derived from the application of different protocols to determine the K_d (composition of the contact solution, solid/liquid ratio, etc.) is an increase in the variability of the range of values of this parameter for a given group of soils with similar characteristics, this being a limitation to select an estimate for K_d to be used in models implemented in decision support systems. In contrast, when the same experimental procedure was used the variability of K_d values decreased substantially, the remaining variability being attributed to the existing differences among soils within the group. Then, a harmonisation of experimental procedures to determine K_d values is strongly recommended.

The K_d obtained for the Spanish soils can also be compared with available data in the literature. The IAEA TRS-364 has been considered to date as a handbook of

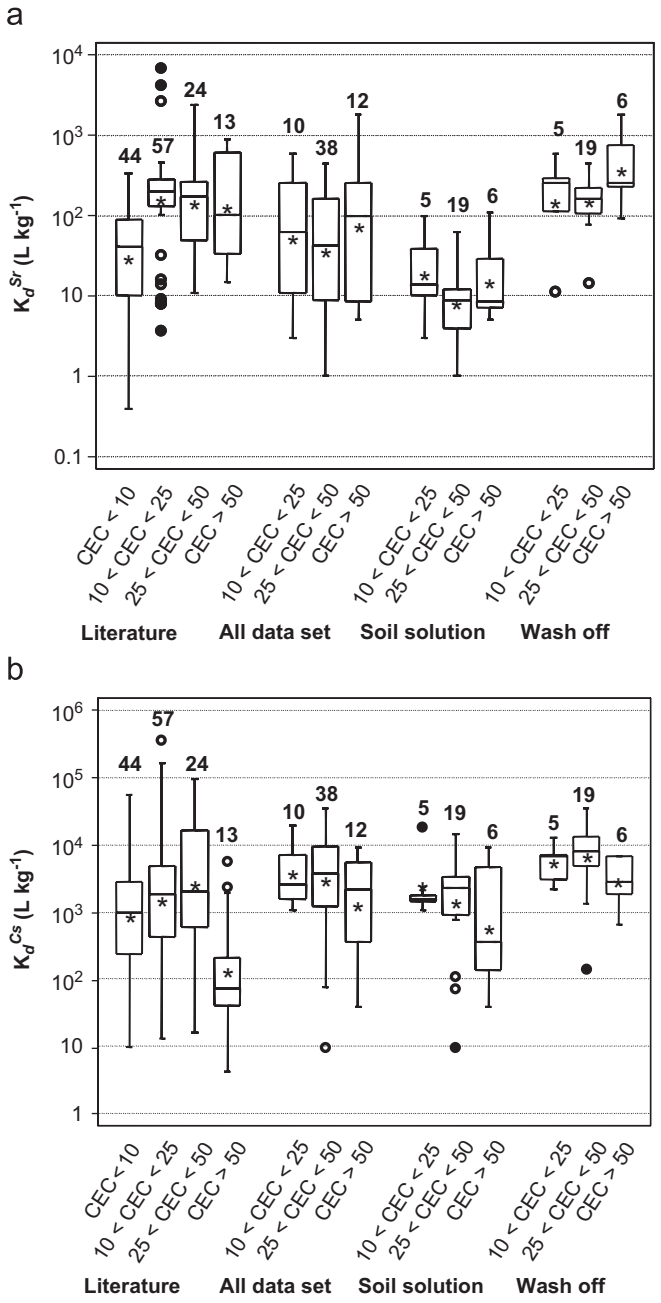

Fig. 2. Box-and-whisker plots of (a) K_d (Sr) and (b) K_d (Cs), grouped according to ranges of values of CEC (cmol$_c$ kg^{-1}). The box encloses the middle 50%, and the median is represented as a horizontal line inside the box. Vertical lines extend to the point within 1.5 interquartile ranges. Other symbols represent geometrical mean (*) and points at >1.5 (○) and >3 (●) interquartile ranges.

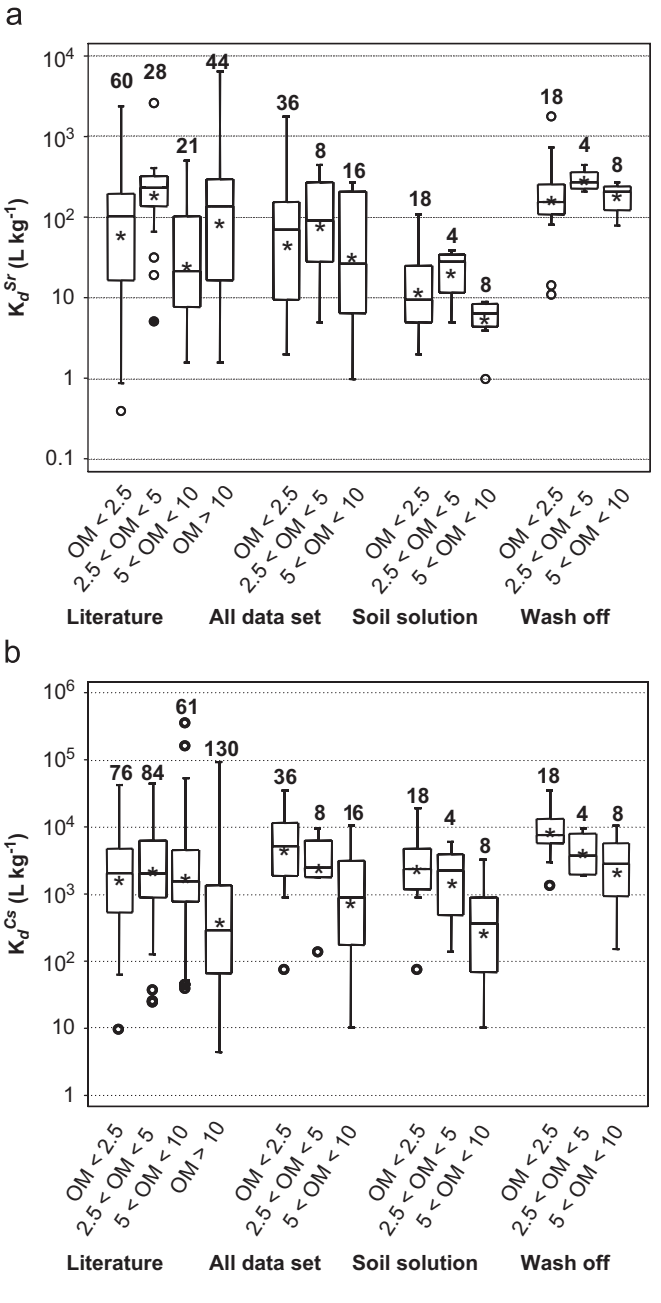

Fig. 3. Box-and-whisker plots of (a) K_d (Sr) and (b) K_d (Cs), grouped according to ranges of values of OM percentage. The box encloses the middle 50%, and the median is represented as a horizontal line inside the box. Vertical lines extend to the point within 1.5 interquartile ranges. Other symbols represent geometrical mean (*) and points at >1.5 (○) and >3 (●) interquartile ranges.

reference for radionuclide K_d (IAEA, 1994), but much work has been carried out recently that makes it possible to improve the ranges of K_d values (Gutierrez and Fuentes, 1991; Agapkina et al., 1995; Vidal et al., 1995; Yasuda et al., 1995; Rauret and Firsakova, 1996; Roca et al., 1997; Mollah and Ullah, 1998; EPA, 1999; Elejalde et al., 2000; Sokolik et al., 2001; Tianwei et al., 2001; Sanchez et al., 2002; Camps et al., 2003; Camps et al., 2004; Dewiere et al., 2004; Twining et al., 2004). An overall data set including the K_d values obtained from the two experimental procedures was considered for the soils of the Spanish territory to facilitate comparison with literature data. For this latter data set soils with OM content >10% and CEC <10 cmol$_c$ kg^{-1} were not available for comparison. When comparing the population created by the overall K_d (Sr) and K_d (Cs) data sets, the percentiles were similar to those from the recent literature, for all the soil grouping criteria

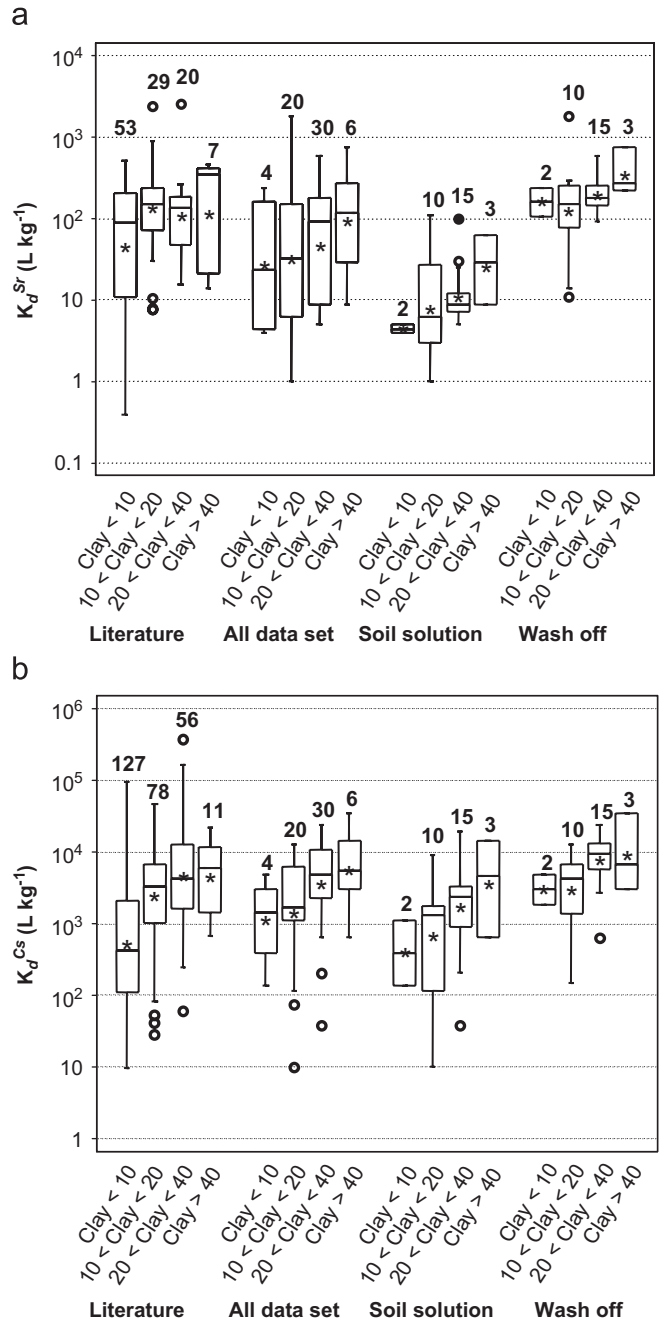

Fig. 4. Box-and-whisker plots of (a) K_d (Sr) and (b) K_d (Cs), grouped according to ranges of values of clay percentage. The box encloses the middle 50%, and the median is represented as a horizontal line inside the box. Vertical lines extend to the point within 1.5 interquartile ranges. Other symbols represent geometrical mean (*) and points at >1.5 (○) and >3 (●) interquartile ranges.

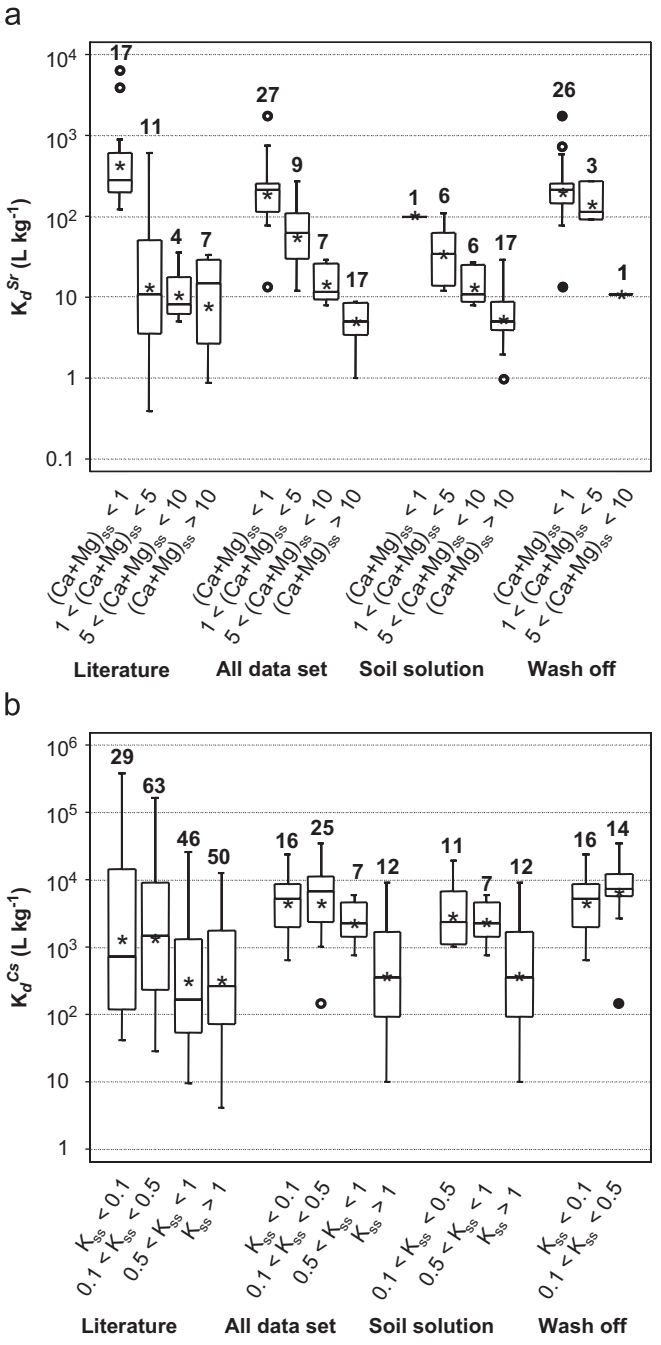

Fig. 5. Box-and-whisker plots of (a) K_d (Sr) and (b) K_d (Cs), grouped according to ranges of values of Ca + Mg and K concentrations in soil solution (mmol L^{-1}), respectively. The box encloses the middle 50%, and the median is represented as a horizontal line inside the box. Vertical lines extend to the point within 1.5 interquartile ranges. Other symbols represent geometrical mean (*) and points at >1.5 (○) and >3 (●) interquartile ranges.

considered. Hence, it can be concluded that, in general, the ranges of the K_d values for all the soils examined in this work agreed with the K_d ranges from soils originating from other environmental scenarios and, therefore, prediction models in decision support systems might be extrapolated from one scenario to another with contrasting environmental conditions.

The box-and-whisker plots also allowed evaluating the dependence of the ranges of K_d values on the different soil parameters considered. Figs. 2 and 3 show that no tendency in the K_d value was observed when increasing the CEC or OM content of the soils, except for the K_d (Cs) in Spanish soils, which decreased when increasing OM. However, this tendency can be related rather to an increase

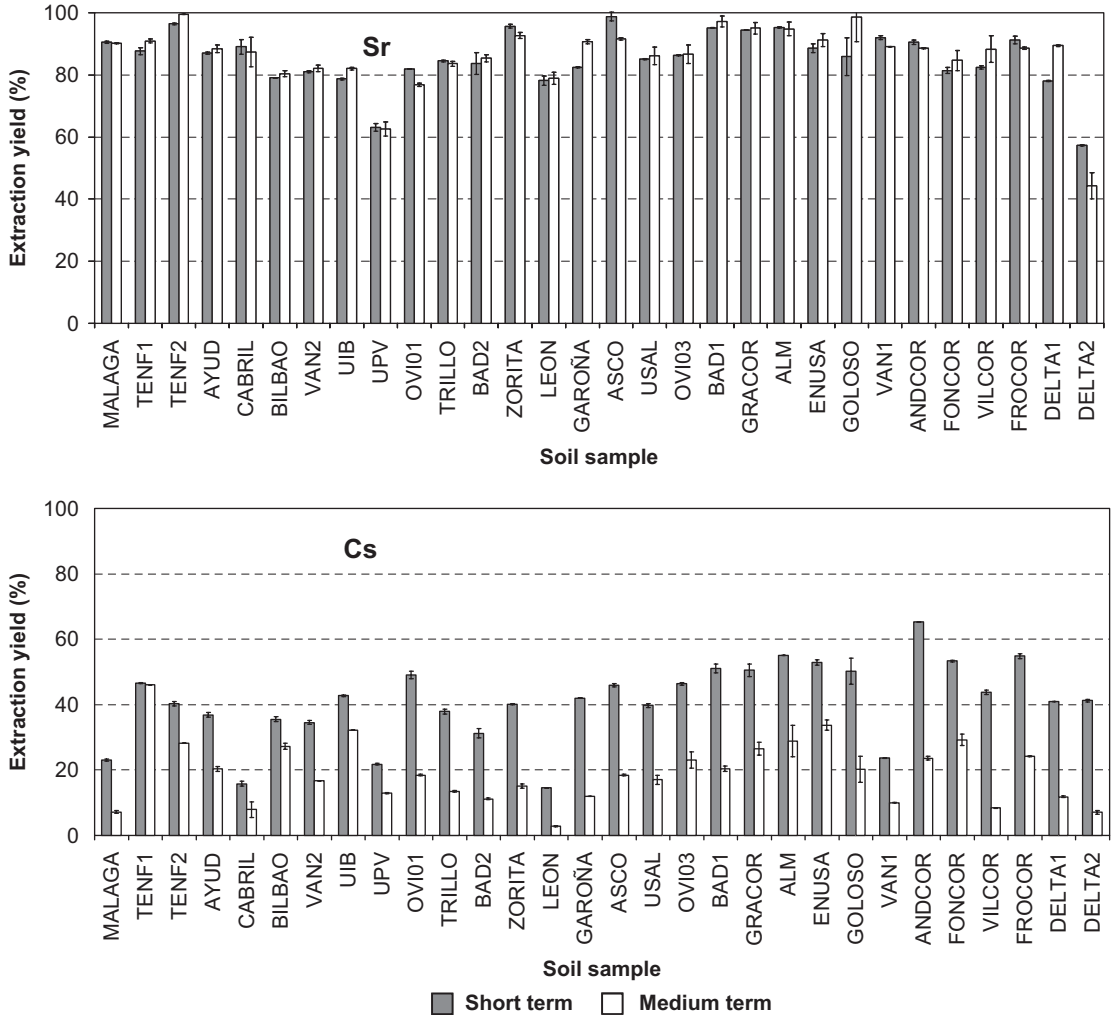

Fig. 6. Radiostrontium and radiocesium extraction yields of soils submitted to 1 (short term) and 20 (medium term) drying–wetting cycles. Error bars indicate one standard deviation.

Table 4
Ranges of radiostrontium and radiocesium $K_d^{adjusted}$ values ($L\,kg^{-1}$)

	Short term				Medium term			
	Sr		Cs		Sr		Cs	
	$K_d^{adjusted}$	n	$K_d^{adjusted}$	n	$K_d^{adjusted}$	n	$K_d^{adjusted}$	n
Minimum	15		280		15		635	
Maximum	2010		151 670		1940		488 060	
Median	245		15 335		240		33 870	
	$<10^2$	5	$<10^2$	0	$<10^2$	4	$<10^2$	0
	10^2–10^3	24	10^2–10^3	2	10^2–10^3	25	10^2–10^3	1
	10^3–10^4	1	10^3–10^4	8	10^3–10^4	1	10^3–10^4	4
	10^4–10^5	0	10^4–10^5	19	10^4–10^5	0	10^4–10^5	21
	$>10^5$	0	$>10^5$	1	$>10^5$	0	$>10^5$	4

in the clay content (see Fig. 4), than to a decrease in OM (Staunton, 1994; Absalom et al., 1995; Rigol et al., 1998). Apart from clay for the K_d (Cs), the only soil parameter that had an effect on K_d values, in both literature and Spanish data sets, was the soil solution composition, (Ca + Mg) for radiostrontium, and K for radiocesium, as observed in Fig. 5. These cationic species are the main competing major ions of radiostrontium and radiocesium, respectively, and a high concentration of them in soil solution may contribute to a decrease in K_d.

3.4. Estimation of radionuclide sorption reversibility

The reversibility of the sorption process was estimated from the quantification of the radionuclide extractability. Fig. 6 shows the radiostrontium and radiocesium extraction yields obtained from soil samples originated from the sorption experiments, and submitted to DW cycles. The short-term scenario was defined by those soils submitted to 1 DW cycle, while those submitted to 20 DW cycles defined the medium-term scenario.

Regarding the short-term data, and as described elsewhere, radiostrontium yields were systematically higher than those of radiocesium for all soils (Valcke, 1993; Roig et al., 1998). Radiostrontium extraction yields in the short-

term ranged from 98.8% in the ASCO soil to 57.3% in the DELTA2 soil, while for radiocesium the range was between 65.3% for the ANDCOR soil and 14.6% for the LEON soil. The correlation between the K_d values from the wash-off procedure and extraction yields was non-significant for radiostrontium, while for radiocesium it was very weak (Pearson coefficient of 0.54), confirming that the reversibility of the sorption cannot be predicted from sorption data, and suggesting that both parameters have to be quantified for a better prediction of the impact of a contamination event.

As deduced from the extraction yields of samples submitted to 20 DW cycles, aging was not a relevant process for radiostrontium in the examined soils, since the extraction yields were not statistically lower than those obtained after the application of 1 DW cycle. On the contrary, the reversibility of radiocesium sorption decreased in the medium-term, as deduced by the significant decrease in radiocesium extraction yields in all soils, with the exception of the TENF1 soil. Decreases averaged 2.4-fold, with a maximum decrease of 5.2-fold for the LEON soil. The correlation between the K_d (Cs) values and extraction yields in the medium-term was even worse than in the short-term (Pearson coefficient of 0.24), thus indicating that not only the initial sorption reversibility but also the sorption dynamics cannot be explained or predicted from sorption data.

3.5. Risk assessment from sorption–desorption data

From the individual quantification of the K_d and the estimation of the sorption reversibility with the single extraction procedure, a $K_d^{adjusted}$ was calculated for all the scenarios studied as the ratio of the K_d versus the extraction yield. The $K_d^{adjusted}$ concept is similar to a total K_d calculated by correcting the reversible K_d by the available pool of radionuclide participating in the solid phase–soil solution equilibria (Hilton and Comans, 2001). The comparison of $K_d^{adjusted}$ values permitted the establishment of relative scales of expected mobility for the target radionuclides in the different soils considered here, both in the short and in the medium term after the radioactive release. Thus, the higher the K_d and the lower the extraction yield, the higher the retention capacity of the soil towards a given radionuclide, and thus the lower the expected mobility and derived risk.

The calculated $K_d^{adjusted}$ values are summarised in Table 4. As in the previous section, only the K_d values derived from the wash-off solution procedure were used in the calculations. The results are organised as ranges of values, indicating the minimum, maximum and median values, and the number of soils within each range. It is important to highlight how the pattern of sorption differed from that of reversibility, thus justifying the making of predictions on the impact of a contamination event on the basis of the $K_d^{adjusted}$ values. As an example to illustrate this, while the UPV soil had the lowest K_d (Sr) among the soils tested, its desorption yield was the second lowest, while the opposite was observed for the TENF2, with the second largest K_d (Sr), but also the second highest desorption yield. For this radionuclide, and as aging was not a relevant process, the values of the $K_d^{adjusted}$(Sr) did not significantly change with time (only the $K_d^{adjusted}$(Sr) of the ZORITA soil shifted to a higher range of values). Moreover, as the values of reversibility were reasonably high for all the soils, the $K_d^{adjusted}$(Sr) depended mostly on the values of the K_d (Sr). Hence, the prediction on the impact of a radiostrontium release to these soils does not require considering significant changes with time due to the low significance of radiostrontium sorption dynamics.

As would be expected from the higher K_d (Cs) and lower desorption yield values, the $K_d^{adjusted}$(Cs) was much higher than the $K_d^{adjusted}$(Sr), in general, by around two orders of magnitude. As shown for radiostrontium, the calculation of the $K_d^{adjusted}$(Cs) was justified by the different sorption–desorption patterns observed among the soils examined. A few examples may illustrate this statement. For instance, the ALM and DELTA2 soils had almost identical K_d (Cs), but their extraction yields in the medium term differed by a factor of 4, while the UIB soil had the third highest K_d (Cs), but also the third highest extraction yield. This caused the sequence of soils with increased $K_d^{adjusted}$(Cs) to differ from those with increased K_d (Cs). Moreover, the sequences of soils also differed when considering short- or medium-term predictions (details not shown here). Therefore, for this radionuclide, the dynamics aspects of its interaction must be taken into account when assessing the risk derived from a contamination event.

It is difficult to compare the $K_d^{adjusted}$ values obtained here with values from soils of other areas, due to the different experimental conditions used in calculating the K_d and sorption reversibility. Taking into account this limitation, the $K_d^{adjusted}$(Sr) of soils of the Chernobyl area were one order of magnitude lower than the $K_d^{adjusted}$(Sr) of the soils examined in the present work (Vidal et al., 1995), while the differences for the $K_d^{adjusted}$(Cs) were of two orders of magnitude (Vidal et al., 1995; Rigol et al., 1999; Camps et al., 2003). The main reason for this is the low clay content in the soils of the Chernobyl-affected area, since they were mostly podzols and organic soils.

4. Conclusions

The examination in terms of sorption (RIP; distribution coefficient) and desorption (sorption reversibility) of radiostrontium and radiocesium in a high number of soils in Spain confirmed that the data obtained overlapped with the ranges of values found in soils from other climatic areas. The examination described here also confirmed that risk assessment exercises based on the use of mechanistic models to predict sorption–desorption data could be easily extrapolated from a scenario to another of contrasting characteristics.

When the sorption data are not described from mechanistic models but quantified from batch experiments, experimental conditions for the laboratory tests must be carefully selected to predict behaviour and to compare environmental scenarios, since these factors have a significant effect on the eventual predicted risk. Thus, the batch protocols must simulate field scenarios. In the present study it is difficult to choose between soil solution and soil wash-off solution media. Probably, an intermediate situation such as a soil wash-off solution using a lower liquid–solid ratio that ensured a reasonable concentration of cationic species in solution, would be the most appropriate.

Regardless of the fact that the initial retention capacity of a soil can be high for a given radionuclide, as was the case here for radiocaesium for most mineral soils, if the aging process is shown to be relevant, it is advisable to design dynamic environmental decision-support systems to better assess the medium-term situation after a contamination event and to evaluate the significance of natural attenuation.

Acknowledgements

This research was funded by the Spanish Government (CICYT, contract PPQ2002-00264). C. J. Gil-García acknowledges the Ministerio de Educación, Cultura y Deporte for a PhD fellowship. The authors thank Universidad de Salamanca, Universidad Politécnica de Valencia, Universidad de Oviedo, Universidad de Extremadura, Universidad de León, Universitat de les Illes Balears, ENRESA, ENUSA, SCAR (Generalitat de Catalunya), Universidade da Coruña and Universidad de Málaga for the soil samples supplied. The authors also thank Dr. A. Sahuquillo for the use of MATCONTROL facilities to prepare the samples.

References

Absalom, J.P., Young, S.D., Crout, N.M.J., 1995. Radio-cesium fixation dynamics: measurement in six Cumbrian soils. Eur. J. Soil Sci. 46 (3), 461–469.

Absalom, J.P., Young, S.D., Crout, N.M.J., Nisbet, A.F., Woodman, R.F.M., Smolders, E., Gillett, A.G., 1999. Predicting soil to plant transfer of radiocesium using soil characteristics. Environ. Sci. Technol. 33 (8), 1218–1223.

Adams, F., Burmester, C., Hue, N.V., Long, F.L., 1980. A comparison of column-displacement and centrifuge methods for obtaining soil solutions. Soil Sci. Soc. Am. J. 44, 733–735.

Agapkina, G.I., Tikhomirov, F.A., Shcheglov, A.I., Kracke, W., Bunzl, K., 1995. Association of Chernobyl derived ^{239,240}Pu, ^{241}Am, ^{90}Sr and ^{137}Cs with organic matter in the soil solution. J. Environ. Radioact. 29 (3), 257–269.

ASTM, 2001. ASTM D4319-93, Standard test method for distribution ratios by the short-term batch method.

Bachhuber, H., Bunzl, K., Schimmack, W., 1982. The migration of ^{137}Cs and ^{90}Sr in multilayered soils: results from batch, column and fallout investigations. Nucl. Technol. 59, 291–301.

Burt, R. (Ed.), 2004. Soil survey laboratory methods manual. Investigations Report No 42, Version 4.0, Natural Resources Conservation Service, USDA, Washington.

Camps, M., Rigol, A., Vidal, M., Rauret, G., 2003. Assessment of the suitability of soil amendments to reduce ^{137}Cs and ^{90}Sr root uptake in meadows. Environ. Sci. Technol. 37, 2820–2828.

Camps, M., Rigol, A., Hillier, S., Vidal, M., Rauret, G., 2004. Quantitative assessment of the effects of agricultural practices designed to reduce ^{137}Cs and ^{90}Sr soil–plant transfer in meadows. Sci. Total Environ. 332, 23–38.

Cremers, A., Elsen, A., De Preter, P., Maes, A., 1988. Quantitative analysis of radiocesium retention in soils. Nature 335, 247–249.

De Preter, P., Van Loon, L., Maes, A., Cremers, A., 1991. Solid/liquid distribution of radiocesium in Boom clay. A quantitative interpretation. Radiochim. Acta 52–53, 299–302.

Dewiere, L., Bugai, D., Grenier, C., Kashparov, V., Ahamdach, N., 2004. ^{90}Sr migration to the geo-sphere from a waste burial in the Chernobyl exclusion zone. J. Environ. Radioact. 74 (1–3), 139–150.

Elejalde, C., Herranz, M., Legarda, F., Romero, F., 2000. Determination and analysis of distribution coefficients of ^{137}Cs in soils from Biscay (Spain). Environ. Pollut. 110 (1), 157–164.

EPA, 1999. Understanding variation in partition coefficient, K_d, values. EPA 402-R-99-004B, United States Environmental Protection Agency, Office of Air and Radiation.

Gutierrez, M., Fuentes, H.R., 1991. Competitive adsorption of cesium, cobalt and strontium in conditioned clayey soil suspensions. J. Environ. Radioact. 13 (4), 271–282.

Hilton, J., Comans, R.N.J., 2001. Chemical forms of radionuclides and their quantification in environmental samples. In: Van der Stricht, E., Kirchmann, R. (Eds.), Radioecology, Radioactivity and Ecosystems. Fortemps, Liège, pp. 99–111.

IAEA, 1994. Handbook of parameter values for the prediction of radionuclide transfer in temperate environments. Technical Reports Series No. 364, International Atomic Energy Agency, Vienna.

ISO, 1995. Soil quality. Determination of organic and total carbon after dry combustion (elementary analysis). ISO 10694.

Krom, M.D., 1980. Spectrophotometric determination of ammonia: a study of a modified Berthelot reaction using salicylate and dichloroisocyanurate. Analyst 105, 305–316.

Mollah, A.S., Ullah, S.M., 1998. Determination of distribution coefficient of ^{137}Cs and ^{90}Sr in soil from AERE, Savar. Waste Manage. 18 (4), 287–291.

Mueller, G., Gastner, M., 1971. The ''Karbonat-Bombe,'' a simple device for the determination of the carbonate content in sediments, soils, and other materials. Neues Jahrb. Mineral. Monatsh. 10, 466–469.

OECD, 2000. OECD guideline 106. Guideline for the testing of chemicals: adsorption–desorption using a batch equilibrium method.

Rauret, G., Firsakova, S. (Eds.), 1996. Transfer of radionuclides through the terrestrial environment to agricultural products, including the evaluation of agrochemical practices, ECP-2. Final Report, EUR 16528 EN, Luxembourg.

Rigol, A., Vidal, M., Rauret, G., Shand, C.A., Cheshire, M.V., 1998. Competition of organic and mineral phases in radiocesium partitioning in organic soils of Scotland and the area near Chernobyl. Environ. Sci. Technol. 32 (5), 663–669.

Rigol, A., Roig, M., Vidal, M., Rauret, G., 1999. Sequential extractions for the study of radiocaesium and radiostrontium dynamics in mineral and organic soil from Western Europe and Chernobyl areas. Environ. Sci. Technol. 33, 887–895.

Roca, M.C., Vallejo, V.R., Roig, M., Tent, J., Vidal, M., Rauret, G., 1997. Prediction of cesium-134 and strontium-85 crop uptake based on soil properties. J. Environ. Qual. 26, 1354–1362.

Roig, M., Vidal, M., Rauret, G., 1998. Estimating the radionuclide available fraction in mineral soils using an extraction technique. Analyst 123, 519–526.

Roig, M., Vidal, M., Rauret, G., Rigol, A., 2007. Prediction of radionuclide aging in soils from the Chernobyl and Mediterranean areas. J. Environ. Qual. 36, 943–952.

Sanchez, A.L., Smolders, E., Van den Brande, K., Merckx, R., Wright, S.M., Naylor, C., 2002. Predictions of in situ solid–liquid distribution of radiocaesium in soils. J. Environ. Radioact. 63, 35–47.

Sauvé, S., Hendershot, W., Allen, H.E., 2000. Solid-solution partitioning of metals in contaminated soils: dependence on pH, total metal burden and organic matter. Environ. Sci. Technol. 34, 1125–1131.

Sheppard, M.I., Thibault, D.H., Smith, P.A., 1992. Effect of extraction techniques on soil pore-water chemistry. Comm. Soil Sci. Plant Anal. 23 (13–14), 1643–1662.

Smolders, E., Van den Brande, K., Merckx, R., 1997. Concentrations of ^{137}Cs and K in soil solution predict the plant availability of ^{137}Cs in soils. Environ. Sci. Technol. 31 (12), 3432–3438.

Sokolik, G.A., Ivanova, T.G., Leinova, S.L., Ovsiannikova, S.V., Kimlenko, I.M., 2001. Migration ability of radionuclides in soil-vegetation cover of Belarus after Chernobyl accident. Environ. Int. 26 (3), 183–187.

Staunton, S., 1994. Adsorption of radiocesium on various soils: interpretation and consequences of the effects of soil: solution ratio and solution composition on the distribution coefficient. Eur. J. Soil Sci. 45 (4), 409–418.

Sweeck, L., Wauters, J., Valcke, E., Cremers, A., 1990. The specific interception potential of soils for radiocesium. In: Desmet, G., Nassimbeni, P., Belli, M. (Eds.), Transfer of Radionuclides in Natural and Seminatural Environments, EUR 12448. Elsevier Applied Science, pp. 249–258.

Tianwei, Q., Hongxiao, T., Jiajun, C., Sheng, W.J., Chunli, L., Guibin, W., 2001. Simulation of the migration of ^{85}Sr in Chinese loess under artificial rainfall condition. Radiochim. Acta 89 (6), 403–406.

Trueba, C., Millán, R., Schmid, T., Lago, C., Gutiérrez, J., 2000. Estimación de índices de vulnerabilidad radiológica para los suelos peninsulares españoles. Colección Documentos Ciemat, Ciemat, Madrid.

Twining, J.R., Payne, T.E., Itakura, T., 2004. Soil–water distribution coefficients and plant transfer factors for ^{134}Cs, ^{85}Sr and ^{65}Zn under field conditions in tropical Australia. J. Environ. Radioact. 71 (1), 71–87.

Valcke, E., 1993. The behaviour dynamics of radiocaesium and radiostrontium in soils rich in organic matter. Ph.D. Thesis, Katholieke Universiteit Leuven (KUL), Belgium.

Vidal, M., Roig, M., Rigol, A., Llauradó, M., Rauret, G., Wauters, J., Elsen, A., Cremers, A., 1995. Two approaches to the study of radiocaesium partitioning and mobility in agricultural soils from the Chernobyl area. Analyst 120, 1785–1791.

Wauters, J., Sweeck, L., Valcke, E., Elsen, A., Cremers, A., 1994. Availability of radiocaesium in soils: a new methodology. Sci. Total Environ. 157, 239–248.

Wauters, J., Elsen, A., Cremers, A., Konoplev, A.V., Bulgakov, A.A., Comans, R.N.J., 1996. Prediction of solid liquid distribution coefficients of radiocaesium in soils and sediments. Part two: a simplified procedure for the solid characterization. Appl. Geochem. 11, 589–594.

Yasuda, H., Uchida, S., Muramatsu, Y., Yoshida, S., 1995. Sorption of manganese, cobalt, zinc, strontium and cesium onto agricultural soils: statistical analysis on effects of soil properties. Water Air Soil Pollut. 83, 85–96.

Applied Radiation and Isotopes 67 (2009) 367

Contents lists available at ScienceDirect

Applied Radiation and Isotopes

journal homepage: www.elsevier.com/locate/apradiso

Corrigendum

Corrigendum to "Radionuclide sorption–desorption pattern in soils from Spain" [Appl. Radiat. Isot. 66(2) (2008) 126–138]

C.J. Gil-García, A. Rigol, G. Rauret, M. Vidal *

Departament de Química Analítica, Universitat de Barcelona, Martíi Franqués 1-11, 3a Planta, 08028 Barcelona, Spain

The authors regret that an incorrect version of Table 1b was shown in the original manuscript. The correct version of Table 1b is now reproduced below:

Table 1b Summary of soil characteristics

Soil sample	FC (%)	Exchangeable cations ($cmol_c\,kg^{-1}$)					Soil solution ($mmol\,L^{-1}$)				EC ($\mu S\,cm^{-1}$)	RIP ($mmol\,kg^{-1}$)
		Na	K	Ca	Mg	NH_4^+	Na	K	Ca	Mg		
MALAGA	43.3	0.76	2.0	12.8	3.6	0.14	0.69	0.42	1.7	0.63	327	5958 (120)
TENF1	29.4	19.6	10.2	10.2	2.8	0.17	27.2	1.5	1.2	0.35	523	6669 (422)
TENF2	42.4	1.4	1.6	12.1	14.1	0.34	8.2	0.84	4.1	6.4	477	6758 (304)
AYUD	31.7	0.33	1.0	13.7	4.4	0.14	1.3	0.98	10.3	6.8	404	4929 (355)
CABRIL	29.0	0.26	0.66	7.8	4.1	0.08	0.51	0.13	0.44	0.46	89	4852 (669)
BILBAO	30.1	0.40	1.7	15.4	1.4	0.17	0.82	0.95	3.8	0.57	220	4419 (474)
VAN2	27.2	0.71	0.76	13.4	1.1	0.19	1.9	0.13	5.5	0.59	271	4488 (111)
UIB	26.7	0.91	1.7	16.1	1.0	0.20	1.0	1.2	17.6	1.6	435	7000 (454)
UPV	19.2	1.0	0.74	9.2	0.45	0.16	0.39	0.90	17.3	0.60	2001	3213 (88)
OVI01	29.4	0.6	0.39	9.8	0.91	0.91	1.8	0.55	24.6	3.9	584	3221 (586)
TRILLO	26.6	0.12	0.79	13.8	1.7	0.11	0.18	0.96	7.6	1.6	231	2897 (205)
BAD2	22.6	0.59	0.77	9.9	1.5	0.15	1.4	0.48	6.6	1.1	235	2594 (110)
ZORITA	20.0	0.13	0.48	9.3	1.2	0.11	0.38	0.33	3.4	0.39	237	2371 (187)
LEON	32.9	0.83	0.40	24.5	2.3	0.27	2.9	0.16	26.3	4.1	580	2314 (189)
GAROÑA	32.1	0.84	1.4	11.9	1.5	0.21	0.60	2.7	18.7	3.1	486	2080 (256)
ASCO	24.2	0.44	0.84	22.7	1.6	0.12	0.69	1.0	15.8	2.5	1547	2034 (233)
USAL	33.2	0.45	1.7	12.4	3.0	0.30	0.51	1.4	5.0	1.7	318	1874 (238)
OVI03	26.3	0.67	0.40	11.9	0.94	0.72	1.7	0.43	20.4	3.2	413	1718 (94)
BAD1	17.0	0.48	0.62	5.5	1.7	0.18	2.0	0.63	4.3	2.2	297	1523 (162)
GRACOR	29.2	0.64	0.19	5.4	1.1	0.18	3.3	0.16	6.0	2.3	239	1017 (42)
ALM	21.0	0.60	0.41	4.1	0.76	0.21	0.69	0.42	1.7	0.63	283	1002 (23)
ENUSA	20.2	0.39	0.30	7.2	0.56	0.17	0.17	0.17	1.3	0.17	197	744 (76)
GOLOSO	16.9	0.15	0.24	6.6	0.94	0.16	0.55	1.3	16.2	3.3	278	672 (30)
VAN1	6.2	0.77	0.34	12.5	0.93	0.15	3.4	0.34	14.0	4.6	397	660 (98)
ANDCOR	40.2	0.96	0.40	3.5	4.0	1.9	3.9	1.9	4.5	21.8	921	366 (28)
FONCOR	28.5	0.98	0.40	13.5	2.5	0.36	8.4	1.7	38.4	12.5	951	340 (24)
VILCOR	20.1	0.58	0.30	4.4	0.5	0.26	3.1	1.5	27.4	5.1	489	225 (6)
FROCOR	23.7	3.4	2.7	6.8	5.1	2.6	91.2	23.7	52.1	72.5	2300	179 (3)
DELTA1	28.9	1.9	2.9	33.9	7.2	0.16	58.2	5.6	30.6	19.9	3010	1186 (96)
DELTA2	56.1	2.2	3.5	52.0	8.6	0.06	128	2.0	43.5	20.4	3390	1463 (117)

FC: Field capacity; EC: Electrical conductivity; RIP: Radiocaesim interception potential, mean values (SD) for $n = 4$.

DOI of original article: 10.1016/j.apradiso.2007.07.032
* Corresponding author. Tel.: +34 934039276; fax: +34 934021233.
E-mail address: miquel.vidal@ub.edu (M. Vidal).

doi:10.1016/j.apradiso.2008.11.004

3.2

New best estimates for radionuclide solid–liquid distribution coefficients in soils. Part 1: radiostrontium and radiocaesium

C. Gil-García, A. Rigol, M. Vidal

Journal of Environmental Radioactivity, 100, 690–696, 2009

Páginas 91-98

Journal of Environmental Radioactivity 100 (2009) 690–696

Contents lists available at ScienceDirect

Journal of Environmental Radioactivity

journal homepage: www.elsevier.com/locate/jenvrad

New best estimates for radionuclide solid–liquid distribution coefficients in soils, Part 1: radiostrontium and radiocaesium

C. Gil-García, A. Rigol, M. Vidal*

Departament de Química Analítica – Universitat de Barcelona, Martí i Franquès 1-11, 3a Planta, 08028 Barcelona, Spain

ARTICLE INFO

Article history:
Received 31 July 2007
Received in revised form
4 July 2008
Accepted 7 October 2008
Available online 25 November 2008

Keywords:
Distribution coefficient
Soil
Radiostrontium
Radiocaesium
Radiocaesium interception potential
Cationic exchange capacity
Soil solution

ABSTRACT

Best estimates for the solid-liquid distribution coefficients (K_d) of radiostrontium and radiocaesium for various soil types, were derived from geometric means (GM) calculated from grouping soils by texture and organic matter content, and also using soil cofactors governing soil–radionuclide interaction. The K_d (Sr) GM for Sand, Loam, Clay and Organic groups were similar, although the value for the Sand group was significantly lower. The Sr cofactor approach, based on the ratios of cation exchange capacity (CEC) to Ca and Mg concentrations in the soil solution, leads to K_d (Sr) GM with a lower variability, from which best estimates could be proposed. The K_d (Cs) GM for Sand and Organic groups differed, although similar values were obtained for Loam and Clay groups. Grouping the K_d (Cs) according to the Radiocaesium Interception Potential (RIP) and the RIP divided by the K concentration in the soil solution also allows to suggest K_d (Cs) best estimates with a lower variability.

1. Introduction

The chemical form and speciation of radionuclides greatly affects their movement through environmental media and uptake by biota. Specifically, the way that a radionuclide is bound to solids determines the amount of radionuclide in solution, which directly influences the fraction of radionuclide that may be incorporated into organisms.

Dissolved radionuclide ions bind to solid surfaces by a number of processes often classified under the broad term of sorption. Although significant progress has been made in describing sorption on heterogeneous solids as a weighted result of sorption on homogeneous surfaces, models for the describing radionuclide sorption are still mostly based on empirical values of solid-liquid distribution coefficients (K_d). This is the simplest sorption model and consists of the ratio of the concentration of radionuclide sorbed on a specific solid to the concentration of radionuclide in a specified liquid phase at equilibrium (K_d, L/kg). The K_d-based model does not assume sorption mechanisms, nor does it contain a quantification of the capacity and selectivity of the sorption sites or the competition from other ions to fill the sorption sites. Moreover, the K_d-based model relies on the hypothesis that the radionuclide bound to the soil solid phase is in equilibrium with the radionuclide in the soil solution, and thus can exchange with it. Therefore, the K_d should strictly only be used for radionuclides whose sorption obeys an instantaneous, reversible, linear equilibrium. However, the time elapsed since incorporation of the radionuclide is known to affect K_d, since a fraction of the radionuclide taken up may become fixed by the solid phase (an aging effect related to sorption dynamics), and thus no longer participate in the soil–soil solution equilibrium. Besides this, the many different approaches used to determine K_d values, and the contrasting experimental conditions applied in each case, lead to wide ranges of K_d values for similar soil and radionuclide combinations. This makes it difficult to compare K_d values derived from laboratory experiments.

As K_d is one of the most significant parameters in predicting the fate of a radionuclide in the environment, it is a common input in risk assessment models. Some efforts have been made to create a K_d database for soils and to establish ranges of values for a specific radionuclide and soil type, as in the case of the *Handbook of Parameter Values for the Prediction of Radionuclide Transfer in Temperate Environments*, TRS 364 (IAEA, 1994) and related compendiums from which K_d data originated (Sheppard and Thibault, 1990; Thibault et al., 1990). Now, more than 15 years after the creation of the previous K_d database, it is time to revise K_d ranges by including data from post-Chernobyl research and the mechanisms behind soil–radionuclide interaction. With this aim, in 2003 the International Atomic Energy Agency launched the programme on

* Corresponding author. Tel.: +34 934039276; fax: +34 934021233.
E-mail address: miquel.vidal@ub.edu (M. Vidal).

0265-931X/$ – see front matter © 2008 Elsevier Ltd. All rights reserved.
doi:10.1016/j.jenvrad.2008.10.003

Environmental Modelling for Radiation Safety (IAEA EMRAS), with a Working Group devoted to the "Revision of the TRS-364", which revised K_d values in parallel with other transfer parameters. This is the first in a series of three papers, in which we propose new best estimates of K_d for a large number of radionuclides. Part 1 is a general introduction to experimental methods for estimating K_d values, and it focuses on radiostrontium and radiocaesium. Part 2 deals with naturally occurring radionuclides, and Part 3 proposes best estimates for a miscellany of radionuclides, although emphasis is given to heavy metal radionuclides, iodine, selenium, antimony, americium and plutonium.

2. Experimental methods used to estimate K_d values

2.1. K_d values from field contaminated soils

K_d values can be quantified from the radionuclide level in the soil solid phase divided by the concentration of the radionuclide in soil solution obtained from the contaminated soil, as done for other pollutants (Goody et al., 1995; Sanchez et al., 2002). This approach is reliable when the level of contamination is high enough to disregard the uncertainty in obtaining and measuring the soil solution. However, it may lead to K_d values higher than those resulting from a laboratory sorption test because the radionuclide quantified in the solid phase of the contaminated soil may include sorbed radionuclide that is not available for exchange with the soil solution due to the time elapsed since radionuclide incorporation.

2.2. Laboratory sorption experiments

The most common approach in laboratory studies is to perform sorption experiments on non-contaminated soils, mainly using batch methods. Experimental conditions may be extremely different from one experiment to another, although standardized protocols are increasingly recommended by several organizations (OECD, 2000; ASTM, 2003).

Sorption experiments are conducted at various radionuclide activity and (more pertinently) mass concentrations, in different hydrochemical and mineralogical contexts. Experimental conditions, such as the composition of the contact solution, contact (shaking) time, volume/mass ratios, and filtration of the resulting solution, often differ among laboratory studies (Benes et al., 1994). As the competitive effect of major ions has been widely described, especially when dealing with specific sorption sites, sorption experiments should be performed that simulate as closely as possible field conditions of interest, for example by reproducing the pH and ionic composition of the soil solution in the sorption medium (Staunton, 2004; Gil-García et al., 2008).

Experiments should not be performed at higher concentrations than could be expected after a radioactive release, since there may be a limited number of selective sites for radionuclide sorption, and at high concentrations non specific sites could be involved in radionuclide sorption. In particular, excessively high mass concentrations may arise in simulations of radionuclide sorption using stable or very long-lived isotopes of the element or analogue elements.

2.3. Laboratory mass transport experiments

Another experimental approach is to derive K_d values from the diffusion pattern of a radionuclide in compacted samples, in column or diffusion cells (García-Gutiérrez et al., 2004; Montavon et al., 2006). In a porous medium like soils, an effective diffusion coefficient (D_e; m^2/s) must be defined. Only the pores that contribute to the transport of the dissolved radionuclide species need to be considered (the diffusion-accessible porosity, Φ), although in most cases (especially when the relative saturation tends to one) to use the total porosity (ε) is a sufficiently correct approach. In the case of radionuclides with significant sorption, an apparent diffusion coefficient (D_a; m^2/s) can be calculated from the diffusion profile into the sample. This diffusion coefficient takes into account the retardation of the radionuclide due to its interaction with the porous material. We may write:

$$D_a = D_e/f_{ret} \quad (1)$$

where f_{ret} is the Retardation Factor. If we assume a linear sorption pattern, with a constant K_d in the range of concentrations studied, the f_{ret} can be defined as:

$$f_{ret} = 1 + (\rho/\varepsilon)K_d \quad (2)$$

where ρ is the dry bulk density of the soil.

Few data comparing K_d values from batch and diffusion experiments are available to date, since most experiments have been carried out with pure mineral phases (Wang et al., 2003), thus conclusions on whether the batch sorption methods over or underestimate K_d values are contradictory (Ochs et al., 2001). However, mostly due to differences in experimental conditions, such as the volume/mass ratio and contact time, more cases are described where the K_d derived from diffusion experiments were lower than those derived from batch experiments than *vice versa* (Okamoto et al., 1999; Fernández-Torrent et al., 2005).

3. Data collection and treatment

3.1. Data collection and acceptance

Data of the present compilation come from field and laboratory experiments with various contamination sources, considering the scenario of soils contaminated by radioisotopes, and from references mostly from 1990 onwards, including data in the previous TRS-364 and related reports (Sheppard and Thibault, 1990; Thibault et al., 1990; IAEA, 1994), reviewed papers, and grey literature (PhD theses, reports). In most cases, data from diffusion experiments, studies using other materials (for example sediments; pure soil phases such as clays or Fe–Mn–Al oxides; rock materials) and from stable elements are not considered. Data from radioisotopes of the same element are pooled.

3.2. Data treatment

For both radionuclides, K_d values were grouped according to two criteria. On one hand, soils were grouped according to the sand and clay mineral percentages referred to the mineral matter, and the organic matter (OM) content in the soil. This defined the 'texture/OM' criterion, which was similar to the criterion followed in the previous TRS-364. The thresholds defining each soil group within the texture/OM criterion were the result of discussions within the Working Group. In short, a soil was included in the Organic group if the organic matter content was $\geq$20%. For the mineral soils, three groups were created according to the sand and clay percentages referred to the mineral matter:

Sand group: sand fraction $\geq$65% and clay fraction $<$18%
Clay group: clay fraction $\geq$35%
Loam group: rest of cases

Moreover, an additional Unspecified group was created for soils without characterization data, or for mineral soils with unknown sand and clay contents.

Improved knowledge of the interaction mechanisms of certain radionuclides in soils allows to review K_d values in terms of a more fundamental description of underlying processes. Thus, the second criterion was to group soils regarding specific soil factors governing the radionuclide–soil interaction ('cofactor' criterion). The cofactors depended on the radionuclide considered. An advantage of using cofactors for grouping soils is that the variability of K_d ranges for a given soil group may decrease considerably with respect to the variability observed when the classification is based solely on sand, clay and organic matter contents, thus improving the best estimate for a given soil group.

After grouping the K_d values, the following data set descriptors were calculated: n: number of observations; GM: geometric mean; GSD: geometric standard deviation; Min–Max: minimum and maximum values. The GM and GSD were calculated when the number of observations was $\geq$3. When $n = 2$, min and max values were given, while only the single value could be given when $n = 1$.

As the log-transformed K_d were normally distributed in most cases, the exploratory and ANOVA analysis were performed with log K_d data. The exploratory analysis was based on box-and-whisker plots (*StatGraphics Plus 5.1*) and, besides exploring the data population, it was useful to exclude data points to decrease data variability. A data point was excluded when it was beyond three times the interquartile ranges defined by the box-and-whisker plots. Although in a few cases the log K_d were not normally

distributed, or the standard deviations of the soil groups were not statistically comparable, the ANOVA analysis, based on Fisher's Least Significant Differences test (*StatGraphics Plus 5.1*), was useful to identify which soil groups were statistically different, although some results must be treated with precaution.

The best estimates were the calculated GM of the K_d values when they were significantly different between soil groups. When they were not, the best estimates were proposed from an expert judgment of the GM values.

4. Description of ranges of K_d values: derivation of K_d best estimates

4.1. The case of radiostrontium

4.1.1. Best estimates of K_d (Sr) for soils grouped according to the texture/OM criterion

Table 1 summarizes the ranges of values of K_d (Sr), obtained for the different soil groups. Data originated from 28 accepted references, which led to 255 observations. As could be expected given the soil parameters governing radiostrontium interaction, geometric means (GM) increase with increasing the clay content, and the maximum value is observed for the Organic group. The increase in the GM with increasing the clay and organic matter contents, and the variability of data were similar to that of the previous TRS-364, in which the GM values for Sand, Loam, Clay and Organic groups were 13, 20, 110, and 150 L/kg, respectively. However, the ANOVA analysis of the present compilation showed that only the GM of the Sand group was statistically different. Therefore, the modellers and end-users of the K_d (Sr) estimates may consider to use the individual GM values for each soil type as best estimates, or instead to use the value of 20 L/kg for Sand soils, and a value around 70 L/kg for the rest of soil types.

4.1.2. Best estimates of K_d (Sr) for soils grouped according to the cofactor criterion

The solid–liquid partitioning of a number of radionuclides (RN), such as radiostrontium, may be better understood by reference to the partitioning of an analogue (sorption competitive) ion (AN), characterized by similar sorption behaviour. In this approach:

$$K_d(\mathrm{RN}) = K_d(\mathrm{AN}) \times K_c(\mathrm{RN/AN}) \quad (3)$$

where the K_d (RN) is calculated by a linear amplification of the K_d (AN) by a factor equal to the RN–AN selectivity coefficient at the sorption sites (K_c (RN/AN)).

K_d (Sr) can be predicted from the ratio of the Ca and Mg in the exchangeable complex (in $cmol_c/kg$) to the sum of the concentrations of Ca and Mg in the soil solution ($Ca_{ss} + Mg_{ss}$, in $cmol_c/L$) (Rauret and Firsakova, 1996; Hilton and Comans, 2001), amplified by the trace selectivity coefficient Sr-to-Ca and Sr-to-Mg, K_c(Sr/Ca–Mg), which corresponds to the equation (4):

$$K_d(\mathrm{Sr}) = K_c(\mathrm{Sr/Ca{-}Mg})\frac{\mathrm{Ca_{exch}} + \mathrm{Mg_{exch}}}{\mathrm{Ca_{ss}} + \mathrm{Mg_{ss}}} \quad (4)$$

In most cases similar trace selectivity coefficients Sr-to-Ca and Sr-to-Mg may be assumed to derive a simpler model, as the K_c (Sr/Ca–Mg) is reported to be close to 1 (Valcke, 1993). Therefore, equation (4) can be simplified to:

$$K_d(\mathrm{Sr}) = \frac{\mathrm{Ca_{exch}} + \mathrm{Mg_{exch}}}{\mathrm{Ca_{ss}} + \mathrm{Mg_{ss}}} \quad (5)$$

If data on exchangeable cations is not available, they can be substituted by the cationic exchange capacity (CEC, in $cmol_c/kg$, which is usually quantified in routine soil analysis). This is a satisfactory approach for estimating K_d (Sr), especially when dealing with soils with saturated exchange complex (Rauret and Firsakova, 1996).

Another approach to the prediction of K_d (Sr) is based on correlating K_d (Sr) to other soil properties that are easily measured in routine studies. An example of this is to relate the K_d (Sr) to the Cation Distribution Ratio (CDR), defined as the value of the cation exchange capacity (CEC, $cmol_c/kg$) divided by the electrical conductivity (EC, mS/cm) in the soil solution (Yasuda and Uchida, 1993). This correlation is easily explained by the fact that electrical conductivity is governed by the concentrations of major cations in the soil solution, especially Ca and Mg:

$$\mathrm{EC(mS/cm)} \approx 1000\,x\left[\mathrm{Na_{ss}} + \mathrm{K_{ss}} + \mathrm{NH_{4ss}^{+}} + \mathrm{Mg_{ss}} + \mathrm{Ca_{ss}}\right](\mathrm{cmol_c/L}) \quad (6)$$

K_d (Sr) can be predicted from the CDR using the following equation:

$$K_d(\mathrm{Sr})(\mathrm{L/kg}) = 2.1\,x\,\mathrm{CDR(L/kg)} \quad (7)$$

We regrouped K_d (Sr) according to CEC and to the ratio of the CEC to $(Ca + Mg)_{ss}$. Although the use of the CEC as a cofactor is not strictly appropriate, since as seen in equations (4) and (5) it does not predict the K_d (Sr), it is however widely (and often wrongly) accepted that K_d (Sr) varies accordingly to CEC, thus being here interesting to compare it with a suitable cofactor, as the CEC/$(Ca + Mg)_{ss}$ ratio. Results are shown in Table 2. To group K_d (Sr) according to the CEC values was a slightly worse approach than the texture/OM criterion, since there is no consistent dependence between CEC values and K_d (Sr). However, grouping according to the CEC/$(Ca + Mg)_{ss}$ ratio led to ranges with a lower variability (generally one order of magnitude lower), which also have a lower GSD, while the K_d (Sr) GM consistently increased with increasing CEC/$(Ca + Mg)_{ss}$ ratios.

Fig. 1a illustrates the exploratory analysis of the three grouping approaches with the box-and-whiskers plots for all cases. In just two classes a few points were excluded since they were beyond the

Table 1
K_d (Sr) for soils grouped according to texture/OM criterion (L/kg).

Soil group	*n*	GM	GSD	Min	Max	# Ref.
All soils	255	52	6	0.4	6500	28
Sand	65	22	6	0.4	2424	19
Loam	120	57	5	2	2549	12
Clay	19	95	4	9	747	5
Organic	37	110	6	3	6500	10
Unspecified	14	73	3	8	267	8

n: number of observations; GM: geometric mean; GSD: geometric standard deviation; Min–Max: minimum and maximum values; # Ref.: number of references serving as data sources.

Table 2
K_d (Sr) for soils grouped according to cofactor criterion (L/kg).

Soil groups	*n*	GM	GSD	Min	Max
CEC < 10	50	21	4	0.4	332
10 < CEC < 20[a]	44	200	2	33	462
20 < CEC < 50	82	62	6	1	6500
CEC > 50	25	94	6	5	1764
$CEC/M_{ss} < 15$	25	4	2	0.4	15
$15 < CEC/M_{ss} < 150$	28	22	3	4	111
$150 < CEC/M_{ss} < 500$[a]	18	170	2	77	269
$CEC/M_{ss} > 500$	25	320	2	81	1764

n: number of observations; GM: geometric mean; GSD: geometric standard deviation; Min–Max: minimum and maximum values.

[a] Data beyond the threshold of 3 times the interquartile ranges were excluded.

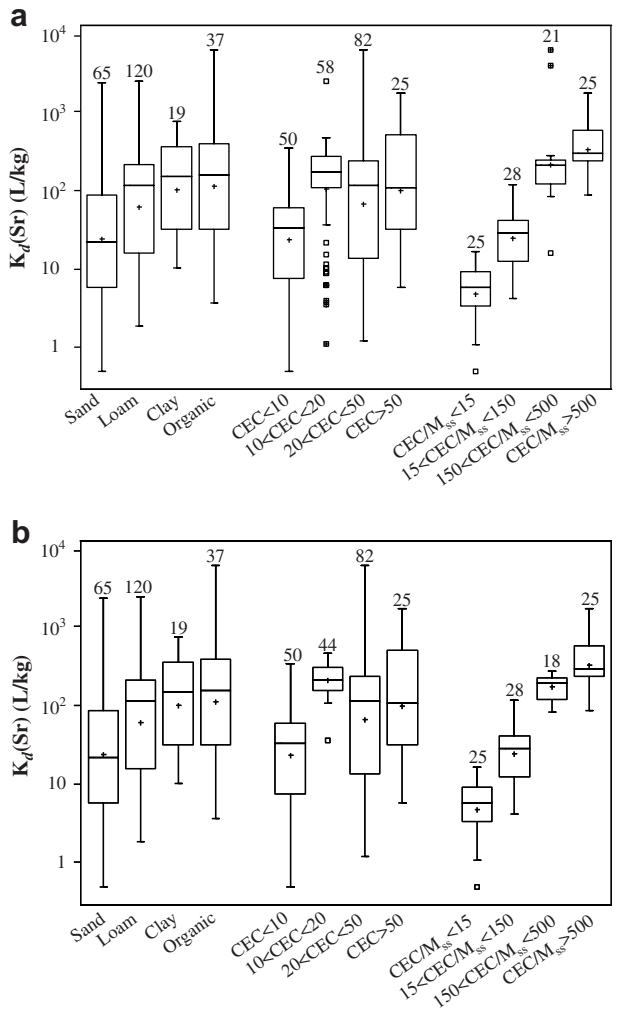

Fig. 1. Box-and-whisker plots of K_d (Sr) values grouped according to texture/OM and cofactor criteria. The box encloses the middle 50%, and the median is represented as a horizontal line inside the box. Vertical lines extend to the point within 1.5 interquartile range. Other symbols represent GM (+), points at >1.5 interquartile ranges (□), points at >3 interquartile ranges (⊞). (a) Complete data set. (b) Data beyond the threshold of 3 interquartile ranges were excluded.

threshold of 3 times the interquartile ranges, and the resulting GM, GSD, and box-and-whiskers plots were recalculated. This process was repeated until no further data points to be excluded were suggested by the exploratory analysis. The number of excluded points depended on the quality of the cofactor adopted: 14 points were excluded in the $10 < CEC < 20$ class (13 in the lower range and 1 in the upper range), while only 3 points in the $150 < CEC/M_{ss} < 500$ class (1 in the lower range and 2 in the upper range). The resulting populations had lower variability, with a GSD around 1. As all the GM values using the CEC/M_{ss} criterion were significantly different, the best estimates could be defined by their values.

The main difficulty of the cofactor approach based on the CEC/M_{ss} ratio is obtaining data on the soil solution composition, which is not always characterized in routine soil analysis. Since exchangeable Ca and Mg are more often quantified, Table 3 shows a summary of K_d (Ca), K_d (Mg) and K_d (Ca + Mg) derived from the ratios of the exchangeable Ca and Mg, and their concentrations in the corresponding soil solution. This should help modellers and end-users to estimate the Ca and Mg concentrations in the soil solution, if these data are not available. As expected, the distribution coefficients of these major elements increased with increasing clay content, and they were higher for organic than for mineral soils, thus following a similar pattern to the K_d (Sr).

Table 3
K_d (Ca), K_d (Mg), and K_d (Ca + Mg) for soils grouped according to texture/OM criterion (L/kg).

	Soil groups	*n*	GM/Value	GSD	Min	Max	# Ref.
Ca	All soils	34	8	3	0.7	110	2
	Sand	7	3	4	0.7	28	2
	Loam	21	8	3	2	89	2
	Clay	5	16	3	6	49	2
	Organic	1	110	–	–	–	1
Mg	All soils	30	4	3	0.4	45	1
	Sand	6	1	4	0.4	16	1
	Loam	20	5	3	0.9	45	1
	Clay	4	7	3	2	29	1
Ca + Mg	All soils	65	12	6	0.3	647	6
	Sand	18	3	3	0.3	26	5
	Loam	22	7	3	1	66	2
	Clay	4	10	3	5	35	1
	Organic	17	68	4	7	647	4
	Unspecified	4	82	1	56	129	1

n: number of observations; GM: geometric mean; GSD: geometric standard deviation; Min–Max: minimum and maximum values; # Ref.: number of references serving as data sources.

The fact that the approach based on the $CEC/(Ca + Mg)_{ss}$ ratios led to obtain K_d (Sr) best estimates with a lower variability confirms that the cofactor criterion is better than texture/OM criterion for grouping soils. In fact, the $CEC/(Ca + Mg)_{ss}$ ratio is satisfactory for predicting K_d (Sr) from soil data obtained in routine analysis. Statistical analysis of the whole data set using a multiple regression with CEC and $(Ca + Mg)_{ss}$ confirmed that more than 82% of the variance of the K_d (Sr) could be explained, and that the log K_d (Sr) strongly correlated to the log $(CEC/(Ca + Mg)_{ss})$ [$\log K_d\,(Sr) = -0.05\,(\pm 0.09) + 0.87\,(\pm 0.04) \times \log (CEC/(Ca + Mg)_{ss})$; $r = 0.90$; 82% of the variance explained; $n = 99$]. After excluding 3 points beyond the threshold of 3 times the interquartile ranges, correlation improved [$\log K_d\,(Sr) = -0.05\,(\pm 0.09) + 0.86\,(\pm 0.03) \times \log (CEC/(Ca + Mg)_{ss})$; values $r = 0.95$; 90% of the variance explained; $n = 96$; see Fig. 2]. The value of the slope, lower than unity, can be explained by the fact that, for soils with unsaturated exchangeable complex, the prediction based on CEC, instead of on $(Ca + Mg)_{exch}$, overestimates K_d (Sr). Nevertheless, the use of the CEC and the soil solution composition (which is a compulsory step to improve the K_d (Sr) predictions) is satisfactory enough for an excellent estimate of K_d (Sr) in all kind of soils. Therefore, rather than using a best estimate for K_d (Sr) for a given soil type, the straightforward calculation of K_d (Sr) from the above correlations can be a much better approach.

4.2. The case of radiocaesium

4.2.1. Best estimates of K_d (Cs) for soils grouped according to texture/OM criterion

Table 4 summarizes the ranges of values of K_d (Cs) obtained for all soil groups. Data are from 32 accepted references, which led to

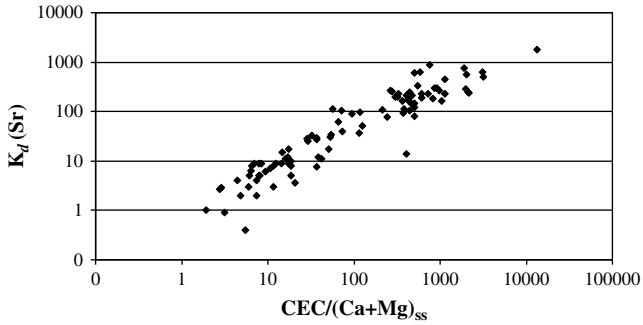

Fig. 2. Variation of the K_d (Sr) according to the CEC to $(Ca + Mg)_{ss}$ ratio.

469 observations. As could be expected by the soil parameters governing radiocaesium, the K_d (Cs) GM increased with increasing clay content, while the minimum value was observed for the Organic group. However, the GM for the Loam and Clay groups was not statistically different. This is already an improvement with respect to the data included in the previous TRS-364, since the GM values for Sand, Loam, Clay and Organic groups were 270, 4400, 1800, and 270 L/kg, respectively. This implied that the highest GM value was for the Loam group, conclusion that was not consistent with the mechanisms behind radiocaesium interaction in soils. Regarding data variability, the values for the mineral soils were within three orders of magnitude, while for the Organic group the range was of 4 orders of magnitude. The larger range of values for this last category is explained by the fact that soil was considered within the Organic group if it had over 20% organic matter content. However, the mineral phases still govern radiocaesium sorption in soils with up to 90% organic matter content, thus potentially having K_d (Cs) as high as those in mineral soils (Rigol et al., 1998). Therefore, and from the analysis of the data presented in Table 2, possible best estimates for the K_d (Cs) (besides using the individual GM values) could be 530 L/kg for sandy soils, 270 L/kg for organic soils, and a recalculated value of around 3700 L/kg for loam and clay soils.

4.2.2. Best estimates of K_d (Cs) for soils grouped according to the cofactor criterion

K_d (Cs) values were also grouped using the cofactor approach based on the Radiocaesium Interception Potential (RIP) concept. The RIP value is an estimate of the capacity of a given soil to specifically sorb Cs. The most common protocol to determine RIP is based on preequilibrating the samples with a solution containing 100 mmol/L of Ca and 0.5 mmol/L of K (m_K). After preequilibrating the samples, these are equilibrated with the same solution, but labelled with radiocaesium. The distribution coefficients (K_d (Cs)) are obtained by measuring the radiocaesium activity in the supernatant, before and after equilibration. The calculated product K_d (Cs) $\times$ m_K defines the RIP value (in mmoL/kg). Details can be found elsewhere (Wauters et al., 1996a).

RIP is related to the content and selectivity of expandable clays, especially illite and other 2:1 phyllosilicates, in which Frayed Edge Sites (FES) – which are specific sites for Cs sorption – are present (Sweeck et al., 1990). Other exchange sites are of little relevance for Cs sorption (Brouwer et al., 1983; Cremers et al., 1988; Vidal et al., 1995), except when dealing with soils with extremely low clay content (for example, with an organic matter content over 90%; highly sandy podzols) in which Cs may also be sorbed at other, less specific sites (Rigol et al., 1998).

As Cs sorption is governed by the FES, the Cs solid–liquid distribution coefficient at these sites (K_d^{FES} (Cs)) accounts for more than 80% of the total sorption process (Vidal et al., 1995). The K_d^{FES} (Cs) can be predicted by dividing the RIP value by the sum of K and NH_4^+ concentrations in the soil solution, the latter amplified by the NH_4-to-K trace selectivity coefficient in the FES (K_c^{FES} (NH_4/K)) (Sweeck et al., 1990). This parameter, which can easily be quantified by laboratory experiments, ranges from 4 to 8 for soils in which specific sites govern Cs sorption quantitatively, and is as low as 2 in those soils where sorption occurs basically at regular exchange sites (Wauters et al., 1996b; Rigol et al., 1998).

For a more accurate prediction of K_d (Cs) a second term must be added to account for Cs sorption at regular exchange sites (K_d^{RES} (Cs)). This term is the sum of the exchangeable K and NH_4^+ divided by the sum of K and NH_4^+ concentrations in the soil solution (in mmol/L), assuming a selectivity coefficient NH_4/K of approximately 1 at these sites. The global equation from sorption at specific and regular sites may be written as follows:

$$K_d(\mathrm{Cs}) = K_d^{FES}(\mathrm{Cs}) + K_d^{RES}(\mathrm{Cs}) = \frac{\mathrm{RIP}}{K_{ss} + K_c^{FES}(\mathrm{NH_4/K}) \times \mathrm{NH_{4ss}^+}} + \frac{\mathrm{K_{exch}} + \mathrm{NH_{4exch}^+}}{\mathrm{K_{ss}} + \mathrm{NH_{4ss}^+}} \quad (8)$$

For the case of highly saline soils near to marshlands and with high Na concentrations in the soil solution, equation (8) may be slightly modified to include the potential competitive role of Na and its effect on the quantification of K_d^{FES}, correcting the Na concentration by the Na-to-K trace selectivity coefficient in the FES, K_d^{FES} (Na/K). As this coefficient is approximately 0.02 (Wauters et al., 1996a), the role of Na will have a significant effect only where an unusually high Na concentration occurs.

Since Na and NH_4^+ concentrations are generally much lower than K concentrations (as is the case for most agricultural systems with mineral soils) we can simplify equation (8). As the value of K_d^{FES} (Cs) is much larger than the value of K_d^{FES} (Cs), K_d (Cs) is reasonably well predicted by the following equation, except for those soil types (such as upland peat soils or soils affected by flooding) in which $NH_{4\,ss}^+$ can be significant:

$$K_d(\mathrm{Cs}) = \frac{\mathrm{RIP}}{K_{ss}} \quad (9)$$

Therefore, K_d (Cs) can be grouped according to the RIP values of soils and the ratio RIP/K_{ss}. Results are summarized in Table 5. The cofactor approach led to obtain K_d (Cs) GM with a lower variability than when using the texture/OM criterion. Besides, the GM for all soil groups was significantly different, thus allowing to derive in this case the K_d (Cs) best estimates straightforwardly from the GM values. Fig. 3 illustrates an exploratory analysis of the three grouping approaches with the box-and-whiskers plots for all cases. No points were beyond the threshold of 3 times the interquartile ranges, despite the high degree of heterogeneity in data sources.

As described for radiostrontium, the cofactor approach based on the RIP/K_{ss} ratios actually yields excellent predictions of K_d (Cs) from soil data obtained in routine analysis. The RIP alone explained a 54% of the total data variance and it was well correlated with the K_d (Cs) [$\log K_d$ (Cs) $= 0.3\ (\pm 0.2) + 0.94\ (\pm 0.05) \times \log$ RIP; $r = 0.74$; $n = 257$]. Describing the relationship between variants with a multiple regression, the use of RIP and K_{ss} explained around the

Table 4
K_d (Cs) for soils grouped according to texture/OM criterion (L/kg).

Soil Group	n	GM	GSD	Min	Max	# Ref.
All soils	469	1200	7	4	375 000	32
Sand	114	530	6	10	35 210	19
Loam	191	3500	4	39	55 100	17
Clay	36	5500	4	566	375 000	9
Organic	108	270	7	4	95 000	14
Unspecified	20	1700	5	40	55 000	8

n: number of observations; GM: geometric mean; GSD: geometric standard deviation; Min–Max: minimum and maximum values; # Ref.: number of references serving as data sources.

Table 5
K_d (Cs) for soils grouped according to the cofactor criterion (L/kg).

Soil groups	n	GM	GSD	Min	Max
RIP < 150	47	74	2	10	726
150 < RIP < 1000	78	320	6	10	34 400
1000 < RIP < 2500	72	2400	4	62	95 000
RIP > 2500	60	7200	4	220	375 000
RIP/K_{ss} < 100	37	85	3	10	697
100 < RIP/K_{ss} < 1000	85	240	5	20	5836
1000 < RIP/K_{ss} < 10 000	78	2000	4	62	34 400
RIP/K_{ss} > 10 000	57	9900	4	220	375 000

n: number of observations; GM: geometric mean; GSD: geometric standard deviation; Min–Max: minimum and maximum values.

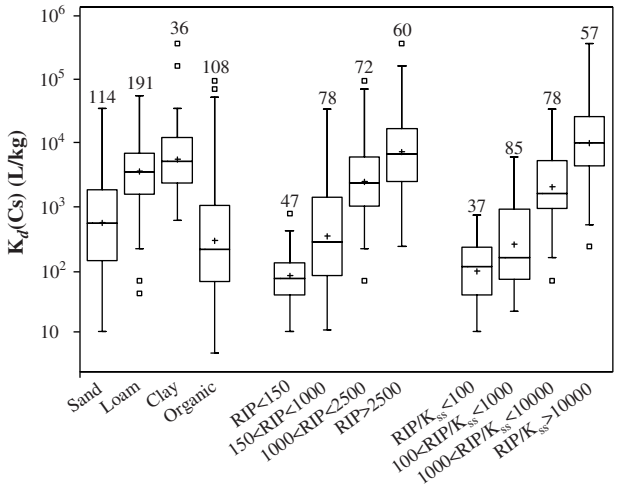

Fig. 3. Box-and-whisker plots of K_d (Cs) values grouped according to the texture/OM and cofactor criteria. The box encloses the middle 50%, and the median is represented as a horizontal line inside the box. Vertical lines extend to the point at 1.5 interquartile range. Other symbols represent GM (+), and points at >1.5 interquartile ranges (□).

70% of the total variance, with the following regression equation: $\log K_d$ (Cs) = 0.1 (±0.1) + 0.98 (±0.04) × log RIP − 0.53 (±0.04) × log K_{ss}. Finally, the RIP/K_{ss} ratios explained around a 65% of total variance of the K_d (Cs) data, and the statistical analysis confirmed that log K_d (Cs) correlated well with log (RIP/K_{ss}), as seen in Fig. 4 [log K_d (Cs) = 0.94 (±0.04) × log (RIP/K_{ss}); $r = 0.78$; $n = 257$]. The predictions were satisfactory without including data regarding NH_4^+ in the soil solution (NH_{4ss}). This can be partially explained by the fact that most soils with RIP data were mineral (177 out of 257) and thus the NH_{4ss} was low and easily omitted. In fact, in the statistical analysis of the population for which all the variants including the NH_{4ss} were available ($n = 110$), the use of NH_{4ss} did not lead to an improvement in the prediction of K_d (Cs).

As for radiostrontium, the quantification of the cationic composition of the soil solution (or of the contact solution in sorption experiments) is necessary for good estimates of K_d (Cs). As the exchangeable K is more often quantified in soil analysis than K_{ss}, modellers may find useful to have data on K_d (K) to derive one variant from the other. Table 6 summarizes the K_d (K) obtained for all soil categories, which can be used to estimate K_{ss} from exchangeable K. However, the ANOVA analysis showed than only the GM of the Sand group was significantly lower, although the GM increased with the clay content.

A major limitation of the cofactor approach in predicting K_d (Cs) is the fact that a K_d value must be obtained to quantify the RIP value. To date, attempts to predict the RIP value from soil properties have been only partially successful. Waegeneers et al. (1999) showed

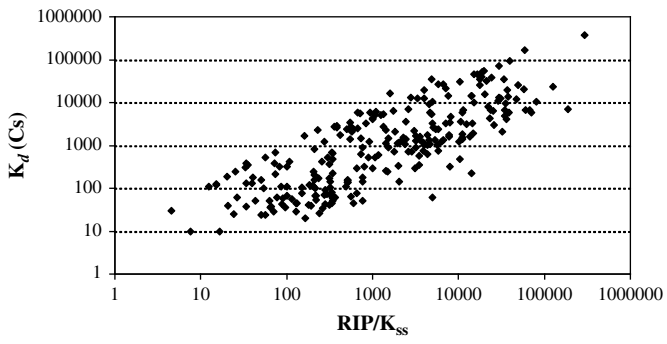

Fig. 4. Variation of the K_d (Cs) according to the RIP to K_{ss} ratio.

Table 6
K_d (K) for soils grouped according to texture/OM criterion (L/kg).

Soil group	*n*	GM	GSD	Min	Max	# Ref.
All soils	237	13	4	0.7	911	9
Sand	60	3	3	0.7	179	8
Loam	81	20	4	2	911	5
Clay	12	43	3	9	294	2
Organic	76	19	3	2	134	5
Unspecified	8	11	3	4	178	2

n: number of observations; GM: geometric mean; GSD: geometric standard deviation; Min–Max: minimum and maximum values; # Ref.: number of references serving as data sources.

that the RIP value depends not only on the clay content, but also on the type of clay and geological origin of the soil. In that work, after performing a stepwise regression analysis on two sets of soils, the clay content alone accounted for up to 71% of the variance of the RIP in the most favourable set of soils, whereas for another set of soils it explained only 13% of the variance. The regression improved when silt content and pH were added to clay content, depending on the origin of the soils. Regarding the K_d database compiled here – and making no distinctions regarding soil geological origin or clay type (information that is not available) – the clay content alone explains 40% of the variance of the RIP values, and there was a good correlation between the two variants [log RIP = 1.8 (±0.1) + 1.0 (±0.1) × log clay; $r = 0.64$; $n = 108$]. Including the silt content explains the 60% of the total variance [log RIP = 1.5 (±0.1) + 0.9 (±0.1) × log clay + 0.45 (±0.06) log silt]. When the organic soils were excluded from this analysis, the clay content alone explained up to 57% of the variance, with an improved correlation [log RIP = 2.1 (±0.1) + 0.95 (±0.09) × log clay; $r = 0.76$; $n = 86$], while the inclusion of the silt content increased this to 62% [log RIP = 1.6 (±0.2) + 0.8 (±0.1) × log clay + 0.5 (±0.3) log silt]. Although the RIP values could be predicted from clay and silt contents, the low explained variance and the limitations of the correlations suggest that quantifying the RIP leads to better estimates of K_d (Cs).

5. Conclusions and recommendations

A considerable amount of data has been added to the new K_d database compared to the previous TRS-364, despite the constraints applied to accept data. However, the large number of experimental approaches used to quantify K_d values is partially responsible for the wide ranges of values that can be found for a given radionuclide-soil type combination.

Focusing on radiostrontium and radiocaesium shows that soil–radionuclide interactions are governed by many factors that depend on the radionuclide and on various soil properties. Although the quality and quantity of mineral matter is one of the key soil properties governing radionuclide interaction, deriving K_d best estimates from soil groups based on soil texture and organic matter content is only a partially satisfactory approach for these radionuclides. It is thus recommended that wherever possible consideration and use be made of additional soil and radionuclide properties (cofactors), for better proposal of K_d best estimates with a lower variability. The main soil parameters (cofactors) governing the interaction should be measured and monitored to improve the prediction of K_d, and they should also be included in models of environmental decision support systems. As shown here, clear examples are RIP and K (and NH_4^+) status for radiocaesium; CEC and Ca and Mg concentrations for radiostrontium. When these data are available, modellers can straightforwardly calculate the values of K_d (Sr) and K_d (Cs) from well established correlations, rather than relying on best estimates derived from ranges of values for a given soil group.

Acknowledgements

This research was carried out in the frame of the IAEA' Programme on Environmental Modelling for Radiation Safety, EMRAS, within the Working Group "Revision of the TRS-364". The research was funded by the Spanish Government (CICYT, contracts PPQ2002-00264 and CTM2005-03847; Secretaría General para la Prevención de la Contaminación y el Cambio Climático del Ministerio de Medio Ambiente, contracts 1.2-193/2005/3-B and 240/2006/2-1.2).

References

ASTM, 2003. American Society for Testing and Materials D4646-03. Standard Test Method for 24-h Batch-type Measurement of Contaminant Sorption by Soils and Sediments. ASTM Publications, PA.

Benes, P., Stamberg, K., Stegmann, R., 1994. Study of the kinetics of the interaction of Cs-137 and Sr-85 with soils using a batch method: methodological problems. Radiochim. Acta 66/67, 315–321.

Brouwer, E., Baeyens, B., Maes, A., Cremers, A., 1983. Cesium and rubidium ion equilibria in illite clay. J. Phys. Chem. 87, 1213–1219.

Cremers, A., Elsen, A., De Preter, P., Maes, A., 1988. Quantitative analysis of radiocesium retention in soils. Nature 335, 247–249.

Fernández-Torrent, R., Vidal, M., Rauret, G., Rigol, A., 2005. Laboratory experiments to characterize radionuclide diffusion in soils. In: The 2nd International Conference on Radioactivity in the Environment. Aix-en-Provence, France.

García-Gutiérrez, M., Cormenzara, J.L., Missana, T., Mingarro, M., 2004. Diffusion coefficient and accessible porosity for HTO and $^{36}Cl^-$ in compacted FEBEX bentonite. Appl. Clay Sci. 26, 65–75.

Gil-García, C.J., Rigol, A., Rauret, G., Vidal, M., 2008. Radionuclide sorption-desorption pattern in soils from Spain. Appl. Radiat. Isot. 66, 126–138.

Goody, D.C., Shand, P., Kinniburgh, D.G., Van Riemsdijk, W.H., 1995. Field-based partition coefficients for trace elements in soil solutions. Eur. J. Soil Sci. 46, 265–285.

Hilton, J., Comans, R.N.J., 2001. Chemical forms of radionuclides and their quantification in environmental samples. In: Van derStricht, E., Kirchmann, R. (Eds.), Radioecology, Radioactivity and Ecosystems. Fortemps, Liège, pp. 99–111.

International Atomic Energy Agency. Handbook of Parameter Values for the Prediction of Radionuclide Transfer in Temperate Environments. Technical Report No 364. Vienna, 1994.

Montavon, G., Alhajji, E., Grambow, B., 2006. Study of the interaction of Ni^{2+} and Cs^+ on MX-80 bentonite. Effect of compaction using the capillary method. Environ. Sci. Technol. 40, 4672–4679.

Ochs, M., Lothenbach, B., Wanner, H., Sato, H., Yui, M., 2001. An integrated sorption–diffusion model for the calculation of consistent distribution and diffusion coefficients in compacted bentonite. J. Contam. Hydrol. 47, 283–296.

OECD, 2000. OECD Guideline 106. Guideline for the testing of chemicals: Adsorption–desorption using a batch equilibrium method.

Okamoto, A., Idemitsu, K., Furuya, H., Inagaki, Y., Arima, T., 1999. Distribution coefficients and apparent diffusion coefficients of caesium in compacted bentonites. Mater. Res. Sou. Symp. Proc. 556, 1091–1098.

Rauret, G., Firsakova, S., 1996. The Transfer of Radionuclides through the Terrestrial Environment to Agricultural Products, including the Evaluation of Agrochemical Practices. EUR 16528 EN. European Commission, Luxembourg.

Rigol, A., Vidal, M., Rauret, G., Shand, C.A., Cheshire, M.V., 1998. Competition of organic and mineral phases in radiocaesium partitioning in organic soils of Scotland and the area near Chernobyl. Environ. Sci. Technol. 32, 663–669.

Sanchez, A.L., Smolders, E., Van den Brande, K., Merckx, R., Wright, S.M., Naylor, C., 2002. Predictions of in situ solid/liquid distribution of radiocaesium in soils. J. Environ. Radioact. 63, 35–47.

Sheppard, M.I., Thibault, D.H., 1990. Default soil solid/liquid partition coefficients, K_ds, for four major soil types: a compendium. Health Phys. 59, 471–482.

Staunton, S., 2004. Sensitivity of the distribution coefficient, K_d, of nickel to changing soil chemical properties. Geoderma 122, 281–290.

Sweeck, L., Wauters, J., Valcke, E., Cremers, A., 1990. The specific interception potential of soils for radiocesium. EUR 12448. In: Desmet, G., Nassimbeni, P., Belli, M. (Eds.), Transfer of Radionuclides in Natural and Seminatural Environments. Elsevier Applied Science, pp. 249–258.

Thibault, D.H., Sheppard, M.T., Smith, P.A., 1990. A Critical Compilation and Review of Default Soil Solid/Liquid Partition Coefficients, K_d, for Use in Environmental Assessments. AECL 10125. Atomic Energy of Canada Limited, Pinawa, Manitoba Canada, 113 pp.

Valcke, E., 1993. The Behaviour Dynamics of Radiocesium and Radiostrontium in Soils Rich in Organic Matter. Doctoral thesis. Katholieke Universiteit Leuven, Belgium.

Vidal, M., Roig, M., Rigol, A., Llauradó, M., Rauret, G., Wauters, J., Elsen, A., Cremers, A., 1995. Two approaches to the study of radiocaesium partitioning and mobility in agricultural soils from the Chernobyl area. Analyst 120, 1785–1791.

Waegeneers, N., Smolders, E., Merckx, R., 1999. A statistical approach for estimating the radiocesium interception potential of soils. J. Environ. Qual. 28, 1005–1011.

Wang, X.K., Montavon, G., Grambow, B., 2003. A new experimental design to investigate the concentration dependent diffusion of Eu(III) in compacted bentonite. J. Radioanal. Nucl. Chem. 257, 293–297.

Wauters, J., Elsen, A., Cremers, A., Konoplev, A., Bulgakov, A.A., Comans, R.N.J., 1996a. Prediction of solid liquid distribution coefficients of radiocaesium in soils and sediments. Part one: a simplified procedure for the solid phase characterization. Appl. Geochem. 11, 589–594.

Wauters, J., Vidal, M., Elsen, A., Cremers, A., 1996b. Prediction of solid liquid distribution coefficients of radiocaesium in soils and sediments. Part two: a new procedure for solid phase speciation of radiocaesium. Appl. Geochem. 11, 595–599.

Yasuda, H., Uchida, S., 1993. Statistical approach for the estimation of strontium distribution coefficient. Environ. Sci. Technol. 27, 2462–2465.

3.3

New best estimates for radionuclide solid–liquid distribution coefficients in soils. Part 2. Naturally occurring radionuclides

H. Vandenhove, C. J. Gil-García, A. Rigol, M. Vidal.

Journal of Environmental Radioactivity, 100, 697–703, 2009

Páginas 101-108

Journal of Environmental Radioactivity 100 (2009) 697–703

Contents lists available at ScienceDirect

Journal of Environmental Radioactivity

journal homepage: www.elsevier.com/locate/jenvrad

New best estimates for radionuclide solid–liquid distribution coefficients in soils. Part 2. Naturally occurring radionuclides

H. Vandenhove [a,*], C. Gil-García [b], A. Rigol [b], M. Vidal [b]

[a] Belgian Nuclear Research Centre, Biosphere Impact Studies, Boeretang 200, 2400 Mol, Antwerp, Belgium
[b] University of Barcelona, Barcelona, Spain

ARTICLE INFO

Article history:
Received 22 August 2007
Received in revised form
11 March 2009
Accepted 13 March 2009
Available online 18 April 2009

Keywords:
Lead
pH
Polonium
Radium
Soil
Solid liquid distribution coefficient
Thorium
Uranium

ABSTRACT

Predicting the transfer of radionuclides in the environment for normal release, accidental, disposal or remediation scenarios in order to assess exposure requires the availability of an important number of generic parameter values. One of the key parameters in environmental assessment is the solid liquid distribution coefficient, K_d, which is used to predict radionuclide–soil interaction and subsequent radionuclide transport in the soil column. This article presents a review of K_d values for uranium, radium, lead, polonium and thorium based on an extensive literature survey, including recent publications. The K_d estimates were presented per soil groups defined by their texture and organic matter content (Sand, Loam, Clay and Organic), although the texture class seemed not to significantly affect K_d. Where relevant, other K_d classification systems are proposed and correlations with soil parameters are highlighted. The K_d values obtained in this compilation are compared with earlier review data.

1. Introduction

Naturally occurring radionuclides are present in many natural resources. High concentrations of these radionuclides are often found in certain geological materials, namely igneous rocks and ores. Human activities that exploit these resources may lead to enhanced concentrations of naturally occurring radionuclide materials (NORM) and (or) enhanced potential for exposure to NORM in products, by-products and wastes. Activities involving the extraction, exploitation and processing of materials containing NORM include the mining and processing of uranium and metal ores, the combustion of fossil fuels, production of natural gas and oil, and the phosphate industry. If wastes containing NORM are not properly managed, large areas of contamination can result, due to the large quantities of wastes associated with these activities (IAEA, 2003). NORM-containing wastes from outside the nuclear fuel cycle have received increasing attention lately, due not only to the existing large amounts, but to the potential long-term hazards resulting from the fact that NORM comprise long-lived radionuclides with relatively high radiotoxicities (IAEA, 2003).

The radionuclides present at these sites can enter the food chain directly via the soil–plant–animal pathway, or indirectly by the use of contaminated groundwater or surface water for irrigation purposes or drinking water. To assess the uptake in the food chain and by biota in general and to predict human exposure, knowledge on the environmental parameters governing radionuclide mobility and uptake is indispensable.

The solid–liquid distribution coefficient, K_d (the ratio of the concentration of the radionuclide in the soil solid phase to the concentration in the (soil) solution, L kg^{-1}), describes the sorption processes that control radionuclide interaction in soils, thus affecting subsequent radionuclide transport in the soil profile and radionuclide accumulation in surface soils. Sorption is element and soil-type dependent, and is affected by soil mineralogy (e.g. clay content and type, iron oxides and hydroxides), organic matter content and soil geochemistry (pH, presence of colloids, presence of counter-ions, …), and by the experimental method used for its quantification. The K_d is based on the equilibrium concept. It relies on the hypothesis that the radionuclide on the solid phase is in equilibrium with the radionuclide in solution, and thus can exchange with it. However, elapse time since the addition of the radionuclide is known to affect the value of K_d, since a fraction of the added radionuclide may become fixed by the solid phase (an aging effect related to sorption dynamics). Most laboratory tests

* Corresponding author. Tel.: +32 14332114; fax: +32 14321056.
E-mail address: hvandenh@sckcen.be (H. Vandenhove).

0265-931X/$ – see front matter © 2009 Elsevier Ltd. All rights reserved.
doi:10.1016/j.jenvrad.2009.03.014

are, in principle, designed to obtain the so-called exchangeable K_d (K_d^{exch}). However, a K_d deduced from a laboratory test cannot be unequivocally considered to be a K_d^{exch}, since the nature of the sorption process for a given radionuclide may lead to a *quasi* instantaneous irreversible sorption, and, in other cases, long contact times, for instance, may result in a fraction of the radionuclide activity becoming irreversible sorbed, and thus no longer participating in the soil – soil solution equilibria (Gil-Garcia et al., 2009). Besides for trace experiments, only pseudo-equilibrium may be reached as sorption processes associated with the absorption on clay lattices can be slow and equilibrium may not be reached during the time available for the experiments. Hence, the large number of approaches used to quantify K_d values, and the contrasting experimental conditions applied in each case, lead to wide ranges of K_d values being obtained for similar soil and radionuclide combinations. The variation in approaches adopted often makes it difficult to compare among K_d values derived from laboratory experiments.

For field experiments, the K_d values can be quantified from the radionuclide concentration in the soil solid phase divided by the concentration of the radionuclide in the soil solution obtained from the contaminated soil (Gooddy et al., 1995). This approach may lead to K_d values higher than those resulting from a laboratory sorption test, because the radionuclide quantified in the solid phase of the contaminated soil may include sorbed radionuclide not available for exchange with the soil solution due to the time elapsed since the radionuclide incorporation.

This paper is Part 2 of a series of three papers, in which we propose new best estimates of K_d for a high number of radionuclides, in the frame of the activities of a Working Group addressing the revision of the *Handbook of Parameter Values for the Prediction of Radionuclide Transfer in Temperate Environments* – TRS-364 (IAEA, 1994), within the IAEA-EMRAS programme. Here emphasis is given to uranium (U), radium (Ra), lead (Pb), polonium (Po) and thorium (Th). The new K_d estimates should be suitable for use in probabilistic assessment of radionuclide fate in soils. Though these generic data are perhaps not useful to assess site-specific impact, they may be useful for preliminary or screening assessments. Besides obtaining the K_d best estimates for soils grouped on the basis of their texture (sand and clay percentages in the mineral matter) and organic matter content, this paper also attempts to elucidate other soil properties responsible for radionuclide interaction in soils. These other properties, alone or combined with textural information, can be used as cofactors for classification of soils in order to reduce the variability of the derived K_d best estimates.

2. Data collection and treatment

2.1. Data collection and data acceptance

Literature collection consisted on peer-reviewed publications as well as reports. About 30 references were retained after a critical reading and data were retained/excluded based on a number of constraints. These references are reported in Annex. Data were only accepted if the measurements were done under relevant and realistic conditions (e.g. the K_d values obtained under extreme salt concentrations were excluded). Only K_d values reported for soils were considered, and K_d values obtained for pure phases (e.g. minerals, humic and fulvic acids), sediments or for special substrates (e.g. U-rocks, U-tailings, sludge from the phosphate industry) were excluded. No *in situ* K_d data for soils in vicinity of NORM extraction or exploitation areas were included. Similarly, K_d values derived from chemical extractions were neither considered. Summary data from reviews were also excluded, except where mentioned. The minimal soil information required for K_d data to be accepted was the concentration of radionuclides in the soil and the contamination type. The reported and collected K_d should best be referred to as apparent K_d as equilibrium may not always be the case.

Additionally to K_d data, information was collected on experimental conditions for sorption tests, soil type, pH, sand and clay content, organic matter content, cation exchange capacity (CEC), E_h, $CaCO_3$ content, amorphous Fe content, exchangeable Ca and Mg and soil solution concentrations of HCO_3^-, Ca^{2+} and Mg^{2+}.

The increased knowledge of interaction mechanisms between certain radionuclides and solid materials allows reviewing K_d values in terms of a more fundamental description of underlying processes. Soil *cofactors* that influence soil–radionuclide interactions may be identified as K_d categorization factors. Such soil grouping based on cofactors may result in a decreased variability of K_d compared to the variability observed when the classification is based solely on sand, clay and organic matter contents. For the different radionuclides evaluated in this study, several soil factors were screened for their suitability as co-factor. The pH was retained as suitable cofactor for grouping K_d(U), K_d(Th) and K_d(Pb).

2.2. Data treatment and statistical analysis

As in the other papers of the series, the K_d values were grouped according to two criteria. Soils were initially grouped according to the sand and clay contents, referred to the mineral matter, and organic matter (OM) content, as in the former TRS-364. This defined the 'texture/OM' criterion. The thresholds to define each soil group were accepted by the Working Group. In short, a soil was included in the Organic group if the organic matter content was $\geq$20%. For the mineral soils, three groups were created according to the following criteria: Sand group: sand fraction $\geq$65%; clay fraction $<$18%; Clay group: clay fraction $\geq$35%; Loam group: rest of cases. Additionally, an Unspecified group was designed for mineral soils with unknown sand and clay contents, or soils with unknown characteristics.

Soils were also grouped in specific cases according to a second criterion regarding specific soil factors governing the radionuclide–soil interaction ('cofactor' criterion). The cofactor depended on the radionuclide considered, and permitted to decrease the variability of K_d ranges for a given soil group. The most important cofactor used here was the soil pH.

For all groups considered, the following dataset descriptors were calculated: geometric mean (GM), geometric standard deviation (GSD), arithmetical mean (AM), standard deviation (SD), minimum (min) and maximum (max) values. The GM and GSD are preferred to AM and SD since K_d values are generally log-normally distributed (distribution is normal after log-transformation of the data), although GM and GSD were only calculated if the number of observations (n) was higher than 2. The number of observations is given, together with the number of references serving as data sources.

Statistical analysis of data was performed with the statistical software packages *Statistica for Windows* (Statsoft, 2004). Outlier analysis was performed using box–whisker plots. A value was defined an outlier if it was over 1.5-times the interquartile range (for the log-transformed data). Significant differences were considered at $p = 0.05$, and mean values were ranked by Tukey's multiple range tests when more than two groups were compared with ANOVA. Correlations between K_d or log K_d and soil parameters were considered significant if $p < 0.05$. Multiple regression analysis was performed with the stepwise backward, stepwise forward or standard method.

3. Description of ranges of K_d values: derivation of K_d best estimates

3.1. The case of uranium

3.1.1. Best estimates of K_d(U) for soils grouped according to the texture/OM criterion

About 20 references were identified that reported a total of 178 observations for the sorption of uranium onto soils. This is a larger number than the 45 observations compiled by Sheppard and Thibault (1990), reported in the former TRS-364 (IAEA, 1994). Table 1 shows the K_d(U) for soils grouped according to texture and organic matter criterion. The ranges within one soil group have a variability from 2 to 5 orders of magnitude, while the GM differed among soil groups maximum a factor of 40. Clay soils showed the lowest K_d, while the Organic group had the highest. The K_d GM were not significantly different between all soil groups, thus suggesting that grouping the K_d values for different soil types was statistically not fully justified since the K_d(U) was little affected by soil texture.

Sheppard et al. (2006) compiled the K_d(U) values for soils within a pH range of 4–8.8, and they recommended K_d(U) values of 40, 200, 200 and 2000 L kg^{-1}, for Sand, Loam, Clay, and Organic soils, respectively. The present data collection included soils with the pH range of 2–12. Recalculating the GM values with the K_d data from 4 to 8.8 range, the resulting K_d(U) estimates were 170, 380, 30, 1800 L kg^{-1}, thus indicating that the pattern shown in Table 1 was not changed. The recommended values in the former TRS-364 were, respectively, 33, 12, 1500 and 400 L kg^{-1}. Overall, the largest discrepancies were observed for Clay soils. A reason for that may be that under present data compilation estimates were based on a larger number of observations (for TRS-364, the K_d estimate for the Clay group was derived from 7 observations) and only data representative for soils were assembled, excluding data obtained for other materials, such as sediments and pure mineral phases. In earlier compilations (Sheppard and Thibault, 1990; Sheppard et al., 2006) also K_d(U) values for non-soils (e.g. pure clays) were included.

3.1.2. Soil variables affecting K_d(U)

As the differences in experimental conditions cause minor changes in K_d(U), a significant amount of variability can be attributed to the fact that uranium sorption is affected by soil properties other than soil texture such as pH, content of amorphous iron oxides, soil organic matter content, cation exchange capacity, and phosphate status (EPA, 1999).

EPA (1999) performed an extensive review of K_d(U) values for soils, crushed rock material and single-mineral phases, which indicated that pH and dissolved carbonate concentrations were the two most important factors influencing the sorption behaviour of U(VI), which is the dominant U species in agricultural soils. At pH below 5, U(VI) is present as the uranyl ion, UO_2^{2+}. At a higher pH, the uranyl ion hydrolyzes, forming a number of aqueous hydroxide complexes, which dominate U(VI) speciation in the absence of dissolved inorganic ligands (carbonate, fluoride, sulphate and phosphate). At the pH range of 6–10, highly soluble carbonate complexes dominate (the acid biphosphate, bicarbonate and tricarbonate) (Langmuir, 1978). Since U speciation is related to pH, the K_d(U) values show a specific trend in relation to the pH. In general, the sorption of uranium by soils is low at pH values less than 3, increases rapidly with increasing pH from 3 to 5, reaches a maximum in the pH range from 5 to 7, and then decreases with increasing pH at pH values greater than 7 (EPA, 1999). Table 2 presents the K_d(U) values collected in the present dataset grouped according to 3 pH-categories. These three pH categories were selected based on the U chemistry and related sorption behaviour and since further breaking up in pH categories (e.g. 3–5, 5–6, 6–7, >7) did not result in significant differences between additional groups (e.g. between 5–6 and 6–7 pH-groups). A significant 10-fold higher K_d(U) value is observed for the 5–7 pH range. Though significantly different K_d values can be assigned to the pH categories, data variability was as high as 3–4 orders of magnitude.

Echevarria et al. (2001) also explored the effect of soil characteristics on U sorption. They found no significant effect of clay or organic matter. However, they did find a significant relation between soil K_d and pH. For soils in 5.5–8.8 pH range they deduced a linear relationship: $\log K_d = -1.29\ (\pm 0.17) \times \mathrm{pH} + 11.0\ (\pm 1.2)$, $R^2 = 0.76$. Vandenhove et al. (2007) examined the effect of soil pH on uranium availability for 18 spiked soils, and a similar linear decrease of $\log K_d$ with pH was observed for soils with pH ≥ 6 [$\log K_d = -1.18 \times \mathrm{pH} + 10.8$, $R^2 = 0.65$], which was explained by the increased amount of soluble uranyl–carbonate complexes at high pH. Sheppard et al. (2006) found the following correlation for soils with pH ranging from 5.5 to 8.8: $\log K_d = -1.07\ (\pm 0.13) \times \mathrm{pH} + 9.8\ (\pm 0.9)$, $R^2 = 0.41$.

Based on the K_d(U) values compiled for the present dataset and solely considering soils in the 5.5–8.8 pH range (as Echevarria et al., 2001 and Sheppard et al., 2006) the regression equation was $\log K_d = -0.77\ (\pm 0.11) \times \mathrm{pH} + 7.7\ (\pm 0.7)$, $R^2 = 0.30$ ($p < <0.001$) ($n = 110$) (Fig. 1). The correlation parameters are in agreement with those found by the above authors. The smaller R^2 (0.30) than that obtained by Echevarria et al. (2001) and Vandenhove et al. (2007) is quite understandable since this compilation contains many different experimental protocols (and experimenters) for obtaining K_d values. Hence, for soils with a pH applicable for agricultural soils, K_d can be predicted according to the observed linear pH-dependence of $\log K_d$. For pH < 5.5, only 20% of the variation in $\log K_d$ is explained by pH (Fig. 1).

The relative low percentage of explained variance by the K_d(U)–pH correlation indicated that the K_d(U) cannot be univariantly predicted in our dataset from pH variation. Significant sources of variability in the relationship between K_d(U) and pH are the heterogeneity in soil mineralogy (e.g. soils containing larger percentages of iron oxide minerals and mineral coatings, and/or clay minerals exhibit higher sorption than soils dominated by

Table 1
K_d(U) (L kg^{-1}) for soils grouped according to the texture/OM criterion. Number of entries (n), geometric mean (GM), geometric standard deviation (GSD), arithmetical mean (AM), standard deviation (SD), minimum (min) and maximum (max) values and number of references from which entries were extracted (# ref).

Soil group	n	GM	GSD	AM	SD	min	max	# ref
All soils	178	200	12	200	6700	0.7	66,667	22
Sand	50	110^{bc,*}	12	2100	9500	0.7	66,667	8
Loam	84	310^{ab}	12	2500	6300	0.9	38,710	12
Clay	12	28^{c}	7	120	170	3	480	3
Organic	9	1200^{a}	6	2900	2800	33	7600	7
Unspecified	23	170^{abc}	6	860	1700	16	6200	5

* Values with different letters are significantly different at $p < 0.05$.

Table 2
K_d(U) (L kg^{-1}) classified according to pH. Number of entries (n), geometric mean (GM), geometric standard deviation (GSD), arithmetical mean (AM), standard deviation (SD), minimum (min) and maximum (max) values and number of references from which entries were extracted (# ref).

Soil group	n	GM	GSD	AM	SD	min	max	# ref
pH < 5	36	71^{b,*}	11	540	1200	0.7	6700	16
5 ≤ pH < 7	77	740^{a}	8	4000	9800	2.6	66,667	17
pH ≥ 7	61	68^{b}	8	450	1100	0.9	6160	14

* Values with different letters are significantly different at $p < 0.05$.

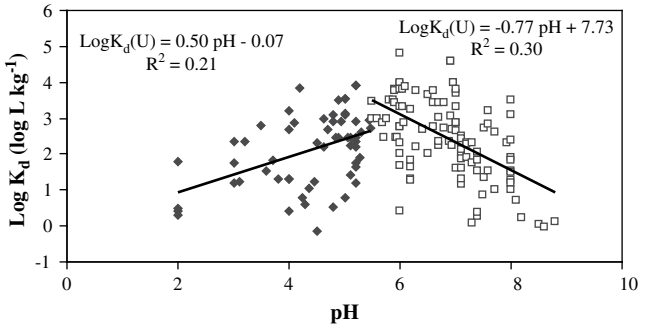

Fig. 1. Log K_d(U) (L kg^{-1}) as function of pH.

quartz and feldspar minerals (EPA, 1999) and the organic matter content).

Many studies corroborate the importance of iron oxides/hydroxides for the adsorption of U (Hsi and Langmuir, 1985; Waite et al., 1994; Duff and Amrhein, 1996; Payne et al., 1996). The positively charged U-species are sorbed to the negatively charged surfaces of the sesquioxides or U-species become structurally incorporated in the iron-oxides (coatings) over the many dissolution–precipitation cycles of these amorphous or poorly crystalline iron oxides (Sowder et al., 2003).

Organic matter and clay minerals provide exchange sites and as such are expected to increase sorption of UO_2^{2+} and other positively-valent U-forms. The influence of organic matter (OM) on U mobility is twofold: a decreased mobility through sorption by exchange and an increased mobility following formation of organic complexes and colloids. In absence of large amounts of organic matter and clay, U is considered to be relatively mobile. The role of humic substances in the mobility of U^{+6} was investigated for a sandy podzol (Crançon and van der Lee, 2003). Uranium was found to be strongly retained by the bulk soil mainly due to organic aggregates and organic coatings on quartz. A large fraction of U^{+6} was found to be associated to humic colloids in soil, thus forming a potential mobile uranium phase.

For soils with pH < 6, Vandenhove et al. (2007) reported very significant correlations between K_d(U) and organic matter [$K_d(U) = 1963 \times OM - 5432$, $R^2 = 0.78$], and amorphous iron content [$K_d(U) = 1.02 \times Fe_{amorphous} + 1691$, $R^2 = 0.88$]. Considering the whole pH domain, these relationships remained significant [$K_d(U) = 1591 \times OM - 3362$, $R^2 = 0.70$; $K_d(U) = 1.08 \times Fe_{amorphous} + 2783$, $R^2 = 0.88$]. For the present compilation for all soils or for soils with pH < 6, OM did not explained K_d observed (log K_d vs OM: $R^2 = 0.02$; K_d vs OM: $R^2 = 0.002$). Also the amount of amorphous iron oxides and hydroxides did not explain the observed K_d ($R^2 < 0.02$).

Additional single and multiple regression analyses were performed with the present data compilation, but no additional significant correlations were obtained.

For U we would hence recommend the following K_d values (L kg^{-1}) (GSD between brackets): 70 (10) for soils of pH < 5 or pH ≥ 7 and 750 (8) for soils of 5 ≤ pH < 7. Alternatively, for soils with a pH adequate for agricultural practice (5.5–8.8), K_d could be predicted using the regression equation $\log K_d(U) = -0.77\ (\pm 0.11) \times pH + 7.7\ (\pm 0.7)$.

3.2. The case of radium

3.2.1. Best estimates of K_d(Ra) for soils grouped according to the texture/OM criterion

Only 7 references were identified that reported suitable K_d(Ra) values (total of 51 entries) for soils following the constraints set to compile the present dataset. Earlier reviews contained even fewer entries (Sheppard and Thibault (1990) reported in IAEA (1994): 15 observations; and Sheppard et al. (2006): comprising 37 observations).

Table 3 shows K_d values for Ra classified according to the texture and organic matter criterion. Geometric means were highest for Clay soils and lowest for Loam soils. Considering the high affinity of Ra for the regular exchange sites (Simon and Ibrahim, 1990), the higher K_d(Ra) value observed for Clay soils than for Loam soils can be explained by the generally higher CEC of clay soils, which thus have a higher sorption capacity.

K_d(Ra) estimates were generally not significantly different between soil groups, due to a variability of 2–5 orders of magnitude. For Clay soils and especially for Organic soils very low numbers of K_d were available which makes it difficult to deduce best estimates for these groups.

Sheppard et al. (2006) recommended a K_d(Ra) value of 47 L kg^{-1} irrespective of soil type. The overall geometric mean observed in the present compilation (2500 L kg^{-1}) is about 2 orders of magnitude higher. Sheppard et al. (2006) proposed a downward revision of the former TRS-364 estimates, where values of 490, 36,000, 9000 and 2400 L kg^{-1} were recommended for Sand, Loam, Clay, and Organic groups, respectively.

3.2.2. Soil variables affecting the K_d(Ra)

As radium occurs in the environment as a divalent cation, with a high affinity for regular exchange sites, in geochemical equilibrium models, often data for barium, which may act as analogue, are recommended for assessing the behaviour of radium. Simon and Ibrahim (1990) reported that organic matter sorbs about 10 times as much radium as clay. Vandenhove and Van Hees (2007) exploring the effect of soil properties on the radium availability in a small-scale study covering 8 soils, concluded that K_d(Ra) could be predicted by CEC [$K_d(Ra) = 0.71 \times CEC - 0.64$, $R^2 = 0.3$] and soil organic matter content [$K_d(Ra) = 27 \times OM - 27$, $R^2 = 0.4$]. However, these correlations were not significant with the K_d(Ra) values of the present compilation. Multiple regression analysis didn't either result in significant regressions.

Calcium levels in the soil solution or exchangeable phase significantly affect the K_d(Ra) values. This is illustrated by the extremely high K_d(Ra) values recorded by Nathwani and Phillips (1979) when they measured K_d(Ra) values in soils equilibrated with a 0.025 mM Ca^{2+} solution, whereas in common agricultural soils the soil pore water contains a 100–1000 times higher Ca^{2+} concentration. Table 3 also shows the geometric means and ranges recalculated when excluding these data, which led to a significant reduction of the variability. Insufficient entries for soil solution

Table 3
K_d(Ra) (L kg^{-1}) for soils grouped according to the texture/OM criterion. Number of entries (n), geometric mean (GM), geometric standard deviation (GSD), arithmetical mean (AM), standard deviation (SD), minimum (min) and maximum (max) values and number of references from which entries were extracted (# ref).

Soil group	n	GM	GSD	AM/value	SD	min	max	# ref
All soils	51	2500	13	34,000	130,000	12	950,000	8
All soils*	47	1800	10	11,000	21,000	12	100,000	7
Sand	20	3100[ab]	8	9600	12,000	49	40,000	4
Loam	19	1100[b]	17	15,000	32,000	12	120,000	5
Loam*	17	710	14	8600	20,000	12	80,000	4
Clay	6	38,000[a]	12	200,000	37,000	696	950,000	3
Clay*	4	13,000	10	41,000	47,000	696	100,000	2
Organic	1			200				1
Unspecified	4	1200	1	1300	500	785	1890	1

* K_d estimates excluding the data from Nathwani and Phillips (1979) with very low Ca^{2+} concentration in external solution; values with different letters are significantly different at $p < 0.05$.

concentrations of Ca were available to assess the impact of Ca-concentration on K_d(Ra). For 60% of entries information was available on exchangeable Ca and Mg content, but these parameters did not significantly explain the variation in the K_d(Ra) observed.

The classification of K_d values by soil group does not result in significant differences between the soil classes. However, a more suitable parameter for classifying K_d values (pH, CEC, OM) could not be suggested either. Additional research to collate K_d(Ra) values, especially for clayey and organic soils is recommended. Furthermore, a more methodical soil characterisation is advised in order to be able to deduce the processes ruling radium sorption and to allow for prediction of K_d(Ra) from soil parameters.

3.3. The case of lead

3.3.1. Best estimates of K_d(Pb) for soils grouped according to the texture/OM criterion

The main source of ^{210}Pb in the environment is from the decay of ^{222}Rn gas evolved from the soil into the atmosphere, with a subsequent deposit on the soil in association with aerosols via washouts and sedimentation. Other sources include burning of fossil fuels, phosphate fertilizers and tetraethyl lead in petrol. Several sources have reported that superphosphate fertilizers contain significant concentrations of ^{210}Pb (Amaral et al., 1992). Lead has three known oxidations states 0, +2, and +4, but the most common redox state encountered in the environment is the divalent form. Lead sorption increases with increasing pH and by the amount of clays, oxides, hydroxides and organic matter (EPA, 1999). Anionic constituents may influence sorption by formation of precipitates of minerals or by reducing sorption through complex formation.

Table 4 summarizes the K_d(Pb) for soils grouped according to the texture and organic matter criterion. Only a very few references reporting K_d(Pb) values for Pb radioisotopes were found. The K_d(Pb) estimate for the Sand group was significantly different from the GM of the other soil groups. The GM reported in the former TRS-364 (13 entries) were 270, 16,000, 540 and 22,000 L kg^{-1}, respectively, for Sand, Loam, Clay, and Organic soils. For present compilation, estimates are hence higher for the Clay group, lower for Organic soils, and similar for Sand and Loam groups.

3.3.2. The effect of pH on the K_d(Pb)

Soil pH is reported to be the most important factor controlling lead mobility (EPA, 1999). Rieuwerts et al. (2006) reported that a regression analysis showed that pH accounted for 68% of the variance in the Pb fraction extracted with $CaCl_2$. A significant correlation was found between log K_d(Pb) and pH [log K_d(Pb) = 0.37 (±0.08) × pH + 1.25 (±0.45), $R^2 = 0.52$, $p = 0.002$, $n = 21$] (Fig. 2).

Table 4
K_d(Pb) (L kg^{-1}) for soils classified according to the texture/OM and pH criteria. Number of entries (n), geometric mean (GM), geometric standard deviation (GSD), arithmetical mean (AM), standard deviation (SD), minimum (min) and maximum (max) values and number of references from which entries were extracted (# ref).

Soil group	n	GM	GSD	AM	SD	Min	max	# ref
All soils	23	2100	10	15,000	33,000	25	127,544	5
Sand	9	220	4	400	430	25	1349	2
Loam	5	10,000	3	15,000	16,000	3600	43,000	2
Clay	2			66,000	86,000	5396	127,544	2
Organic	5	2500	3	3700	3800	880	10,266	2
Unspecified	2			59,000	61,000	15,849	102,410	2
3 ≤ pH ≤ 6.4	13	570[b,*]	6	1519	1870	25	6200	2
6.4 < pH ≤ 8.3	8	7900[a]	7	26,329	43,062	301	127,544	3

* Values with different letters are significantly different at $p < 0.05$.

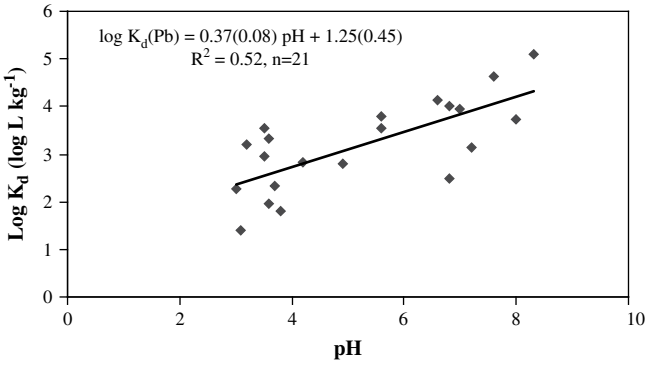

Fig. 2. Dependence of log K_d(Pb) (L kg^{-1}) on pH.

EPA (1999) reported a K_d(Pb) look-up table in function of pH. Table 4 also includes the K_d(Pb) estimates from data of the present compilation for similar pH ranges to those defined by EPA (1999). These GM values correspond within a factor two with the GM calculated with the values of the EPA data, it is, respectively 940 and 3342 L kg^{-1} for the 4.0–6.3 and for the 6.4–8.7 pH range. The EPA dataset includes data from stable and radioactive Pb species.

For Pb we recommend K_d estimates based on the pH classification criterion or to calculate K_d with the regression equation presented in Fig. 2.

Correlations between any other soil characteristic and (log)K_d(Pb) were not significant.

3.4. The case of polonium

3.4.1. Best estimates of K_d(Po) for soils grouped according to the texture/OM criterion

As described for Pb, polonium (^{210}Po) originates mostly from ^{222}Rn, fossil fuels, and superphosphate fertilizers (Amaral et al., 1992). Only two references were found recording K_d(Po) data. Most data are for Loam and Sand groups, with values not statistically different (Table 5). For Clay and Organic soils, the number of data is too limited to be able to propose best estimates. Therefore, a K_d(Po) value of 200 L kg^{-1} can be recommended irrespective of soil type. Values from the former TRS-364 (with 51 observations) were 150, 400, 2700 and 6600, for Sand, Loam, Clay, and Organic soils, respectively. Values were very much in agreement since they were based on virtually the same references (Hansen and Watters, 1971), although now subsoil data were excluded.

3.4.2. Soil variables affecting the K_d(Po)

Regarding correlations between soil variables and K_d(Po), 18% of the variation in log K_d(Po) was explained by pH (log K_d(Po) = 0.22 (±0.70) + 0.33 (±0.11) × pH, $R^2 = 0.18$, $p = 0.006$, $n = 42$) and 24% of

Table 5
K_d(Po) (L kg^{-1}) for soils classified according to the texture/OM criterion. Number of entries (n), geometric mean (GM), geometric standard deviation (GSD), arithmetical mean (AM), standard deviation (SD), minimum (min) and maximum (max) values and number of references from which entries were extracted (# ref).

Soil group	n	GM	GSD	AM/value	SD	min	max	# ref
All soils	42	180	5	560	1140	12	7020	1
Sand	14	100	6	740	1900	17	7020	1
Loam	27	230	4	460	460	12	1830	1
Clay	1			732				1

the variation was explained by clay content ($\log K_d(Po) = 1.75\ (\pm 0.19) + 0.034\ (\pm 0.010) \times$ Clay, $R^2 = 0.24$, $p = 0.002$, $n = 40$). No correlation was observed between K_d(Po) and CEC alone, as observed previously (Hansen and Watters, 1971).

Further research is required to assemble additional K_d(Po) values (especially for Clay and Organic soils) together with relevant soil parameters (pH, texture, OM, CEC) in order to better understand processes ruling Po sorption and to predict Po sorption from soil parameters.

3.5. The case of thorium

3.5.1. Best estimates of K_d(Th) for soils grouped according to the texture/OM criterion

Table 6 shows K_d(Th) estimates for soils grouped according to the texture and organic matter criterion. The GM of K_d(Th) were low for Sand and Organic soils, and high for Loam soils. Only GM of Sand and Loam soils were significantly different. Within each soil group there was a large variability from 2 to 4 orders of magnitude. The former TRS-364 report (19 entries) best estimates were 3000, 3300, 5400, and 89,000 for Sand, Loam, Clay, and Organic soil, respectively. The high value for the organic group is due to inclusion of very high K_d(Th) values (up to 8.8×10^4 L kg^{-1}) most probably resulting from data including precipitation reactions (see below).

3.5.2. Soil variables affecting the K_d(Th)

More than 99% of natural thorium exists in the form of ^{232}Th. Thorium occurs only in the +4 oxidation state in nature. In natural waters the concentrations of dissolved thorium are very low. Thorium can form various aqueous complexes with inorganic anions such as dissolved carbonate, phosphate, nitrate, which will increase the concentration of dissolved thorium. Thorium containing minerals, such as thorite, monazite and zircon, do not dissolve readily in low-temperature surface and groundwater (EPA, 1999 and references therein). The maximum concentration of dissolved thorium that may occur in low-temperature aqueous systems can be predicted by the solubility of hydrous thorium oxide (Ryan and Rai, 1987).

Iron and manganese oxides are expected to be more important adsorbents for thorium than silica. Humic substances are considered particularly important in Th sorption. But the very high K_d(Th) values reported by Thibault et al. (1990) and by Sheppard and Thibault (1990) for organic soils (up to 8.8×10^8 L kg^{-1}) should be viewed with caution according to EPA (1999) due to precipitation of thorium compounds.

Based on two simplifying assumptions [Th precipitates at concentrations larger than 10^{-9} M (at $10^{-2.6}$ M if pH < 5), and that for lower concentrations Th sorption can be predicted by pH], EPA (1999) proposed a K_d(Th) look-up table with a rough K_d(Th) estimate of 300,000 L kg^{-1} if Th concentrations exceed 10^{-9} M (or $10^{-2.6}$ M if pH < 5), and a range of K_d(Th) depending on pH. After rearranging the data of the present compilation in a similar way, and excluding data from *in situ* K_d(Th) (in which Th is expected to be part of the solid mineral phases, thus leading to higher K_d(Th) values), the ranges of the K_d(Th) corresponded well with the observations by EPA (1999) (Table 7).

Based on data from present compilation and on the pH effect on K_d(Th), we would recommend the following K_d(Th) estimates (L kg^{-1}) (GSD between brackets): 1000 (15), 3000 (8) and 300 (7) for the pH groups pH < 5, 5 ≤ pH < 8, pH ≥ 8, respectively.

Table 6
K_d(Th) (L kg^{-1}) for soils classified according to the texture/OM criterion. Number of entries (n), geometric mean (GM), geometric standard deviation (GSD), arithmetical mean (AM), standard deviation (SD), minimum (min) and maximum (max) values and number of references from which entries were extracted (# ref).

Soil group	n	GM	GSD	AM	SD	min	max	# ref
All soils	46	1900	10	16,000	42,000	19	250,000	8
Sand	12	700^{b,*}	11	10,000	28,000	35	100,000	3
Loam	6	18,000^{a}	4	53,000	97,000	5000	250,000	2
Clay	7	4500^{ab}	3	7400	8000	800	24,000	2
Organic	5	730^{ab}	44	19,000	35,000	19	80,000	3
Unspecified	16	1500	5	8900	25,000	207	100,000	3

* Values with different letters are significantly different at $p < 0.05$.

Table 7
K_d(Th) (L kg^{-1}) ranges based on pH.

		pH range		
		3–5	5–8	8–10
EPA (1999)	Range	62–6200	1700–170,000	20–2000
Present compilation	Range	19–10,200	100–100,000	35–3200
	GM(GSD)	1275(15)^{ab,*}	3261(8)^{a}	310(7)^{b}
	n	11	26	$n = 6$

* Values with different letters are significantly different at $p < 0.05$.

4. Conclusions

Solid–liquid distribution coefficients (K_d) for the naturally radionuclides U, Ra, Pb, Po and Th were reviewed, and grouped according to soil texture and organic matter criterion, and were relevant, according to other soil characteristics, such as pH.

The K_d values were generally about 10-fold higher for Ra, Pb and Th than for Po and U. Though the number of observations compiled in the present database doubled the former TRS-364 report, the number of observations is still limited, particularly for Clay and Organic groups, and K_d estimates are associated with large uncertainties. Significant differences were observed in the K_d estimates between textural classes only in a few cases. For the radionuclides considered, K_d is hence largely texture-independent and grouping based on soil texture classes should be discouraged. Instead, pH is generally a more appropriate classification parameter. Therefore, the K_d prediction could be significantly improved by a more thorough description of the soil characteristics. More specifically, information on factors influencing sorption as pH, CEC, clay content, OM content and concentration of counter ions should be collated, and increase in the research to increase the understanding in the mechanisms governing radionuclide–soil interaction is encouraged, especially for Ra and Po. For U, Th and Pb, K_d categorization or estimation is best done on the basis of pH.

Whatever the classification system applied, K_d estimates are associated with large uncertainties. Proposed best estimates, mostly derived from the GM values, may be suitable for screening assessments, but more site specific K_d values will be required for predicting effective impact.

Acknowledgements

Steve Sheppard of ECOMatters Inc. is acknowledged for providing us internal reports not available for distribution from which an important number of useful observations for Canadian soils could be extracted. This research was carried out in the frame of the IAEA' Programme on Environmental Modelling for Radiation Safety, EMRAS, within the Working Group "Revision of the TRS-364". The research was partially funded by the Spanish Government (CICYT, contracts PPQ2002-00264 and CTM2005-03847; Secretaría General para la Prevención de la Contaminación y el

Cambio Climático del Ministerio de Medio Ambiente, contracts 1.2-193/2005/3-B and 240/2006/2-1.2).

References

Amaral, E.C.S., Carvalho, Z.L., Godoy, J.M., 1992. Transfer of ^{226}Ra and ^{210}Pb to forage and milk in a Brazilian high natural radioactivity region. Radiat. Prot. Dosim. 24, 119–121.

Crançon, P., van der Lee, J., 2003. Speciation and mobility of uranium (VI) in humic-contain soils. Radiochim. Acta 91 (11), 673–679.

Duff, M.C., Amrhein, C., 1996. U (VI) sorption on goethite and soil in carbonate solutions. Soil Sci. Soc. Am. J. 60, 1393–1400.

Echevarria, G., Sheppard, M., Morel, J.L., 2001. Effect of pH on the sorption of uranium in soils. J. Environ. Radioactiv. 53, 257–264.

EPA (Environmental Protection Agency), 1999. Understanding Variation in Partitioning Coefficients, K_d, Values: Volume II: Review of Geochemistry and Available K_d Values for Cadmium, Caesium, Chromium, Lead, Plutonium, Radon, Strontium, Thorium, Tritium and Uranium. US-EPA, Office of Air and Radiation, Washington, USA. EPA 402-R-99-004B.

Gil-Garcia, C., Rigol, A., Vidal, M., 2009. New best estimates for radionuclide solid–liquid distribution coefficients in soils. Part 1: Radiocaesium and radiostrontium. J. Environ. Radioact 100, 690–696.

Gooddy, D.C., Shand, P., Kinniburgh, D.G., Van Riemsdijk, W.H., 1995. Field-based partition coefficients for trace elements in soil solutions. Eur. J. Soil Sci. 46, 265–285.

Hansen, W.R., Watters, R.L., 1971. Unsupported ^{210}Po oxide in soil. Soil adsorption and characterisation of soil solution species. Soil Sci. 112, 145–155.

Hsi, C.K.D., Langmuir, D., 1985. Adsorption of uranyl onto ferric oxy-hydroxides: application of the surface complexation site-binding model. Geochim. Cosmochim. Acta 49, 1931–1941.

IAEA (International Atomic Energy Agency), 1994. Handbook of Parameter Values for the Prediction of Radionuclide Transfer in Temperate Environments (TRS-364).

IAEA (International Atomic Energy Agency), 2003. Extent of Environmental Contamination by Naturally Occurring Radioactive Material (NORM) and Technological Options for Remediation. Technical report series 419. STI/DOC/010/419, ISBN 92-0-112503-8.

Langmuir, D., 1978. Uranium solution–mineral equilibria at low temperature with applications to sedimentary ore deposits. Geochim. Cosmochim. Acta 42, 547–569.

Nathwani, J.S., Phillips, C.R., 1979. Adsorption of ^{226}Ra by soils in the presence of Ca^{+2} ions: specific adsorption(II). Chemosphere 8, 293–299.

Payne, T.E., Davis, J.A., Waite, T.D., 1996. U sorption on ferrihydrite – effects of phosphate and humic acid. Radiochim. Acta 74, 239–243.

Rieuwerts, J.S., Ashmore, M.R., Farago, M.E., Thornton, I., 2006. The influence of soil characteristics on the extractability of Cd, Pb and Zn in upland and moorland soils. Sci. Tot. Environ. 366, 864–875.

Ryan, J.L., Rai, D., 1987. Thorium(IV) hydrous oxide solubility. Inorg. Chem. 26, 4140–4142.

Sheppard, M.I., Thibault, D.H., 1990. Default solid/liquid partitioning coefficients, K_ds, for four major soil types: a compendium. Health Phys. 59 (4), 471–482.

Sheppard, S.C., Sheppard, M.I., Tait, J.C., Sanipelli, B.L., 2006. Revision and meta-analysis of selected biosphere parameter values for chlorine, iodine, neptunium, radium, radon and uranium. J. Environ. Radioactiv. 89, 115–137.

Simon, S.L., Ibrahim, S.A., 1990. Biological uptake of radium by terrestrial plants. In: The Environmental Behaviour of Radium, vol. 1, IAEA. Technical report series no. 310, pp. 545–599.

Sowder, A.G., Bertsch, P.M., Morris, P.J., 2003. Partitioning and availability of uranium and nickel in contaminated riparian sediments. J. Environ. Qual. 32, 885–898.

Statsoft Inc., 2004. STATISTICA (Data analysis software system), version 6. www.stat.com.

Thibault, D.H., Sheppard, M.I., Smith, P.A., 1990. A Critical Compilation and Review of Default Soil Solid/Liquid Partition Coefficients, K_d, for Use in Environmental Assessments. AECL 10125. Atomic Energy of Canada Limited, Pinawa, Manitoba, Canada, 113 pp.

Vandenhove, H., Van Hees, M., Wouters, K., Wannijn, J., 2007. Can we predict uranium bioavailability based on soil parameters? Part 1: Effect of soil parameters on soil solution uranium concentration. Environ. Pollut. 145, 587–595.

Vandenhove, H., Van Hees, M., 2007. Predicting radium availability and uptake from soil properties. Chemosphere 69 (4), 664–674.

Waite, T.D., Davis, J.A., Payne, T.E., Waychunas, G.A., Xu, N., 1994. U (VI) sorption to ferrihydrite: application of the surface complexation model. Geochim. Cosmochim. Acta 58, 5465–5478.

Annex: Selected literature used for data compilation

Barnett, M.O., Jardine, P.M., Brooks, S.C., Selim, H.M., 2000. Adsorption and transport of uranium(VI) in subsurface media. Soil Sci. Soc. Am. J. 65, 908–917.

Bell, J., Bates, H., 1988. Distribution coefficients of radionuclides between soils and groundwaters and their dependence on various test parameters. Sci. Tot. Environ. 69, 297–317.

Crançon, P., van der Lee, J., 2003. Speciation and mobility of uranium(VI) in humic-containing soils. Radiochim. Acta 91, 673–679.

Echevarria, G., Sheppard, M., Morel, J.L., 2001. Effect of pH on the sorption of uranium in soils. J. Environ. Radioact. 53, 257–264.

Gooddy, D.C., Shand, P., Kinniburgh, D.G., Van Riemsdijk, W.H., 1995. Field-based partition coefficients for trace elements in soil solutions. Eur. J. Soil Sci. 46, 265–285.

Hansen, W.R., Watters, R.L., 1971. Unsupported ^{210}Po oxide in soil. Soil adsorption and characterisation of soil solution species. Soil Sci. 112, 145–155.

Johnson, W.H., Serkiz, S.M., Jonhson, L.M., Clarck, S.B., 1995. Uranium partitioning under acidic conditions in a sandy soil aquifer. U.S. Department of Energy Report, WSRC-MS-94–0528 (DOE).

Legoux, Y., Blain, G., Guillaumont, R., Ouzounian, G., Brillard, L., Hussonnois, M., 1992. K_d measurements of activation, fission and heavy metals in water/solid phase systems. Radiochim. Acta 58/59, 211–218.

Nathwani, J.S., Phillips, C.R., 1979. Adsorption of ^{226}Ra by soils. Chemosphere 8, 285–291.

Nathwani, J.S., Phillips, C.R., 1979. Adsorption of ^{226}Ra by soils in the presence of Ca^{+2} ions: specific adsorption(II). Chemosphere 8, 293–299.

Payne, T.E., Harries, J.R., 2000. Adsorption of Cs and U(VI) on soils of the Australian arid zone. Radiochim. Acta 88, 799–802.

Sastre, J., Rauret, G., Vidal, M., 2006. Sorption–desorption tests to assess the risk derived from metal contamination in mineral and organic soils. Environ. Int. 33, 246–256.

Sauvé, S., Hendershot, W., Allen, H.E., 2000. Solid-solution partitioning of metals in contaminated soils: dependence on pH, total metal burden, and organic matter. Environ. Sci. Technol. 34, 1125–1131.

Sheppard, M.I., Thibault, D.H., 1991. A four-years mobility study of selected trace elements and heavy metals. J. Environ. Qual. 20, 101–114.

Sheppard, M.I., Sheppard, S.C., 1987. A solute transport model evaluated on two experimental systems. Ecol. Model. 37, 191–206.

Sheppard, S.C., Eveden, W.G., 1988. The assumption of linearity in soil and plant concentration ratios: an experimental evaluation. J. Environ. Radioact. 7, 221–247.

Sheppard, S.C., Eveden, W.G., Pollock, J.R., 1989. Uptake of natural radionuclides by field and garden crops. Can. J. Soil Sci. 69, 751–767.

Sheppard, S.C., Sheppard, M.I., Tait, J.C., Sanipelli, B.L., 2006. Revision and meta-analysis of selected biosphere parameter values for chlorine, iodine, neptunium, radium, radon and uranium. J. Environ. Radioact. 89, 115–137.

Sheppard, S.C., Sheppard, M.I., Ilin, M., Tait, J., Sanipelli, B., 2004. Primordial radionuclides in Canadian background sites: secular equilibrium and isotopic differences. Ecomatters report written under contract for Canadian. Nuclear Safety Commission.

Tyler, G., Olsson, T., 2002. Conditions related to solubility of rare and minor elements in forest soils. J. Plant Nutr. Soil Sci. 165, 594–601.

EPA-United States Environmental Protection Agency, 1999. Understanding variation in partition coefficient, K_d, values: vol. II. Review of geochemistry and available values for cadmium, caesium, chromium, lead, plutonium, radon, strontium, thorium, tritium and uranium, 402-R-99-004B.

EPA-United States Environmental Protection Agency, 1999. Partition coefficients for metals in surface water, soil, and waste. Technical report, p. 74.

Vandenhove, H., Antunes, K., Wannijn, J., Duquène, L., Van Hees, M., 2007b. Method of diffusive gradient in thin films (DGT) compared with other testing methods to predict uranium phytoavailability. Sci. Tot. Environ. 373, 542–555.

Vandenhove, H., Van Hees, M., 2007. Predicting radium availability and uptake from soil properties. Chemosphere 69 (4), 664–674.

Vandenhove, H., Van Hees, M., Wouters, K., Wannijn, J., 2007a. Can we predict uranium bioavailability based on soil parameters? Part 1: effect of soil parameters on soil solution uranium concentration. Environ. Pollut. 145, 587–595.

Willet, I.R., Bond, W.J., 1995. Sorption of manganese, uranium and radium by highly weathered soils. J. Environ. Qual. 24, 834–845.

Zheng, Z., Tokunaga, T.K., 2003. Influence of calcium carbonate on U(VI) sorption to soils. Environ. Sci. Technol. 37, 5603–5608.

Zheng, Z., Wan, J., 2005. Release of contaminated U(VI) from soils. Radiochim. Acta 93, 211–217.

3.4

New best estimates for radionuclide solid–liquid distribution coefficients in soils. Part 3: miscellany of radionuclides (Cd, Co, Ni, Zn, I, Se, Sb, Pu, Am, and others)

C. J. Gil-García, K. Tagami, S. Uchida, A. Rigol, M. Vidal.

Journal of Environmental Radioactivity, 100, 704–715, 2009

Páginas 111-122

Journal of Environmental Radioactivity 100 (2009) 704–715

Contents lists available at ScienceDirect

Journal of Environmental Radioactivity

journal homepage: www.elsevier.com/locate/jenvrad

New best estimates for radionuclide solid–liquid distribution coefficients in soils. Part 3: miscellany of radionuclides (Cd, Co, Ni, Zn, I, Se, Sb, Pu, Am, and others)

C. Gil-García [a], K. Tagami [b], S. Uchida [b], A. Rigol [a], M. Vidal [a,*]

[a] Departament de Química Analítica, Universitat de Barcelona; Martí i Franquès 1-11, 3a Planta, 08028 Barcelona, Spain
[b] Office of Biospheric Assessment for Waste Disposal, National Institute of Radiological Sciences, Anagawa 4-9-1, Inage, Chiba 263-8555, Japan

ARTICLE INFO

Article history:
Received 31 July 2007
Received in revised form
22 October 2008
Accepted 1 December 2008
Available online 25 December 2008

Keywords:
Distribution coefficient
Soil
Radionuclides
Heavy metals
Iodine
Selenium
Antimony
Americium
Plutonium

ABSTRACT

New best estimates for the solid–liquid distribution coefficient (K_d) for a set of radionuclides are proposed, based on a selective data search and subsequent calculation of geometric means. The K_d best estimates are calculated for soils grouped according to the texture and organic matter content. For a limited number of radionuclides this is extended to consider soil cofactors affecting soil–radionuclide interaction, such as pH, organic matter content, and radionuclide chemical speciation. Correlations between main soil properties and radionuclide K_d are examined to complete the information derived from the best estimates with a rough prediction of K_d based on soil parameters. Although there are still gaps for many radionuclides, new data from recent studies improve the calculation of K_d best estimates for a number of radionuclides, such as selenium, antimony, and iodine.

1. Introduction

There is a significant amount of qualitative and quantitative data on the interaction of a limited number of radionuclides in soils (radiocaesium, radiostrontium, and several naturally occurring radionuclides, such as uranium). However, there are evident gaps in the available interaction data for a large number of radionuclides. This is particularly true for the quantification of the solid–liquid distribution coefficient (K_d) and its dependency on soil type and characteristics.

Recently, there has been increased interest in certain radionuclides with limited environmental impact to date, but which are of increasing importance for the management of radioactive waste. The list of radionuclides in this field is very extensive, and models designed to forecast their impact in the geo and biosphere, in case of continuous or accidental releases and waste management, suffer from the limited number of available input data.

This is the last in a series of three papers in which we propose new best estimates of K_d for a large number of radionuclides (although we emphasise heavy metals, iodine, selenium, antimony, plutonium, and americium radioisotopes). As in the preceding two papers, data for estimates of K_d come from field and laboratory experiments, with various contamination sources, mainly considering soils contaminated by radioisotopes.

Besides obtaining K_d best estimates for soils grouped on the basis of their texture (sand and clay percentages of the mineral matter) and organic matter content, we also elucidate the more significant soil properties responsible for radionuclide interaction in soils. These properties may be as significant as mineral and organic matter contents in governing soil-radionuclide interaction and alone or combined with textural information they can be used as cofactors to classify soils, thus reducing the variability of K_d best estimates. We apply this approach to pH – since it strongly affects the sorption of heavy metal radionuclides – and radionuclide chemical speciation – which may also affect the K_d for several radionuclides, since different species (such as oxidized-reduced species and oxyanions) may display contrasting sorption behaviour. We further comment on other factors potentially affect radionuclide K_d, such as the content of Fe and Al oxides and organic matter, microbial activity and the water regime of the soil.

* Corresponding author. Tel.: +34 934039276; fax: +34 934021233.
E-mail address: miquel.vidal@ub.edu (M. Vidal).

0265-931X/$ – see front matter © 2008 Elsevier Ltd. All rights reserved.
doi:10.1016/j.jenvrad.2008.12.001

2. Data collection and treatment

2.1. Data collection and acceptance

As in the rest of the papers of this series, data of the present compilation come from field and laboratory experiments considering the scenario of soils contaminated by radioisotopes, and from references mostly from 1990 onwards, including data in the previous TRS-364 and related reports (Sheppard and Thibault, 1990; Thibault et al., 1990; IAEA, 1994). Constraints for data acceptance led to reject data from diffusion experiments, from other materials, such as sediments or pure soil phases, and from stable elements. Data from radioisotopes of the same element were pooled.

2.2. Data treatment

For all radionuclides, K_d values were grouped according to two criteria. On one hand, soils were grouped according to the sand and clay mineral percentages referred to the mineral matter, and the organic matter (OM) content in the soil. This defined the 'texture/OM' criterion, which was similar to the criterion followed in the previous TRS-364. The thresholds defining each soil group were as follows:

- Organic group: soil with an organic matter content $\geq$20%.
- Mineral soils: three soil groups were created according to the sand and clay percentages referred to the mineral matter:
  - Sand group: sand fraction $\geq$65% and clay fraction $<$18%
  - Clay group: clay fraction $\geq$35%
  - Loam group: rest of cases

Moreover, an additional Unspecified group was created for soils without characterization data, or for mineral soils with unknown sand and clay contents.

Soils were also grouped according to a second criterion regarding specific soil factors governing the radionuclide-soil interaction ('cofactor' criterion). The cofactors depended on the radionuclide considered, and permitted to decrease the variability of K_d ranges for a given soil group.

After grouping K_d values, the following dataset descriptors are calculated: n: number of observations; GM: geometric mean; GSD: geometric standard deviation; min–max: minimum and maximum values. The GM and GSD are calculated when the number of observations was $\geq$3. When $n = 2$, min and max values are given, while only the single value could be given when $n = 1$.

As the log-transformed K_d are normally distributed in most cases, the exploratory and ANOVA analyses are performed with log K_d data. The exploratory analysis is based on box-and-whisker plots (*StatGraphics Plus 5.1*), and it is useful to exclude potential outliers and thus to decrease data variability (those data beyond three times the interquartile ranges). The ANOVA analysis, based on the Fisher' Least Significant Differences criterion (*StatGraphics Plus 5.1*), is useful to identify which soil groups are statistically different, although some derived results must be treated with precaution.

Best estimates are the calculated GM of K_d values when they are significantly different between soil groups. When they are not, best estimates are proposed from an expert judgment of the GM values.

3. Description of ranges of K_d values: derivation of K_d best estimates

3.1. The case of heavy metal radionuclides

3.1.1. Best estimates of K_d for soils grouped according to the texture/OM criterion

Table 1 summarizes the dataset descriptors of K_d for Cd, Co, Cr, Cu, Ni, and Zn, for all the soil groups. Best estimates from the previous TRS-364 document are also included (IAEA, 1994). The data variability was high, although the previous TRS value and the new GM were reasonably similar (or of the same order of magnitude) with clear exceptions: Co in Clay and Organic soils, and Cr in Sand and Clay groups. In the case of Co and Cr in the Clay group, the previous TRS-364 estimates were the minimum and maximum values, respectively, of the recalculated ranges.

Although there was no consistent relationship between K_d GM and soil texture, the new GM had a more logical variation with respect to soil texture than TRS-364 values. For a few radionuclides (Cu, Co, and Ni) K_d increased with clay content, while for the rest of radionuclides this pattern was not observed. Excluding the Unspecified soils, maximum K_d was for the Organic soils in the cases of Cd, Cr, and Ni.

Exploratory analysis showed that all points were within the threshold of 3 times the interquartile ranges, with the single exception of the 2 L/kg value in the Clay group for Zn. As this point can be considered as a potential outlier, it was excluded and the resulting GM and GSD were recalculated. Excluding this point meant that the increases in the GM of K_d (Zn) were also related with increases in the clay content.

However, and despite the trends observed with the GM and the clay content, the ANOVA analyses confirmed that there was not a direct correlation between the GM and the soil groups, surely due to the large data variability, thus making it difficult to derive clear best estimates for all the metals. The statistical differences between soil groups depended on each metal, as shown in Table 1.

3.1.2. Best estimates of K_d for soils grouped according to the cofactor criterion

The K_d for heavy metal radionuclides are strongly dependent on soil properties such as pH, and the content of Fe and Mn oxides, clay, and organic matter (Sauvé et al., 2000; Staunton, 2004). Moreover, they depend on whether the batch experiments have been carried out with or without a certain concentration of stable isotopes used as carriers. In most cases, the concentration of the stable carrier is similar to those used in regular sorption experiments with stable isotopes (for instance, in the 10^{-6}–10^{-8} M range). This means that we can include experiments performed with stable isotopes in the present database.

An extensive examination of the multivariate correlations between soil parameters and K_d is beyond the scope of the present work, so is deriving a complete model for the K_d prediction. However, we can provide modellers and end-users with some indications regarding how to use better estimators of K_d than those based solely on texture and organic matter content. Table 2 shows a summary of the best correlations (K_d vs. soil parameters) obtained for all radionuclides. An examination of simple regressions between soil parameters and K_d values confirmed that the best correlations were obtained between K_d and the pH of the sorption experiments. The correlations improved when the organic soils were excluded from the regression analysis, especially for Cd and Cu. Cr is an exception since its speciation is an additional factor affecting K_d (EPA, 1999). While in a reduced form (Cr(III)), K_d (Cr) follows the same pH dependence as other metals (EPA, 1999). However, when experiments are performed with Cr(VI), the anionic character of the Cr(VI) species makes that the pH dependence is the opposed to that of the other metals. This information is crucial and it is not always reported in the literature. The presence together of data from experiments performed with Cr(III) and Cr(VI) means that there is no statistical correlation between K_d (Cr) and pH. However, when only using soils with data corresponding to Cr(VI), an excellent negative correlation is observed between the two variables.

Multiple regression analyses were also performed on K_d data. Examples of cases in which the inclusion of the clay and/or the

Table 1
K_d for heavy metal radionuclides for soils grouped according to the texture/OM criterion (L/kg). *n*: number of observations; GM: geometric mean; GSD: geometric standard deviation; min–max: minimum and maximum values; # ref.: number of references serving as data sources.

Radionuclide	Soil group	*n*	TRS value	GM/Value	GSD	min	max	# ref.
Cd	All soils	61	–	150	9	2	7000	11
	Sand	30	74	110[a]	8	2	1770	5
	Loam	5	40	100[a,b]	7	9	1700	4
	Clay	4	540	130[a,b]	15	7	2721	3
	Organic	13	810	650[b]	6	10	7000	6
	Unspecified	9	–	68	15	6	4360	4
Co	All soils	118	–	480	16	2	103 595	8
	Sand	18	60	260[a,b]	18	5	36 756	4
	Loam	71	1300	810[b,c]	15	2	103 595	5
	Clay	10	540	3800[c]	6	540	99 411	3
	Organic	17	990	87[a]	9	4	5800	4
	Unspecified	2	–	–	–	126	14 971	2
Cr	All soils	31	–	40	20	1	7943	6
	Sand	9	67	8[a]	8	1	100	4
	Loam	9	30	45[a,b]	23	1	1585	3
	Clay	5	1500	14[a,b]	20	1	1500	2
	Organic	6	270	160[b]	10	8	2905	3
	Unspecified	2	–	–		4778	7943	2
Cu	All soils	11	–	530	3	76	2733	4
	Sand	2	–	–	–	128	333	1
	Loam	1	–	490[a]	–	–	–	1
	Clay	2	–	–	–	1401	2733	1
	Organic	4	–	320[a]	3	76	883	2
	Unspecified	2	–	–	–	501	2120	2
Ni	All soils	64	–	280	7	3	7250	12
	Sand	26	400	130[a]	10	3	7250	4
	Loam	14	300	180[a]	5	8	1163	6
	Clay	12	670	930[b]	2	247	3187	5
	Organic	8	1100	1100[b]	2	406	4990	3
	Unspecified	4	–	480	8	22	2333	3
Zn	All soils[d]	92	–	950	11	0.9	153 070	11
	Sand	17	200	110[a]	23	0.9	27 816	6
	Loam	48	1300	2400[b]	4	211	153 070	4
	Clay[d]	8	2400	2445[b,c]	2	480	6945	3
	Organic	12	1600	570[c]	8	10	7630	6
	Unspecified	7	–	240	35	5	6216	5

[a,b,c] GM values with different letters were significantly different at $p < 0.05$.
[d] Data beyond the threshold of 3 times the interquartile ranges were excluded.

Table 2
Correlations between the K_d for heavy metal radionuclides and main soil properties (n = number of observations; r = correlation coefficient).

	Regression equations	*n*	*r*	% variance
Cd – All soils	$\log K_d = 0.8\ (0.4) + 0.21\ (0.07) \times \text{pH}$	55	0.38	13
	$\log K_d = -0.1\ (0.5) + 0.34\ (0.08) \times \text{pH} + 0.4\ (0.1) \times \log \text{OM}$	54	0.49	24
Cd – Mineral soils	$\log K_d = -0.7\ (0.4) + 0.41\ (0.06) \times \text{pH}$	43	0.71	49
Co – All soils	$\log K_d = -0.7\ (0.3) + 0.63\ (0.05) \times \text{pH}$	113	0.75	56
	$\log K_d = -1.5\ (0.4) + 0.74\ (0.06) \times \text{pH} + 0.5\ (0.2) \times \log \text{OM}$	110	0.77	59
Co – Mineral soils	$\log K_d = -1.2\ (0.4) + 0.71\ (0.06) \times \text{pH}$	97	0.76	58
Cr (VI) – All soils	$\log K_d = 4.7\ (0.6) - 0.52\ (0.08) \times \text{pH}$	12	−0.89	78
Cu – Mineral soils	$\log K_d = -3\ (1) + 0.8\ (0.1) \times \text{pH}$	5	0.95	88
Ni – All soils	$\log K_d = 0.1\ (0.3) + 0.34\ (0.05) \times \text{pH}$	58	0.68	46
	$\log K_d = -1.6\ (0.5) + 0.55\ (0.06) \times \text{pH} + 0.27\ (0.09) \times \log \text{clay}$	38	0.82	67
	$\log K_d = -0.7\ (0.3) + 0.41\ (0.04) \times \text{pH} + 0.7\ (0.1) \times \log \text{OM}$	58	0.84	70
Ni – Mineral soils	$\log K_d = -0.6\ (0.3) + 0.43\ (0.04) \times \text{pH}$	51	0.82	66
	$\log K_d = -1.6\ (0.5) + 0.55\ (0.06) \times \text{pH} + 0.27\ (0.09) \times \log \text{clay}$	38	0.82	67
	$\log K_d = -0.9\ (0.3) + 0.45\ (0.04) \times \text{pH} + 0.6\ (0.1) \times \log \text{OM}$	51	0.86	74
Zn – All soils	$\log K_d = -0.1\ (0.5) + 0.52\ (0.08) \times \text{pH}$	88	0.55	30
	$\log K_d = -1.0\ (0.6) + 0.6\ (0.1) \times \text{pH} + 0.5\ (0.2) \times \log \text{OM}$	86	0.59	35
Zn – Mineral soils[a]	$\log K_d = -1.2\ (0.5) + 0.71\ (0.09) \times \text{pH}$	75	0.69	47
	$\log K_d = -1.8\ (0.6) + 0.8\ (0.9) \times \text{pH} + 0.5\ (0.2) \times \log \text{OM}$	73	0.71	50

[a] Data without outliers.

Table 3
K_d for heavy metal radionuclides for mineral soils grouped according to the pH (L/kg). *n*: number of observations; GM: geometric mean; GSD: geometric standard deviation; min–max: minimum and maximum values.

Radionuclide	Soil group	*n*	GM	GSD	min	max
Cd	pH < 5	8	11	3	2	64
	5 ≤ pH < 6.5	11	18	4	6	250
	pH ≥ 6.5	24	380	6	4	4360
Co	pH < 5	21	12	5	2	153
	5 ≤ pH < 6.5	50	1100	5	29	99 411
	pH ≥ 6.5	26	4600	4	547	103 595
Ni	pH < 5	10	15	2	3	48
	5 ≤ pH < 6.5	11	58	4	7	1100
	pH ≥ 6.5	30	820	4	40	7250
Zn	pH < 5	9	8	8	1	301
	5 ≤ pH < 6.5	49	1600	6	6	30 157
	pH ≥ 6.5[a]	17	4300	4	437	153 070

[a] Data beyond the threshold of 3 times the interquartile ranges were excluded.

organic matter contents significantly improved the correlations are also given in Table 2. In some cases, over 70% of the variance was explained by these soil variables, thus confirming good K_d data prediction. If data regarding these soil properties are available, these regression equations can therefore be considered as alternatives to the use of best estimates based on the calculation of the GM.

Considering the key role of pH in K_d variability, the K_d for heavy metals can be grouped according to pH ranges in the mineral soils. Ideally, this exercise should be undertaken for each textural class, but the dataset is not large enough to do it. Establishing common pH ranges for all metals is difficult and range thresholds are arbitrarily set up. Table 3 shows the grouping based on pH ranges for those metals with sufficient data. The exploratory analysis of the data showed that for Zn two points could be excluded since they were beyond the threshold of 3 times the interquartile ranges. The K_d GM for all metals increased when the pH increased, and their variability was much lower than those obtained using the texture/OM criterion. Fig. 1 compares the box-and-whisker plots derived using the soil group criterion with those from the pH criterion. The ANOVA analyses confirmed the excellence of the pH cofactor criterion, since all the GM were statistically different, with the single exception of the GM calculated for Cd in the pH < 5, and 5 ≤ pH < 6.5 soil groups. Therefore, it is recommended to group soils with respect to their pH, while the GM of each soil group can be proposed as the best estimate for that range of pH. For Cd, a best estimate of 15 L/kg can be proposed for soils with pH < 6.5.

3.2. The case of radioiodine

3.2.1. Best estimates of K_d (I) for soils grouped according to the texture/OM and speciation criteria

Table 4 shows the dataset descriptors for radioiodine K_d (K_d (I)) for soils classified according to the texture/OM criterion. Comparing the GM of the mineral soils, there is a gradual increase in the K_d (I) with increasing clay content, and the K_d (I) for organic soils were higher than for mineral soils. However, none of these trends was statistically significant. The GM of the present compilation was similar to those given in the previous TRS-364.

Table 4 also shows the GM values distinguishing between the iodine species; distinction that was not made in the previous TRS-364. At the usual soil pH and redox potential, iodide and iodate are the anionic species of iodine that can be found in soils (Fukui et al., 1996). In anoxic conditions, iodide may prevail over iodate. Although to take into account iodine speciation is usually recommended as a means of decreasing data variability, a quick look at the data indicates that a non significant effect of iodine species was observed by examining the GM of K_d (I) derived from sorption experiments including both iodide and iodate compounds, although iodate is commonly accepted to have a stronger sorption than iodide (Fukui et al., 1996). This point is more extensively discussed in the following section.

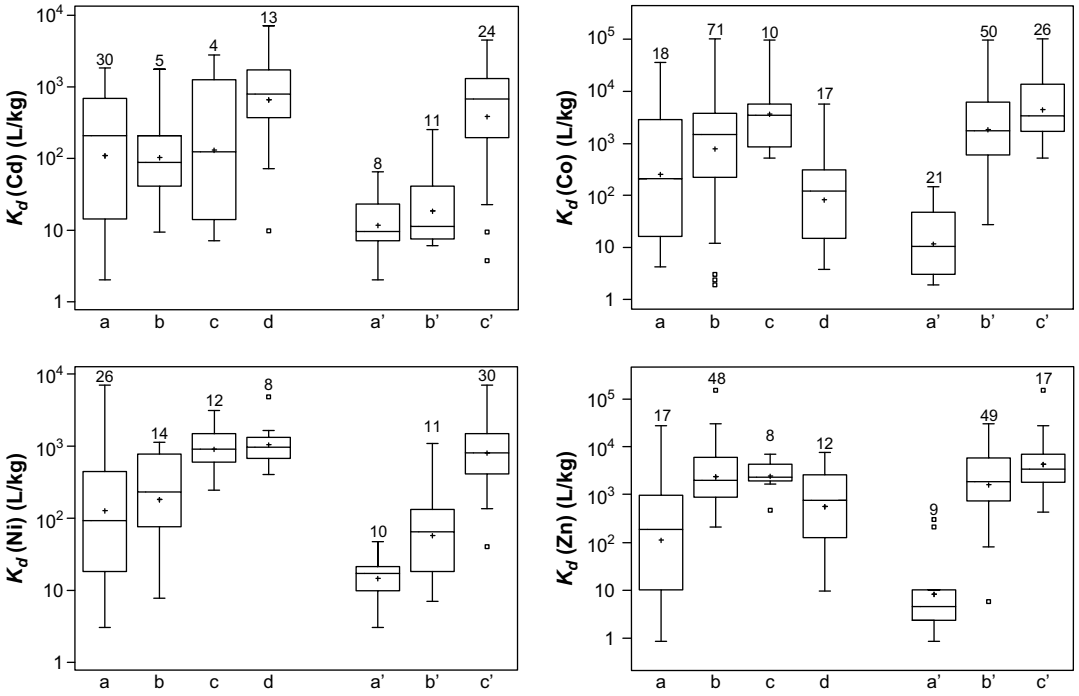

Fig. 1. Box-and-whisker plots of K_d for Cd, Co, Ni, and Zn, for all soils grouped according to the texture/OM criterion (a: Sand; b: Loam; c: Clay; d: Organic) and for mineral soils grouped according to pH criteria (a′: pH < 5; b′: 5 ≤ pH < 6.5; c′; pH ≥ 6.5). The box encloses the middle 50%, and the median is represented as a horizontal line inside the box. Vertical lines extend to the point at 1.5 interquartile ranges. Other symbols represent GM (+) and points at >1.5 interquartile ranges (□).

Table 4
K_d (I) for soils grouped according to the texture/OM criterion and speciation (L/kg). *n*: number of observations; GM: geometric mean; GSD: geometric standard deviation; min–max: minimum and maximum values; # ref.: number of references serving as data sources.

Iodine species	Soil group	*n*	TRS value	GM/Value	GSD	min	max	# ref.
All data	All soils	250	–	7	5	0.01	581	9
	Sand	48	1	4[a]	7	0.01	134	7
	Loam	129	4	8[a]	4	0.2	538	6
	Clay	19	18[c]	11[a,b]	5	1	180	5
	Organic	11	27	32[b]	3	8	581	4
	Unspecified	43	–	4	6	0.1	368	2
I^-	All soils	157	–	5	6	0.01	581	6
	Sand	37	–	4[a]	8	0.01	134	5
	Loam	74	–	7[a]	5	0.2	531	4
	Clay	13	–	7[a]	6	1	123	2
	Organic	9	–	36[b]	4	8	581	3
	Unspecified	24	–	3	6	0.1	368	2
IO_3^-	All soils	67	–	8	4	0.4	538	2
	Sand	6	–	4	5	0.4	41	1
	Loam	41	–	9	4	1	538	2
	Clay	–	–	–	–	–	–	–
	Organic	1	–	13	–	–	–	1
	Unspecified	19	–	8	5	0.4	58	2

[a,b] GM values with different letters were significantly different at $p < 0.05$.
[c] The previous TRS-364 suggested a value of 1.8×10^2 L/kg, which is interpreted as a mistake.

From the GM calculated based on the texture/OM criterion, it is difficult to derive best estimates that distinguish between mineral soil groups. Therefore, a K_d (I) best estimate of 7 L/kg could be proposed for mineral soils, while the GM of the Organic group could serve as K_d (I) best estimate for organic soils.

3.2.2. Soil variables affecting the K_d (I)

Previous studies show that the sorption of the anionic iodine species in soils is strongly affected by the experimental conditions, such as contact time, solid–liquid ratio, and temperature (Fukui et al., 1996; Ashworth and Shaw, 2006) and soil properties such as organic matter and Al and Fe oxides (Fukui et al., 1996; Yoshida et al., 1998). The relative significance of each soil factor is in turn affected by microbial biomass, the water regime of the soil (which also affects the redox potential) and pH (Sheppard, 2003). The effect of these soil factors should be considered along with iodine speciation.

Table 5 summarizes the best correlations between the K_d (I) and soil properties, with data of the present compilation. These correlations agree with those previously reported in the literature. The most significant regressions were found for organic matter and total Fe content in soils (Muramatsu et al., 1990; Yoshida et al., 1998). The variability of K_d data is better explained by a multiple regression with organic matter and Fe contents. This is particularly true when examining only the iodide data; more than 50% of its total variance can be explained by these two soil properties.

It is obvious that univariant correlations are not enough to describe the K_d (I) variability. An example of this is the complex dependency of K_d (I) on the water regime, as shown in Table 6 (Muramatsu et al., 1990; Yoshida et al., 1995, 1998). At short contact times the effect of water regime on K_d (I) is clearly more significant than the iodine species involved in the sorption process. This is probably due to changes in microbial activity. When soil samples are dried, and the microbial activity is reduced, there is a strong decrease in iodine sorption (Bunzl and Schimmack, 1991). However, in sufficiently waterlogged soils leading to anoxic scenarios iodide sorption could be lower at long contact times (more than 35 days) than sorption in oxic scenarios (Ashworth and Shaw, 2006). In a similar study, iodate sorption was higher than iodide in soils dried at 100 °C, while in the same air-dried soils the two species showed a similar K_d value (Fukui et al., 1996). In all, this indicates a complex dependency of K_d (I) on organic matter and water content, microbial activity and oxidizing-reducing conditions.

As the correlations with the clay content were mostly not statistically significant, it is no correct to derive the K_d (I) best estimates regarding for the textural classes of mineral soils. Instead we should group the K_d (I) with respect to organic matter content, or better, consider both the organic matter and Fe content to calculate the best estimates. As an example of this, Table 6 shows the K_d (I) GM according to organic matter content. In all cases the K_d GM increase with increasing organic matter content, leading to ranges of values with less variability than those derived on the basis of the clay content, and with comparable values for all the iodine species. This can also be seen in Fig. 2, which shows the results of the exploratory analysis of K_d (I) data, distinguishing between soil and organic matter grouping criteria, and iodine speciation. Therefore, and although all the GM were not significantly different, the organic matter for soil grouping is recommended over the texture/OM criterion for a better proposal of K_d (I) best estimates.

Table 5
Correlations between K_d (I) and main soil properties (n = number of observations; r = correlation coefficient).

	Regression equations	*n*	*r*	% variance
All data	$\log K_d = 0.63\ (0.04) + 0.6\ (0.1) \times \log OM$	227	0.55	30
	$\log K_d = -1.4\ (0.4) + 0.6\ (0.1) \times \log Fe$	124	0.44	18
	$\log K_d = -0.6\ (0.4) + 0.7\ (0.1) \times \log OM + 0.3\ (0.1) \times \log Fe$	124	0.63	39
I^-	$\log K_d = 0.6\ (0.1) + 0.6\ (0.1) \times \log OM$	139	0.58	33
	$\log K_d = -2.8\ (0.6) + 0.9\ (0.2) \times \log Fe$	62	0.58	32
	$\log K_d = -1.5\ (0.6) + 0.7\ (0.1) \times \log OM + 0.5\ (0.2) \times \log Fe$	62	0.74	53
IO_3^-	$\log K_d = 0.64\ (0.09) + 0.6\ (0.1) \times \log OM$	67	0.45	19
	$\log K_d = -1.6\ (0.6) + 0.6\ (0.2) \times \log Fe$	61	0.45	19
	$\log K_d = -0.8\ (0.6) + 0.5\ (0.2) \times \log OM + 0.4\ (0.2) \times \log Fe$	61	0.56	30

Table 6
K_d (I) for soils grouped according to water regime, organic matter content and speciation criteria (L/kg) (n = number of observations; organic matter content (OM) in % w/w).

The effect of water content (Muramatsu et al., 1990)						
	Soil – treatment	n	GM/Value	GSD	min	max
I^-	Sand – air dried	1	28	–	–	–
	Sand – water saturated	1	32	–	–	–
	Unspecified – air dried	9	19	6	0.8	470
	Unspecified – water saturated	9	550	6	8	7000
IO_3^-	Sand – air dried	1	28	–	–	–
	Sand – water saturated	1	35	–	–	–
	Unspecified – air dried	9	15	7	0.7	550
	Unspecified – water saturated	9	680	7	8	7500

K_d (I) grouped according to the organic matter content						
	Soil group	n	GM	GSD	min	max
All data	OM < 2	75	2[a]	6	0.01	57
	2 ≤ OM < 5	106	9[b]	3	0.6	538
	5 ≤ OM < 10	27	18[c]	4	2	262
	OM ≥ 10	19	34[c]	3	8	581
I^-	OM < 2	49	1[a]	6	0.01	25
	2 ≤ OM < 5	60	8[b]	3	0.6	134
	5 ≤ OM < 10	16	16[b,c]	4	2	262
	OM ≥ 10	14	37[c]	4	8	581
IO_3^-	OM < 2	18	4[a]	5	0.4	57
	2 ≤ OM < 5	35	8[a,b]	3	2	538
	5 ≤ OM < 10	9	17[b]	3	4	127
	OM ≥ 10	5	26[b]	2	10	86

[a,b,c] GM values with different letters were significantly different at $p < 0.05$.

3.3. The cases of radioselenium and radioantimony

Table 7 summarizes the K_d (Se) GM for soils grouped according to the texture/OM criterion. They are significantly lower for the Sand group, while for the rest of soils there were not statistically significant differences. More data are required for the organic soils, only with one additional observation with respect to the previous TRS-364. Comparing the present GM with those from the previous TRS-364, the GM derived from the present compilation was systematically lower. Therefore, a best estimate of 55 L/kg can be proposed for the K_d (Se) in sandy soils, and a common value of around 230 L/kg for loam and clay soils.

Selenium interaction in soils depends on Se speciation, which is affected by pH, redox potential and microbial activity. Selenite is considered to be the most important Se form in soils, with a significant degree of sorption on soil particles. Most sorption experiments are carried out with this anionic form. Selenate is less abundant, since its sorption is very low and it is easily leachable. K_d (Se) of the selenate species is usually considered to be zero (Ylaranta, 1983). The contribution of each soil component to Se sorption is not yet clear, although Fe and Al oxides are considered to be major sorbents of Se (Nakamaru et al., 2005). Moreover, selenite sorption can be affected by pH and soil solution composition (for instance, concentration of phosphate), as well as by microbial activity (Fevrier et al., 2007). Since we had no data on Fe available, we checked univariate relationships with other soil components. In general their significance was low, the best correlation being with the organic matter content ($r = 0.39$; 15% of the variance explained). The inclusion of the clay content increased the explained variance, but only up to 20%. Complete correlations between soil properties and K_d (Se) can be found in Nakamaru et al. (2005).

Table 7 also shows the best estimates of K_d (Sb) for soils grouped according to the texture/OM criterion. The K_d (Sb) GM gradually increased from the Sand to the Clay groups, while for the Organic soils the best estimate had an intermediate value. As for Se, the comparison of these new GM with those from the previous TRS-364 confirmed that the new GM was systematically lower. With the exception of the organic soils, for which more data are required to derive a suitable K_d (Sb) best estimate, the ANOVA analysis confirmed that the GM of the mineral soils were significantly different, and therefore they could be taken as the best estimates of K_d (Sb) in mineral soils.

At the pH and potential redox that are expected in soils, the most important Sb species is the oxyanion (SbO_3^-). Reported data seem to correlate Sb sorption to soil pH, as well as with the

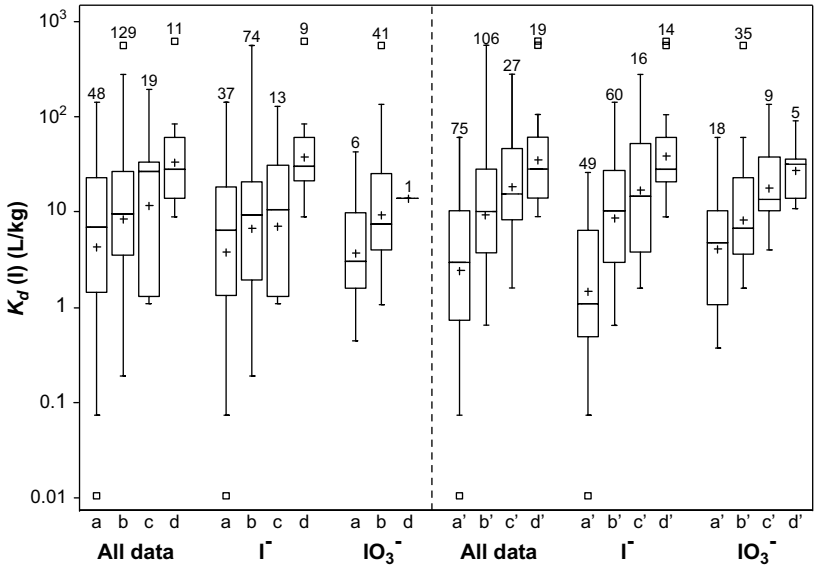

Fig. 2. Box-and-whisker plots of K_d (I) for soils grouped according to the texture/OM criterion (a: Sand; b: Loam; c: Clay; d: Organic), organic matter content (a′: OM < 2; b′: 2 ≤ OM < 5; c′; 5 ≤ OM < 10; d′: OM ≥ 10), and speciation criteria. The box encloses the middle 50%, and the median is represented as a horizontal line inside the box. Vertical lines extend to the point at 1.5 interquartile ranges. Other symbols represent GM (+) and points at >1.5 interquartile ranges (□).

Table 7
K_d (Se) and K_d (Sb) for soils grouped according to the texture/OM criterion (L/kg). *n*: number of observations; GM: geometric mean; GSD: geometric standard deviation; min–max: minimum and maximum values; # ref.: number of references serving as data sources.

Radionuclide	Soil group	*n*	TRS value	GM	GSD	min	max	# ref.
Se	All soils	172	–	200	3	4	2130	10
	Sand	15	150	56	5	4	1616	6
	Loam	101	490	220	3	12	1606	4
	Clay	33	740	240	3	22	2130	6
	Organic	2	1800	–	–	230	1800	2
	Unspecified	21	–	230	2	20	618	3
Sb	All soils	152	–	62	4	0.6	2065	5
	Sand	19	45	17	6	0.6	472	4
	Loam	92	150	61	3	4	2065	2
	Clay	18	240	140	2	38	614	2
	Organic	3	540	75	8	8	540	2
	Unspecified	20	–	99	4	4	612	2

presence of other anions in the soil solution (similar to the case described for selenite). Thus, K_d (Sb) is expected to increase with decreasing pH, and to increase with increasing amounts of Fe and Al oxides in the solid phase (Nakamaru et al., 2006). However, the best univariate correlation with the data in the present database was with CEC ($r = 0.48$; 22% of explained variance) while a multiple regression with pH and clay, and pH and CEC explained 23% and a 28% of the total variance, respectively. More research is therefore required for a better understanding of Sb sorption in soils.

3.4. The cases of americium and plutonium

Table 8 shows the descriptors of the dataset of K_d (Am) for soils grouped on the basis of the texture/OM criterion. K_d (Am) GM increased with increasing clay content, but only one value was available for the Clay group, which originated from the previous TRS-364. The Organic group had an intermediate GM value. This radionuclide belongs to the group of radionuclides with the highest GM from the whole dataset, although the variability for all soil groups was quite large; K_d (Am) varies over a range of more than 3 orders of magnitude. However, the exploratory analysis based on the box-and-whisker plots did not show any point beyond 3 times the interquartile ranges. The new GM appears to make more sense than those in the previous TRS-364, since the previous values did not gradually increase with the clay content. Moreover, the GM for the Organic group in the previous TRS-364 is an outstandingly high value, virtually considered as an outlier by the exploratory analysis. As Table 8 shows, the new GM for the Organic group is around 40 times lower. Therefore, the GM can serve as best estimates for the Sand and Loam groups, although more data is needed to propose a best estimate for clay soils.

K_d (Am) is expected to depend on the soil pH and on the sand and clay contents (Allard et al., 1984; Roussel-Debet, 2005). The univariate correlations between K_d (Am) and soil properties in this database partially confirm this assumption; the best correlations were for pH ($r = 0.35$; 11% of the variance explained) and sand content ($r = -0.48$; 21% of the variance explained). Multiple regressions did not lead to a better description of K_d (Am) variability. If Organic soils are excluded, the same univariate correlation was found with the sand content, while the best correlation was obtained with the clay content ($r = 0.53$; 26% of the variance explained). Therefore, grouping K_d (Am) on the basis on the soil group criterion appears to be a satisfactory approach for this radionuclide.

Table 8 also shows the GM of K_d (Pu) for soils classified according to the texture/OM criterion. As for Am, K_d (Pu) best estimates increased from the Sand to the Clay groups, with the Organic group having an intermediate best estimate value, but in this case no significant differences were observed, excepting when comparing the Sand and Clay groups. The new GM was of the same order of magnitude as the GM from the previous TRS-364, although the previous value for the Clay group was significantly higher. This could be due to the constraints applied to build up the present database, where data from pure clay minerals were excluded, whereas values from clay phases are often found in previous databases.

Plutonium speciation affects the quantification of K_d (Pu) and this causes variability of K_d (Pu) data. Reduced species of Pu (Pu (III,IV)) are expected to have higher K_d (Pu) than oxidized (Pu (V,VI)) and organic bound Pu (Skipperud et al., 2000). Sorption experiments are often performed with oxidized species, although this information is not always reported, and K_d (Pu) may be derived from data from various Pu species.

Table 8
K_d (Am) and K_d (Pu) for soils grouped according to the texture/OM criterion (L/kg). *n*: number of observations; GM: geometric mean; GSD: geometric standard deviation; min–max: minimum and maximum values; # ref.: number of references serving as data sources.

Radionuclide	Soil group	*n*	TRS value	GM/Value	GSD	min	max	# ref.
Am	All soils	62	–	2600	6	50	110 000	6
	Sand	17	2000	1000[a]	7	67	37 000	4
	Loam	31	990	4200[b]	6	50	48 309	5
	Clay	1	8100	8100	–	–	–	1
	Organic	13	110 000	2500[a,b]	5	210	110 000	4
Pu	All soils	62	–	740	4	32	9610	7
	Sand	11	540	400[a]	4	33	6865	5
	Loam	27	1200	950[a,b]	4	100	9610	4
	Clay	10	4900	1800[b]	2	430	7600	4
	Organic	6	1800	760[a,b]	4	90	2951	4
	Unspecified	8	–	230	5	32	2100	2

[a,b] GM values with different letters were significantly different at $p < 0.05$.

Table 9
K_d for a miscellany of radionuclides for soils grouped according to the texture/OM criterion (L/kg). *n*: number of observations; GM: geometric mean; GSD: geometric standard deviation; min–max: minimum and maximum values; # ref.: number of references serving as data sources.

Radionuclide	Soil group	n	TRS value	GM/Value	GSD	min	max	# ref.
Ac	All soils	4	–	1700	3	450	5400	1[a]
	Sand	1	450	450	–	–	–	1
	Loam	1	1500	1500	–	–	–	1
	Clay	1	2400	2400	–	–	–	1
	Organic	1	5400	5400	–	–	–	1
Ag	All soils	9	–	380	7	36	15 000	5
	Sand	3	90	130	5	36	695	3
	Loam	1	120	120	–	–	–	1[a]
	Clay	1	180	180	–	–	–	1[a]
	Organic	2	15 000	–	–	4400	15 000	2
	Unspecified	2	–	–	–	115	398	2
As	All soils	7	–	550	5	25	2991	3
	Sand	4	–	210	5	25	1350	2
	Loam	1	–	1000	–	–	–	1
	Unspecified	2	–	–	–	2512	2991	2
Ba	Loam	1	–	0.4	–	–	–	1
Be	All soils	5	–	990	3	240	3 000	2
	Sand	1	240	240	–	–	–	1[a]
	Loam	1	810	810	–	–	–	1[a]
	Clay	1	1300	1300	–	–	–	1[a]
	Organic	1	3000	3000	–	–	–	1[a]
	Unspecified	1	–	1300	–	–	–	1
Bi	All soils	6	–	480	2	120	1500	2
	Sand	2	120	–	–	120	490	2[a,b]
	Loam	1	400	400	–	–	–	1[a]
	Clay	1	670	670	–	–	–	1[a]
	Organic	1	1500	1500	–	–	–	1[a]
	Unspecified	1	–	490	–	–	–	1[b]
Br	All soils	4	–	56	3	15	180	1[a]
	Sand	1	15	15	–	–	–	1
	Loam	1	49	49	–	–	–	1
	Clay	1	74	74	–	–	–	1
	Organic	1	180	180	–	–	–	1
Ce	All soils	11	–	1200	5	122	20 000	5
	Sand	3	490	400	1	316	490	3
	Loam	4	8100	3000	3	652	8100	4
	Clay	3	20 000	910	15	122	20 000	2
	Organic	1	3000	3000	–	–	–	1[a]
Cl	All soils	22	–	0.3	3	0.04	1.2	4
	Sand	3	–	0.5	4	0.1	1.1	2
	Loam	10	–	0.4	3	0.04	0.9	3
	Clay	5	–	0.2	3	0.06	0.9	4
	Organic	2	–	–	–	0.1	1.2	2
	Unspecified	2	–	–	–	0.1	0.2	1
Cm	All soils	18	–	9300	4	186	51 900	2
	Sand	5	4000	3400	14	186	30 920	2
	Loam	9	18 000	19 000	2	6809	51 900	2
	Clay	1	5400	5400	–	–	–	1[a]
	Organic	3	12 000	7400	2	5056	12 000	2
Dy	All soils	2	–	–	–	820	2100	1[b]
	Sand	1	–	820	–	–	–	1
	Unspecified	1	–	2100	–	–	–	1
Fe	All soils	23	–	880	2	220	4900	2
	Sand	4	220	320	1	220	424	2
	Loam	12	810	890	2	291	2231	2
	Clay	4	160	1600	1	1185	2240	2
	Organic	3	4900	1400	3	521	4900	2
Ga	All soils	2	–	–	–	280	310	1[b]
	Sand	1	–	310	–	–	–	1
	Unspecified	1	–	280	–	–	–	1
H	Sand	1	–	0.1	–	–	–	1
Hf	All soils	6	–	2500	3	450	8500	2
	Sand	2	450	–	–	450	3270	2[a,b]
	Loam	1	1500	1500	–	–	–	1[a]
	Clay	1	2400	2400	–	–	–	1[a]
	Organic	1	5400	5400	–	–	–	1[a]
	Unspecified	1	–	8500	–	–	–	1[b]
Hg	Unspecified	1	–	6300	–	–	–	1
Ho	All soils	4	–	930	3	240	3000	1[a]
	Sand	1	240	240	–	–	–	1
	Loam	1	810	810	–	–	–	1
	Clay	1	1300	1300	–	–	–	1
	Organic	1	3000	3000	–	–	–	1

(*continued on next page*)

Table 9 (*continued*)

Radionuclide	Soil group	n	TRS value	GM/Value	GSD	min	max	# ref.
In	All soils	2	–	–	–	240	730	1[b]
	Sand	1	–	240	–	–	–	1
	Unspecified	1	–	730	–	–	–	1
Ir	Unspecified	15	–	3	–	1	11	1
La	Sand	1	–	5300	–	–	–	1[b]
Lu	Sand	1	–	5100	–	–	–	1[b]
Mn	All soils	83	–	1200	9	36	79 044	4
	Sand	13	49	980	14	40	79 044	4
	Loam	56	720	1100	8	60	77 079	3
	Clay	10	180	4500	13	139	57 215	3
	Organic	3	490	160	4	36	490	2
	Unspecified	1	–	10 000	–	–	–	1
Mo	All soils	9	–	38	3	7	130	5
	Sand	2	7	–	–	7	82	2
	Loam	1	130	130	–	–	–	1[a]
	Clay	1	90	90	–	–	–	1[a]
	Organic	2	27	–	–	18	27	2
	Unspecified	3	–	37	3	13	109	3
Na	All soils	30	–	3	3	0.2	26	1
	Sand	6	–	2	4	0.4	23	1
	Loam	20	–	5	2	0.3	26	1
	Clay	4	–	2	6	0.2	11	1
Nb	All soils	11	–	1500	4	160	8370	3
	Sand	2	160	–	–	160	187	2
	Loam	5	540	2500	3	540	8370	2
	Clay	3	900	2400	2	900	4729	2
	Organic	1	2000	2000	–	–	–	1[a]
Np	All soils	26	–	36	6	1.3	1200	3
	Sand	8	4	14	4	3	108	3
	Loam	12	25	23	4	1.3	117	3
	Clay	2	55	–	–	20	55	2
	Organic	4	1200	810	1	500	1200	3
P	All soils	6	–	87	5	9	760	2
	Sand	2	9	–	–	9	760	2
	Loam	2	30	–	–	30	380	2
	Clay	1	49	49	–	–	–	1[a]
	Organic	1	110	110	–	–	–	1[a]
Pa	All soils	4	–	2000	3	540	6600	1[a]
	Sand	1	540	540	–	–	–	1
	Loam	1	1800	1800	–	–	–	1
	Clay	1	2700	2700	–	–	–	1
	Organic	1	6600	6600	–	–	–	1
Pd	All soils	6	–	180	2	55	670	2
	Sand	2	55	–	–	55	127	2[a,b]
	Loam	1	180	180	–	–	–	1[a]
	Clay	1	270	270	–	–	–	1[a]
	Organic	1	670	670	–	–	–	1[a]
	Unspecified	1	–	170	–	–	–	1[b]
Pm	All soils	2	–	–	–	450	450	1[b]
	Sand	1	–	450	–	–	–	1
	Unspecified	1	–	450	–	–	–	1
Pt	Unspecified	15	–	24	–	12	83	1
Rb	All soils	4	–	210	3	55	670	1[a]
	Sand	1	55	55	–	–	–	1
	Loam	1	180	180	–	–	–	1
	Clay	1	270	270	–	–	–	1
	Organic	1	670	670	–	–	–	1
Rh	Unspecified	12	–	4	–	0.6	29	1
Ru	All soils	15	–	270	8	5	66 000	5
	Sand	3	55	36	6	5	172	3
	Loam	3	990	300	3	82	990	3
	Clay	4	400	500	2	203	989	3
	Organic	1	66 000	66 000	–	–	–	1[a]
	Unspecified	4	–	140	3	34	490	2
Sc	All soils	2	–	–	–	670	3500	1[b]
	Sand	1	–	670	–	–	–	1
	Unspecified	1	–	3500	–	–	–	1
Si	All soils	4	–	130	3	33	400	1[a]
	Sand	1	33	33	–	–	–	1
	Loam	1	110	110	–	–	–	1
	Clay	1	180	180	–	–	–	1
	Organic	1	400	400	–	–	–	1

Table 9 (*continued*)

Radionuclide	Soil group	n	TRS value	GM/Value	GSD	min	max	# ref.
Sm	All soils	4	–	930	3	240	3000	1[a]
	Sand	1	240	240	–	–	–	1
	Loam	1	810	810	–	–	–	1
	Clay	1	1300	1300	–	–	–	1
	Organic	1	3000	3000	–	–	–	1
Sn	All soils	12	–	1600	6	130	31 000	4
	Sand	2	130	–	–	130	169	2[a,b]
	Loam	1	450	450	–	–	–	1[a]
	Clay	1	670	670	–	–	–	1[a]
	Organic	1	1600	1600	–	–	–	1[a]
	Unspecified	7	–	4100	5	328	31 000	3
Ta	All soils	5	–	780	3	240	3000	2
	Sand	2	240	–	–	240	379	2[a,b]
	Loam	1	810	810	–	–	–	1[a]
	Clay	1	1300	1300	–	–	–	1[a]
	Organic	1	3000	3000	–	–	–	1[a]
Tb	All soils	2	–	–	–	5400	6600	1[b]
	Sand	1	–	5400	–	–	–	1
	Unspecified	1	–	6600	–	–	–	1
Tc	All soils	33	–	0.2	9	0.01	11	4
	Sand	5	0.1	0.04	3	0.01	0.1	2
	Loam	14	0.1	0.07	3	0.01	0.9	4
	Clay	3	1	0.09	10	0.02	1	2
	Organic	11	2	3	3	0.9	11	2
Te	All soils	2	–	–	–	180	790	1[b]
	Sand	1	–	180	–	–	–	1
	Unspecified	1	–	790	–	–	–	1
Tm	Sand	1	–	330	–	–	–	1[b]
V	All soils	2	–	–	–	180	410	1[b]
	Sand	1	–	180	–	–	–	1
	Unspecified	1	–	410	–	–	–	1
Y	All soils	7	–	47	4	10	375	1
	Sand	5	–	22	2	10	47	1
	Organic	2	–	–	–	260	375	1
Zr	All soils	11	–	410	21	2	10 300	4
	Sand	4	600	32	16	2	600	3
	Loam	2	2200	–	–	2200	8100	2
	Clay	2	3300	–	–	3300	10 300	2
	Organic	2	7300	–	–	23	7300	2
	Unspecified	1	–	480	–	–	–	1[b]

[a] K_d estimates from the TRS-364 (IAEA, 1994).
[b] K_d estimates from neutron activation analyses (Zuyi et al., 2000).

For Pu the best correlation was with the sand content ($r = -0.50$; 22% of the variance explained). Multiple regressions did not lead to a significantly better description of K_d (Pu) variability, except for the sand and CEC combination that allowed us to explain 26% of the variance. When excluding Organic soils, similar correlations with the sand content were found ($r = -0.51$; 24% of the variance explained). However, grouping K_d (Pu) on the basis on the texture/OM criterion to derive a best estimate for each soil group is not a fully satisfactory option for this radionuclide.

3.5. Best estimates for a miscellany of radionuclides

Table 9 summarizes the descriptors of K_d data for a miscellany of radionuclides. No new data were available for a few radionuclides (Ac, Br, Ho, Pa, Rb, Si and Sm) and so the data presented in Table 9 for these radionuclides come from the previous TRS-364. For a number of radionuclides (for example, Ag, Be, Bi, Hf, Mo, P, Pd, Sn and Ta) although some new data were available, most also comes from the previous TRS-364. On the other hand, data for elements not present in the previous TRS-364 (As, Ba, Cl, Dy, Ga, H, Hg, In, Ir, La, Lu, Na, Pm, Pt, Rh, Sc, Tb, Te, Tm, V, and Y) have been included.

It is rather difficult to derive best estimates from the GM and values of Table 9, due to the low number of observations for many radionuclides, and the low number of references serving as data sources. In a few cases, only a distinction of K_d for mineral and organic soils can be proposed, as is the case of Np and Tc. Data often come from a single reference, such as the TRS-364 itself, related reports (Sheppard and Thibault, 1990; Thibault et al., 1990) or the work by Zuyi et al., 2000, where the K_d values come from experiments that use neutron activation analysis. Examples of other publications that are practically single source for specific radionuclides are: Gooddy et al., 1995, for Y and Zr; Yasuda et al., 1996, for Ir, Pt and Rh; Echevarria et al., 2003, for Tc; De Brouwere et al., 2004, for As and P; Echevarria et al., 2005, for Nb; and Nakamaru and Uchida, 2008, for Sn.

In some cases, the addition of new data has caused major changes in the GM with respect to those suggested by the previous TRS-364, especially because the criteria for accepting data are more strict here than in TRS-364. Some of the largest discrepancies are in the Clay and Organic classes, since for a reduced number of radionuclides (for example, Ag, Ce, Cm, Fe, Mn, Np and Zr) the previous GM are now the maximum value of the new range of values. Therefore, the new GM is clearly lower. For Ru, as no new value has been added, its estimate is the same as in the previous TRS-364, although the outstandingly high value of 66 000 L/kg must be used with caution.

4. Conclusions and recommendations

Although an important amount of data has been added to the new K_d compilation, there are evident gaps for a large number of radionuclides that are of increasing interest for waste management.

This fact restricts the possibility of proposing best estimates in most cases, and GM and single values must be considered only as approximate values, suitable for screening purposes, but not for specific risk assessments.

While for several radionuclides soil classification based on texture and organic matter content are satisfactory for deriving best estimates, the variability of the range of values decreases when other cofactors are used for soil grouping. Therefore, modellers and end-users can choose to use the best estimates derived from the GM values of K_d for soils arranged according to texture and organic matter or, when available, according to other criteria such as pH and speciation. Moreover, modellers and end-users can consider using existing single and multiple correlations between soil properties and K_d to derive best estimates from soil properties, especially in those cases where the K_d variance explained is significant.

Acknowledgements

This research was carried out in the frame of the IAEA' Programme on Environmental Modelling for Radiation Safety, EMRAS, within the Working Group "Revision of the TRS-364". The research was funded by the Spanish Government (CICYT, contracts PPQ2002-00264 and CTM2005-03847; Secretaría General para la Prevención de la Contaminación y el Cambio Climático del Ministerio de Medio Ambiente, contracts 1.2-193/2005/3-B and 240/2006/2-1.2).

References

Allard, B., Olofsson, U., Torstenfelt, B., 1984. Environmental actinide chemistry. Inorg. Chem. Acta. 94, 205–221.
Ashworth, D.J., Shaw, G., 2006. Effects of moisture content and redox potential on in situ K_d values for radioiodine in soil. Sci. Total Environ. 359, 244–254.
Bunzl, K., Schimmack, W., 1991. Kinetics of the sorption of ^{137}Cs, ^{85}Sr, ^{57}Co, ^{65}Zn and ^{109}Cd by the organic horizons of a forest soil. Radiochim. Acta. 54, 97–102.
De Brouwere, K., Smolders, E., Merckx, R., 2004. Soil properties affecting solid–liquid distribution of As(V) in soils. Eur. J. Soil Sci. 55, 165–173.
Echevarria, G., Morel, J.L., Florentin, L., Leclerc-Cessac, E., 2003. Influence of climatic conditions, soil type and plant physiology on $^{99}TcO_4^-$ uptake by crops. J. Environ. Radioact. 70, 85–97.
Echevarria, G., Morel, J.L., Leclerc-Cessac, E., 2005. Retention and phytoavailability of ^{95}Nb in soils. J. Environ. Radioact. 78, 343–352.
Environmental Protection Agency, 1999. Understanding Variation in Partitioning Coefficients, Kd, Values. In: Review of Geochemistry and Available Kd Values for Cadmium, Caesium, Chromium, Lead, Plutonium, Radon, Strontium, Thorium, Tritium and Uranium, vol. 2. US-EPA, Office of Air and Radiation EPA 402-R-99-004B, Washington, USA.
Fevrier, L., Martin-Garin, A., Leclerc-Cessac, E., 2007. Variation of the distribution coefficient K_d of selenium in soils under various microbial states. J. Environ. Radioact. 97, 189–205.
Fukui, M., Fujikawa, Y., Satta, N., 1996. Factors affecting interaction of radioiodide and iodate species with soil. J. Environ. Radioact. 31, 199–216.
Gooddy, D.C., Shand, P., Kinniburgh, D.G., Van Riemsdijk, W.H., 1995. Field-based partition coefficients for trace elements in soil solutions. Eur. J. Soil Sci. 46, 265–285.
International Atomic Energy Agency, 1994. Handbook of parameter values for the prediction of radionuclide transfer in temperate environments. Technical Report No 364, Vienna.
Muramatsu, Y., Uchida, S., Sriyotha, P., Sriyotha, K., 1990. Some considerations on the sorption and desorption phenomena of iodide and iodate on soil. Water Air Soil Pollut. 49, 125–138.
Nakamaru, Y., Tagami, K., Uchida, S., 2005. Distribution coefficient of selenium in Japanese agricultural soils. Chemosphere 58, 1347–1354.
Nakamaru, Y., Tagami, K., Uchida, S., 2006. Antimony mobility in Japanese agricultural soils and the factors affecting antimony sorption behavior. Environ. Pollut. 141, 321–326.
Nakamaru, Y., Uchida, S., 2008. Distribution coefficients of tin in Japanese agricultural soils and the factors affecting tin sorption behavior. J. Environ. Radioact. 99, 1003–1010.
Roussel-Debet, S., 2005. Experimental values for ^{241}Am and $^{239+240}$Pu Kd's in French agricultural soils. J. Environ. Radioact. 79, 171–185.
Sauvé, S., Hendershot, W., Allen, H., 2000. Solid-solution partitioning of metals in contaminated soils: dependence on pH, total metal burden, and organic matter. Environ. Sci. Technol. 34, 1125–1131.
Sheppard, S.C., 2003. Interpolation of solid/liquid partition coefficients, K(d), for iodine in soils. J. Environ. Radioact. 70, 21–27.
Sheppard, M.I., Thibault, D.H., 1990. Default soil solid/liquid partition coefficients, Kds, for four major soil types: a compendium. Health Phys. 59, 471–482.
Skipperud, L., Oughton, D., Salbu, B., 2000. The impact of Pu speciation on distribution coefficients in Mayak soil. Sci. Total Environ. 257, 81–93.
Staunton, S., 2004. Sensitivity of the distribution coefficient, K_d, of nickel to changing soil chemical properties. Geoderma 122, 281–290.
Thibault, D.H., Sheppard, M.T., Smith, P.A., 1990. A Critical Compilation and Review of Default Soil Solid/Liquid Partition Coefficients, Kd, for Use in Environmental Assessments. AECL 10125, Atomic Energy of Canada Limited, Pinawa, Manitoba Canada, 113 pp.
Ylaranta, T., 1983. Sorption of selenite and selenate in the soil. Ann. Agric. Fenn. 22, 29–39.
Yasuda, H., Ambe, S., Uchida, S., 1996. Distribution coefficient of platinum group metals between soil solid and liquid phases. Environ. Technol. 17, 1151–1154.
Yoshida, S., Muramatsu, Y., Uchida, S., 1995. Adsorption of I^- and IO_3^- onto 63 Japanese soils. Radioisotopes 44, 837–845.
Yoshida, S., Muramatsu, Y., Uchida, S., 1998. Soil-solution distribution coefficients, Kd's, of I^- and IO_3^- for 68 Japanese soils. Radiochim. Acta. 82, 293–297.
Zuyi, T., Xiangke, W., Xiongxin, D., Jinzhou, D., 2000. Adsorption characteristics of 47 elements on a calcareous soil, a red earth and an alumina: a multitracer study. Appl. Radiat. Isot. 52, 821–829.

Further reading

Agapkina, G.I., Tikhomirov, F.A., Shcheglov, A.I., Kracke, W., Bunzl, K., 1995. Association of Chernobyl derived ^{239,240}Pu, ^{241}Am, ^{90}Sr and ^{137}Cs with organic matter in the soil solution. J. Environ. Radioact. 29, 257–269.
Bachhuber, H., Bunzl, K., Schimmack, W., 1985. Spatial variability of the distribution coefficients of ^{137}Cs, ^{65}Zn, ^{85}Sr, ^{57}Co, ^{109}Cd, ^{141}Ce, ^{103}Ru, ^{95m}Tc and ^{131}I in a cultivated soil. Nucl. Technol. 72, 359–371.
Bell, J., Bates, T.H., 1988. Distribution coefficients of radionuclides between soils and groundwaters and their dependence on various test parameters. Sci. Total Environ. 69, 297–371.
Christensen, T.H., Lehmann, N., Jackson, T., Holm, P.E., 1996. Cadmium and nickel distribution coefficients for sandy aquifer minerals. J. Contam. Hydrol. 24, 75–84.
Colle, C., 2006. Transfert de l'iode 129 dans la biosphere – étude bibliographique, IRSN Report for ANDRA, CRPPSTR060007.
Colle, C., Mauger, S., Massiani, C., Kashparov, A.A., Grasset, G., 2002. Behaviour of chlorine (^{36}Cl) in cultivated terrestrial ecosystems. Radioprotection-Colloques 37, 491–496.
Darcheville, O., Février, L., Haichar, F.Z., Berge, O., Martin-Garin, A., Renault, P., 2008. Aqueous, solid and gaseous partitioning of selenium in an oxic sandy soil under different microbiological states. J. Environ. Radioact. 99, 981–992.
Denys, S., 2001. Prédiction de la phytodisponibilité de deux radionucléides (^{63}Ni et ^{99}Tc) dans les sols, PhD Thesis, Sciences Agronomiques, Nancy Univ.
Echevarria, G., 1996. Contribution à la prévision des transferts sol-plante des radionucléides, PhD Thesis, Sciences Agronomiques, Nancy Univ.
Ferrand, E., 2005. Étude de la spéciation en solution, de la rétention dans les sols et du transfert sol-plante du Zr, PhD Thesis, Paris VI Pierre et Marie Curie Univ.
John, M.K., Saunders, W.M.H., Watkinson, J.H., 1975. Selenium adsorption by New Zealand soils. I. Relative adsorption of selenite by representative soils and the relation to soil properties. N.Z.J. Agric. Res. 19, 143–151.
Kotova A.Y., 1998. A study into the mechanisms of ^{90}Sr, ^{106}Ru, ^{137}Cs, and ^{144}Ce sorption and bioavailability in different soil types, PhD thesis, Obninsk Univ.
Lakin, H.W., 1972. Selenium accumulation in soils and its absorption by plants and animals, Geo. Soc. Am. Bull. 83, 173–181.
Massoura, S.T., 2005. Fate of ^{36}Cl in the soil-plant system through isotopic exchange processes, ANDRA post-doc report, CRP1INR050001.
Mu, D.H., Du, J.Z., Li, D.J., Song, H.Q., Yan, S.P., Gu, Y.J., 2006. Sorption/desorption of radiozinc on the surface sediments. J. Anal. Chem. 267, 585–589.
Pinel, F., 2002. Chimie de ^{63}Ni et de ^{137}Cs dans le système sol-plante, PhD Thesis, Montpellier Univ.
Pinel, F., Leclerc-Cessac, E., Staunton, S., 2003. Relative contributions of soil chemistry, plant physiology and rhizosphere induced changes in speciation on Ni accumulation in plants shoots. Plant Soil 255, 619–629.
Rigol, A., Aldaba, D., Fernández-Torrent, R., Rauret, G., Vidal, M. Laboratory experiments to characterize radionuclide diffusion in unsaturated soils. Anal. Chim. Acta., submitted for publication.
Sastre, J., Rauret, G., Vidal, M., 2007. Sorption-desorption tests to assess the risk derived from metal contamination in mineral and organic soils. Environ. Int. 33, 246–256.
Shang, Z.R., Leung, J.K.C., 2003. ^{110m}Ag root and foliar uptake in vegetables and its migration in soil. J. Environ. Radioact. 68, 297–307.
Sheppard, S.C., Sheppard, M.I., Tait, J.C., Sanipelli, B.L., 2006. Revision and meta - analysis of selected biosphere parameter values for chlorine, iodine, neptunium, radium, radon and uranium. J. Environ. Radioact. 89, 115–137.
Smolders, E., Brans, K., Földi, A., Merckx, R., 1999. Cadmium fixation in soils measured by isotopic dilution. Soil Sci. Soc. Am. J. 63, 78–85.
Sokolik, G.A., Ivanova, T.G., Leinova, S.L., Ovsiannikova, S.V., Kimlenko, I.M., 2001. Migration ability of radionuclides in soil-vegetation cover of Belarus after Chernobyl accident. Environ. Int. 26, 183–187.
Staunton, S., Barthes, M., Leclerc-Cessac, E., Pinel, E., 2002. Effect of sterilization, incubation time, solution composition and soil: solution ratio on the isotopic exchange of nickel in two contrasting soils. Eur. J. Soil Sci. 53, 655–662.

Tipping, E., Woof, C., Kelly, M., Bradshaw, K., Rowe, J.E., 1995. Solid-solution distributions of radionuclides in acid soils: application of the Wham Chemical speciation model. Environ. Sci. Technol. 29, 1365–1372.

Twining, J.R., Payne, T.E., Itakura, T., 2004. Soil-water distribution coefficients and plant transfer factors for ^{134}Cs, ^{85}Sr and ^{65}Zn under field conditions in tropical Australia. J. Environ. Radioact. 71, 71–87.

Willett, I.R., Bond, W.J., 1995. Sorption of manganese, uranium, and radium by highly weathered soils. J. Environ. Qual. 24, 834–845.

Yasuda, H., Uchida, S., Muramatsu, Y., Yoshida, S., 1995. Sorption of manganese, cobalt, zinc, strontium and cesium onto agricultural soils: statistical analysis on effects of soil properties. Water Air Soil Pollut. 83, 85–96.

3.5

The use of hard and soft modelling to predict radiostrontium solid-liquid distribution coefficient in soils

C. J. Gil-García, A. Rigol M, Vidal.

Enviado a la revista *Chemosphere* para su publicación

Páginas 125-143

The use of hard- and soft-modelling to predict radiostrontium solid-liquid distribution coefficients in soils.

Carlos J. Gil-García, Anna Rigol*, Miquel Vidal

Departament de Química Analítica, Universitat de Barcelona, Martí i Franqués 1-11, 3ª Planta, 08028 Barcelona, Spain.

*Corresponding author: Tel.: +34 934021277; Fax: +34 934021233; e-mail: annarigol@ub.edu

ABSTRACT

The solid-liquid distribution coefficient (K_d) is the parameter that governs the incorporation of contaminants in soils. Its estimation allows the prediction of the fate of contaminants in the short- and long-term after a contamination event. Here, the K_d of radiostrontium (K_d(Sr)), a radionuclide of significant environmental interest, was predicted using hard models, which are based on knowledge of the mechanisms governing its sorption, and using PLS-based soft models, using a large data set based on the characteristics of the main soil parameters. The two approaches were tested and compared for 30 soils in Spain. Correlations between the predicted and experimental values of K_d(Sr) obtained using hard- and soft-modelling showed slopes close to 1 and regression coefficients higher than 0.95, which confirms that both approaches are able to obtain satisfactory estimates for K_d(Sr) from soil parameters.

Keywords: radiostrontium; soil; sorption; distribution coefficient; hard modelling; soft modelling.

1. Introduction

Radiostrontium is a radionuclide of significance resulting from the fallout from nuclear weapons testing, accidental releases from radioactive and nuclear facilities, and radioactive waste. Soils are typically a target of radioactive releases as well as an intermediate in their subsequent fate within the environment, and an understanding of the interactions of radiostrontium in soils is necessary to predict its mobility within other environmental compartments, to assess the subsequent risk, and to propose countermeasures that minimise the incorporation of radiostrontium into the trophic chain.

The main mechanism of radiostrontium sorption by the soil solid phase is ion exchange (Valcke, 1993; Rigol et al., 1999; Sysoeva et al., 2005), and this mechanism is strongly associated with the regular exchange sites (RES) in clays and organic matter. Thus, the soil sorption capacity for radiostrontium varies with the cationic exchange capacity (CEC); the CEC depends on the content of soil organic matter (SOM) and clays and the cationic composition of the soil exchange complex, especially those species competing with radiostrontium for the sorption sites, such as Ca and Mg.

The extent of radionuclide sorption onto the solid phase is often quantified using the solid-liquid distribution coefficient (K_d), which is useful when making assessments of the overall mobility and likely residence times of radionuclides in soils. The K_d is the ratio of the radionuclide concentration sorbed onto a specified solid phase to the radionuclide concentration in the liquid phase in contact with the solid phase. The K_d approach does not explicitly account for sorption mechanisms, and it is an operational parameter that depends on the characteristics of the liquid and solid phases and on the methodology applied for its determination. The K_d can be quantified using various approaches based on column and mass transport experiments (Bachhuber et al., 1982; Dewiere et al., 2004), batch tests (Bunzl et al., 1985; Benes et al., 1994; Twining et al., 2004; Wang et al., 2005), or in situ quantification of the soil solution obtained in field conditions (Agapkina, 1995; Goody et al., 1995). All of these approaches generate K_d values that may vary within a range of 2 or 3 orders of

magnitude, even for similar soils, indicating that not all laboratory methods are reliable for estimating the field values of the K_d of radiostrontium (K_d(Sr)). Moreover, default or best-estimate values exhibit large variability and are thus not useful for prediction purposes (Sheppard and Thibault, 1990; Gil-García et al., 2009). Therefore, models to predict the K_d(Sr) derived from laboratory experiments using the soil parameters governing radiostrontium sorption are needed to estimate the K_d(Sr) for a target soil with lower variability.

Hard modelling is the most frequently applied approach to predict the K_d(Sr) on the basis of general soil properties (Yasuda and Uchida, 1993; Ishikawa et al., 2009) or by reference to the partitioning of an analogue (sorption competitive) ion that is characterised by similar sorption behaviour, which are Ca and Mg in the case of radiostrontium (Valcke, 1993; Rauret and Firsakova, 1996; Hilton et al., 2001; Camps et al., 2003). Soft models, which make use of chemometric tools, are complementary to hard models and can also be applied to predict the K_d using soil parameters. Soft models examine similarities between soil samples or measured soil properties and find mathematical relationships that may allow the K_d parameter to be predicted from the quantification of soil parameters without the restrictions of hard models. Thus, the observed relationships are not supported by mathematical expressions that describe the underlying physicochemical phenomena. Partial least squares regression (PLS) is a soft modelling tool that is often used for the prediction of quantitative information from multivariate linear responses, and it has been increasingly used for the prediction of radioecological processes (Sonesten, 2001; Rigol et al., 2008).

In this paper, we predict the K_d(Sr) of 30 soils originating from zones in the Spanish territory, including soils from areas near nuclear power plants and other radioactive facilities. The experimental values of K_d(Sr) were previously obtained using sorption batch experiments, and the experimental data were used to construct and validate the soft and hard models that were developed.

2. Material and methods

2.1. Soil sample characteristics

The 30 soils under study were collected throughout Spain, including in locations near radioactive facilities and nuclear power plants. Samples were taken from the surface layer (0-10 cm depths), air-dried, sieved and homogenised prior to analyses and experiments.

Table 1 summarises the ranges for values of the general and specific quantified soil characteristics. Individual values are available elsewhere (Gil-García et al., 2008). Soils were mineral-based with a maximum C_{org} content of less than 10%. Most soils had a loamy texture, and a few had clay (5 soils) and sandy (1 soil) textures. Unlike soils from temperate areas, many of these soils had a clay content over 20%, pH value over 8, and $CaCO_3$ content over 25%.

2.2. Determination of radiostrontium solid-liquid distribution coefficients

The K_d(Sr) values were derived from two batch sorption tests, differing in the composition of the contact solution. The first set of data was obtained in a medium that simulated the cationic composition of the soil solution. Soil samples (1 g) were equilibrated for 16 h with 50 mL of a solution representing the cationic composition of the soil solution of each soil. After four pre-equilibrations, soils were equilibrated for 24 h with the same solution but were labelled with ^{85}Sr (SR85ELSB45; CERCA-LEA Framatome). The K_d(Sr) values were determined by measuring the ^{85}Sr level in the supernatant before and after equilibration.

A second data set was obtained from batch experiments with a contact solution derived from the soil wash-off. This solution was obtained by equilibrating soil samples (1 g) in water (30 mL g^{-1}) using end-over-end shaking for 16 h. Subsequently, the wash-off solution in contact with the soil was spiked with ^{85}Sr and shaken for 24 h. The K_d(Sr) values were calculated from ^{85}Sr levels in the supernatant before and after equilibration. Further details about the determination of the K_d(Sr) are available elsewhere (Gil-García, 2008).

Table 1. Ranges of values for the soil characteristics.

Variable	Code	Unit	Min	Max	AM[a]	GM[b]
pH	pH	-	4.3	9.2	7.0	6.9
Organic carbon	C_{org}	%	0.2	9.4	3.3	2.1
Carbonate content	$CaCO_3$	%	1	51	13.9	6.6
Cationic exchange capacity	CEC	$cmol_c\ kg^{-1}$	21.3	89.3	42.2	39.0
Exchangeable Na	Na_{exch}	$cmol_c\ kg^{-1}$	0.12	19.6	1.4	0.69
Exchangeable K	K_{exch}	$cmol_c\ kg^{-1}$	0.19	10.2	1.3	0.81
Exchangeable Ca	Ca_{exch}	$cmol_c\ kg^{-1}$	3.5	52.0	13.1	10.8
Exchangeable Mg	Mg_{exch}	$cmol_c\ kg^{-1}$	0.45	14.1	2.7	1.8
Exchangeable NH_4^+	NH_{4exch}	$cmol_c\ kg^{-1}$	0.06	2.6	0.36	0.22
Clay fraction (wrt. initial soil weight)	Clay	%	6.3	52.4	22.9	20.7
Sand fraction (wrt. initial soil weight)	Sand	%	4.5	86.8	43.1	36.8
Field capacity	FC	%	6.2	56.1	27.8	26.1
Electrical conductivity	EC	$\mu S\ cm^{-1}$	89	3390	738	481
Wash-off experiments						
Na in the contact solution	Na_{ss}	$mmol\ L^{-1}$	0.01	3.6	0.35	0.11
K in the contact solution	K_{ss}	$mmol\ L^{-1}$	0.02	0.35	0.095	0.075
Ca in the contact solution	Ca_{ss}	$mmol\ L^{-1}$	0.01	6.6	0.70	0.29
Mg in the contact solution	Mg_{ss}	$mmol\ L^{-1}$	0.01	0.76	0.12	0.065
NH_4^+ in the contact solution	NH_{4ss}	$mmol\ L^{-1}$	0.02	0.96	0.091	0.047
Soil solution experiments						
Na in the contact solution	Na_{ss}	$mmol\ L^{-1}$	0.17	128	11.8	2.0
K in the contact solution	K_{ss}	$mmol\ L^{-1}$	0.13	23.7	1.8	0.79
Ca in the contact solution	Ca_{ss}	$mmol\ L^{-1}$	0.44	52.1	14.3	8.3
Mg in the contact solution	Mg_{ss}	$mmol\ L^{-1}$	0.17	72.5	6.8	2.4
NH_4^+ in the contact solution	NH_{4ss}	$mmol\ L^{-1}$	0.016	11.4	1.1	0.24
Strontium distribution coefficient						
Wash-off experiments	K_d	$L\ kg^{-1}$	11	1764	262	172
Soil solution experiments	K_d	$L\ kg^{-1}$	1	110	19	10

[a]AM = arithmetic mean;

[b]GM = geometric mean

2.3. Data treatment

Whereas the application of the hard-model was carried out for the global data set, the application of the soft-model was carried out for three K_d(Sr) data sets: K_d(Sr) from the wash-off experiments, K_d(Sr) from the soil solution experiments, and the global data set. Single and multiple linear correlations related to the hard models were performed using STATGRAPHICS Plus (StatPoint Technologies, US) software, whereas Unscrambler® 6.11a software (CAMO ASA, Norway) was used to carry out the soft modelling based on Partial Least Squares regression (PLS).

The errors of the correlations between K_d(Sr) experimental and K_d(Sr) predicted values from the various models were evaluated as Root Mean Square Errors:

$$RMSE = \sqrt{\frac{\sum_{i=1}^{n} (y^i_{experimental} - y^i_{predicted})^2}{n}} \qquad (1)$$

3. Results and discussion

3.1. Hard-modelling

Several studies reported in the literature have attempted to directly estimate the solid-liquid distribution coefficient of selected contaminants, including heavy metals and radionuclides, using single or multiple linear correlations with soil properties (Sauvé et al., 2000). Here, we examined single correlations of the K_d(Sr) values from the wash-off and soil solution data sets with a number of soil characteristics that are determined in routine soil analyses, specifically pH, C_{org}, CEC, clay, $CaCO_3$, Ca_{exch}, $(Ca + Mg)_{exch}$, and electrical conductivity (EC). The correlations were not significant at the 95% confidence level, with a few exceptions that included K_d vs. CEC and $CaCO_3$ in the wash-off data set and K_d vs. EC for the wash-off and soil solution data sets (Table 2). These findings indicated that the K_d(Sr) cannot be directly estimated from single correlations with soil properties. However, the significant correlations that were observed emphasise the two major factors affecting radiostrontium sorption in soils: the number of sorption sites in the soil (here represented by the CEC) and the concentration of

competing cations in the contact solution (here represented by the EC). When a multiple correlation is considered by calculating the regression coefficients of K_d(Sr) vs. CEC and EC, improved correlations are observed for both data sets, thus confirming the previous hypotheses. These results agree with those found by Yasuda and Uchida (1993), in which the correlation between the K_d(Sr) and the Cation Distribution Ratio (CDR, calculated from the CEC/EC ratio) yielded regression coefficients around 0.6.

Table 2. Significant correlations between K_d(Sr) and soil properties (n = 30; r = correlation coefficient).

Data set	Regression equations	r
Single correlations		
Wash-off	$K_d(Sr) = 6\ (\pm 3)\ CEC$	0.35
	$\log K_d(Sr) = 2.5\ (\pm 0.2) - 0.3\ (\pm 0.1) \log CaCO_3$	0.40
	$\log K_d(Sr) = 3.6\ (\pm 0.5) - 0.5\ (\pm 0.2) \log EC$	0.46
Soil solution	$\log K_d(Sr) = 2.9\ (\pm 0.5) - 0.7\ (\pm 0.2) \log EC$	0.55
Multiple correlations		
Wash-off	$\log K_d(Sr) = 2.0\ (\pm 0.5) + 1.7\ (\pm 0.4) \log CEC - 0.9\ (\pm 0.2)$ logEC	0.76
Soil solution	$\log K_d(Sr) = 2.1\ (\pm 0.7) + 0.8\ (\pm 0.5) \log CEC - 0.9\ (\pm 0.2)$ logEC	0.61

To improve the K_d(Sr) estimation, predictions based on the mechanisms governing radiostrontium incorporation in soils can be performed. The sorption of radiostrontium can be depicted as the result of a competition with an analogue ion with similar sorption behaviour to that of radiostrontium. In soils, these analogues are Ca and Mg (Valcke, 1993):

$$K_d(Sr) = K_d(Ca + Mg) \cdot K_c(Sr / Ca - Mg) \qquad (2)$$

Here, the K_c(Sr/Ca–Mg) term is the Sr to Ca–Mg selectivity coefficient at the sorption sites. The combined Ca + Mg distribution coefficient can be calculated by dividing the exchangeable Ca and Mg (in $cmol_c\ kg^{-1}$) by the sum of the Ca and Mg concentrations in the contact soil solution (Ca_{ss} and Mg_{ss} in $cmol_c\ L^{-1}$), and the Ca contribution is amplified by the respective selectivity coefficient (K_c(Ca/Mg)) (Rauret et al., 1996; Hilton et al., 2001):

$$K_d(Sr) = \frac{Ca_{exch} + Mg_{exch}}{K_c(Ca/Mg) \cdot Ca_{ss} + Mg_{ss}} \cdot K_c(Sr/Ca - Mg) \qquad (3)$$

The $K_c(Ca/Mg)$ values were determined for each sample from the $K_d(Ca)/K_d(Mg)$ ratios, and they ranged from 0.1 to 11.5 with a geometrical mean of 1.5, which agrees with previously reported values (Valcke, 1993).

The regression equation obtained from the modelling exercise ($\log K_d(Sr)_{exp}$ = 1.07 (±0.06) $\log K_d(Sr)_{pred}$, r = 0.86, n = 60) showed a satisfactory correlation between the predicted and experimental $K_d(Sr)$ values with a slope close to 1 and an RMSE of 19 and 212 for the soil solution and wash-off data, respectively.

As the Sr-to-Ca, Sr-to-Mg, and Ca-to-Mg selectivity coefficients approach one, the model described by equation 3 can be simplified to that shown in equation 4:

$$K_d(Sr) = \frac{Ca_{exch} + Mg_{exch}}{Ca_{ss} + Mg_{ss}} \qquad (4)$$

The regression equation obtained from the new modelling exercise ($\log K_d(Sr)_{exp}$ = 1.02 (±0.05) $\log K_d(Sr)_{pred}$, r = 0.92, n = 60) was similar to that obtained with equation 3, yielding a slightly better regression coefficient and a lower RMSE of 16 and 199 for the soil solution and wash-off data, respectively. A final, further simplification of the model uses CEC instead of $(Ca + Mg)_{exch}$ if the latter data are not available. This may be a satisfactory approach for estimating the $K_d(Sr)$, especially when dealing with soils with a saturated exchange complex (Rauret et al., 1996). Therefore, the hard model would employ equation 5 for the prediction.

$$K_d(Sr) = \frac{CEC}{Ca_{ss} + Mg_{ss}} \qquad (5)$$

As shown in Fig. 1a, the regression equation obtained from the final hard modelling exercise ($\log K_d(Sr)_{exp}$ = 1.01 (±0.04) $\log K_d(Sr)_{pred}$, r = 0.94, n = 60) was also similar to those obtained previously with an RMSE of 10 and 187 for the soil solution and wash-off data,

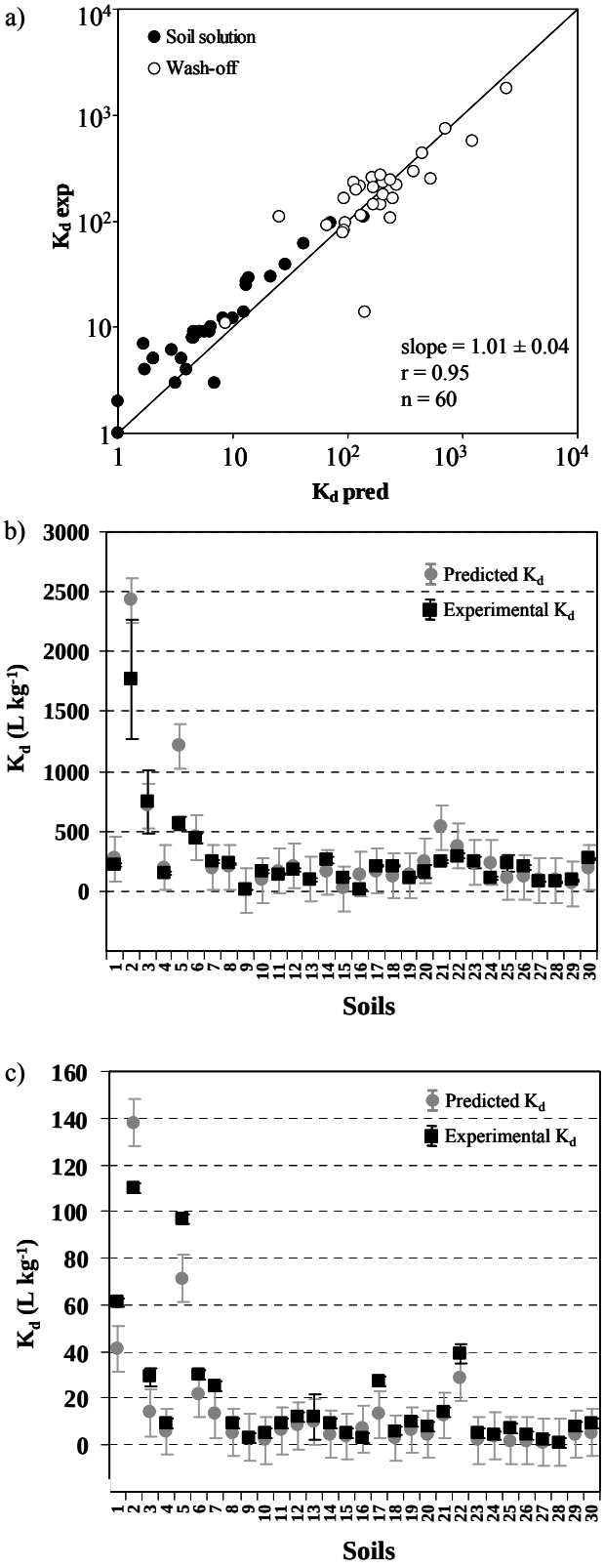

Fig 1. Hard-modelling results: (a) experimental vs. predicted $K_d(Sr)$, in which the solid line represents the ideal $K_d(Sr)_{exp} = K_d(Sr)_{pred}$ relationship; (b) comparison of individual values for the soil solution data for all soils; (c) comparison of individual values for the wash-off data for all soils. Error bars indicate the uncertainty of replicates for the experimental values and the RMSE for predicted values.

respectively, thus confirming the robustness of the hard model when the concentrations of Mg and Ca in the contact solution are retained in the equations. Individually predicted K_d(Sr) values were compared with those obtained experimentally, and the proposed model succeeded in predicting individual K_d(Sr) values; accounting for the associated error, agreement between the two sets of values was observed for the soil solution data (Fig. 1b) and the wash-off data (Fig. 1c). This model also improved previously reported approaches, especially those based on suggesting default or predicted values from general soil properties (Sheppard and Thibault, 1990; Yasuda and Uchida, 1993) and even those in which the prediction was based solely on the Ca status in the soil (Ishikawa et al., 2009).

3.2. Soft-modelling

3.2.1. Theoretical approach

A data matrix was constructed with rows related to the soil samples and columns corresponding to the soil variables to predict the K_d(Sr) from soil properties using soft-modelling. To assume normal distributions of variables for multivariate analysis and to confer more stability to the regression model, data were transformed to logarithmic units with the exception of pH, which already showed a normal distribution. Data were also autoscaled prior to analysis, i.e., mean centred (each element subtracted by its mean column) and scaled to unit variance (each element divided by the standard deviation of its column). This process gave the same weight to all variables in the analyses.

PLS is a multivariate regression method that builds a model between a sample variable (y) and a set of other sample descriptors (X) for predictive purposes. The PLS model is built in a low-dimensional space formed by PLS components and seeks a maximum covariance model of the relationship between the X- and y-space (Boardman et al., 1981; Wold et al., 1983). The construction of the PLS regression model, $y = XB$, consists of the creation of the PLS space and the calculation of the model regression coefficients (B) in this space. Full cross-validation was used to determine the number of PLS components to be included in the regression model, for which the RMSE reached its minimal value.

PLS was first used to ascertain the relevance of the soil variables for the prediction of the

K_d(Sr) by examining the quality parameters of the model and the value and sign of the regression coefficients, B. In the second stage, the quality of the PLS model was tested by representatively dividing the population of samples into a calibration set, used to establish the model, and a prediction set, used to validate externally the predictive ability of the model. The data set for calibration was selected using the Kennard-Stone algorithm (Kennard and Stone, 1969). The remaining samples were used as the prediction set.

Further details on the theoretical background of the applied multivariate calibration methods and on the software are available elsewhere (Esbensen et al., 1994).

3.2.2. Relevance of variables to predict the K_d(Sr) using PLS

The relevance of the soil variables used for the prediction of the K_d(Sr) values was ascertained by examining the quality parameters of the model and the value and sign of the regression coefficients. The soil solution, the wash-off and the global data sets were modelled separately to reveal which variables better explained K_d(Sr) in each data set. Table 3 summarises the statistical description of the cross-validated PLS models obtained in each case. Suitable models were obtained for the three data sets with an explained y cumulative variance higher than 80%. Four PLS components were required to explain the maximum y cumulative variance for the soil solution and wash-off data sets although satisfactory results were also obtained with three PLS components. Moreover, models obtained for the soil solution data set showed better statistical parameters than those obtained for the wash-off data set. For the global data set, the best model was obtained with only three PLS components, likely due to the larger number of samples and the wider range of values for some of the variables, especially for the predicted K_d(Sr) variable. All of the statistical parameters of this model improved substantially when compared with the models derived from the individual data sets. Satisfactory regressions with slopes close to 1 were obtained for the three sets of data, confirming the absence of bias in the models. Moreover, the RMSE values were approximately half the value of those observed when hard modelling was applied.

The regression coefficients of the PLS models obtained for the three data sets were compared to identify the most relevant variables to describe the K_d(Sr) variation for each data set. The direction and magnitude of the influence of soil variables on K_d(Sr) can generally be

Table 3. Description of the cross-validated PLS models**.**

Data set	n	Number of PLS components	y explained cumulative variance (%)	RMSE [a]	Experimental vs. predicted regression [b]	
					slope	r
Soil solution	30	3	89	15	1.03 ± 0.06	0.94
	30	4	93	7.5	1.01 ± 0.05	0.96
Wash-off	30	3	82	145	1.01 ± 0.03	0.89
	30	4	85	93	1.00 ± 0.03	0.91
Soil solution + wash-off	60	3	94	70	1.00 ± 0.03	0.97

[a] Value calculated after back-transforming the logarithmic predicted values to original K_d(Sr) units.

[b] Offsets of all experimental vs. predicted regressions were found not to be statistically significant.

associated with the sign and the magnitude of its regression coefficient, respectively. However, because soil variables may be partially correlated, their related regression coefficients cannot be considered in an individual or completely independent way, and only the most salient trends in the regression coefficients can be safely used for chemical interpretation. Similar patterns for the regression coefficients were obtained for all of the data sets. As an example, Fig. 2 shows those coefficients obtained for the global data set. High negative regression coefficients were obtained for Ca and Mg concentrations in soil solutions, and high positive regression coefficients were obtained for exchangeable cations (especially Mg), CEC and C_{org}. Other variables describing significant soil properties, such as pH and texture, had regression coefficients with a lower significance. The relevance of these variables agreed with the mechanisms governing the sorption process described for K_d(Sr), as shown in the previous section. As the K_d(Sr) is directly related to exchangeable Ca and Mg and to the CEC, an increase in these parameters provoked an increase in the K_d(Sr), which was confirmed by the positive regression coefficients for these factors. Conversely, an increase in the Ca and Mg concentrations in the soil solution may contribute to a decrease in K_d(Sr), which was confirmed by their high negative regression coefficients.

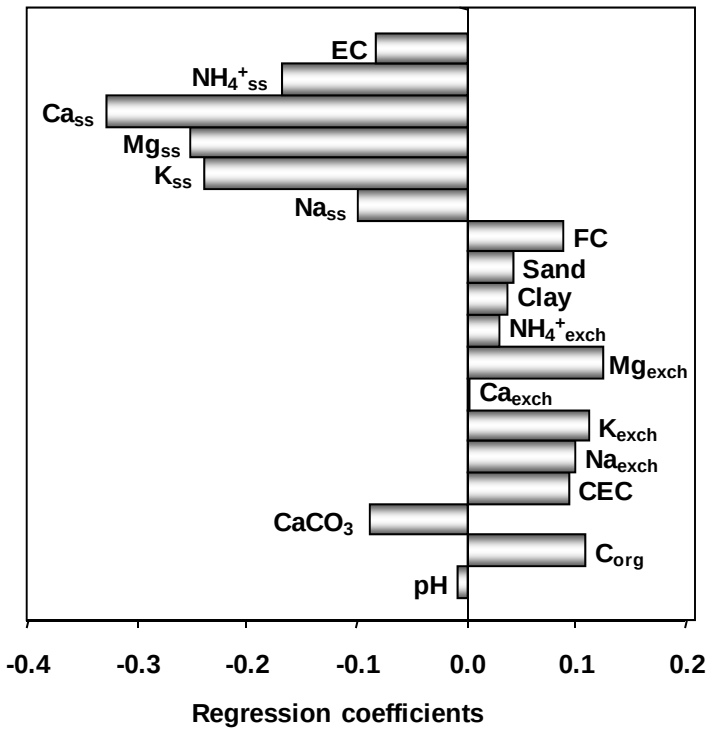

Fig. 2. Regression coefficients of the PLS model with the soil solution + wash-off dataset.

3.2.3. Construction and external validation of the PLS model

Whereas the satisfactory results obtained with hard modelling guaranteed that the model could be extrapolated to other samples, soft modelling requires a further step to demonstrate the potential usefulness of the PLS model to predict K_d(Sr) values of samples not used for model calibration. Thus, external validation was performed using the global data set because this set provided a more satisfactory model in terms of statistical parameters and applicability to a wider range of soil samples with different properties. The population of samples was representatively divided into a calibration set, used to establish the model, and a prediction set, used to externally validate the predictive ability of the model.

The calibration set (n = 32) was selected for calibration using the Kennard-Stone algorithm (Kennard et al., 1969). The remaining data (n = 28) were used as the prediction set and compared with the experimental values. The PLS model obtained with the calibration set showed a pattern of regression coefficients similar to that obtained in the previous section with the global data set. Moreover, despite the smaller number of samples used for the calibration, the correlation parameters were almost identical because with three PLS components, the y explained cumulative variance was 94%, the slope of the correlation was 1.00 ± 0.04 and r = 0.97; the RMSE was the same order of magnitude as for the global dataset. Once the PLS model was constructed, it was externally validated with the prediction set. As shown in Fig. 3a, an excellent correlation between the predicted and experimental K_d(Sr) values was obtained with a slope of unity. This result confirmed the robustness and the absence of bias in the PLS model.

Individual K_d(Sr) predicted values were back-transformed to the original units and compared with those obtained experimentally. As shown in Fig. 3b and 3c, the PLS model succeeded in predicting K_d(Sr) values from soil properties because the predicted values, with RMSE values of 4.5 and 68 for the soil solution and wash-off datasets, respectively, often agreed with the experimental ones within the corresponding error.

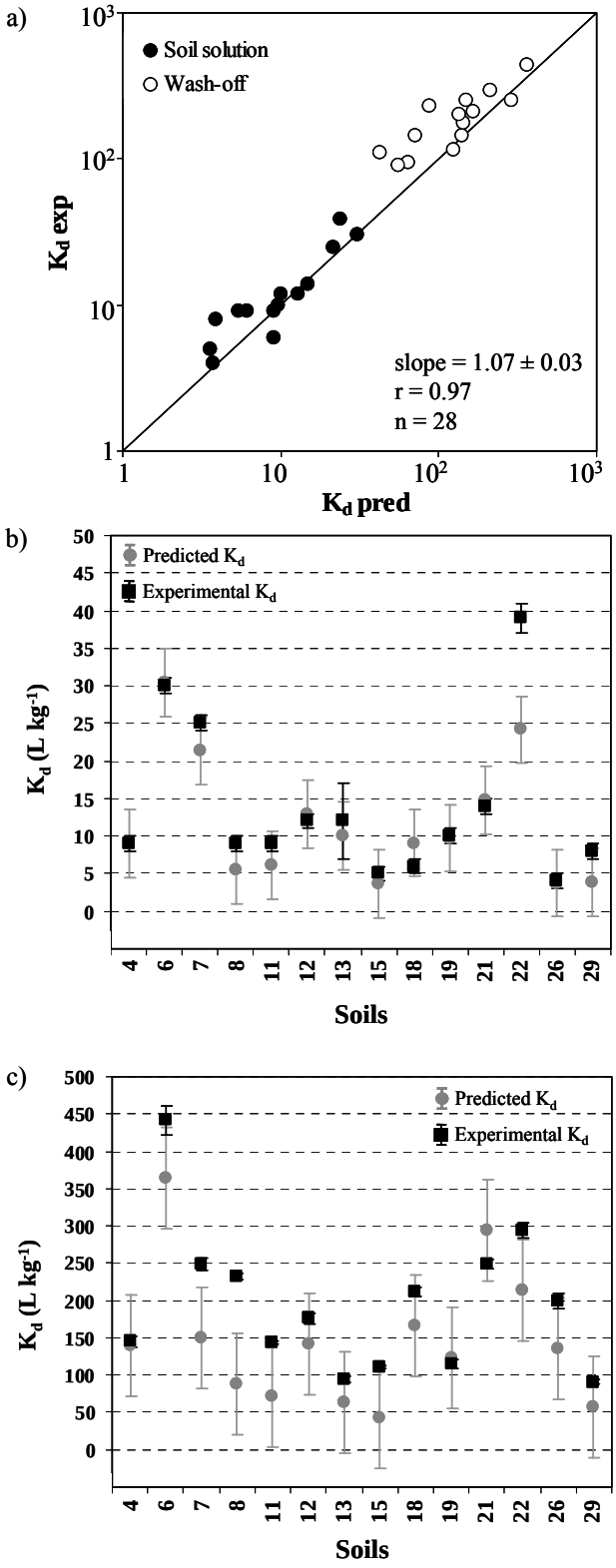

Fig. 3. Soft-modelling results: (a) experimental vs. predicted $K_d(Sr)$, in which the solid line represents the ideal $K_d(Sr)_{exp} = K_d(Sr)_{pred}$ relationship; (b) comparison of individual values for the soil solution data for the soils of the prediction set; (c) comparison of individual values for the wash-off data for the soils of the prediction set. Error bars indicate the uncertainty of replicates for the experimental values and the RMSE for predicted values.

4. Conclusions

Hard- and soft-models produced excellent results for the prediction of K_d(Sr) values from soil parameters. However, both models required measurements of minimum, key significant data, including the quantification of the concentrations of competitive species in the soil solution.
The hard-modelling approach is useful when the interaction mechanisms are well-known and the key data are available. However, this approach neglects variable interactions (synergisms and antagonisms) and works by fitting a fixed correlation to the variation of the data, allowing less freedom in the interpretation of the results. Moreover, complete knowledge of all events and mechanisms involved in environmental processes is hardly ever achieved in practice, and this consideration makes complete reliance on mechanistic models risky.

In this work, soft-modelling methodologies were found to be an excellent option for the interpretation and prediction of environmental processes. The semi-empirical models underlying PLS are more forgiving of a lack of knowledge, and consequently, they are often preferable in situations where only partial mechanistic information is available. However, these models require representative and large environmental data sets. The quality of the prediction and derived diagnostics from PLS modelling may also provide more insight into the data and their relationships, as well as into their deficiencies, than mechanistic modelling.

Acknowledgements

This research was funded by the Spanish Government (CICYT, contracts PPQ2002-00264 and CTM2005-03847/TECNO) and the Generalitat de Catalunya (contract 2009SGR1188). C.J. Gil-García acknowledges the Ministerio de Educación, Cultura y Deporte for a PhD fellowship. The authors thank Universidad de Salamanca, Universidad Politécnica de Valencia, Universidad de Oviedo, Universidad de Extremadura, Universidad de León, Universitat de les Illes Balears, ENRESA, ENUSA, SCAR (Generalitat de Catalunya), Universidade da Coruña and Universidad de Málaga for the soil samples supplied.

References

Agapkina, G.I., Tikhomirov, F.A., Shcheglov, A.I., Kracke, W., Bunzl, K., 1995. Association of Chernobyl derived ^{239,240} Pu, ^{241}Am, ^{90}Sr and ^{137}Cs with organic matter in the soil solution. J. Environ. Radioactiv. 29, 257-269.

Bachhuber, H., Bunzl, K., Schimmack, W., 1982. The migration of ^{137}Cs and ^{90}Sr in multilayered soils: results from batch, column and fallout investigations. Nucl. Technol. 59, 291-301.

Benes, P, Stamberg, K., Stegmann, R., 1994. Study of the kinetics of the interaction of Cs-137 and Sr-85 with soils using a batch method: methodological method. Radiochim. Acta 66/67, 315-321.

Boardman, A. E., Hui, B. S., Wold, H., 1981. The partial least squares-fix point method of estimating interdependent systems with latent variables. Comm. Statist. Theory Methods 10, 613-639.

Bunzl, K, Schultz, W., 1985. Distribution coefficients of ^{137}Cs and ^{85}Sr by mixtures of clay and humic material. J. Radioanal. Nucl. Ch. 90, 23-37.

Camps, M., Rigol, A., Vidal, M., Rauret, G., 2003. Assessment of the suitability of soil amendments to reduce ^{137}Cs and ^{90}Sr root uptake in meadows. Environ. Sci. Technol. 37, 2820-2828.

Dewiere, L., Bugai, D., Grenier, C., Kashparov, V., Ahamdach, N, 2004. ^{90}Sr migration to the geo-sphere from a waste burial in the Chernobyl exclusion zone. J. Environ. Radioactiv. 74, 139-150.

Esbensen, K., Schönkopf, S., Midtgaard, T., 1994. Multivariate Analysis in Practice. Computer-Aided Modelling AS, Norway.

Gil-García, C. , Rigol, A., Rauret, G., Vidal, M., 2008. Radionuclide sorption-desorption pattern in soils from Spain. Appl. Radiat. Isotopes 66, 126-138.

Gil-García, C., Rigol, A., Vidal, M., 2009. New best estimates for radionuclide solid-liquid distribution coefficient in soils. Part 1: radiostrontium and radiocaesium. J. Environ. Radioactiv. 100, 690-696.

Goody, D.C., Shand, P., Kinniburgh, D.G., Van Riemsdijk, W.H., 1995. Field-based partition coefficients for trace elements in soil solutions. Eur. J. Soil Sci. 46, 265-285.

Hilton, J., Comans, R. N. J., 2001. Chemical forms of radionuclides and their quantification in environmental samples. In: Van Der Stricht, E., Kirchmann, R. (Eds.). Radioecology, Radioactivity and Ecosystems. Fortemps, Liège, Belgium, pp 99-111.

Ishikawa, N.J., Uchida, S. Tagami, K. 2009. Estimation of soil–soil solution distribution coefficient of radiostrontium using soil properties. Applied Radiation and Isotopes 67, 319–323.

Kennard, R., Stone, L.A., 1969. Computer aided design of experiments. Technometrics 11, 137-148.

Rauret, G., Firsakova, S., 1996. The transfer of radionuclides through the terrestrial environment to agricultural products, including the evaluation of agrochemical practices. EUR 16528 EN, European Commission, Luxembourg.

Rigol, A., Roig, M., Vidal, M., Rauret, G., 1999. Sequential extractions for the study of radiocaesium and radiostrontium dynamics in mineral and organic soils from Western Europe and Chernobyl areas. Environ. Sci. Technol. 33, 887-895

.

Rigol, A., Camps, M., de Juan, A., Rauret, G., Vidal, M., 2008. Multivariate soft-modelling to predict radiocesium soil-to-plant transfer. Environ. Sci. Technol. 42, 4029-4036.

Sauvé, S., Hendershot, W., Allen, H. E., 2000. Solid-solution partitioning of metals in contaminated soils: dependence on pH, total metal burden, and organic matter. Environ. Sci. Technol. 34, 1125-1131.

Sheppard, M. I., Thibault, D. H., 1990. Default soil solid / liquid partition coefficients, Kds, for 11 four major soil types: a compendium. Health Phys. 59, 471-482

.

Sonesten, L., 2001. Land use influence on ^{137}Cs levels in perch (Perca fluviatilis L.) and roach (Rutilus rutilus L.). J. Environ. Radioactiv. 55, 125-143.

Sysoeva, A. A., Konopleva, I. V., Sanzharova, N. I., 2005. Bioavailability of radiostrontium in soil: Experimental study and modelling. J. Environ. Radioactiv. 81, 269-282.

Twining, J.R., Payne, T.E., Itakura, T., 2004. Soil-water distribution coefficients and plant transfer factors for ^{134}Cs, ^{85}Sr and ^{65}Zn under field conditions in tropical Australia. J. Environ. Radioactiv. 71, 71-87.

Valke, E., 1993. The behaviour dynamics of radiocaesium and radiostrontium in soils rich in organic matter. Ph. D. Thesis, Katholieke Universiteit Leuven (KUL), Belgium.

Wang, G., Staunton, S., 2005. Evolution of Sr distribution coefficient as a function of time, incubation conditions and measurement technique. J. Environ. Radioactiv. 81, 173-185.

Wold, S., Martens, H., Wold. H., 1983. The multivariate calibration problem in chemistry solved by the PLS method. Lect. Notes Math. 973, 286-293.

Yasuda, H., Uchida, S., 1993. Statistical approach for the estimation of strontium distribution coefficient. Environ. Sci. Technol. 27, 2462-2465.

3.6

Comparison of mechanistic and PLS-based models to predict radiocaesium distribution coefficient in soils

C. J. Gil-García, A. Rigol, M. Vidal.

Enviado a la revista *Journal of Hazardous Materials* para su publicación

Páginas 147-170

Comparison of mechanistic and PLS-based models to predict radiocaesium distribution coefficients in soils

C. J. Gil-García, A. Rigol, M. Vidal*

Departament de Química Analítica, Universitat de Barcelona, Martí i Franqués 1-11, 3ª Planta, 08028 Barcelona, Spain.

*Corresponding author: Tel.: +34 934039276; Fax: +34 934021233

E-mail address: miquel.vidal@ub.edu (M. Vidal)

Abstract

Radiocaesium sorption interaction descriptors were examined in 30 soils from the Spanish territory. Mechanistic and PLS-based models were used to predict the solid-liquid distribution coefficients of radiocaesium (K_d(Cs)) from soil properties, and the values obtained were compared with the experimental ones, which were derived from batch experiments using two contact solutions: one simulated the composition of the soil solution and the other was the wash-off of the soil. Several mechanistic models of different complexity were tested based on the Radiocaesium Interception Potential (RIP), with satisfactory coincidence between experimental and predicted values. A simplified model based on either the RIP or the clay cantent, and K status in the soil was proposed. Various multivariant, soft models, constructed using Partial Least Square Regression (PLS), were also evaluated. The RIP, the clay content and the K and NH_4^+ were also identified by the PLS-models as the most relevant soil parameters in the prediction of K_d. The goodness of these models was demonstrated by an excellent concordance between experimental and predicted values.

Keywords: radiocaesium; soil; sorption; radiocaesium interception potential; distribution coefficient; modelling

1. Introduction

Knowledge of the behaviour of radionuclides in the environment is necessary to predict the impact of a radioactive contamination and to assess the derived risk. Mobility of radionuclides within the environment is mainly controlled by their sorption in soils, and by the reversibility of this process.

Radiocaesium is one of the radionuclides that has deserved a larger number of studies in the environment, because it was the most relevant radionuclide affecting European ecosystems following the Chernobyl accident. Numerous works in the literature focused on describing the mechanisms governing its sorption in soils and its subsequent mobility in the soil-plant system [1-3]. It was shown that radiocaesium sorption is controlled by ionic exchange at two types of sites with varying sorption affinities: the high-affinity Frayed Edge Sites (FES), which are interlattice sites at the end of the expanded clay layers, and the low-affinity Regular Exchange Sites (RES), which are at the organic matter phases and also at external positions in clay minerals. With the exception of soils with a high organic matter content or with a negligible 2:1 phyllosilicate content, the FES govern radiocaesium sorption, which also ensures a high sorption irreversibility.

The solid-liquid distribution coefficient (K_d) is a useful parameter for the characterization of the radionuclide behaviour at solid-liquid interfaces. Although it is not a thermodynamic constant, the K_d integrates simultaneous physicochemical processes, and it is highly dependent on liquid and solid phase characteristics. The quantification of K_d values can be undertaken using various experimental approaches [4-6], although batch experiments are the most widely used approach [7,8]. Therefore, whereas there is a general consensus on the use of the K_d as an input data for environmental decision support systems, there is still a major concern due to the apparently high variability of the K_d data, because they depend not only on the soil characteristics, but also on the experimental conditions applied, mainly the cationic composition of the contact solution, contact time, and concentration of stable element related to the radioisotope. Recently reported works succeeded in reducing the variability of the radiocaesium distribution coefficient (K_d(Cs)) for a given type of soil, based on suggesting a best estimate K_d(Cs) value after grouping soils with respect to textural classes, organic matter content, or on the basis of specific parameters governing radiocaesium interaction in soils,

after discarding not suitable data, due to either be outliers or be generated from not representative experimental conditions [9,10]. However, for a given soil group, the K_d(Cs) best estimate still had a variability of a few orders of magnitude, and a univariant correlation between K_d(Cs) values and a given soil property could not be properly established, thus reducing the possibility of calculating an individual K_d(Cs) value for a fully characterized soil.

Here we tested two modelling approaches to be able to describe the range of K_d(Cs) values experimentally obtained for a set of soils [11], and to predict individual K_d(Cs) from soil properties. A hard model was constructed based on the knowledge of the radiocaesium interaction in soils, mainly on the basis on the Radiocaesium Interception Potential (RIP) concept, the cationic composition of the contact solution, and the clay content in the soil samples. This approach was compared with a soft model based on the use of the Partial Least Square Regression (PLS), which had been successfully applied to predict other radiological parameters such as soil-plant transfer [12], or the distribution coefficient of other radionuclides [13].

2. Material and methods

2.1. Soil sample

30 agricultural soils were sampled in locations near to radioactive facilities and nuclear power plants in Spain. Samples were taken from the surface layer (0-10 cm depth) without the vegetation, air-dried, sieved through 2-mm sieves and homogenized in 5-10 L cylinder bottles during 90 h with a roller table prior to analyses and experiments.

2.2. General soil characteristics

Table 1 summarizes the ranges of values for the general and specific quantified soil characteristics. Individual values are available elsewhere [11]. Soils were mineral-based, with a maximum C_{org} content lower than 10%. Most soils had a loamy texture, and a few had clay

Table 1. Range of values for the soil characteristics (AM: arithmetic mean; GM: geometric mean)

Variable	Code	Unit	Min	Max	AM	GM
pH	pH	-	4.3	9.2	7.0	6.9
Organic carbon	C_{org}	%	0.2	9.4	3.3	2.1
Carbonate content	$CaCO_3$	%	1	51	13.9	6.6
Cationic exchange capacity	CEC	$cmol_c\ kg^{-1}$	21.3	89.3	42.2	39.0
Exchangeable Na	Na_{exch}	$cmol_c\ kg^{-1}$	0.12	19.6	1.4	0.69
Exchangeable K	K_{exch}	$cmol_c\ kg^{-1}$	0.19	10.2	1.3	0.81
Exchangeable Ca	Ca_{exch}	$cmol_c\ kg^{-1}$	3.5	52.0	13.1	10.8
Exchangeable Mg	Mg_{exch}	$cmol_c\ kg^{-1}$	0.45	14.1	2.7	1.8
Exchangeable NH_4^+	NH_{4exch}	$cmol_c\ kg^{-1}$	0.06	2.6	0.36	0.22
Clay fraction (wrt. initial soil weight)	Clay	%	6.3	52.4	22.9	20.7
Sand fraction (wrt. initial soil weight)	Sand	%	4.5	86.8	43.1	36.8
Field capacity	FC	%	6.2	56.1	27.8	26.1
Electrical conductivity	EC	$\mu S\ cm^{-1}$	89	3390	738	481
Wash-off experiments						
Na in the contact solution	Na_{ss}	$mmol\ L^{-1}$	0.01	3.6	0.35	0.11
K in the contact solution	K_{ss}	$mmol\ L^{-1}$	0.02	0.35	0.095	0.075
Ca in the contact solution	Ca_{ss}	$mmol\ L^{-1}$	0.01	6.6	0.70	0.29
Mg in the contact solution	Mg_{ss}	$mmol\ L^{-1}$	0.01	0.76	0.12	0.065
NH_4 in the contact solution	NH_{4ss}	$mmol\ L^{-1}$	0.02	0.96	0.091	0.047
Soil solution experiments						
Na in the contact solution	Na_{ss}	$mmol\ L^{-1}$	0.17	128	11.8	2.0
K in the contact solution	K_{ss}	$mmol\ L^{-1}$	0.13	23.7	1.8	0.79
Ca in the contact solution	Ca_{ss}	$mmol\ L^{-1}$	0.44	52.1	14.3	8.3
Mg in the contact solution	Mg_{ss}	$mmol\ L^{-1}$	0.17	72.5	6.8	2.4
NH_4 in the contact solution	NH_{4ss}	$mmol\ L^{-1}$	0.016	11.4	1.1	0.24
Radiocaesium distribution coefficient						
Wash-off experiments	K_d	$L\ kg^{-1}$	153	34945	8203	5239
Soil solution experiments	K_d	$L\ kg^{-1}$	10	19437	3111	1185

(5 soils) and sandy (1 soil) textures. Unlike soils from temperate areas, many of the examined soils had clay content over 20%, pH value over 8, and $CaCO_3$ content over 25 %.

2.3. X-Ray Diffraction (XRD) analyses of the soil samples.

Soil samples were also analysed by the XRD to quantify the total content of phyllosilicates and 2:1 phyllosilicates, among other crystalline phases. The determination of the soil mineralogy was carried out with powder samples, whereas for the determination of the 2:1 phyllosilicates it was necessary to prepare oriented aggregates. The fraction smaller than 2 μm was obtained by sedimentation in aqueous media, and the characterization of phyllosilicates was performed in the oriented aggregates submitted to several treatments (air dried, solvation with ethylene glycol, and thermal treatment at 550ºC).

The diffractograms were obtained from 3º to 70º 2θ with a step of 0.03º and a counting time of 1 s, whereas for the oriented aggregates they were obtained from 3º to 40º 2θ with a step of 0.02º and a counting time of 1.5 s. External standard was used in all cases for quantification.
Table 2 lists the main crystalline phases quantified in the examined soils. Phyllosilicate content ranged from 6.8% at ALM to 71.9% at CABRIL, whereas the 2:1 phyllosilicates content ranged from 4.3% at ALM soil to 64% at CABRIL.

2.4. Determination of radiocaesium solid–liquid distribution coefficients

The K_d(Cs) values were determined using two batch sorption tests, differing in the composition of the contact solution. A first set of data was obtained in a medium that simulated the cationic composition of the soil solution. Soil samples (1 g) were equilibrated for 16 h with 50 mL of a solution representing the cationic composition of the soil solution of each soil. After four pre-equilibrations, soils were equilibrated for 24 h with the same solution, but were labelled with ^{137}Cs (CS137ELSB45; LEA FRAMATONE). The K_d(Cs) values were determined by measuring the ^{137}Cs level in the supernatant before and after equilibration.

Table 2. Main crystalline phases quantified by XRD analyses (%, wrt initial soil weight)

	Quartz	Calcite+Dolomite	Phyllosilicates	Illite	Smectite	Vermiculite	2:1 phyllosilicates[a]
ALM	86	nd[b]	6.8	4.2	nd	0.1	4.3
ANDCOR	<5	< 3	12.2	7.2	nd	5.0	12.2
ASCO	21	50	13.9	10.7	nd	0.3	11.0
AYUD	26	16	50.2	44.2	0.5	Nd	44.7
BAD1	67	nd	26.5	11.4	10.3	Nd	21.7
BAD2	57	<5	34.6	10.4	19.3	Nd	29.7
BILBAO	29	nd	30.3	25.1	0.6	Nd	25.7
CABRIL	25	nd	71.9	64.0	nd	Nd	64.0
DELTA1	nd	<5	30.0	24.0	nd	0.3	24.3
DELTA2	10	59	14.4	9.8	nd	Nd	9.8
ENUSA	59	nd	15.9	9.1	0.2	0.6	9.9
FONCOR	26	nd	13.3	6.0	nd	0.5	6.5
FROCOR	31	nd	18.4	10.5	0.2	0.7	11.4
GAROÑA	31	44	19.1	12.2	1.0	Nd	13.2
GOLOSO	23	nd	7.4	3.6	1.4	Nd	5.0
GRACOR	46	nd	37.4	4.1	nd	1.5	5.6
LEON	52	nd	34.4	17.5	nd	Nd	17.5
MALAGA	18	18	63.8	34.5	10.9	Nd	45.3
OVI01	38	nd	43.0	9.9	nd	Nd	9.9
OVI03	55	nd	30.7	4.9	nd	0.9	5.8
TENF1	<5	nd	49.4	28.2	4.4	1.5	34.1
TENF2	5	nd	42.9	0.9	28.8	0.4	30.1
TRILLO	19	56	19.2	14.2	nd	Nd	14.2
UIB	25	30	32.8	26.5	0.7	Nd	27.2
UPV	<5	70	16.7	16.7	nd	Nd	16.7
USAL	39	<3	22.9	9.4	10.3	Nd	19.7
VAN1	33	33	10.9	8.4	0.5	0.1	9.1
VAN2	27	38	30.9	22.3	nd	0.6	22.9
VILCOR	77	nd	18.6	7.8	nd	1.1	8.9
ZORITA	21	50	22.0	16.4	nd	0.3	16.7

[a] 2:1 phyllosilicates: sum of illite, smectite and vermiculite contents

[b] nd = not detected

A second dataset was obtained with a contact solution derived from the soil wash-off. This solution was obtained by equilibrating soil samples (1 g) in water (30 mL g^{-1}), using end-over-end shaking for 16 h. Subsequently, the wash-off solution in contact with the soil was spiked with ^{137}Cs and shaken for 24 h. The $K_d(Cs)$ values were calculated from ^{137}Cs levels in the supernatant before and after equilibration.

The ^{137}Cs activity was measured in samples derived from the sorption experiments in 20 mL capacity polyethylene vials using a solid scintillation detector (PACKARD MINAXI 5000 Series), equipped with a 3-inch NaI (Tl activated) crystal. Measurement time was set to obtain RSD < 0.5%.

Table 1 also includes the ranges of $K_d(Cs)$ obtained in the two contact media. From the statistical descriptors it could be observed that the $K_d(Cs)$ values obtained in the batch experiments with the contact solution that simulated the soil solution composition were systematically lower

2.5. Radiocaesium-specific soil parameters

2.5.1. Determination of Radiocaesium Interception Potential

In a soil homoionically saturated with K or NH_4^+, which are competitive species for Cs, the sorption of this radionuclide at the FES depends on the total capacity of these sites ([FES]), the sorption selectivity of Cs compared with that of the competitive ion ($K_C^{FES}(Cs/X)$) and the concentration of the competitive ion in the contact, aqueous phase (m_X), as shown in the following equation [1]:

$$K_d^{FES}(Cs) = \frac{[FES]}{m_X} \cdot K_C^{FES}(Cs/X) \qquad (1)$$

Due to the fact that the FES capacity is difficult to measure, one of the approaches for the prediction of the $K_d^{FES}(Cs)$ is based on the use of the Radiocaesium Interception Potential (RIP) concept, which represents the $K_d^{FES}(Cs) \cdot m_X$ product and estimates the soil ability for specific radiocaesium sorption because it also gives a direct measure of $K_C^{FES}(Cs/X) \cdot [FES]$.

The RIP was determined in K and NH_4^+ scenarios (RIP_K and RIP_N). RIP_K was determined after preequilibrating the soil sample (1 g) with 50 mL of a solution containing 100 mmol L^{-1} in Ca and 0.5 mmol L^{-1} in K (K_{ss} = 0.5). After four preequilibrations, soils were equilibrated for 24 h with the same solution, but labelled with ^{137}Cs, and the related $K_d(Cs)$ was determined. The calculated product $K_d(Cs) \cdot K_{ss}$ was associated with the RIP_K value [14]. RIP_N was determined using the same procedure, but using a solution 0.5 mmol L^{-1} in NH_4^+.

2.5.2. Changes in the K_d(Cs) due to changes in NH_4^+ concentration in the contact solution

The $K_d(Cs)$ were obtained in a solution with Ca and K (100 and 10 mmol L^{-1} respectively; K_d(Ca-K)) and in additional five solutions with the same concentration of Ca and K, but increasing NH_4^+ concentrations (0.50, 1.0, 2.5, 4, 5 mmol L^{-1}; K_d (Ca-K-NH_4)), to evaluate the response of the system to increasing concentrations of NH_4^+ in the mixed Ca-K-NH_4^+ scenarios. Soil samples (1g) were preequilibrated with 50 mL of these solutions and, after 3 preequilibrations, soils were equilibrated for 24 h with the same solution, but labelled with ^{137}Cs.

If radiocaesium sorption were governed by the RES, the $K_d(Cs)$ should not change since NH_4^+ and K are equally competitive at these sites and, consequently, the ratio K_d(Ca-K)/K_d(Ca-K-NH_4) would tend to unity. If radiocaesium sorption were associated with the FES, the $K_d(Cs)$ should be sensitive to the changes of NH_4^+ concentrations in the contact solution, because NH_4^+ is more competitive than K at these sites. This last case is described by the following equation [15,16]:

$$\frac{K_d(Ca-K)}{K_d(Ca-K-NH_4)} = 1 + K_C^{FES}(NH_4/K)\frac{NH_{4,ss}}{K_{ss}} \qquad (2)$$

where K_{ss} and $NH_{4,ss}$ are the K and NH_4^+ concentrations in the contact solution in mmol L^{-1}, K_d(Ca-K) and K_d(Ca-K-NH_4) are the K_d in absence or presence of NH_4^+, respectively, and K_C^{FES} (NH_4/K) is the NH_4-to-K selectivity coefficient at FES.

2.6. Quality control

Intermediate activity solutions of ^{137}Cs were prepared by diluting weighed amounts of commercial solutions of each radionuclide with deionised water, and used as internal controls for measurements with the PACKARD MINAXI 5000 Series instrument. Additionally, blank experiments without soil sample but applying the same procedures for the sorption tests were carried out in parallel for each set of analysis.

2.7. Data treatment

The application of soft models was carried out considering three $K_d(Cs)$ datasets depending on the models examined: $K_d(Cs)$ from the wash-off experiments, $K_d(Cs)$ from the soil solution experiments, or the global dataset. The application of the hard models was only carried out considering the global dataset. Single and multiple linear correlations related to the hard models were performed using STATGRAPHICS Plus (StatPoint Technologies, US) software, whereas Unscrambler® 6.11a software (CAMO ASA, Norway) was used to carry out the soft modelling based on Partial Least Squares regression (PLS).

3. Results and discussion

3.1. Use of mechanistic models

3.1.1. Construction of the global mechanistic model and estimation of the $K_C^{FES}(NH_4/K)$

As radiocaesium sorption in soils is controlled by FES and RES, two contributions are expected for the total $K_d(Cs)$ in soils, the $K_d^{FES}(Cs)$ and the $K_d^{RES}(Cs)$. The relative weight of each contribution depends on the soil type.

The $K_d^{FES}(Cs)$ can be predicted by dividing the RIP_K value (in mmol kg^{-1}) by the sum of K, NH_4^+ and Na concentrations in the soil solution (in mmol L^{-1}), but amplifying the NH_4^+ and Na contributions by the respective selectivity coefficient in FES ($K_c^{FES}(NH_4/K)$; $K_c^{FES}(Na/K)$,

because at the FES the relative selectivity of these monovalent cations differs from 1. The K_d^{RES}(Cs) can be calculated by dividing the sum of the exchangeable K, NH_4^+ and Na (in mmol kg^{-1}) by the sum of K, NH_4^+ and Na concentrations in the soil solution. The equation derived may be written as follows:

$$K_d(Cs) = K_d^{FES}(Cs) + K_d^{RES}(Cs) = \frac{RIP_K}{K_{ss} + K_C^{FES}(NH_4/K)\cdot NH_{4,ss} + K_C^{FES}(Na/K)\cdot Na_{ss}} + \frac{K_{exch} + NH_{4,exch} + Na_{exch}}{K_{ss} + NH_{4,ss} + Na_{ss}} \quad (3)$$

Sodium has little significance in Cs sorption, excepting for saline soils, and a good estimator of the K_c^{FES}(Na/K) is 0.02. Regarding the role of NH_4^+, its inclusion in the prediction of K_d^{FES}(Cs) requires a proper quantification of the K_c^{FES}(NH_4/K) value. K_c^{FES}(NH_4/K) could be determined using two approaches. Firstly, from the ratio between the RIP obtained in K and NH_4^+ scenarios [17] and secondly, from the changes in the K_d(Cs) after changing the NH_4^+ concentration in the contact solution in mixed Ca-K-NH_4^+ scenarios, as described in section 2.5.2.

Table 3 presents the K_c^{FES}(NH_4/K) values obtained by the two approaches, whereas Fig. 1 displays four examples of the examination of the changes of K_d(Cs) with increasing NH_4^+ concentration, in which the K_c^{FES}(NH_4/K) derived from the slope of the K_d(Ca-K)/K_d(Ca-K-NH_4) vs. $NH_{4,ss}$/ K_{ss} correlation. The quantification of the K_c^{FES}(NH_4/K) coefficient depended on the approach followed, because the values derived from the mixed scenario experiments were consistently higher (around 2.3-fold higher, as a mean value) than those derived from the RIP ratio. It is the first time that a systematic comparison of K_c^{FES}(NH_4/K) coefficients derived from the two approaches is performed, and reasons for this finding may lay in the lower K and NH_4^+ concentrations used for the RIP calculations that may not ensure homoionic FES in soils with high clay content. Focusing on the range of values derived from both approaches, the fact that the K_c^{FES}(NH_4/K) values were consistently higher than 1 confirmed that the radiocaesium sorption were governed in these soils by the presence of FES.

Table 3. RIP_K (mmol kg^{-1}), RIP_N (mmol kg^{-1}), and K_C^{FES} (NH_4/K) values obtained. AM: arithmetic mean; GM: geometric mean.

Soil			K_c (NH_4/K)	
Sample	RIP_K	RIP_N	RIP ratio	Mixed scenario
ALM	1002	316	3.2	8.7
ANDCOR	366	140	2.6	6.2
ASCO	2034	512	4.0	6.5
AYUD	4929	1368	3.6	7.5
BAD1	1523	376	4.1	8.3
BAD2	2594	613	4.2	6.2
BILBO	4419	2052	2.2	9.4
CABRIL	4852	1234	3.9	10.2
DELTA1	1186	298	4.0	7.2
DELTA2	1463	337	4.3	7.4
ENUSA	744	249	3.0	7.3
FONCOR	340	128	2.7	4.4
FROCOR	179	74	2.4	7.7
GAROÑA	2080	749	2.8	5.3
GOLOSO	672	204	3.3	5.2
GRACOR	1017	303	3.4	8.3
LEON	2314	910	2.5	10.0
MALAGA	5958	1824	3.3	6.9
OVI01	3221	1009	3.2	8.3
OVI03	1718	825	2.1	7.6
TENF1	6669	4914	1.4	4.4
TENF2	6758	2128	3.2	5.0
TRILLO	2897	838	3.5	7.4
UIB	7000	1595	4.4	7.1
UPV	3213	714	4.5	7.6
USAL	1874	753	2.5	5.7
VAN1	660	205	3.2	6.2
VAN2	4488	803	5.6	8.0
VILCOR	225	103	2.2	5.1
ZORITA	2371	687	3.5	6.8
Min	179	74	1.4	4.4
Max	7000	4914	5.6	10.2
AM	2626	875	3.3	7.1
GM	1760	557	3.2	6.9

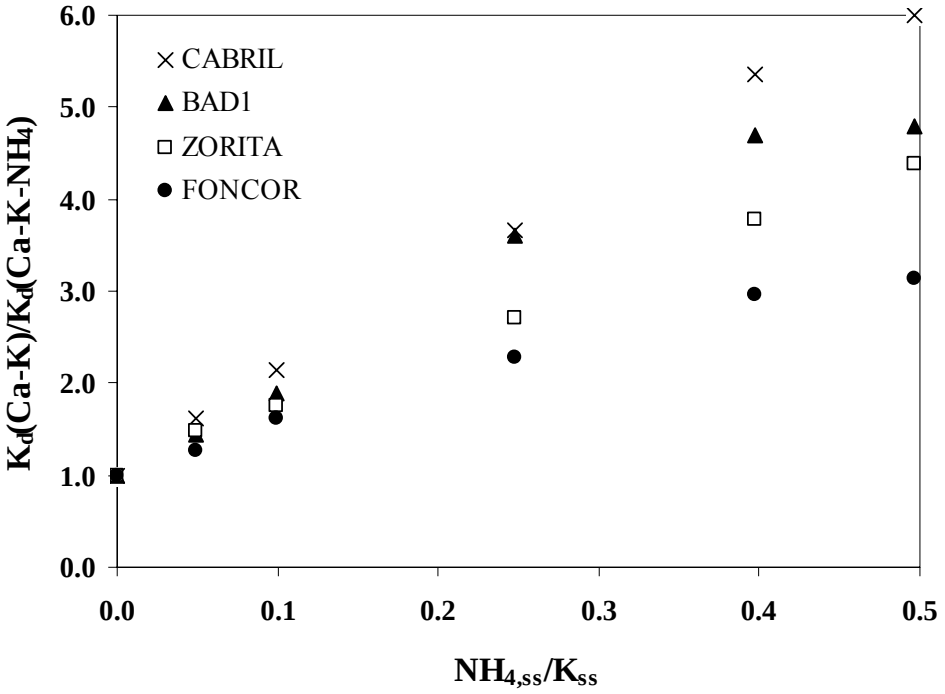

Fig. 1. Response of the K_d(Cs) to increasing NH_4^+ concentrations in a Ca-K-NH_4 scenario in four of the soils of the data set: (A) Foncor, (B) Zorita, (C) Bad1 and (D) Cabril soils.

3.1.2. Prediction of the K_d(Cs) on the basis of the global and simplified equations

The use of the $K_c^{FES}(NH_4/K)$ values derived from either the RIP ratio or the mixed scenario experiments did not affect the mechanistic model, because similar experimental vs. predicted K_d(Cs) were obtained ($\log K_d(Cs)_{exp}$ = 0.98 (±0.02) $\log K_d(Cs)_{pred}$, n = 60; r = 0.94; and $\log K_d(Cs)_{exp}$ = 1.04 (±0.02) $\log K_d(Cs)_{pred}$, n = 60; r = 0.90, respectively). Both cases showed that the multiple correlation represented by equation (3) succeeded in predicting the K_d(Cs) in soils. As an example, Fig. 2 shows the results of the prediction exercise from equation (3) by using the $K_c^{FES}(NH_4/K)$ derived from the mixed scenario experiments.

The use of equation (3) requires a full characterization of the soils. Therefore, simpler models could be necessary in case there is a limited soil characterization. First of all, a general value of 5 can be taken for $K_C^{FES}(NH_4/K)$ in case its value is unknown for a given soil, as it has been suggested previously (Vidal et al., 1995) and it also consistent with the arithmetic mean value of all the $K_C^{FES}(NH_4/K)$ values obtained in the present work. Additionally, the role of Na can be disregarded, due to the low value of the $K_C^{FES}(Na/K)$. With these two assumptions,

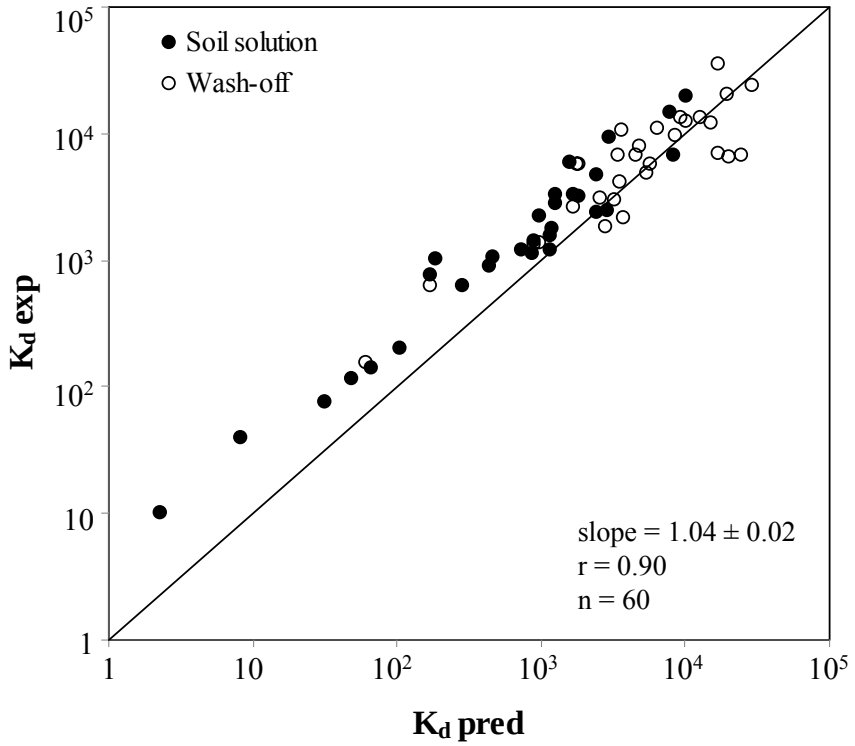

Fig. 2. Prediction of $K_d(Cs)$ values with Equation 2, using $K_c^{FES}(NH_4/K)$ values derived from mixed scenario experiments, in which the solid line represents the ideal $K_d(Cs)_{exp} = K_d(Cs)_{pred}$ relationship.

the model still predicted well the experimental values of the $K_d(Cs)$, because the resulting correlation was similar to those obtained before ($\log K_d(Cs)_{exp}$ = 1.01(±0.02) $\log K_d(Cs)_{pred}$, n=60, r = 0.92).

Further assumptions to simplify the model might have a more significant effect on the correlations. One option could be to focus on the $K_d^{FES}(Cs)$ and to neglect the $K_d^{RES}(Cs)$. A rapid calculation confirmed that for many soils the $K_d^{FES}(Cs)$ accounted for more than 90% of the global $K_d(Cs)$, but in a few soils the percentages decreased down to 53% (as here the FROCOR soil). As the additional information to calculate the $K_d^{RES}(Cs)$ is the concentration of cations in the exchangeable complex and this information is frequently available, this simplification would not have a significant added value. Another option is not to include the NH_4^+ data. The NH_4^+ concentration, and thus its role in the prediction of $K_d(Cs)$, could be high in wet and peat soils, whereas it decreases in mineral soils to lower values than that of K. The resulting equation of this additional simplification would be as follows:

$$K_d(Cs) = K_d^{FES}(Cs) + K_d^{RES}(Cs) = \frac{RIP_K}{K_{ss}} + \frac{K_{exch}}{K_{ss}} \quad (4)$$

The correlation obtained with the simplified equation was slightly worse than the previous correlations ($logK_d(Cs)_{exp}$ = 0.88(±0.02) $logK_d(Cs)_{pred}$, r = 0.89) but it still ensured a proper prediction of the K_d(Cs) values.

A major limitation of these hard models to predict the K_d (Cs) values is the fact that a K_d(Cs) value must be obtained to quantify the RIP_K value. To date, attempts to predict the RIP_K value from soil properties have only been partially successful, because the RIP_K value is multivariantly dependent not only on the clay content, but also on the type of clay and geological origin of the soil [18]. Regarding the data for the examined soils, both the phyllosilicate and 2:1 phyllosilicate contents had similar correlations with the RIP_K values (for instance, RIP_K = 92 (±30) phyllosilicate; n = 30; r = 0.76), because both variables were strongly correlated (r = 0.85). Another parameter that may correlate with the RIP_K is the clay content of the corresponding textural class, which is a parameter easier to be quantified because it does not require additional XRD analyses. For this case the correlation was slightly worst (RIP_K = 130 (±60) clay; n = 30; r = 0.65). The inclusion of the silt content, also derived from the textural analyses, only improved the percentage of the RIP_K variability described in the case of a multiple regression with the phyllosilicate content (RIP_K = 93 (±26) phyllosilicate + 61 (±28) silt -1700 (±1140); r = 0.86). Any of these correlations could be used for the prediction of K_d(Cs) through a previous prediction of the RIP_K values. For instance, when substituting the RIP_K value by its correlation with the clay content a worst correlation was obtained ($logK_d(Cs)_{exp}$ = 0.84(±0.02) $logK_d(Cs)_{pred}$, r = 0.74), but still good enough to be considered as a simpler approach for input data to be used in environmental models and decision support systems, because the prediction of the K_d(Cs) would be based only on general soil properties, such as texture and K status in the exchangeable complex and in soil solution.

3.2 PLS-based soft-modelling

An alternative to hard-modelling to predict K_d(Cs) from soil properties is the use of soft-modelling, which requires a large database of samples and variables, and takes into account

soil properties that either are directly associated with the radiocaesium sorption in soils or affect the sorption process. With the aim of evaluating the capacity of multivariate soft-modelling in the prediction of K_d(Cs) values, a data matrix was constructed with the rows related to the soil samples and columns corresponding to the soil variables. To assume normal distributions of variables, data were transformed to logarithmic units, except pH. Data were also autoscaled prior to analysis, i.e. mean centered (each element subtracted by its mean column) and scaled to unit variance (each element divided by the standard deviation of its column), to give the same weight to all variables in the analyses.

PLS builds a model between a sample variable (y) and a set of other sample descriptors (X) in a low-dimensional space formed by PLS components. It finds the model with the maximum covariance of the relationship between the X- and y-space [19,20], as $y = XB$**,** where B is the matrix of regression coefficients calculated in the PLS space. Full cross-validation was used to determine the number of PLS components that provided a minimal value of the Root Mean Square Error of Cross Validation (RMSECV):

$$\mathrm{RMSECV} = \sqrt{\frac{\sum_{i=1}^{n} (y^{i}_{\mathrm{predicted}} - y^{i}_{\mathrm{experimental}})^{2}}{n}} \qquad (5)$$

Further details on the theoretical background of the PLS method and on the software applied can be found elsewhere [21].

3.2.1. Identification of the relevant variables in the PLS models

PLS was first used to ascertain the relevance of the soil variables for the prediction of the K_d(Cs), by looking at the quality parameters of the models and at the value and sign of the regression coefficients. The soil solution, the wash-off and the global datasets were modelled separately to reveal which variables better explained K_d(Cs) in each dataset. The role of the clay fraction, which is one of the key soil properties affecting radiocaesium interaction in soils, was evaluated by either the content of phyllosilicates determined by mineralogical analysis or the clay content determined by the textural analysis. The weight of RIP_K in the

model was also assessed. Table 4 summarizes the statistical description of the cross-validated PLS model obtained in each case. Four PLS components were considered for comparison

Table 4. Description of the cross-validated PLS models (4 PLS components) to predict K_d(Cs).

Dataset	n	*y* explained cumulative variance (%)	RMSECV[a]	Experimental vs. predicted regression	
				Slope	R
With RIP and total phyllosilicates					
Soil solution	30	85	3700	0.99±0.04	0.90
Wash-off	30	83	3300	1.00±0.02	0.90
Soil solution + wash-off	60	89	4100	1.00±0.02	0.94
With RIP and clay texture					
Soil solution	30	86	3400	0.99±0.04	0.91
Wash-off	30	86	3300	1.00±0.02	0.91
Soil solution + wash-off	60	89	4200	1.00±0.02	0.94
Without RIP and with total phyllosilicates					
Soil solution	30	79	5300	0.99±0.04	0.86
Wash-off	30	67	4100	0.99±0.03	0.79
Soil solution + wash-off	60	84	4100	0.99±0.02	0.91
Without RIP and with clay texture					
Soil solution	30	80	4300	0.99±0.04	0.87
Wash-off	30	70	3600	1.00±0.03	0.81
Soil solution + wash-off	60	85	4100	0.99±0.02	0.92

[a] Value calculated after back-transforming the logarithmic predicted values to original *y* units

purposes, because the *y* explained cumulative variance was higher than 80% in many cases. Additional PLS components improved slightly the quality parameters of the models, but the relevance of variables did not vary.

When RIP_K was one of the variables taken into account to construct the model, almost identical results were obtained for the three data sets and the two selected variables to account for the role of clays. Satisfactory regressions ($r > 0.9$) with slopes close to 1 were obtained, confirming the absence of bias in the models and, therefore, of systematic overestimations or underestimations of K_d(Cs). However, the *y* explained cumulative variance was slightly better for the global dataset due to the wider range of values involved. The RMSECV values, calculated after back-transforming the logarithmic values of predicted K_d(Cs) to the original units, were also very similar for the three models (from 3300 to 4200). The regression coefficients of the PLS models were also compared to identify the most relevant variables to describe the K_d(Cs) variability in each case. The direction and magnitude of the influence of variables can generally be associated with the sign and the magnitude of its regression coefficient. However, as soil variables may be partially correlated, the related regression coefficients cannot be considered in an individual or completely independent way. Only the most salient trends in the regression coefficients can safely be used for chemical interpretation. Fig. 3a shows, as an example, the regression coefficients obtained for the global dataset including RIP_K and clay texture variables. Non significant variations in the relative relevance of variables were observed when phyllosilicates were included instead of clay texture, and similar conclusions could also be drawn from the regression coefficients of the three data sets. Among the clearest trends, the high negative correlation of the concentration of competitive species, K and NH_4^+, in the contact solution was evidenced in the three data sets. Another general trend was the relevance of RIP_K and clay texture that presented high positive regression coefficients. These findings were consistent with the mechanisms governing K_d(Cs) [16,22,23].

As shown in Table 4, when RIP_K was excluded from the databases the quality parameters of the models were still satisfactory, but they worsened with respect to when the RIP_K variable was retained, especially for the datasets with a smaller number of data. Again, the models that considered the clay texture were similar to those that used phyllosilicates. With respect to the regression coefficients (Fig. 3b) the relative relevance of the soil parameters was similar to the

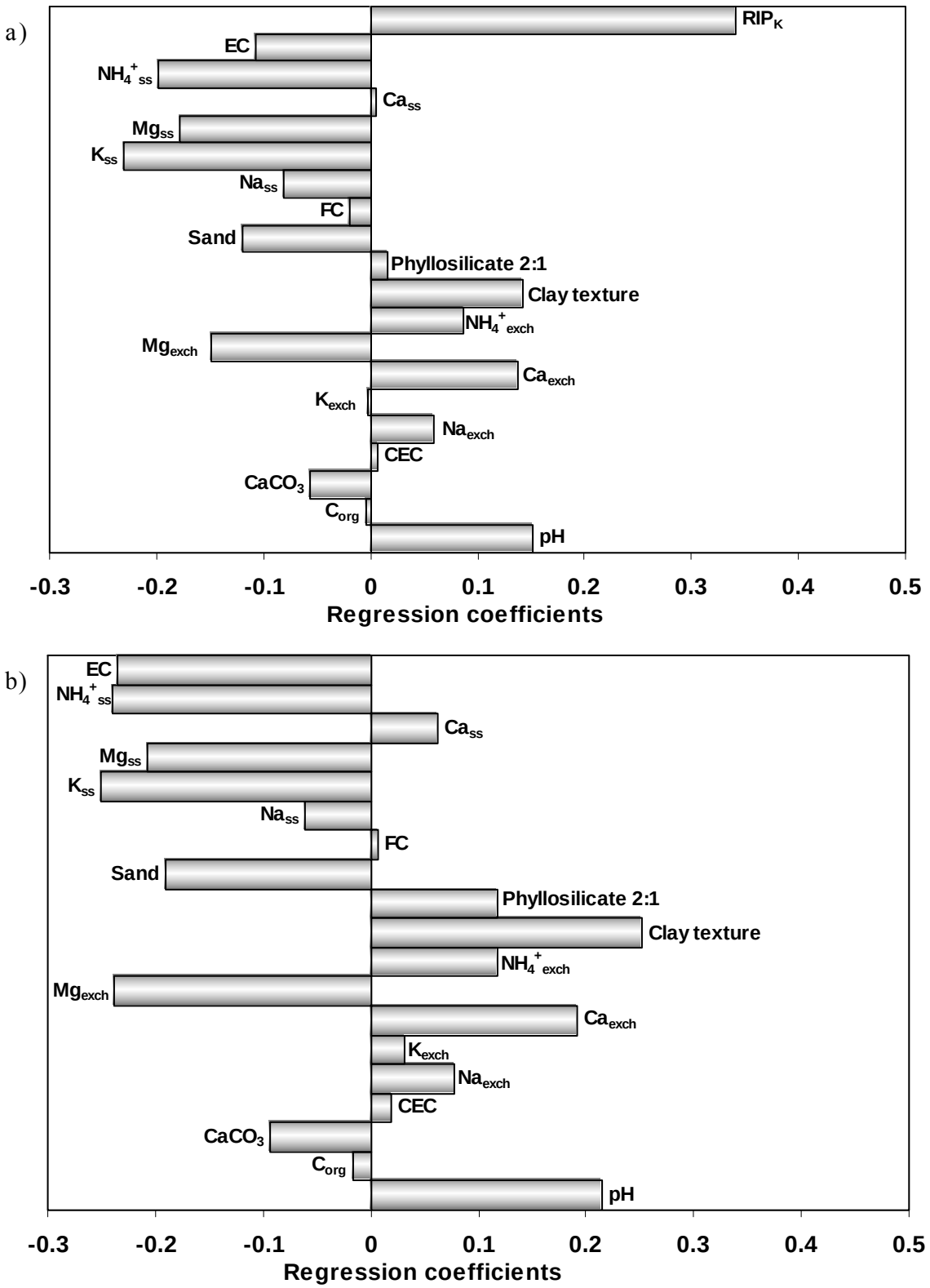

Fig. 3. Regression coefficients of the PLS models using the global dataset and the clay texture to describe the clay content, a) including RIP_K and b) excluding RIP_K.

previous case with RIP_K, except for clay texture, and especially 2:1 phyllosilicate and concentration of cationic species in the contact solution, which gained significance in the prediction of K_d(Cs).

3.2.2. External validation of the PLS models

In contrast to hard-modelling, which employs a fixed equation based on soil parameters to the prediction of K_d(Cs), for the PLS-based models an additional step is required to demonstrate their ability to predict K_d(Cs) values of samples not used for the model calibration. For the external validation step, two thirds of the samples of the global dataset were selected for calibration and to construct the PLS model, using the Kennard-Stone algorithm [24], and the remaining samples were used as the prediction set. This was done including RIP_K and excluding RIP_K, and in each case considering total phyllosilicates or clay texture variables.

The PLS models obtained with the reduced calibration sets had a pattern of regression coefficients and quality parameters similar to those obtained in the previous section, that is, *y* explained cumulative variance was 85% excluding RIP_K and 90% including RIP_K; the slopes were 1; the regression coefficients were > 90; and the RMSECV values were of the same order of magnitude as previously. These statistics confirmed the representativeness of the selected data to construct the new PLS model.

The model was externally validated with the corresponding test set in each case. Figs. 4a and 4b shows, as an example, the correlations between experimental and predicted K_d(Cs) values including or excluding RIP_K, respectively, for data sets with the clay texture variable. The two correlations were satisfactory, with slopes close to unit and regression coefficients close or higher than 0.9. These results confirmed the robustness and the absence of bias in the PLS models, and that the K_d(Cs) could also be predicted with the PLS models without the RIP_K variable.

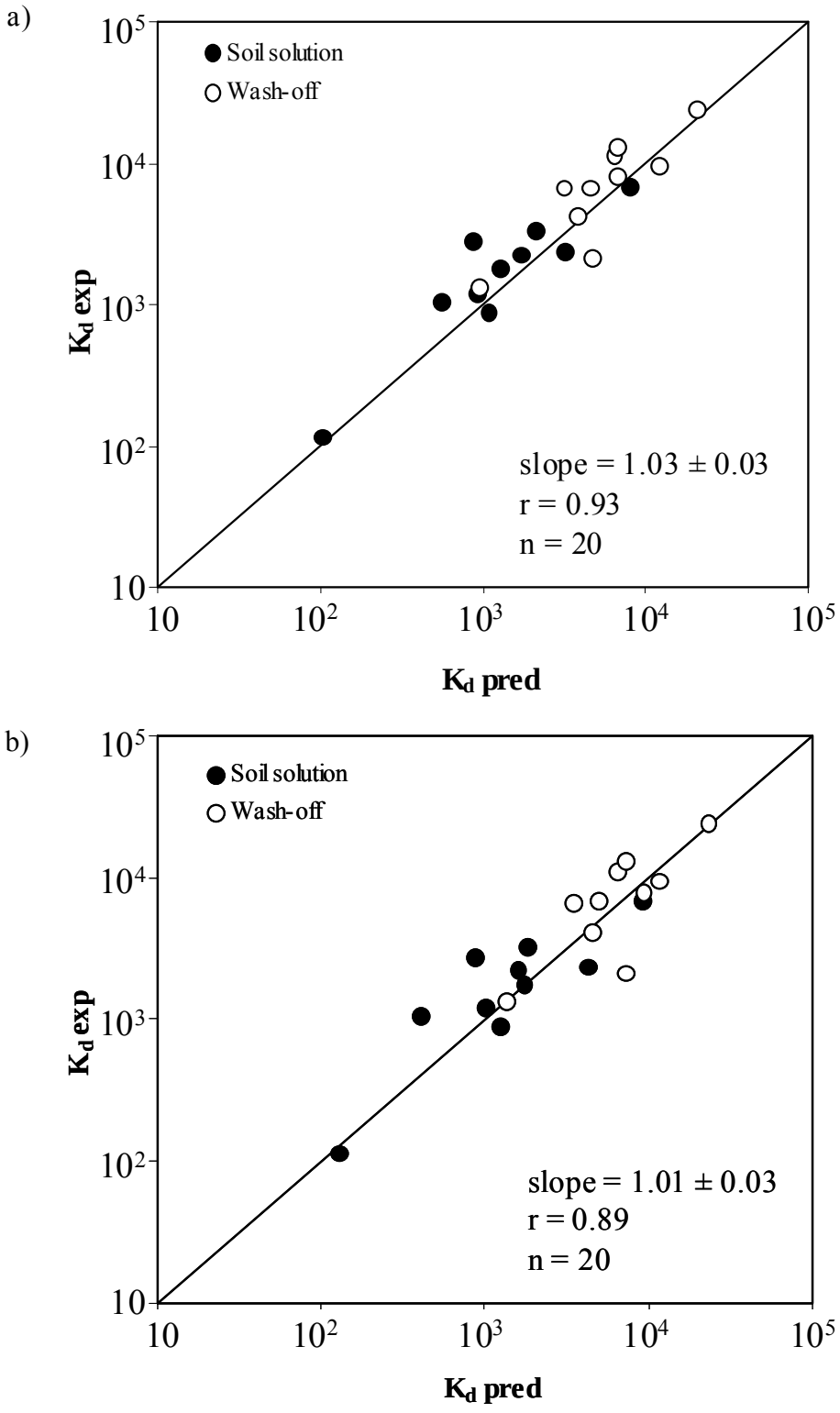

Fig. 4. Validation of the PLS models with the prediction set. Experimental vs. predicted K_d(Cs) correlations obtained with the PLS models using the global dataset and the clay texture to describe the clay content, a) including RIP_K and b) excluding RIP_K, in which the solid line represents the ideal $K_d(Cs)_{exp} = K_d(Cs)_{pred}$ relationship.

4. Conclusions

Both mechanistic and PLS-based models succeeded in predicting K_d(Cs) with very satisfactory correlations between experimental and predicted values. Among mechanistic models, the model with the highest requirements in terms of soil data provided the best prediction. However, it was possible to propose simpler models based on soil properties available from routine analyses, such as clay content and K status in the soil, with also satisfactory results. The PLS-based models confirmed the soil parameters that better explained the variability of K_d(Cs), as the RIP_K, clay content, and NH_4^+ and K status. Only slight differences in the models were observed when using the clay content obtained by textural analysis or the phyllosilicate content obtained by mineralogical analysis, and in all cases the regressions had quality parameters similar to those of the mechanistic models. Although better correlations between experimental and predicted K_d(Cs) were obtained when the RIP_K was included as a soil variable, the prediction of K_d(Cs) was also satisfactory when this specific soil parameter was not considered in the PLS model. As the mechanisms of the interaction of a contaminant in soils are not always well known, PLS-based models are recommended as a powerful approach to examine and to predict the interaction parameters of any contaminant in soils.

Acknowledgements

This research was funded by the Spanish Government (CICYT, contracts PPQ2002-00264 and CTM2005-03847/TECNO) and the Generalitat de Catalunya (contract 2009SGR1188). C. J. Gil-García acknowledges the Ministerio de Educación, Cultura y Deporte for a PhD fellowship. The authors thank Universidad de Salamanca, Universidad Politécnica de Valencia, Universidad de Oviedo, Universidad de Extremadura, Universidad de León, Universitat de les Illes Balears, ENRESA, ENUSA, SCAR (Generalitat de Catalunya), Universidade da Coruña and Universidad de Málaga for the soil samples supplied. The authors also thank Dra. A. Sahuquillo for the use of MATCONTROL facilities to prepare the samples.

References

[1] Cremers, A., Elsen, A., De Preter, P., Maes, A., 1988. Quantitative analysis of radiocaesium retention in soils. Nature 335, 247–249.

[2] Wauters, J., Sweeck, L., Valcke, E., Elsen, A., Cremers, A., 1994. Availability of radiocaesium in soils: A new methodology", Sci. Total Environ. 157, 239-248.

[3] Vidal, M., Roig, M., Rigol, A., Llauradó, M., Rauret, G., Wauters, J., Elsen, A., Cremers, A., 1995. Two approaches to the study of radiocaesium partitioning and mobility in agricultural soils from the Chernobyl area. Analyst 120, 1785-1791.

[4] Bachhuber, H., Bunzl, K., Schimmack, W., 1982. The migration of 137Cs and 90Sr in multilayered soils: results from batch, column and fallout investigations. Nucl. Technol. 59, 291-301.

[5] Sanchez, A.L., Smolders, E., Van den Brande, K., Merckx, R., Wright, S.M., Naylor, C., 2002. Predictions of in situ solid-liquid distribution of radiocaesium in soils. J. Environ. Radioactivity 63, 35- 47.

[6] Dewiere, L., Bugai, D., Grenier, C., Kashparov, V., Ahamdach, N, 2004. ^{90}Sr migration to the geo-sphere from a waste burial in the Chernobyl exclusion zone. J. Environ. Radioactivity 74(1-3), 139-150.

[7] Elejalde, C., Herranz, M., Legarda, F., Romero, F., 2000. Determination and analysis of distribution coefficients of ^{137}Cs in soils from Biscay (Spain). Environ. Pollut. 110(1), 157-164.

[8] Tianwei, Q., Hongxiao, T., Jiajun, C., Sheng, W.J., Chunli, L., Guibin, W., 2001. Simulation of the migration of ^{85}Sr in Chinese loess under artificial rainfall condition. Radiochim. Acta 89(6), 403-406.

[9] Gil-García, C. J., Rigol, A., Vidal, M., 2009. New best estimates for radionuclide solid–liquid distribution coefficients in soils. Part 1: radiostrontium and radiocaesium. J. Environ. Radioact. 100, 690–696.

[10] Vidal, M., Rigol, A., Gil-García, C., 2009. Soil-radionuclide interactions. In: Quantification of radionuclide transfer in terrestrial and freshwater environments for radiological assessments,71-102. IAEA-TECDOC-1616. IAEA, Viena. ISBN: 978-92-0-104509-6

[11] Gil-García, C. J., Rigol, A., Rauret, G., Vidal, M., 2008. Radionuclide sorption-desorption pattern in soils from Spain. Appl. Radiat. Isot. 66, 126-138.

[12] Rigol, A., Camps, M., de Juan, A., Rauret, G., Vidal, M., 2008. Multivariate soft-modelling to predict radiocesium soil-to-plant transfer. Environ. Sci. Technol. 42, 4029-4036.

[13] Gil-García, C. J., Rigol, A., Vidal, M., 2011. The use of hard and soft modelling to predict radiostrontium solid-liquid distribution coefficient in soils. Chemosphere. Submitted

[14] Wauters, J., Elsen, A., Cremers, A., Konoplev, A. V., Bulgakov, A. A., Comans, R. N. J., 1996a. Prediction of solid liquid distribution coefficients of radiocaesium in soils and sediments. Part one: a simplified procedure for the solid characterization. Appl. Geochem. 11, 589-594.

[15] Wauters, J., Vidal, M., Elsen, A., Cremers, A., 1996b. Prediction of solid liquid distribution coefficients of radiocaesium in soils and sediments. Part two: a new procedure for the solid characterization. Appl. Geochem. 11, 595-599.

[16] Rigol, A.; Vidal, M.; Rauret, G.; Shand, C. A.; Cheshire, M. V, 1998. Competition of organic and mineral phases in radiocesium partitioning in organic soils of Scotland and the area near Chernobyl. Environ. Sci. Technol. 32, 663–669.

[17] Sweeck, L., Wauters, J., Valcke, E., Cremers, A., 1990. The specific interception potential of soils for radiocesium, in: Desmet, G., Nassimbeni, P., Belli, M. (Eds.), Transfer of Radionuclides in Natural and Seminatural Environments, EUR 12448, Elsevier Applied Science, pp. 249-258.

[18] Waegeneers, N., Smolders, E., Merckx, R., 1999. A statistical approach for estimating the radiocaesium interception potential of soils, J. Environ. Qual. 28, 1005-1011.

[19] Boardman, A. E., Hui, B. S., Wold, H., 1981. The partial least squares-fix point method of estimating interdependent systems with latent variables. Comm. Statist. Theory Methods 10, 613-639.

[20] Wold, S., Martens, H., Wold. H., 1983. The multivariate calibration problem in chemistry solved by the PLS method. Lect. Notes Math. 973, 286-293.

[21] Esbensen, K., Schönkopf, S., Midtgaard, T., 1994. Multivariate Analysis in Practice. Computer-Aided Modelling AS, Norway.

[22] Staunton, S., 1994. Adsorption of radiocesium on various soils:Interpretation and consequences of the effects of soil:solution ratio and solution composition on the distribution coefficient. Eur. J. Soil Sci., 45, 409–418.

[23] Absalom, J. P.; Young, S. D.; Crout, N. M. J., 1995. Radio-cesium fixation dynamics: measurement in six Cumbrian soils. Eur. J. Soil Sci. 46, 461–469.

[24] Kennard, R., Stone, L.A., 1969. Computer aided design of experiments. Technometrics 11, 137-148.

4. DISCUSIÓN DE RESULTADOS

En este capítulo se realiza una discusión global de los resultados obtenidos, presentando también datos considerados de interés no incluidos en las publicaciones presentadas anteriormente.

La discusión se estructura en tres partes diferenciadas, correspondientes a los objetivos específicos presentados previamente. En primer lugar, se presentan los resultados relacionados con los estudios de sorción-desorción de radioestroncio y radiocesio en suelos del territorio español, incluyendo la caracterización completa de los suelos seleccionados y su agrupación según parámetros generales, y la comparación de los valores del coeficiente de distribución sólido-líquido (K_d) medidos con los obtenidos en suelos pertenecientes a climas templados. En segundo lugar, se resume el estudio crítico sobre los criterios de agrupamiento de los valores de K_d recopilados para una extensa serie de radionucleidos, basados tanto en propiedades edáficas tradicionales (concretamente, textura y contenido de materia orgánica) como, para unos determinados radionucleidos, en parámetros de suelos considerados relevantes para describir sus procesos de sorción, lo que permite también correlacionar los valores de K_d con estas propiedades edáficas clave. Finalmente, se presentan los resultados de predicción de los coeficientes de distribución de radioestroncio y radiocesio a partir de propiedades de suelos, aplicando modelos mecanísticos (duros), desarrollados a partir del conocimiento de los factores que controlan su interacción, y modelos multivariantes blandos basados con el uso de la regresión por mínimos cuadrados parciales (*Partial Least Squares Regression*, PLS).

4.1

Estudios de sorción-desorción de radioestroncio y radiocesio en suelos del territorio español

Como los modelos de predicción del comportamiento y movilidad de radioestroncio y radiocesio que existen en la actualidad han sido construidos, principalmente, a partir de datos pertenecientes a suelos de climas templados y suelos próximos a la central nuclear de Chernóbil, se planteó como objetivo verificar si suelos con diferentes propiedades edáficas, como es el caso de suelos del territorio español, mostrarían una interacción con los radionucleidos (representada mayormente por los valores de los coeficientes de distribución -K_d-) similar a la de los suelos utilizados en la creación de estos modelos. Los resultados de estos estudios se recogieron en la **Publicación 1**.

4.1.1. Selección y caracterización de suelos

La primera etapa del estudio fue la recopilación de muestras de suelos representativas de todo el territorio español. Para ello, se contactó con centros y universidades que participan en el Programa de Vigilancia Radiológica Ambiental, implantado en la zona de influencia de las centrales nucleares y otras instalaciones nucleares y radioactivas, bajo un programa independiente del Consejo de Seguridad Nuclear (PVRAIN). También se contactó con centros y universidades que participan en la red de vigilancia nacional (Revira) no asociada a instalaciones, en concreto la Red de Estaciones de Muestreo (REM), donde la vigilancia se realiza mediante programas de muestreo y análisis llevados a cabo por diferentes laboratorios. De las instituciones que participan en en el PVRAIN, se recibieron muestras de la Universidad Politécnica de Valencia y ENUSA, mientras que de las que participan en la REM se recibieron muestras de la Universidad de Salamanca, Universidad de Asturias, Universidad de Extremadura, Universidad de León, Universitat de les Illes Balears, Universidade da Coruña y Universidad de Málaga. Además de estos suelos, el grupo de investigación realizó una campaña de toma de muestra de suelos cercanos a las centrales nucleares que operan en Cataluña (Ascó y Vandellós), así como en los arrozales del Delta del Ebro.

Una vez recibidos los suelos, se les aplicó una metodología parecida a la utilizada en la preparación de materiales de referencia para el control de la calidad (Llauradó et al., 2001). Las muestras fueron secadas a temperatura ambiente, tamizadas a < 2mm y por último homogeneizadas durante 90 horas utilizando un equipo de homogenización. Tal y como se puede observar en la Figura 4.1, el equipo de homogenización, consta de un bidón con unas palas fijas en su interior, el cual da vueltas sobre sí mismo en una mesa de rodillos o *rollers*. La preparación de los suelos se realizó en las instalaciones que la unidad de MATCONTROL dispone en la Facultat de Química de la Universitat de Barcelona.

Figura 4.1. Tablas de rodillos para la homogenización de materiales (*rollers*).

Una vez preparados los suelos, se procedió a la caracterización de sus propiedades edáficas generales (tales como el pH, el contenido de carbono orgánico y carbonatos, la capacidad de intercambio catiónico (CIC), la concentración de cationes intercambiables y la conductividad eléctrica (CE), y específicas, que son necesarias para los modelos de predicción de la movilidad de radionucleidos en suelos (por ejemplo, la capacidad de campo, la composición catiónica de la solución de contacto y el Potencial de Intercepción de Radiocesio (*Radiocesium Interception Potential,* RIP)). Los datos de caracterización se muestran en las tablas 1a y 1b de la **Publicación 1**.

Los suelos estudiados fueron minerales, con un contenido máximo de carbono orgánico inferior al 10%. Los valores de muchas propiedades generales oscilaron en un intervalo amplio, tal como el pH (4,3 - 9,2), la CIC (de 21,3 a 89,3 cmolc kg^{-1}) y el contenido de carbonatos (que osciló entre por debajo del límite de detección hasta un máximo de 70%). Mayoritariamente, los suelos fueron de textura franca, y sólo una minoría tuvieron textura arenosa (suelo VAN1) o arcillosa (suelos MALAGA, TENF2 y DELTA2). El hecho de que la gran mayoría de suelos tuviera un pH > 8, bajo contenido de materia orgánica, un contenido de $CaCO_3$ > 25%, y que el contenido en arcillas en todos los suelos fuera superior al 10% (y en muchos de ellos ≥ 20%) confirmó las características diferenciadas de los suelos elegidos respecto a las habituales en suelos de clima templados (FAO-UNESCO, 1994).

En lo que hace referencia a la determinación de parámetros específicos, destaca el análisis de la composición catiónica de la solución de contacto y la determinación del RIP_K, que estima la capacidad de sorción específica que tiene un suelo respecto a radiocesio, siendo este parámetro la primera vez que se cuantificó en un número tan elevado de suelos del territorio español. Los valores obtenidos estuvieron comprendidos en un amplio intervalo, desde 179 mmol kg^{-1} en el suelo FROCOR hasta 7000 mmol kg^{-1} en el suelo UIB. Este intervalo de valores coincidió con los intervalos de valores recogidos en la literatura para suelos de la Europa Occidental (Sánchez et al., 2002). La variabilidad que presentan los valores de RIP_K es debida a su estrecha relación con el contenido y el tipo de arcilla que presenta el suelo. La posible correlación entre los valores de RIP_K y las arcillas presentes en las muestras de suelos fue abordada con más detalle en el marco de la **Publicación 6**.

Para estudiar las posibles agrupaciones de suelos existentes en función de sus propiedades edáficas, se realizó un Análisis de Componentes Principales (*Principal Component Analysis*, PCA). Las Figuras 4.2 y 4.3 muestran los gráficos de *scores y loadings* obtenidos en el espacio de los dos primeros componentes principales PC1 y PC2, respectivamente, que explicaron el 50% de la varianza de los datos. La inclusión de dos componentes principales adicionales permitió aumentar el porcentaje explicado hasta el 73%. A partir del gráfico de *scores*, se observó que la gran mayoría de los suelos se agruparon en un único clúster, del que los suelos FROCOR, DELTA1 y DELTA2 estuvieron excluidos. Este comportamiento puede justificarse a partir del análisis de los valores de ciertas propiedades de los suelos. El suelo FROCOR presenta el menor RIP_K y la mayor concentración de elementos en la solución de suelo de entre todos los suelos examinados, mientras que los suelos DELTA1 y DELTA2 son suelos con un elevado contenido en arcillas, pero valores de RIP_K relativamente bajos, y con concentraciones altas de elementos en la solución de suelo. Mirando con detenimiento la agrupación de suelos, a partir de la eliminación de los tres suelos citados, se podría distinguir ciertas nuevas subagrupaciones, como son las de los suelos de MALAGA, TENF1 y TENF2, con valores elevados de RIP, y la de los suelos OVI01, FONCOR y ANDCOR, que tienen los mayores contenidos de carbono orgánico.

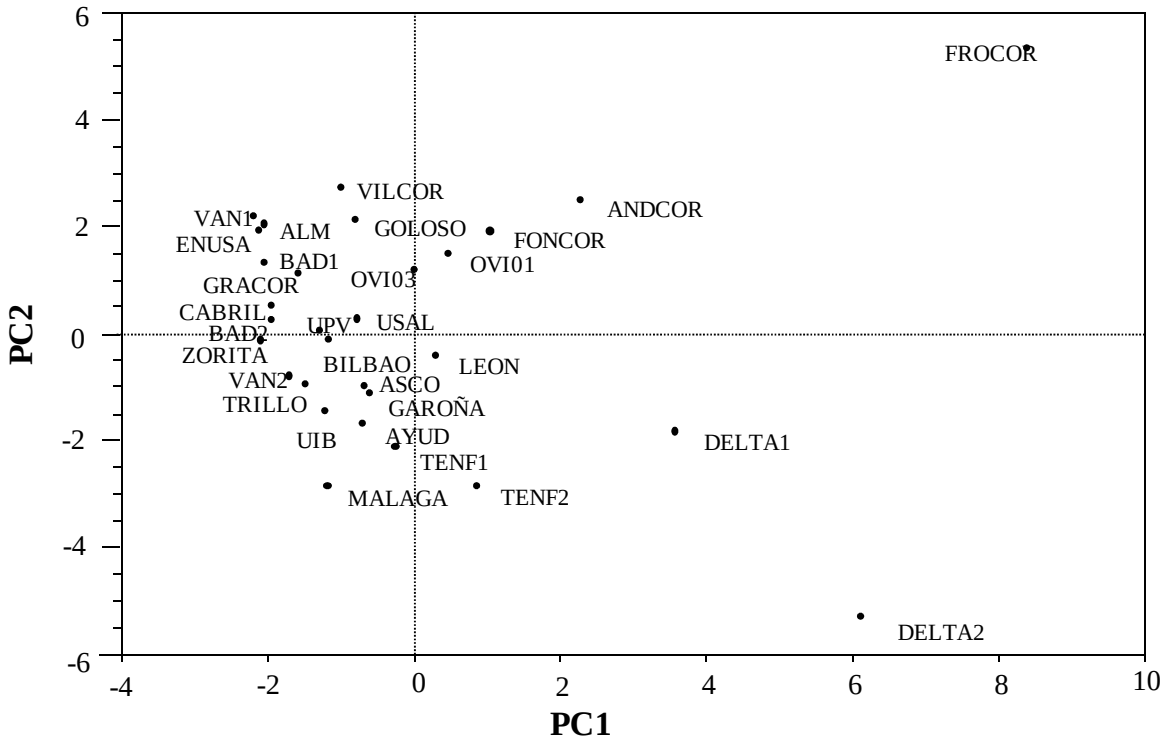

Figura 4.2. Gráfico de *scores* de los suelos analizados.

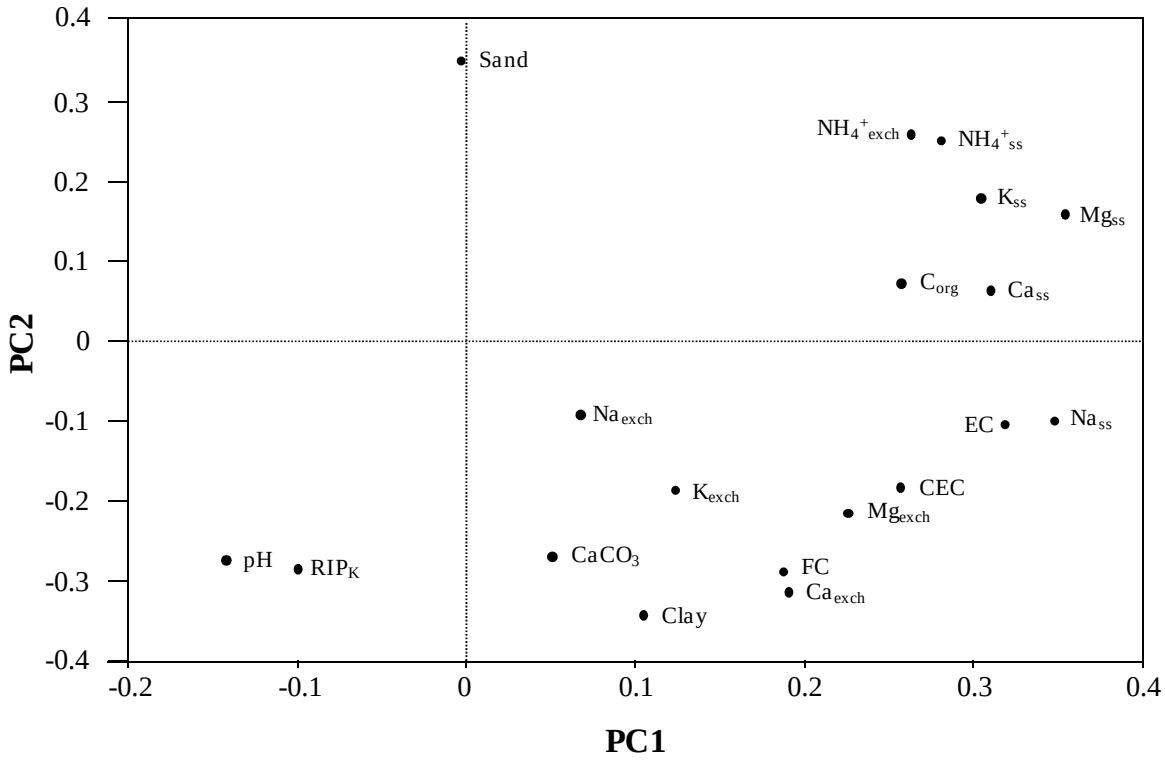

Figura 4.3. Gráfico de *loadings* de las variables de los suelos analizados

El gráfico de *loadings* muestra las variables originales en el nuevo espacio representado por los componentes principales PC1 y PC2, indicando su peso en la creación de los componentes principales. De esta forma cuanto más cercana al centro esté una variable significa que su peso en la creación del componente principal es menor, mientras que cuanto más alejada esté, más peso tiene sobre el componente principal. En este caso, se observa que la variable Arena, influye mucho en el PC2, siendo por el contrario la que menos influye en el PC1. También destaca la fuerte influencia que presentan las variables correspondientes a la composición catiónica de la solución de contacto (K_{ss}, NH_{4ss}, Ca_{ss} y Mg_{ss}) y que se ha demostrado que tiene un rol muy importante en los procesos de sorción. El resto de variables presentan influencias diversas en los dos PC, observándose una gran influencia del pH y RIP_K en el PC2.

4.1.2 Obtención de los coeficientes de distribución de radioestroncio y radiocesio

Una vez se determinaron las propiedades edáficas generales y específicas de todos los suelos, se obtuvieron experimentalmente los coeficientes de distribución sólido-líquido (K_d) de radioestroncio y radiocesio. Su determinación se realizó utilizando la metodología en *batch* con dos soluciones de contacto diferentes. Por un lado, los valores de K_d se obtuvieron en un medio que simulaba la composición catiónica de la solución de suelo. La composición catiónica de la solución de suelo fue determinada con una relación sólido/líquido representativa de la capacidad de campo del suelo, pero la determinación del valor de K_d se obtuvo en una solución con esta composición pero con una relación sólido/líquido 1:10. Por otro lado, los valores de K_d también se determinaron en solución de *wash off*, obtenida tras una extracción del suelo con agua, con una relación sólido/líquido 1:10. La finalidad de esta comparación fue estudiar cómo afectaba la composición de solución de contacto (es decir, el medio iónico con presencia de cationes competitivos para el proceso de sorción) a los valores de K_d.

La Tabla 2 de la **Publicación 1**, muestra los valores obtenidos de K_d para las dos condiciones experimentales estudiadas. Los valores de K_d fueron sistemáticamente mayores para el radiocesio que para el radioestroncio. En lo que hace referencia al efecto de la composición de la solución de contacto, los valores obtenidos en el medio

de la solución de *wash off* fueron superiores a los obtenidos en el medio que simulaba la solución de suelo. Este hecho es consistente con las mayores concentraciones de Ca y Mg en las soluciones de contacto procedentes de la simulación de la solución de suelo, que afectan a la K_d(Sr), y de K y NH_4^+, que controlan los valores de K_d(Cs).

Para elucidar si los suelos del territorio español presentaban datos de K_d similares a los de los suelos de climas templados, se realizó la exploración y comparación de los datos utilizando los denominados diagramas de caja y bigotes. Se escogió este tipo de representación ya que permite en un mismo gráfico presentar varios descriptores estadísticos de un conjunto de datos, como son la mediana y la media aritmética, el primer y tercer cuartil, el valor máximo y valor mínimo, así como valores atípicos. La Figura 4.4 muestra la información que se deriva de este tipo de representación:

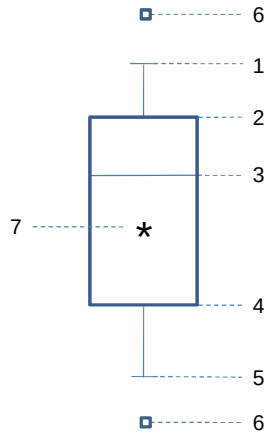

1.-Valor máximo: Es el extremo superior del cuerpo principal de datos.
2.-Tercer cuartil (Q_3): Por debajo de este valor se encuentra como máximo el 75% de los valores de K_d.
3.-Mediana: Coincide con el segundo cuartil. Divide a la distribución en dos partes iguales (50% de los valores a cada lado).
4.-Primer cuartil (Q_1): Por debajo de este valor se encuentra como máximo el 25% de los valores de K_d.
5.-Valor mínimo: Es el extremo inferior del cuerpo principal de datos.
6.-Valores atípicos: Valores apartados del cuerpo principal de datos.
7.-Media aritmética.

Figura 4.4. Información derivada de los diagramas de caja y bigotes.

De forma complementaria a las Figuras 2, 3, 4 y 5 de la **Publicación 1**, las Figuras 4.5 y 4.6 muestran los diagramas construidos a partir de los datos de K_d(Cs) y K_d(Sr) obtenidos en el presente trabajo, en las dos condiciones experimentales, y de datos procedentes de la literatura para suelos de climas templados, agrupados según la textura de la fracción mineral, al ser todos los suelos examinados de tipo mineral. El criterio para la agrupación se define a continuación:

- Suelos Arenosos. La fracción de arena en la materia mineral es mayor del 65%, mientras que la fracción de arcilla es menor que 18%.
- Suelos Arcillosos. La fracción de arcilla en la materia mineral es mayor del 35%.
- Suelos Francos. El resto de suelos minerales.

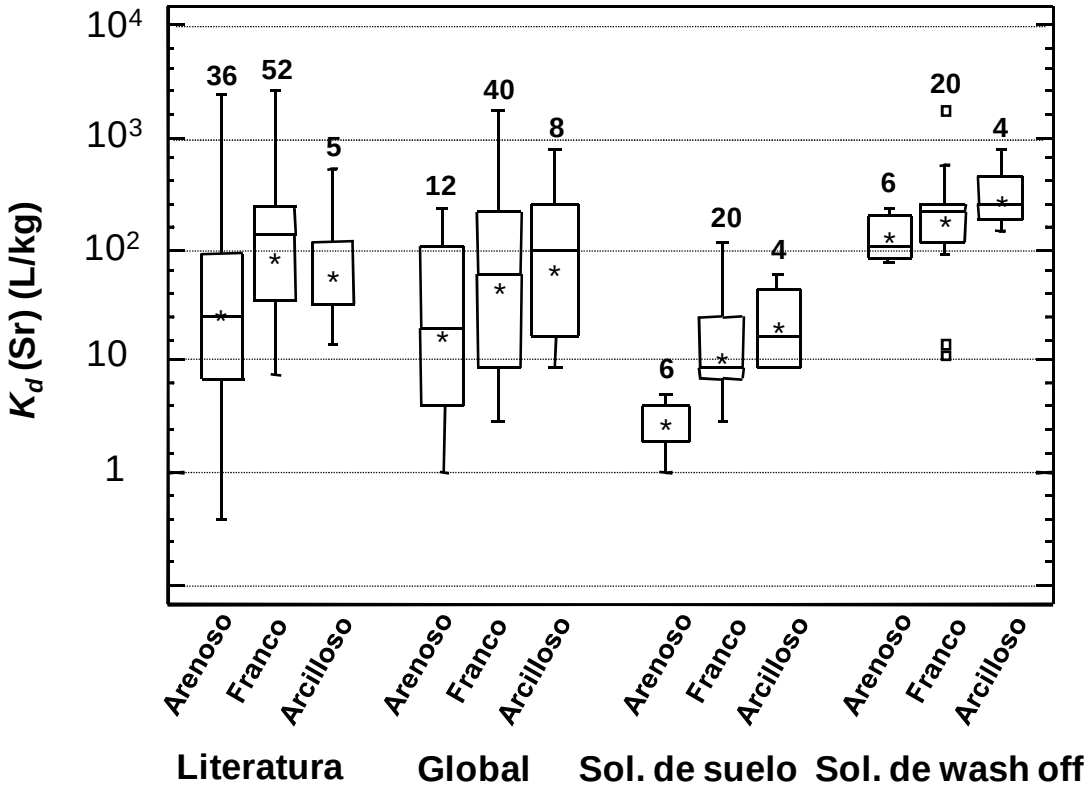

Figura 4.5. Comparación de los intervalos de valores de K_d(Sr) según el criterio de la textura de la fracción mineral

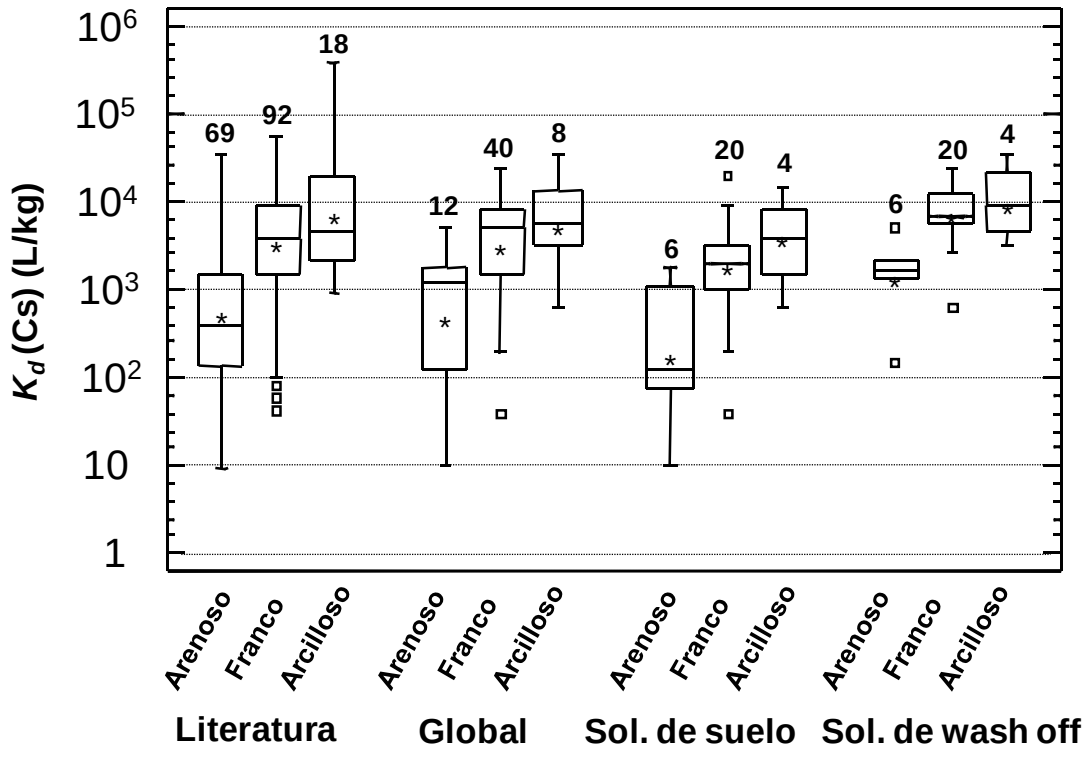

Figura 4.6. Comparación de los intervalos de valores de K_d(Cs) según el criterio de la textura de la fracción mineral

En lo que hace referencia a los valores de K_d(Sr), la Figura 4.5 confirma que los valores obtenidos en el medio que simula la solución de suelo fueron sistemáticamente inferiores a los obtenidos en el medio de la solución de *wash off*. Solamente en el caso del grupo de suelos con textura Franca, hubo un cierto solapamiento de los datos, debido a la variabilidad de éstos en el medio que simula la solución de suelo. La comparación de los valores procedentes de la literatura (procedentes todos de experimentos en *batch*, pero con una gran variabilidad de otras condiciones experimentales) con la población resultante de sumar todos los datos procedentes de los dos medios iónicos (global), mostró que los intervalos se solaparon para todas las clases texturales, con lo que se puede concluir que los intervalos de los valores de K_d(Sr) deducidos a partir de los suelos del territorio español coincidieron con los procedentes de suelos de otros climas.

En líneas generales, estas conclusiones pudieron ser extrapoladas para el caso de K_d(Cs), aunque en este caso el rol de la textura en los valores de K_d(Cs) fue más evidente, ya que los valores de K_d(Cs) aumentaron claramente al pasar de textura Arenosa a Arcillosa. De nuevo se observó que en general los valores obtenidos en el medio iónico de simulación de la solución de suelo, fueron relativamente inferiores a los obtenidos con la solución de *wash off*, y que al comparar el set de datos global no hubo diferencias significativas con los datos procedentes de la literatura.

El claro efecto de la composición catiónica del medio de contacto pone de manifiesto cómo de importante es el protocolo con el que se determine la K_d, ya que para un mismo suelo el valor de K_d puede variar significativamente según las condiciones experimentales aplicadas. Por lo tanto es necesario realizar una armonización de los protocolos existentes para la determinación de la K_d, para permitir una mejor comparación de los valores obtenidos y disminuir las fuentes de variabilidad no intrínsecamente relacionadas con las propiedades de los suelos o de los radionucleidos en estudio. Por otro lado, las comparaciones realizadas entre el set de datos global y los datos procedentes de la literatura, en función de diferentes criterios (por ejemplo, composición catiónica de la solución de contacto; RIP_K; CIC; textura) confirmaron la similitud entre los datos de los suelos de climas templados y los obtenidos con suelos del territorio español. A pesar de la variabilidad observada, esta observación demostró que los mecanismos responsables de la sorción de radioestroncio y radiocesio encontrados en suelos de climas templados son perfectamente aplicables a suelos del territorio español, lo que facilitará su descripción

y predicción, tal como se mostrará en el contexto del tercer objetivo de la presente tesis.

4.1.3. Reversibilidad de la sorción y dinámica de la interacción

Un parámetro importante que controla la concentración de radionucleido en la solución de contacto es la fracción de radionucleido que se encuentra sorbido de forma reversible. Esta fracción puede no ser constante con el tiempo, con lo que hay que considerar aquellos factores que pueden hacer variar la reversibilidad de la sorción con el tiempo.

Se han desarrollado una gran variedad de procedimientos con la finalidad de determinar la reversibilidad de la sorción (Kennedy, 1997). En este caso, se eligió un procedimiento de extracción única en condiciones de intercambio catiónico, y se relacionó el porcentaje de desorción con la fracción reversiblemente sorbida. A su vez, y para obtener información de dinámica, los suelos se sometieron a ciclos de secado-mojado en los que se modificó bruscamente su temperatura y régimen hídrico.

La Tabla 4.1 resume los datos de desorción de la Figura 6 de la **Publicación 1** obtenidos en dos momentos temporales diferentes: corto plazo (con un menor número de ciclos aplicados) y medio plazo.

Tabla 4.1. Porcentajes de desorción obtenidos tras la aplicación de ciclos de secado-mojado. Media aritmética (MA); Desviación estándar (DE), Valores Mínimo (Min) y Máximo (Max).

RN	Momento temporal	MA	DE	Min	Max
Sr	**Corto plazo**	85	9	57	99
	Medio plazo	86	11	44	99
Cs	**Corto plazo**	41	12	14	65
	Medio plazo	19	10	2	46

Para el caso del radioestroncio, la obtención de porcentajes de desorción altos (cercanos al 100% en algún caso), independientemente del número de ciclos aplicados, indicó que desde un principio la fracción de radioestroncio fijada en la fase sólida del suelo fue baja y que su incremento con el tiempo fue menor. Por el contrario, se pudo predecir que la reversibilidad de la sorción de radiocesio no sólo fue baja desde un inicio (mucho más que la de radioestroncio), sino que disminuyó con el tiempo transcurrido desde la sorción, como se deduce de la disminución en sus porcentajes de extracción, lo que se explica por un proceso de envejecimiento de la sorción debido a una migración lenta y continua del radiocesio hacia sitios altamente selectivos de los espacios interlaminares de las arcillas, en los que incluso puede producirse un colapso de las arcillas tras su deshidratación.

Los datos de K_d y de reversibilidad de la sorción han de servir como datos de entrada en los modelos de predicción del riesgo derivado de (posibles) episodios de contaminación. Por lo tanto, si se tiene una combinación de suelo/radionucleido con un valor alto de K_d y un porcentaje bajo de desorción, se está delante de una situación de riesgo bajo, ya que el radionucleido quedará fuertemente retenido, mientras que el escenario de mayor riesgo sería el representado por aquellas combinaciones de suelo/radionucleido con valores bajos de K_d y porcentajes de desorción altos. En el contexto estudiado, para un mismo nivel de concentración de actividad, una contaminación por radioestroncio supondría un mayor riesgo ambiental que una por radiocesio.

4.2

Evaluación de los criterios para el agrupamiento de los valores de K_d en función de propiedades edáficas generales y de factores clave que rigen la interacción suelo-radionucleido

El “Handbook of parameter values for the prediction of radionuclide transfer in temperate environments (TRS-364)” fue publicado en 1994 por el Organismo Internacional de la Energía Atómica (*International Atomic Energy Agency*, IAEA), en colaboración con la Unión Internacional de Radioecología (*International Union of Radioecology*, IUR). Este Handbook es un documento imprescindible en los trabajos de modelización del comportamiento de radionucleidos en el medio ambiente al ser una recopilación de datos disponibles sobre parámetros radioecológicos, usados habitualmente en los modelos de asesoramiento del riesgo sobre el impacto de emisiones accidentales radioactivas. La recopilación incluía datos hasta 1992, con trabajos de varias décadas de antigüedad. En los últimos años, tanto el volumen como la disponibilidad de los datos han aumentado ya que, recientemente, en especial en acciones post-Chernóbil, se han publicado nuevos trabajos recopilatorios sobre parámetros de movilidad de radionucleidos. Es en este contexto que la IAEA se planteó la revisión del documento, en la que participó nuestro grupo de investigación, especialmente en la revisión de datos relacionados con los coeficientes de distribución.

4.2.1. Selección y tratamiento de los datos

Para la nueva versión del Handbook, se utilizaron datos obtenidos a partir de experimentos de laboratorio y de campo, con diferentes fuentes de contaminación, considerando únicamente estudios con suelos. El número final de documentos aceptados como fuentes de información para la construcción de la nueva base de datos de K_d, una vez aplicados filtros estrictos para su aceptación, fue de aproximadamente unos 80, incluyendo artículos de revistas, informes y documentos internos de agencias nucleares internacionales. La base de datos finalmente creada estuvo constituida por más de 2900 datos pertenecientes a 67 elementos. Entre estos, fueron el cesio y el estroncio los elementos con un mayor número de observaciones. Otros elementos como el yodo, uranio, cobalto, potasio, antimonio y selenio, tuvieron también más de 100 datos cada uno.

El análisis de los documentos aceptados permitió la creación de una base de datos en la que, de forma conjunta a los valores de K_d, se incluyeron parámetros de suelo asociados al comportamiento de radionucleidos en suelos e información sobre la metodología analítica utilizada para su determinación. Con la creación de la base de datos se pretendió la mejora en la propuesta de los estimadores de los valores de K_d en suelos de determinadas características, así como reducir su variabilidad. A continuación la Tabla 4.2 muestra los 22 campos obligatorios que se completaron para todos los elementos, además de los campos adicionales para elementos con mayor interés medioambiental.

Debido a que este tipo de datos suele seguir distribuciones de tipo lognormal, los parámetros estadísticos para la estimación del mejor valor de K_d y de su variabilidad fueron la media geométrica y la desviación estándar geométrica, respectivamente. Se siguieron dos aproximaciones para agrupar los datos de K_d recogidos y derivar sus mejores estimadores. Por un lado, se agruparon según el contenido de materia orgánica y textura de la fracción mineral siguiendo el mismo criterio que el TRS 364 anterior. Por otro, lo que constituye una aportación novedosa propuesta en el marco de esta Tesis Doctoral, se agruparon según los parámetros claves que rigen la interacción de radionucleidos en suelos, tal como recogen las **Publicaciones 2, 3 y 4.**

Tabla 4.2. Campos obligatorios y adicionales recopilados en la base de datos.

Elemento	**Campos obligatorios**			
Todos	Tipo documento	Revista	Idioma	Autores
	Volumen	Páginas	Año	Título artículo
	Isótopo	Zona Climática	País	Código suelo
	Clasificación textural	pH	Capacidad de Intercambio Catiónico (CIC)	
	% Arena	% Arcilla	% materia orgánica	K_d
	Comentarios sorción	% desorción	Comentarios desorción	
	Campos adicionales			
Cs	NH_4 + K intercambiable	NH_4 + K solución de suelo	RIP_K	Conductividad eléctrica
Sr	Ca + Mg intercambiable		Ca + Mg solución de suelo	
U	Fe total	$CaCO_3$		

4.2.2. Uso de la textura y el contenido de la materia orgánica como criterios de agrupamiento

En una primera etapa de análisis, los valores de K_d se agruparon según el contenido de materia orgánica y la fracción relativa de las clases texturales “arena” y “arcilla” en la materia mineral, obteniéndose las siguientes clases (IAEA, 2006b):

- Suelos orgánicos: suelos con un contenido en material orgánico > 20%.
- Suelos arenosos: fracción de arena > 65% y fracción de arcilla < 18%.
- Suelos arcillosos: fracción de arcilla > 35%.
- Suelos francos: suelos minerales pertenecientes al resto de casos.
- Suelos inespecíficos: suelos sin información suficiente para ser clasificados en una de las otras categorías.

La Tabla 4.3 muestra, para algunos radionucleidos, la comparación entre la agrupación de los valores de K_d del anterior Handbook TRS 364 con la propuesta en la actual revisión, expresadas como Media Geométrica (MG) con su Desviación Estándar Geométrica (DEG) asociada, junto con los intervalos de valores de K_d obtenidos para

cada una de las clases de la agrupación, así como el número de datos (n) que han sido considerados para su cálculo. Los datos procedentes de la revisión aparecen en las **Publicaciones 2, 3 y 4.**

En general, en la actual revisión se observó un aumento de la variabilidad de los resultados, debido en parte al aumento en observaciones incluidas, mientras que en el TRS 364 algunos datos procedían del mismo trabajo. Detalles para algunos radionucleidos se citan a continuación.

4.2.2.1. Radioestroncio

Los valores de K_d derivados de la revisión fueron en general similares a los incluidos en el TRS 364. En ambos casos se observó como las MG aumentaron de forma consistente al aumentar el contenido de arcillas en las clases texturales, aunque los valores máximos se observaron para los suelos orgánicos. El análisis de la varianza de las series de datos mostró que sólo la MG de los suelos de la categoría “Arenoso” fue estadísticamente diferente a las demás. En función de este criterio de agrupamiento, se puede proponer una valor estimado de K_d(Sr) de 20 L/kg para suelos arenosos, y 70 L/kg para los demás.

4.2.2.2. Radiocesio

La revisión de los datos para radiocesio no sólo supuso un incremento muy significativo en el número de datos incluidos, sino que las nuevas MG aumentaron sistemáticamente con el contenido de arcillas, a diferencia de lo que ocurría con las MG del TRS 364, lo que sí que respondió a lo esperable según los mecanismos que rigen la sorción de radiocesio en suelos. En la nueva revisión, el valor mayor de MG coincidió con los suelos en la clase “Arcilloso”, mientras que en el TRS 364 el valor más grande correspondió a los suelos agrupados como “Franco”, hecho que no se corresponde con los mecanismos de sorción que presenta el radiocesio. En ambos casos, los valores menores de K_d(Cs) fueron para los suelos orgánicos.

Tabla 4.3. Comparación entre las agrupaciones de K_d en el Handbook TRS 364 y en la actual revisión.

		TRS-364				Revisión			
	Clases	**n**	**MG**	**DEG**	**Min - Max**	**n**	**MG**	**DEG**	**Min - Max**
Sr	**Arenoso**	81	$1{,}3 \times 10^{1}$	2	$5{,}5 \times 10^{-1}$ - $3{,}3 \times 10^{2}$	65	$2{,}2 \times 10^{1}$	6	$4{,}0 \times 10^{-1}$ - $2{,}4 \times 10^{3}$
	Franco	43	$2{,}0 \times 10^{1}$	2	$6{,}7 \times 10^{-1}$ - $6{,}0 \times 10^{2}$	120	$5{,}7 \times 10^{1}$	5	$2{,}0$ - $2{,}5 \times 10^{3}$
	Arcilloso	24	$1{,}1 \times 10^{2}$	2	$2{,}0 - 6 \times 10^{3}$	19	$9{,}5 \times 10^{1}$	4	$9{,}0$ - $7{,}5 \times 10^{2}$
	Orgánico	12	$1{,}5 \times 10^{2}$	2	$4{,}1 - 5{,}4 \times 10^{2}$	37	$1{,}1 \times 10^{2}$	6	$3{,}0$ - $6{,}5 \times 10^{3}$
Cs	**Arenoso**	81	$2{,}7 \times 10^{2}$	3	$1{,}8 - 4{,}0 \times 10^{4}$	114	$5{,}3 \times 10^{2}$	6	$1{,}0 \times 10^{1}$ - $3{,}5 \times 10^{4}$
	Franco	54	$4{,}4 \times 10^{3}$	1	$3{,}3 \times 10^{2}$ - $6{,}0 \times 10^{4}$	191	$3{,}5 \times 10^{3}$	4	$3{,}9 \times 10^{1}$ - $5{,}5 \times 10^{4}$
	Arcilloso	28	$1{,}8 \times 10^{3}$	2	$7{,}4 \times 10^{1}$ - $4{,}4 \times 10^{4}$	36	$5{,}5 \times 10^{3}$	4	$5{,}7 \times 10^{2}$ - $3{,}8 \times 10^{5}$
	Orgánico	9	$2{,}7 \times 10^{2}$	4	$2{,}0 \times 10^{-1}$ - $3{,}6 \times 10^{5}$	108	$2{,}7 \times 10^{2}$	7	$4{,}3$ - $9{,}5 \times 10^{4}$
U	**Arenoso**	24	$3{,}3 \times 10^{1}$	3	$5{,}5 \times 10^{-2}$ - $2{,}0 \times 10^{4}$	50	$1{,}1 \times 10^{2}$	12	$7{,}0 \times 10^{-1}$ - $6{,}7 \times 10^{4}$
	Franco	8	$1{,}2 \times 10^{1}$	3	$1{,}7 \times 10^{-2}$ - $9{,}0 \times 10^{3}$	84	$3{,}1 \times 10^{2}$	12	$9{,}0 \times 10^{-1}$ - $3{,}9 \times 10^{4}$
	Arcilloso	7	$1{,}5 \times 10^{3}$	3	4 - $4{,}9 \times 10^{5}$	12	$2{,}8 \times 10^{1}$	7	$2{,}6$ - $4{,}8 \times 10^{2}$
	Orgánico	6	$4{,}0 \times 10^{2}$	3	$2{,}7 - 6{,}0 \times 10^{4}$	9	$1{,}2 \times 10^{3}$	6	$3{,}3 \times 10^{1}$ - $7{,}6 \times 10^{3}$
Th	**Arenoso**	10	$3{,}0 \times 10^{3}$	2	$4{,}5 \times 10^{1}$ - 2×10^{5}	48	$7{,}0 \times 10^{2}$	11	$3{,}5 \times 10^{1}$ - $1{,}0 \times 10^{5}$
	Franco	1	$3{,}3 \times 10^{3}$	--	--	129	$1{,}8 \times 10^{4}$	4	$5{,}0 \times 10^{3}$ - $2{,}5 \times 10^{5}$
	Arcilloso	5	$5{,}4 \times 10^{3}$	3	$3{,}0 \times 10^{1}$ - $9{,}8 \times 10^{5}$	19	$4{,}5 \times 10^{3}$	3	$8{,}0 \times 10^{2}$ - $2{,}4 \times 10^{4}$
	Orgánico	3	$8{,}9 \times 10^{4}$	5	$9{,}0 \times 10^{1}$ - $8{,}8 \times 10^{8}$	11	$7{,}3 \times 10^{2}$	44	$1{,}8 \times 10^{1}$ - $8{,}0 \times 10^{4}$
Cd	**Arenoso**	14	$7{,}4 \times 10^{1}$	2	$3{,}7 - 1{,}5 \times 10^{3}$	30	$1{,}1 \times 10^{2}$	8	$2{,}0$ - $1{,}8 \times 10^{3}$
	Franco	8	$4{,}0 \times 10^{1}$	2	$1{,}6 - 9{,}9 \times 10^{2}$	5	$1{,}0 \times 10^{2}$	7	$9{,}2$ - $1{,}7 \times 10^{3}$
	Arcilloso	10	$5{,}4 \times 10^{2}$	1	$9{,}0 \times 10^{1}$ - $3{,}3 \times 10^{3}$	4	$1{,}3 \times 10^{1}$	15	$6{,}9$ - $2{,}7 \times 10^{3}$
	Orgánico	9	$8{,}1 \times 10^{2}$	2	$8{,}2 - 8{,}1 \times 10^{4}$	13	$6{,}5 \times 10^{2}$	6	$9{,}6$ - $7{,}0 \times 10^{3}$
Pb	**Arenoso**	3	$2{,}7 \times 10^{2}$	2	$2{,}7 - 2{,}7 \times 10^{4}$	9	$2{,}2 \times 10^{2}$	4	$2{,}5 \times 10^{1}$ - $1{,}3 \times 10^{3}$
	Franco	3	$1{,}6 \times 10^{4}$	1	$9{,}9 \times 10^{2}$ - $2{,}7 \times 10^{5}$	5	$1{,}0 \times 10^{4}$	3	$3{,}6 \times 10^{3}$ - $4{,}3 \times 10^{4}$
	Arcilloso	1	$5{,}4 \times 10^{2}$	--	--	2	$6{,}8 \times 10^{4,a}$	--	$5{,}4 \times 10^{3}$ - $1{,}3 \times 10^{5}$
	Orgánico	6	$2{,}2 \times 10^{4}$	1	$8{,}1 \times 10^{3} - 6{,}0 \times 10^{4}$	5	$2{,}5 \times 10^{3}$	3	$8{,}8 \times 10^{2}$ - $1{,}0 \times 10^{4}$
Co	**Arenoso**	33	$6{,}0 \times 10^{1}$	3	$2{,}2 \times 10^{-1}$ - $1{,}6 \times 10^{4}$	18	$2{,}6 \times 10^{2}$	18	$5{,}0$ - $3{,}7 \times 10^{4}$
	Franco	23	$1{,}3 \times 10^{3}$	1	$9{,}9 \times 10^{1}$ - $1{,}8 \times 10^{4}$	71	$8{,}1 \times 10^{2}$	15	$2{,}0$ - $1{,}0 \times 10^{5}$
	Arcilloso	15	$5{,}4 \times 10^{2}$	2	$1{,}5 \times 10^{1}$ - $2{,}0 \times 10^{4}$	10	$3{,}8 \times 10^{3}$	6	$5{,}4 \times 10^{2}$ - $9{,}9 \times 10^{4}$
	Orgánico	6	$9{,}9 \times 10^{2}$	2	$4{,}9 \times 10^{1}$ - $2{,}0 \times 10^{4}$	17	$8{,}7 \times 10^{1}$	9	$4{,}0$ - $5{,}8 \times 10^{3}$
Ni	**Arenoso**	11	$4{,}0 \times 10^{2}$	2	$2{,}0 \times 10^{1}$ - $8{,}1 \times 10^{3}$	26	$1{,}3 \times 10^{2}$	10	$3{,}0$ - $7{,}2 \times 10^{3}$
	Franco	1	$3{,}0 \times 10^{2}$	--	--	14	$1{,}8 \times 10^{2}$	5	$7{,}7$ - $1{,}2 \times 10^{3}$
	Arcilloso	10	$6{,}7 \times 10^{2}$	1	$1{,}6 \times 10^{2}$ - $2{,}7 \times 10^{3}$	12	$9{,}3 \times 10^{2}$	2	$2{,}5 \times 10^{2}$ - $3{,}2 \times 10^{3}$
	Orgánico	6	$1{,}1 \times 10^{3}$	1	$1{,}8 \times 10^{2}$ - $6{,}6 \times 10^{3}$	8	$1{,}1 \times 10^{3}$	2	$4{,}1 \times 10^{2}$ - $5{,}0 \times 10^{3}$
Zn	**Arenoso**	22	$2{,}0 \times 10^{2}$	3	$1{,}1 - 3{,}6 \times 10^{4}$	17	$1{,}1 \times 10^{2}$	23	$9{,}0 \times 10^{-1}$ - $2{,}8 \times 10^{4}$
	Franco	12	$1{,}3 \times 10^{3}$	2	$1{,}1 \times 10^{1}$ - $1{,}6 \times 10^{5}$	48	$2{,}4 \times 10^{3}$	4	$2{,}1 \times 10^{2}$ - $1{,}5 \times 10^{5}$
	Arcilloso	23	$2{,}4 \times 10^{3}$	1	$1{,}5 \times 10^{2} - 4{,}0 \times 10^{4}$	8	$2{,}4 \times 10^{3}$	2	$4{,}8 \times 10^{2}$ - $6{,}9 \times 10^{3}$
	Orgánico	8	$1{,}6 \times 10^{3}$	2	$6{,}7 \times 10^{1}$ - $4{,}0 \times 10^{4}$	12	$5{,}6 \times 10^{2}$	8	$9{,}7$ - $7{,}6 \times 10^{3}$
I	**Arenoso**	22	$1{,}0$	2	$1{,}3 \times 10^{-2}$ - $8{,}5 \times 10^{1}$	48	$4{,}1$	7	$1{,}0 \times 10^{-2}$ - $1{,}3 \times 10^{2}$
	Franco	33	$4{,}5$	2	$8{,}2 \times 10^{-2}$ - $2{,}4 \times 10^{2}$	129	$8{,}0$	4	$2{,}0 \times 10^{-2}$ - $5{,}4 \times 10^{2}$
	Arcilloso	8	$1{,}8 \times 10^{2}$	2	$8{,}2 \times 10^{-2}$ - $3{,}3 \times 10^{1}$	19	$1{,}1 \times 10^{1}$	5	$1{,}0$ - $1{,}8 \times 10^{2}$
	Orgánico	9	$2{,}7 \times 10^{1}$	2	$5{,}0 \times 10^{-1}$ - $1{,}5 \times 10^{3}$	11	$3{,}2 \times 10^{1}$	3	$8{,}5$ - $5{,}8 \times 10^{2}$

4.2.2.3. Uranio

La búsqueda bibliográfica consiguió cuadriplicar el número de valores de K_d(U), en comparación con los que se incluyeron en el TRS 364. Los valores de K_d(U) no mostraron ninguna correlación con el contenido de arcilla en los suelos minerales. Debido a la gran variabilidad de los datos, los valores de MG no fueron estadísticamente diferentes en ningún caso. A diferencia de lo observado en el TRS 364, el valor obtenido para los suelos orgánicos fue mayor que para los suelos minerales.

4.2.2.4. Torio

De la misma forma que para el uranio, la nueva revisión de los datos supuso un aumento considerable del número de valores de K_d(Th) con respecto al número de valores presentes en el TRS 364. El hecho de aumentar el número de observaciones no permitió tampoco observar ninguna relación entre las clases texturales y los valores de K_d(Th). A diferencia de lo observado en el TRS 364, el valor estimado máximo no correspondió a los suelos de la clase “Franco”, sino a los suelos orgánicos.

4.2.2.5. Metales pesados

La revisión de los valores de K_d del TRS 364 correspondientes a los metales pesados supuso un claro aumento del número de observaciones estudiadas. A pesar de la gran variabilidad de los intervalos de valores obtenidos, las nuevas MG sí que aumentaron sistemáticamente con el aumento del contenido en arcillas, a diferencia de lo que se observaba en los valores de MG del TRS 364. Este hecho, observado por ejemplo para Co, Ni y Pb, sugiere que las nuevas MG son más representativas que las anteriores del TRS 364.

4.2.2.6. Radioyodo

Por lo que concierne al radioyodo, la revisión de la K_d(I) también permitió disponer de una base de datos muy superior a la anterior del TRS 364. Las nuevas MG mostraron una tendencia ascendente gradual con el contenido de arcillas, aunque el hecho más destacable fue que el mayor valor de MG correspondió a los suelos orgánicos, a diferencia de lo observado con los valores del TRS 364.

4.2.2.7. Miscelánea de radionucleidos

Si se compara la nueva base de datos creada con la anterior del TRS 364 en referencia a otros radionucleidos, no se encontró nueva información disponible para radioisótopos de algunos elementos (Ac, Br, Ho, Pa, Rb, Si y Sm), y por lo tanto los datos presentados en la Tabla 9 de la **Publicación 4** se corresponden con los datos del documento original. Para un determinado número de elementos (Ag, Be, Bi, Hf, Mo, P, Pd, Sn y Ta), se encontró un número muy reducido de nuevos datos, con lo que para el cálculo de las nuevas MG e intervalos de valores también se incluyó los valores previos del TRS 364. Por el contrario, se encontraron algunos datos para elementos no considerados en el previo TRS 364 (As, Ba, Cl, Cu, Dy, Ga, H, Hg, In, Ir, K, La, Lu, Mg, Na, Pm, Pt, Rh, Sc, Tb, Te, Tm, V e Y), que se incluyeron en esta revisión, aunque en algún caso los datos sólo procedieron de una única referencia.

Para un gran número de radionucleidos fue muy complicado obtener valores de MG para todas las clases, como por ejemplo el Np o el Tc, para los cuales sólo se propuso un valor distinto para suelos orgánicos y minerales.

En algunos casos, la inclusión de nuevos datos provocó un gran cambio en el valor de la MG, en comparación con la propuesta en el previo TRS 364, en parte debido al hecho de que los criterios de aceptación de datos para la nueva base de datos fueron mucho más estrictos que los aplicados en el TRS 364, en el que en algunos casos se aceptaron datos para sedimentos o de fases puras minerales. Las discrepancias más importantes se observaron habitualmente en las clases “Arcilloso” y “Orgánico”, para un número significativo de radionucleidos (por ejemplo, Ag, Ce, Cm, Fe, Mn, Np y Zr), en los cuales el valor previo de la MG pasó a ser el valor máximo de los nuevos intervalos obtenidos, hecho que provocó que la nueva MG fuera claramente menor. Por último, en especial para aquellos casos con un número muy reducido de observaciones, se sospechó de algún error en la confección en la base de datos del TRS 364 para ciertos radionucleidos, como fue el caso del Ru, para el que el valor estimado para suelos orgánicos (66 000 L/kg) debería ser utilizado con cautela.

4.2.3. Uso de otros parámetros como criterios de agrupamiento

Tal y como se puede observar en la Tabla 4.3, al realizar la clasificación de los valores de K_d siguiendo el criterio de textura/materia orgánica, se obtuvieron valores de MG con un mayor sentido químico a partir del conocimiento previo del que se disponen de los mecanismos de interacción de ciertos radionucleidos en suelos. Con todo, los intervalos de valores llegaron a ser de varios órdenes de magnitud, debido a la gran variabilidad de resultados existentes dentro de cada clase del agrupamiento.

Además de la variabilidad inherente a este parámetro, y la originada por las diferentes condiciones experimentales aplicadas para su obtención, se hizo la hipótesis que con criterios de agrupamiento más ajustados a los mecanismos de interacción la variabilidad se vería reducida. Con esta finalidad, se decidió agrupar los valores de K_d en función de aquellas propiedades edáficas específicas, llamadas también *cofactores,* que se había demostrado previamente que intervenían significativamente en los procesos de sorción de algunos radionucleidos. En cada caso, se examinó con detalle los valores frontera de las nuevas categorías de agrupamiento, que se establecieron con la idea de mantener un número de observaciones alto pero que ayudaran a disminuir la variabilidad del valor de la K_d, con el objeto de poder proponer un valor de MG que reflejara y describiera mucho mejor la sorción.

La Tabla 4.4 muestra, para aquellos radionucleidos en los que fue posible realizar la reagrupación de las K_d en función de cofactores de interacción, los valores de la media geométrica (MG), la desviación estándar geométrica (DEG) y los intervalos obtenidos, así como el número de datos (n) que han sido considerados para su cálculo.

4.2.3.1. Radioestroncio

La reagrupación de los datos de K_d(Sr) se hizo siguiendo la información de los mecanismos que rigen su interacción, pero a dos niveles, en función de la información disponible. Por un lado, se realizó la agrupación según el valor de la capacidad de intercambio catiónico (CIC) que presentan los suelos. Esto supuso disminuir el número de observaciones de 255 (para el caso del criterio textura/materia orgánica) a 201. En este caso, se observó que la variabilidad de los intervalos no mejoraba respecto al

Tabla 4.4. Agrupación de los valores de K_d según el criterio de cofactores.

	Clases	n	MG	DEG	Min - Max
Sr	CIC < 10	50	$2{,}1 \times 10^{1}$	4	$4{,}0 \times 10^{-1}$ - $3{,}3 \times 10^{2}$
	10 < CIC < 20	44	$2{,}0 \times 10^{1}$	2	$3{,}3 \times 10^{1}$ – $4{,}6 \times 10^{2}$
	20 < CIC < 50	82	$6{,}2 \times 10^{1}$	2	1,0 – $6{,}5 \times 10^{3}$
	CIC > 50	25	$9{,}4 \times 10^{1}$	6	5,0 – $1{,}8 \times 10^{3}$
	CIC/M_{ss} < 15	25	4,0	2	4,0 – $1{,}5 \times 10^{1}$
	$15 < CIC/M_{ss} < 150$	28	$2{,}2 \times 10^{1}$	3	4,0 – $1{,}1 \times 10^{2}$
	$150 < CIC/M_{ss} < 500$	18	$1{,}7 \times 10^{2}$	2	$7{,}7 \times 10^{1}$ – $2{,}7 \times 10^{2}$
	CIC/M_{ss} > 50	25	$3{,}2 \times 10^{2}$	2	$8{,}1 \times 10^{1}$ – $1{,}8 \times 10^{3}$
Cs	RIP_K < 150	47	$7{,}4 \times 10^{1}$	2	$1{,}0 \times 10^{1}$ – $7{,}3 \times 10^{2}$
	$150 < RIP_K < 1000$	78	$3{,}2 \times 10^{2}$	6	$1{,}0 \times 10^{1}$ – $3{,}4 \times 10^{4}$
	$1000 < RIP_K < 2500$	72	$2{,}4 \times 10^{3}$	4	$6{,}2 \times 10^{1}$ – $9{,}5 \times 10^{4}$
	RIP_K > 2500	60	$7{,}2 \times 10^{3}$	4	$2{,}2 \times 10^{2}$ – $3{,}8 \times 10^{5}$
	RIP_K/K_{ss} > 100	37	$8{,}5 \times 10^{1}$	3	$1{,}0 \times 10^{1}$ – $7{,}0 \times 10^{2}$
	$100 < RIP_K/K_{ss} < 1000$	85	$2{,}4 \times 10^{2}$	5	$2{,}0 \times 10^{1}$ – $5{,}8 \times 10^{3}$
	$1000 < RIP_K/K_{ss} < 10000$	78	$2{,}0 \times 10^{3}$	4	$6{,}2 \times 10^{1}$ – $3{,}4 \times 10^{4}$
	RIP_K/K_{ss} > 10000	57	$9{,}9 \times 10^{3}$	4	$2{,}2 \times 10^{2}$ – $3{,}8 \times 10^{5}$
U	pH < 5	36	$7{,}1 \times 10^{1}$	11	$7{,}0 \times 10^{-1}$ – $6{,}7 \times 10^{3}$
	5 ≤ pH 7	78	$7{,}4 \times 10^{2}$	8	$2{,}6$ – $6{,}7 \times 10^{4}$
	pH ≥ 7	60	$6{,}8 \times 10^{1}$	8	$9{,}0 \times 10^{-1}$ – $6{,}2 \times 10^{3}$
Th	3 ≤ pH < 5	11	$1{,}3 \times 10^{3}$	15	$1{,}9 \times 10^{1}$ – $1{,}0 \times 10^{4}$
	5 < pH < 8	26	$3{,}3 \times 10^{3}$	8	$1{,}0 \times 10^{2}$ – $1{,}0 \times 10^{5}$
	8 < pH ≤ 10	6	$3{,}1 \times 10^{2}$	7	$3{,}5 \times 10^{1}$ – $3{,}2 \times 10^{3}$
Pb	3 ≤ pH < 6,4	13	$5{,}7 \times 10^{2}$	6	$2{,}5 \times 10^{1}$ – $6{,}2 \times 10^{3}$
	6,4 < pH ≤ 8,3	8	$7{,}9 \times 10^{3}$	7	$3{,}0 \times 10^{2}$ – $1{,}3 \times 10^{5}$
Cd	pH < 5	8	$1{,}1 \times 10^{1}$	3	2,0 – $6{,}4 \times 10^{1}$
	5 ≤ pH 6,5	11	$1{,}8 \times 10^{1}$	4	6,2 – $2{,}5 \times 10^{2}$
	pH ≥ 6,5	24	$3{,}8 \times 10^{2}$	6	3,7 – $4{,}4 \times 10^{3}$
Co	pH < 5	21	$1{,}2 \times 10^{1}$	5	2,0 – $1{,}5 \times 10^{2}$
	5 ≤ pH 6,5	50	$1{,}1 \times 10^{3}$	5	$2{,}0 \times 10^{1}$ – $9{,}9 \times 10^{4}$
	pH ≥ 6,5	26	$4{,}6 \times 10^{3}$	4	$5{,}5 \times 10^{2}$ – $1{,}0 \times 10^{5}$
Ni	pH < 5	10	$1{,}5 \times 10^{1}$	2	3,0 – $4{,}8 \times 10^{1}$
	5 ≤ pH 6,5	22	$5{,}8 \times 10^{1}$	4	7,0 – $1{,}1 \times 10^{3}$
	pH ≥ 6,5	30	$8{,}2 \times 10^{2}$	4	$4{,}0 \times 10^{1}$ – $7{,}3 \times 10^{3}$
Zn	pH < 5	9	8,0	8	$0{,}9 \times 10^{-1}$ – $3{,}0 \times 10^{2}$
	5 ≤ pH 6,5	49	$1{,}6 \times 10^{3}$	6	6,2 – $3{,}0 \times 10^{4}$
	pH ≥ 6,5	17	$4{,}3 \times 10^{3}$	4	$4{,}4 \times 10^{2}$ – $1{,}5 \times 10^{5}$
I^-	MO < 2	49	1,0	6	$1{,}0 \times 10^{-2}$ – $2{,}5 \times 10^{1}$
	2 ≤ MO < 5	60	8,0	3	$6{,}0 \times 10^{-1}$ – $1{,}3 \times 10^{2}$
	5 ≤ MO < 10	16	$1{,}6 \times 10^{1}$	4	2,0 – $2{,}6 \times 10^{2}$
	MO ≥ 10	14	$3{,}7 \times 10^{1}$	4	8,0 – $5{,}8 \times 10^{2}$
IO_3^-	MO < 2	18	4,0	5	$4{,}0 \times 10^{-1}$ – $5{,}7 \times 10^{1}$
	2 ≤ MO < 5	35	8,0	3	2,0 – $5{,}3 \times 10^{2}$
	5 ≤ MO < 10	9	$1{,}7 \times 10^{1}$	3	4,0 – $1{,}3 \times 10^{2}$
	MO ≥ 10	5	$2{,}6 \times 10^{1}$	2	$1{,}0 \times 10^{1}$ – $8{,}6 \times 10^{1}$

criterio textura/materia orgánica, y que incluso empeoraba en algún caso, tal como se observa de la comparación con los valores de la DEG o de Min-Max de la Tabla 4.3, o en la Figura 1 de la **Publicación 2**. Este hecho indicó que aunque existía una relación entre el valor de la CIC y la K_d(Sr), evidenciado por los mayores valores de K_d(Sr) al aumentar la CIC, este factor era insuficiente para explicar la variabilidad de la K_d(Sr). Por el contrario, al agrupar los suelos a partir del ratio obtenido entre la CIC y la suma de concentraciones de Ca y Mg en la solución de contacto ($CIC/(Ca+Mg)_{ss}$), aunque se redujo el número de datos a 96, se obtuvieron unos valores de MG con una variabilidad mucho más baja (valores de DEG de 2), indicando que el cofactor propuesto es mejor que el criterio textura/materia orgánica para agrupar los suelos, y confirmando la relación existente entre este ratio y el valor de la K_d(Sr).

4.2.3.2. Radiocesio

El reagrupamiento de los datos de K_d(Cs) también se abordó en dos etapas, en función de la información disponible. El primero sería a partir del parámetro específico de su interacción en suelos, como es el RIP_K. En este caso el número de observaciones decreció de 469 a 257, pero la K_d(Cs) mostró un aumento consistente con el aumento del valor del RIP_K, con variabilidades reducidas respecto al anterior criterio. El segundo nivel de agrupamiento consistió en utilizar la relación entre el RIP_K y la concentración de K en la solución de contacto (RIP_K/K_{ss}), que permitió obtener unos intervalos de valores de K_d(Cs) con una variabilidad aún más baja (en especial, al comparar los valores mínimo y máximo), indicando que el cofactor propuesto permite proponer estimadores de los valores de K_d(Cs) mucho más representativos y que describan de forma más correcta la interacción de este radionucleido en suelos.

4.2.3.3. Uranio

Tal como se describe en la **Publicación 3**, la química del uranio en solución es muy compleja, y su sorción dependerá de su especiación en función del pH, la concentración de carbonatos y el contenido de materia orgánica. En cualquier caso, el criterio de agrupar en función de la textura no es conveniente para este radionucleido, con valores de MG para cada una de las clases que no fueron estadísticamente diferentes entre sí y que no siguieron ninguna relación con el incremento en el contenido de arcillas. Por ello se planteó un reagrupamiento en función del pH, cuya

influencia sobre el comportamiento en solución del uranio está ampliamente confirmada. Los nuevos valores de MG sí que respondieron a la variación del pH, con un valor mayor de K_d(U) en el intervalo de pH 5-7. Los valores para cada clase aún mostraron una gran variabilidad, lo que sugirió que un reagrupamiento univariante como el aquí sugerido era aún insuficiente para este tipo de radionucleido.

4.2.3.4. Torio

Como los valores de K_d(Th) no presentan ninguna correlación con la textura, y sabiendo que la química del Th es muy parecida a la del uranio, se planteó reagrupar los valores de K_d(Th) también en función del pH. Las MG obtenidas fueron similares en cada uno de los intervalos de pH propuestos, presentando en todos ellos unos valores altos, de acuerdo con los intervalos de valores obtenidos. De la misma forma que para el uranio, se recomienda realizar un reagrupamiento en base a más variables.

4.2.3.5. Metales pesados

A pesar de la mejora que supuso la revisión efectuada respecto a los datos inicialmente incluidos en el documento TRS 364, para algunos metales pesados (por ejemplo, Cd y Zn) no se evidenció que la textura y el contenido de arcillas jugaran un papel relevante en la variación de sus K_d. Por ello, se realizó una nueva clasificación siguiendo un criterio de agrupación basado en el pH, ya que numerosos estudios demuestran que los valores de las K_d de metales pesados dependen de variaciones de esta variable. Tal como muestra la Tabla 4.4, con la aplicación de este criterio que diferencia la sorción a pH ácidos, a pH cercanos a la neutralidad, y a pH básicos (excepto para el Pb, para el que el menor número de observaciones aconsejó crear sólo dos categorías), las K_d mostraron un incremento continuo en función del aumento del pH. Además, la variabilidad de los valores de K_d para cada clase, cuantificada por la DEG, disminuyó drásticamente con este criterio.

4.2.3.6. Radioyodo

Como también se ha observado para otros radionucleidos, la sorción de radioyodo muestra una dependencia multivariante con ciertas propiedades edáficas. Como se deriva de la revisión efectuada, la K_d(I) mostró una dependencia significativa con el contenido de materia orgánica, ya que la K_d(I) fue significativamente mayor para los

suelos orgánicos. Este hecho justificó utilizar un criterio de clasificación basado exclusivamente en el contenido de materia orgánica. De forma complementaria, se agruparon los datos en función del estado de oxidación, ya que algunos estudios apuntan a un rol del potencial redox y de la especiación de yodo en su sorción. Tal como muestran los datos de la **Publicación 4**, resumidos aquí en la Tabla 4.4, mientras que se confirmó el rol directo del contenido de la materia orgánica en los valores de la K_d(I), con una mucha menor variabilidad en los valores que la cuantificada en función del criterio anterior, el rol del estado de oxidación y de la especie química involucrada en la cuantificación de la K_d(I) fue despreciable.

4.2.4. Dependencia de la K_d con parámetros de suelo

El estudio anterior demostró que la utilización de propiedades edáficas específicas o cofactores permitió proponer valores estimados de los valores de K_d más representativos y reducir la variabilidad de los intervalos de K_d respecto a la derivada de aplicar el criterio de clasificación por textura/materia orgánica. Con todo, los valores de MG obtenidos a partir de los criterios de agrupamiento sólo permiten proponer un único valor de K_d para aquellos suelos que tengan valores dentro de una categoría determinada. Por consiguiente, el siguiente paso necesario es poder estimar un valor de la K_d a partir de valores individuales de las propiedades edáficas que rigen la interacción de los radionucleidos en suelos. La predicción de los valores individuales de K_d podría llevarse a cabo si las propiedades utilizadas para clasificar las K_d explicaran un porcentaje de varianza de los datos suficientemente alto. Por lo tanto, es necesario examinar las correlaciones uni o multivariantes entre las propiedades edáficas utilizadas como cofactores y las K_d de los radionucleidos correspondientes para comprobar si es posible proponer valores individuales de K_d de ciertos radionucleidos a partir de valores de parámetros que pudieran ser determinados en análisis de rutina.

La Tabla 4.5 muestra las correlaciones obtenidas entre los valores de K_d y las propiedades edáficas específicas de diversos radionucleidos. Los datos de esta tabla se nutren de la información recogida en las **Publicaciones 2, 3 y 4**. Exceptuando el caso del radiocesio, en el que es necesario el cálculo del RIP_K, el resto de propiedades edáficas utilizadas en las correlaciones son de fácil obtención, tal como el pH, el

Tabla 4.5. Correlaciones entre las K_d para una serie de radionucleidos y propiedades edáficas que afectan su sorción (n= nº de observaciones).

Radionucleido	Regresión	n	% varianza
Sr	$\log K_d = -0{,}05 + 0{,}86 \times \log (CEC/(Ca+Mg)_{ss})$	96	90
Cs	$\log K_d = 0{,}30 + 0{,}94 \times \log RIP_K$	257	54
	$\log K_d = 0{,}10 + 0{,}98 \times \log RIP_K - 0{,}53 \times \log K_{ss}$	257	70
	$\log K_d = 0{,}94 \times \log(RIP_K / K_{ss})$	257	65
Uranio (pH > 5,5)	$\log K_d = 7{,}7 - 0{,}8 \times pH$	110	30
Uranio (pH < 5,5)	$\log K_d = -0{,}7 + 0{,}50 \times pH$	64	21
Pb	$\log K_d = 1{,}2 + 0{,}37 \times pH$	21	52
Po	$\log K_d = 0{,}2 + 0{,}3 \times pH$	42	18
	$\log K_d = 1{,}9 + 0{,}03 \times$ Arcilla	40	24
Ra	$K_d = -0{,}64 + 0{,}71 \times CIC$	8	30
	$K_d = -27 + 27 \times MO$	8	40
Cd	$\log K_d = 0{,}8 + 0{,}21 \times pH$	55	13
	$\log K_d = -0{,}1 + 0{,}34 \times pH + 0{,}4 \times \log MO$	54	24
Cd (Suelos minerales)	$\log K_d = -0{,}7 + 0{,}41 \times pH$	43	49
Co	$\log K_d = -0{,}7 + 0{,}63 \times pH$	113	56
	$\log K_d = -1{,}5 + 0{,}74 \times pH + 0{,}5 \times \log MO$	110	59
Co (Suelos minerales)	$\log K_d = -1{,}2 + 0{,}71 \times pH$	97	58
Cr (VI)	$\log K_d = 4{,}7 - 0{,}52 \times pH$	12	78
Cu (Suelos minerales)	$\log K_d = -3 + 0{,}8 \times pH$	5	88
Ni	$\log K_d = 0{,}1 + 0{,}34 \times pH$	58	46
	$\log K_d = -1{,}6 + 0{,}55 \times pH + 0{,}27 \times \log$ Arcilla	38	67
	$\log K_d = -0{,}7 + 0{,}41 \times pH + 0{,}7 \times \log MO$	58	70
Ni (Suelos minerales)	$\log K_d = -0{,}6 + 0{,}43 \times pH$	51	66
	$\log K_d = -1{,}6 + 0{,}55 \times pH + 0{,}27 \times \log$ Arcilla	38	67
	$\log K_d = -0{,}9 + 0{,}45 \times pH + 0{,}6 \times \log MO$	51	74
Zn	$\log K_d = -0{,}1 + 0{,}52 \times pH$	88	30
	$\log K_d = -1{,}0 + 0{,}6 \times pH + 0{,}5 \times \log MO$	86	35
Zn (Suelos minerales)	$\log K_d = -1{,}2 + 0{,}71 \times pH$	75	47
	$\log K_d = -1{,}8 + 0{,}8 \times pH + 0{,}5 \times \log MO$	73	50
$IO_3^- + I^-$	$\log K_d = 0{,}63 + 0{,}6 \times \log MO$	227	30
	$\log K_d = -1{,}4 + 0{,}6 \times \log Fe$	124	18
	$\log K_d = -0{,}6 + 0{,}7 \times \log MO + 0{,}3 \times \log Fe$	124	39
I^-	$\log K_d = 0{,}6 + 0{,}6 \times \log MO$	139	33
	$\log K_d = -2{,}8 + 0{,}9 \times \log Fe$	62	32
	$\log K_d = -1{,}5 + 0{,}7 \times \log MO + 0{,}5 \times \log Fe$	62	53
IO_3^-	$\log K_d = 0{,}64 + 0{,}6 \times \log MO$	67	19
	$\log K_d = -1{,}6 + 0{,}6 \times \log Fe$	61	19
	$\log K_d = -0{,}8 + 0{,}5 \times \log MO + 0{,}4 \times \log Fe$	61	30

MO (% materia orgánica); ss (solución de contacto)

contenido de arcillas, de materia orgánica o de Fe, o la concentración de cationes en la solución de contacto.

Los porcentajes de varianza explicados por algunas correlaciones fueron óptimos en algunos casos, como el radioestroncio, algunos metales pesados (por ejemplo, Ni y Cu en suelos minerales) y radiocesio. Aunque los valores de K_d deducidos de ciertas correlaciones sean un avance respecto de los valores estimados por las MG obtenidas tras la aplicación de los criterios de agrupación descritos en los apartados anteriores, se confirma que la predicción de los valores de la K_d a partir de correlaciones univariantes o bivariantes comporta aún incertidumbres significativas, aunque sean en algunos casos inferiores a las aportadas por otros tipos de información requeridos también por los modelos de predicción de riesgo.

4.3

Predicción de la K_d: modelos mecanísticos y modelos multivariantes blandos

La sección anterior mostró la dificultad en la predicción de valores individuales de K_d de un radionucleido en un suelo, debido a la limitación en la variabilidad descrita por las correlaciones entre la K_d y las propiedades del suelo. Aún así, para ciertos radionucleidos (como es el caso de radioestroncio y radiocesio) pareció posible llevar a cabo este ejercicio de predicción ya que el porcentaje de varianza explicado fue relativamente alto en algunos casos. Es por esto que la predicción de las K_d de estos dos radionucleidos podría realizarse a partir de proponer modelos mecanísticos o duros (*hard-modelling*) basados en el conocimiento de los mecanismos implicados en su sorción en suelos. Por otro lado, es de interés completar esta aproximación con el uso de modelos multivariantes blandos (*soft-modelling*) basados en herramientas quimiométricas, tales como la regresión por mínimos cuadrados parciales (*Partial Least Squares,* PLS) y que no presuponen a priori ninguna correlación entre las propiedades edáficas y la K_d.

Las **Publicaciones 5 y 6** describen la construcción, validación y comparación de los modelos mecanísticos y los multivariantes blandos a partir de los datos obtenidos en la **Publicación 1**, con el objetivo de predecir los valores de la K_d para radioestroncio y radiocesio y así comprobar la flexibilidad y limitaciones de los modelos al ser aplicados a suelos con propiedades edáficas diferentes, y de esta forma evaluar y comparar las ventajas y desventajas de ambos modelos de predicción.

4.3.1. Uso de modelos mecanísticos para la predicción de los coeficientes de distribución de radioestroncio y radiocesio

4.3.1.1 Caso de radioestroncio

Tal como se ha descrito anteriormente, la sorción del radioestroncio está íntimamente relacionada con el contenido de materia orgánica y arcillas. La sorción de radioestroncio se produce en los sitios de intercambio regular (*Regular Exchangeable Sites,* RES), que son los responsables de la capacidad de intercambio catiónico (CIC) de un suelo. Además, la sorción de radioestroncio se ve afectada por la presencia de elementos competitivos, mayoritarios en un suelo, como son Ca y Mg. Este conocimiento permite predecir el valor de $K_d(Sr)$ a partir de la relación entre la suma de concentraciones de Ca y Mg en el complejo de intercambio y la suma de las concentraciones de estos mismos iones en la solución de contacto, pero corrigiendo la contribución de Ca por el coeficiente de selectividad Ca-Mg ($K_C(Ca/Mg)$), tal como muestra la siguiente expresión:

$$K_d(Sr) = \frac{Ca_{exch} + Mg_{exch}}{K_c(Ca/Mg)\cdot Ca_{ss} + Mg_{ss}} \cdot K_C\left(Sr/Ca,Mg\right) \qquad \text{[Ec. 4.1]}$$

Tal como se muestra en la **Publicación 5**, esta ecuación es fácilmente simplificable a partir de ciertas asunciones, tal como la proximidad de los valores de los coeficientes de selectividad Sr/Ca, Sr/Mg y Ca/Mg a la unidad, o el hecho de que para suelos con el complejo de intercambio saturado, la suma de Ca y Mg intercambiables es similar al valor de la CIC, con lo que la ecuación 4.1 puede tomar la siguiente forma:

$$K_d(Sr) = \frac{CIC}{Ca_{ss} + Mg_{ss}} \qquad \text{[Ec. 4.2]}$$

La Tabla 4.6 lista las correlaciones obtenidas en los dos casos con la base de datos global obtenida en el marco de la **Publicación 1**, mientras que las Figuras 4.7a y 4.7b muestran la predicción de los valores de $K_d(Sr)$ para los 60 escenarios estudiados. Los dos modelos tuvieron una pendiente cercana a la unidad (lo que indicó ausencia de sesgo en la predicción global) y un coeficiente correlación suficientemente alto de forma que el porcentaje de varianza explicado fue próximo al 75% o superior.

Tabla 4.6. Correlaciones entre los valores de K_d(Sr) experimentales y los predichos.

	Correlación	r	% varianza
Modelo Ecuación 4.1	$\log K_d(Sr)_{exp} = 1{,}07 \log K_d(Sr)_{pred}$	0,86	74
Modelo Ecuación 4.2	$\log K_d(Sr)_{exp} = 1{,}01 \log K_d(Sr)_{pred}$	0,92	85

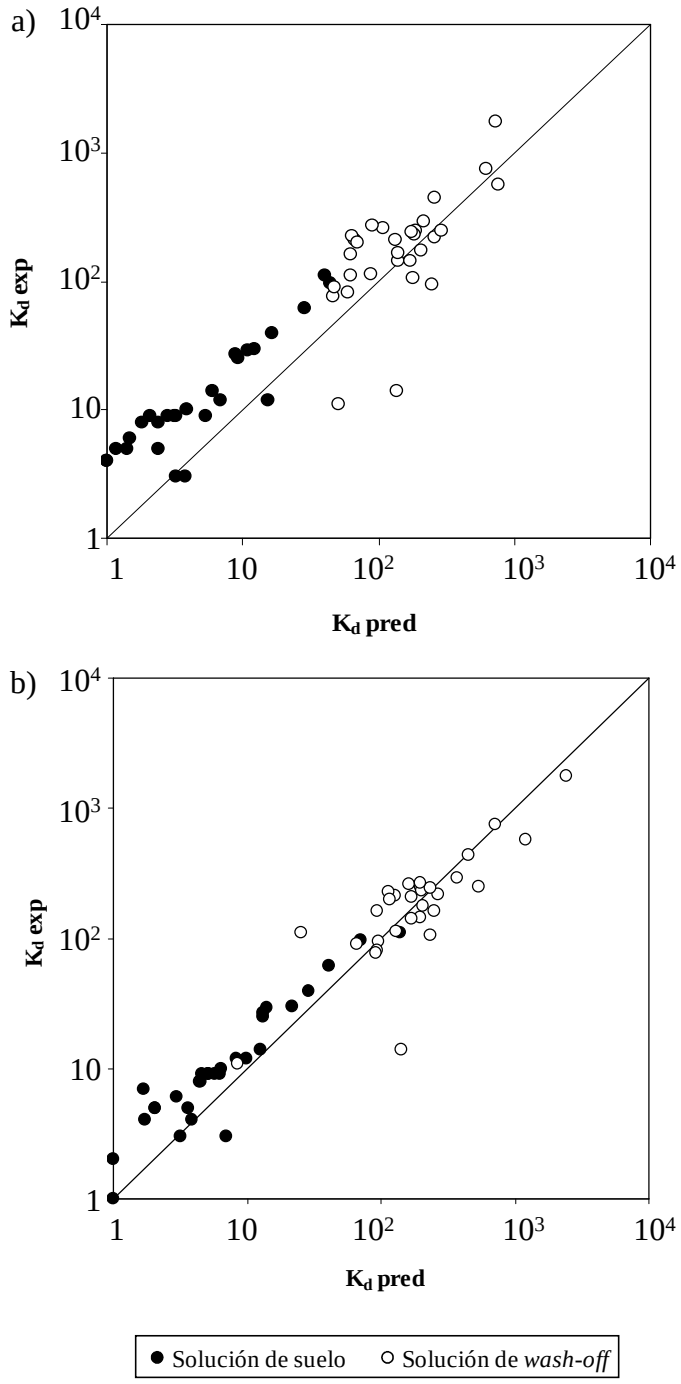

Figura 4.7. Correlación entre los valores de K_d(Sr) experimental y predicho utilizando (a) la ecuación 4.1, y (b) la ecuación 4.2.

4.3.1.2 Caso de radiocesio

4.3.1.2.1. Modelos mecanísticos basados en la predicción de K_d(Cs) a partir de RIP_K

Tal como se describe en la **Publicación 6**, el modelo mecanístico más complejo para radiocesio incluye distinguir dos conjuntos de sitios, los RES y los extremos expandidos de los aluminosilicatos (*Frayed Edge Sites*, FES), siendo estos últimos los que gobiernan la sorción de radiocesio en suelos con un contenido suficiente de estos minerales. En este contexto, el valor de K_d(Cs) global se puede predecir a partir del parámetro RIP_K, de las concentraciones de especies competitivas de Cs en la solución de contacto (K, NH_4 y Na) y en el complejo de intercambio catiónico, según muestra la ecuación 4.3, donde K_c^{FES}(X/Y) es el coeficiente de selectividad entre dos especies X e Y en los FES:

$$K_d(Cs) = K_d^{FES}(Cs) + K_d^{RES}(Cs) = \\ = \frac{RIP_K}{K_{ss} + K_C^{FES}(NH_4/K)\cdot NH_{4,ss} + K_C^{FES}(Na/K)\cdot Na_{ss}} + \frac{K_{exch} + NH_{4,exch} + Na_{exch}}{K_{ss} + NH_{4,ss} + Na_{ss}} \qquad \text{[Ec. 4.3]}$$

Para aplicar este modelo es necesario obtener los K_c^{FES} de Na/K y NH_4/K, ya que no son valores que se puedan derivar directamente de los datos obtenidos en la **Publicación 1**. Mientras que estudios anteriores (Wauters, 1996a) demuestran que el rol de Na es poco relevante, y que además el valor de K_C^{FES}(Na/K) es pequeño (puede tomarse un valor de 0,02), el consenso sobre el valor de K_C^{FES}(NH_4/K) es más complejo, y afecta de forma importante el valor de K_d^{FES}(Cs) al amplificar la concentración de amonio. Tal como recoge la **Publicación 6**, en el marco de esta Tesis Doctoral se obtuvo el valor de K_C^{FES}(NH_4/K) de dos formas diferentes: a partir de la relación RIP_K/RIP_{NH4} y a partir de evaluar la disminución de la K_d(Cs) al aumentar la concentración de NH_4, en escenarios con igual concentración de Ca y de K (experimentos en escenarios mixtos).

La ecuación 4.3, aparentemente compleja, puede ser simplificada en función de hipótesis que se han mostrado como representativas de muchos casos ambientales y que pueden hacerse de forma secuencial o incluso simultánea: contenido despreciable de Na en la mayoría de suelos; substitución de la K_C^{FES}(NH_4/K) por un valor fijo, ya propuesto en algunos estudios anteriores (valor próximo a 5) (Sweeck, 1990); y

contenido despreciable de NH_4, en el supuesto que su concentración será significativa sólo en suelos con un contenido alto de materia orgánica o expuestos a condiciones anóxicas. Con la aplicación de todas estas hipótesis, la ecuación 4.3 toma la siguiente forma:

$$K_d(Cs) = K_d^{FES}(Cs) + K_d^{RES}(Cs) = \frac{RIP_K}{K_{ss}} + \frac{K_{exch}}{K_{ss}} \qquad \text{[Ec. 4.4]}$$

La Tabla 4.7 lista las correlaciones obtenidas con los modelos de las ecuaciones 4.3 y 4.4, a partir de la base de datos global obtenida en el marco de la **Publicación 1**, mientras que las Figuras 4.8a y 4.8b muestran la predicción de los valores de $K_d(Cs)$ para los 60 escenarios estudiados. Dos hechos destacan de las correlaciones obtenidas. Primero, aunque los valores de $K_C^{FES}(NH_4/K)$ obtenidos a partir de la aproximación de escenario mixto fueron sistemáticamente superiores a los obtenidos con la relación RIP_K/RIP_{NH4}, este hecho no afectó de forma significativa la predicción global de los valores de $K_d(Cs)$. En segundo lugar, la comparación entre los dos modelos extremos confirmó lo robusto que es el rol de RIP_K en la predicción de la $K_d(Cs)$ y el efecto prioritario de K sobre NH_4 en suelos minerales, ya que a pesar de todas las simplificaciones, el modelo final fue aún suficientemente bueno, con una pendiente sólo ligeramente inferior a la unidad, y un porcentaje de varianza explicada próximo al 80%.

Tabla 4.7. Correlaciones entre los valores de $K_d(Cs)$ experimentales y predichos.

	Correlación	**r**	**% varianza**
Modelo Ecuación 4.3. K_C^{FES} (NH_4/K) - (RIP_K)	$\log K_d(Cs)_{exp} = 0{,}98 \log K_d(Cs)_{pred}$	0,94	88
Modelo Ecuación 4.3. K_C^{FES} (NH_4/K) - (escenario mixto)	$\log K_d(Cs)_{exp} = 1{,}04 \log K_d(Cs)_{pred}$	0,90	81
Modelo Ecuación 4.4.	$\log K_d(Cs)_{exp} = 0{,}88 \log K_d(Cs)_{pred}$	0,89	79

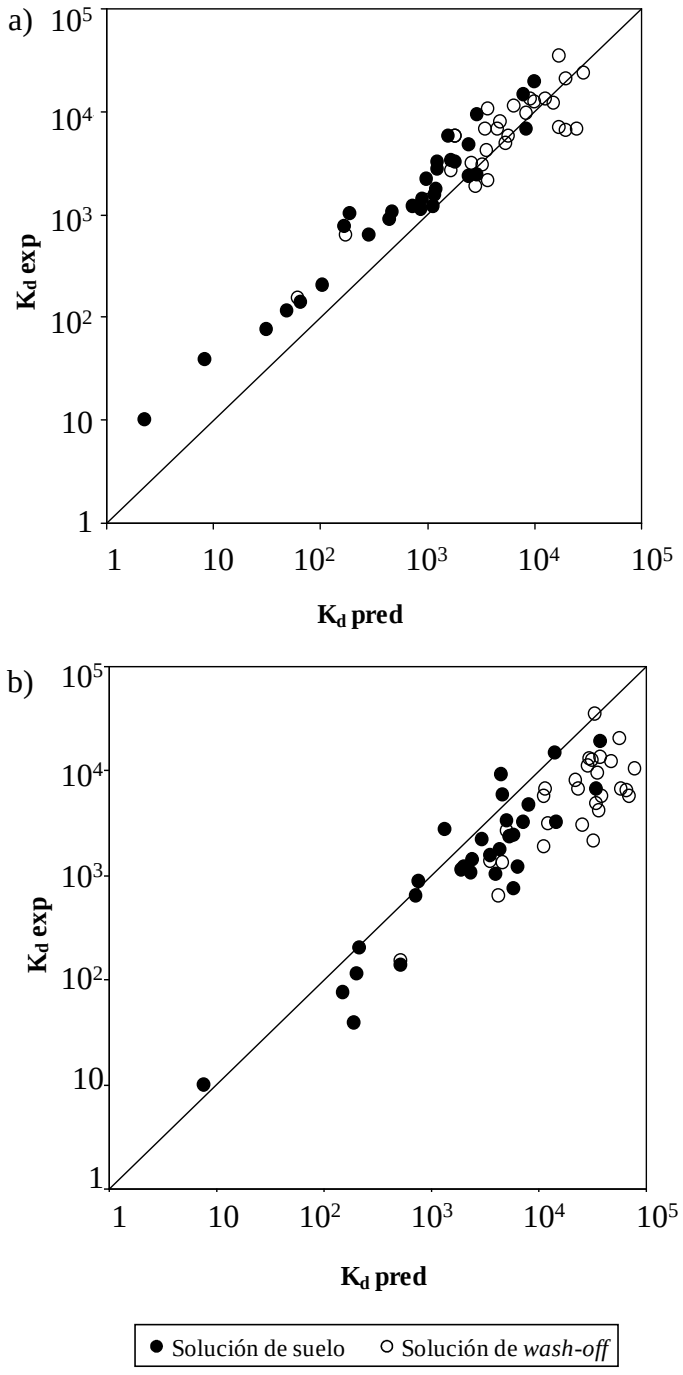

Figura 4.8. Correlación entre los valores de K_d(Cs) experimental y predicha utilizando (a) la ecuación 4.3 (escenario mixto), y (b) la ecuación 4.4.

4.3.1.2.2. Modelos mecanísticos basados en la predicción de RIP_K

La máxima limitación que presenta la aplicación de los dos modelos anteriores (y del resto de modelos mostrados en la **Publicación 6**) es la necesidad de disponer del

valor de RIP_K, que de hecho ya exige el cálculo de una K_d(Cs), aunque en un escenario alejado del contexto medioambiental en el que se pueda encontrar el suelo objeto de estudio. Como el valor de RIP_K está relacionado con la fracción mineral de los suelos, y concretamente con las arcillas, el siguiente paso es plantear si existe correlación posible entre el valor de RIP_K y el contenido y el tipo de arcillas de un suelo.

En este contexto, se realizó la caracterización mineralógica de todos los suelos estudiados mediante la técnica de difracción de rayos X (XRD). Mientras que las Tablas 4.8 y 4.9 muestran las fases cristalinas encontradas en las muestras de suelo, las Figuras 4.9 y 4.10 muestran ejemplos de los difractogramas obtenidos con agregados orientados, con el objeto de poder cuantificar el contenido de varios filosilicatos, y en concreto de los filosilicatos 2:1 (suma de los contenidos de illita, vermiculita y esmectita). En al figura 4.9ª se muestra, como ejemplo, el caso de CABRIL. En el difractograma de la muestra inicial (secada al aire) se observa la presencia de fases cristalinas de illita y caolinita, según los patrones PDF 00-015-0603 y 00-003-0052, respectivamente. La presencia de estos filosilicatos se confirmó según su diferente respuesta tras someter los agregados orientados a un tratamiento con etilenglicol, primero, y a una temperatura de 550 ^oC, posteriormente. Para el caso de la illita, la banda correspondiente a la reflexión de la distancia interlaminar d_{001} (de 9,9 Å, unos 8,9 grados 2θ en las condiciones de medida en las que se obtuvieron los difractogramas) no varia después de los tratamientos, tal como se observa en la Figura 4.9b. En cambio, para el caso de la caolinita, la banda de la reflexión d_{001} (de 7,1 Å, unos 12,5 grados 2θ) permanece igual después de la glicolación, pero desaparece tras el tratamiento térmico, como también se observa en la Figura 4.9b. En el otro ejemplo mostrado (suelo MALAGA) el número de fases cristalinas que se detectó fue superior (ver Figura 4.10a), destacando, además de la presencia de illita y de caolinita, la presencia de otros filosilicatos como vermiculita (PDF 04-013-2154) y esmectita (beidillita: PDF 00-058-2018). Los tratamientos adicionales de los agregados orientados confirmaron la presencia de illita y de caolinita, así como de la esmectita beidillita. Para este último filosilicato 2:1, su banda de la reflexión d_{001} (de 11,8 Å, unos 7,5 grados 2θ) se desplaza a un valor inferior de 2θ tras el tratamiento de glicolación, ya que su d_{001} aumenta hasta 18 Å, mientras que el tratamiento térmico provoca el efecto contrario (disminución de la d_{001} hasta 10 Å) (ver Figura 4.10b).

Tabla 4.8. Análisis mineralógico semicuantitativo de las muestras de suelo (% respecto a materia mineral). Trazas = 1-3%; < 5 = 3-5%.

Suelo	Cuarzo	Feldespatos	Calcita	Dolomita	Yeso	Hornblenda	Actinolita Tremolita	Filosilicatos
ALM	89	4	--	--	--	--	--	7
ANDCOR	<5	10	trazas	--	--	--	55/15	15
ASCO	21	14	31	19	trazas	--	--	14
AYUD	27	<5	14	<5	--	--	--	52
BAD1	68	5,0	--	--	--	--	--	27
BAD2	58	<5	<5	--	--	--	--	35
BILBAO	32	35	--	--	--	--	--	34
CABRIL	26	--	--	--	--	--	--	74
DELTA1	--	trazas	<5	--	trazas	--	--	95
DELTA2	12	trazas	64	6	--	--	--	17
ENUSA	63	20	--	--	--	--	--	17
FONCOR	31	53	---	--	--	--	**--**	16
FROCOR	36	38	--	--	--	5		21
GARONA	32	trazas	40	6	--	--	--	20
GOLOSO	25	67	--	--	--	--	--	8
GRACOR	47	12	--	--	--	<5	--	38
LEON	60	--	--	--	--	--	--	43
MALAGA	18	<5	13	<5	--	--	--	65
OVIO1	47	--	--	--	--	--	--	53
OVIO3	64	--	--	--	--	--	--	36
TENF1	<5	47	--	--	--	--	--	50
TENF2	5	50	--	--	--	--	--	45
TRILLO	20	trazas	49	9	--	--	--	20
UIB	26	9	31	--	--	--	--	34
UPV	<5	trazas	6	65	5	--	--	17
USAL	43	30	trazas	--	--	--	--	25
VAN1	33	22	13	20	--	--	--	11
VAN2	28	trazas	23	16	--	--	--	32
VILCOR	79	trazas	--	--	--	--	--	19
ZORITA	21	20	45	6	--	--	--	8

Tabla 4.9. Análisis mineralógico cuantitativo de los filosilicatos presentes en las muestras de suelo (% respecto a filosilicatos). Trazas = 1-3%; < 5 = 3-5%.

Suelo	Illita	Esmectita	Vermiculita	Caolinita	Clorita	Sepiolita	Observaciones
ALM	62	---	trazas	37	--	--	interestratificado illita/caolinita
ANDCOR	59	---	41	--	--	--	interestratificado vermiculita/illita
ASCO	77	---	trazas	20	trazas	---	interestratificado illita/caolinita
AYUD	88	trazas	--	10	trazas	--	interestratificado illita/caolinita
BAD1	43	39	--	18	--	--	
BAD2	30	56	--	14	--	--	
BILBAO	83	trazas	--	15	--	--	interestratificado vermiculita/illita
CABRIL	89	--	--	11	--	--	
DELTA1	80	--	1	19	--	--	interestratificado vermiculita/illita
DELTA2	68	--	--	32	--	--	
ENUSA	57	trazas	<5	38	--	--	
FONCOR	54	--	5	41	--	--	
FROCOR	57	trazas	4	33	6	--	silice amorfa
GARONA	64	5	--	25	7	--	
GOLOSO	45	18	--	35	--	--	
GRACOR	11	--	4	85	--	--	
LEON	51	--	--	49	--	--	
MALAGA	54	17	--	27	--	--	
OVIO1	23	--	--	77	--	--	silice amorfa
OVIO3	16	--	<5	77	<5	--	
TENF2	2	67	trazas	31	--	--	interestratificado illita/caolinita
TENF1	57	9	<5	31	--	--	interestratificado illita/caolinita
TRILLO	74	--	--	26	--	--	interestratificado illita/caolinita
UIB	81	2	--	17	--	--	interestratificado illita/caolinita
UPV	98	--	--	trazas	--	--	interestratificado illita/esmectita
USAL	41	45	--	14	--	--	
VAN1	77	5	trazas	17	--	--	
VAN2	72	--	trazas	22	<5	--	
VILCOR	42	--	6	46	--	6	
ZORITA	74	--	trazas	26	--	--	interestratificado illita/caolinita

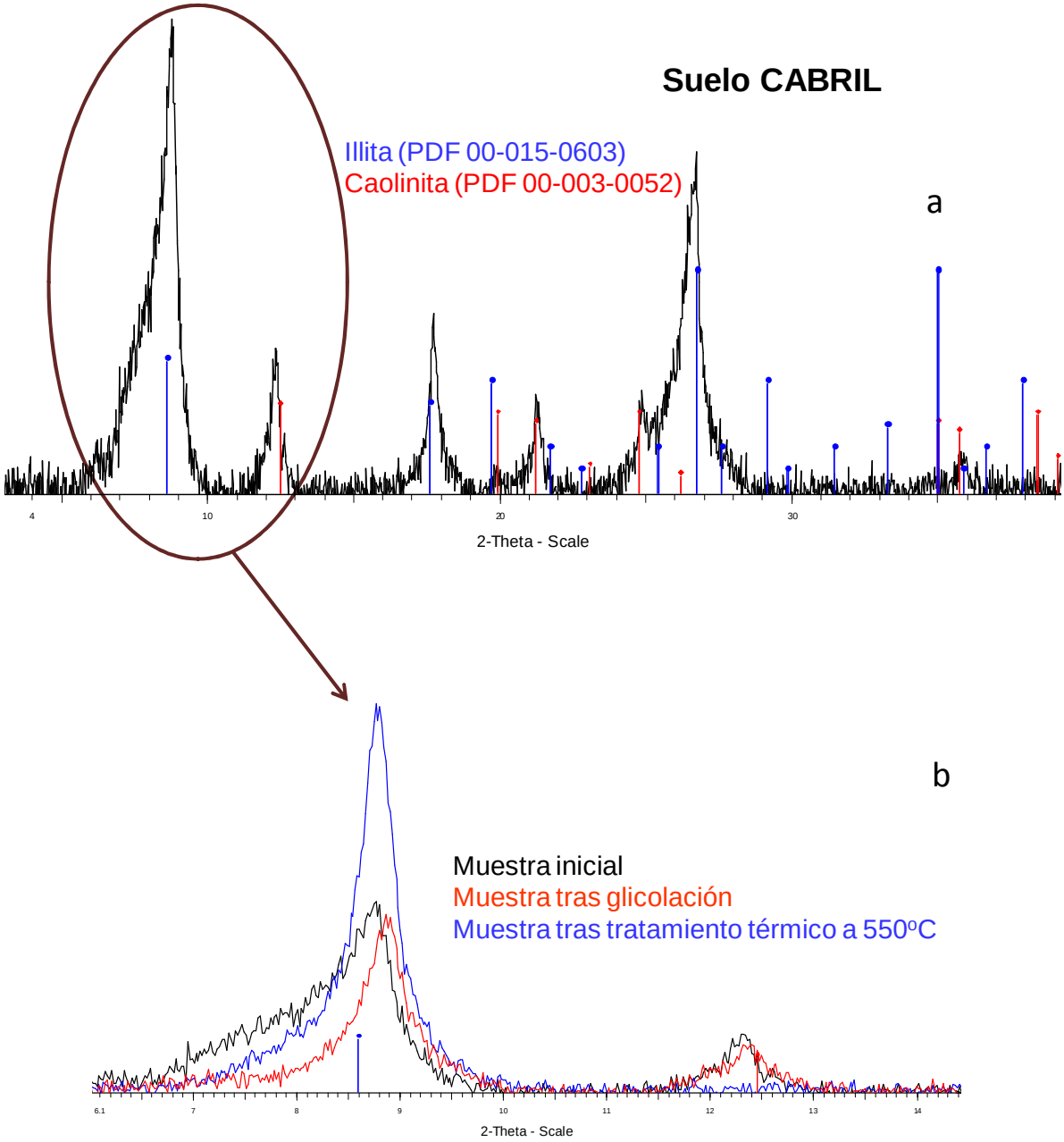

Figura 4.9. Análisis por XRD del suelo CABRIL. (a) Difractograma de la muestra inicial. (b) Ampliación de la zona del difractograma entre los valores 6-14 de la escala de 2θ.

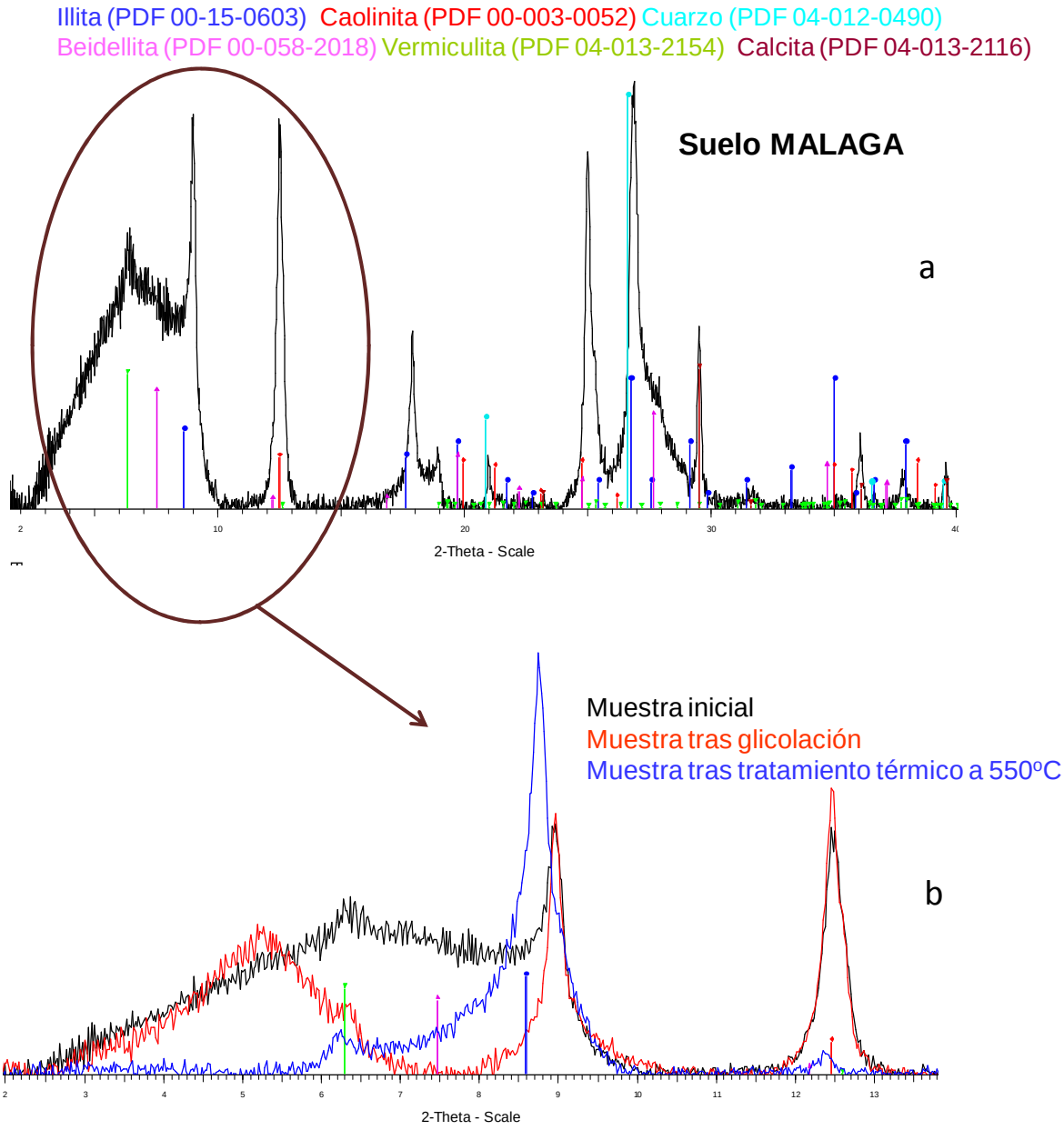

Figura 4.10. Análisis por XRD del suelo MALAGA. (a) Difractograma de la muestra inicial. (b) Ampliación de la zona del difractograma entre los valores 2-14 de la escala de 2θ.

A partir de los datos del contenido de filosilicatos, de filosilicatos 2:1 y del contenido de las fracciones de arcilla y limo derivado del análisis textural, se examinaron las posibles correlaciones entre estas variables y los valores de RIP_K en los 30 suelos examinados. Las correlaciones estadísticamente significativas se incluyen en la Tabla 4.10.

Tal y como podía anticiparse, las correlaciones univariantes que explicaban una mayor varianza fueron con el contenido de filosilicatos y de filosilicatos 2:1. Aunque las pendientes de las correlaciones fueron diferentes, el porcentaje de varianza explicado fue muy similar, ya que ambas variables estaban a su vez correlacionadas. La leve mejora de la correlación con el uso de la variable filosilicatos 2:1 no justifica su obtención para el cálculo del RIP_K, ya que exige un análisis de difracción de rayos X con agregados orientados. Por el contrario, la correlación con el contenido de arcilla derivado del análisis textural (análisis que sí se realiza en rutina) mostró un porcentaje de varianza del RIP_K significativo, superior al 40%. Ninguna correlación múltiple mejoró el porcentaje de varianza explicado, con la excepción de la que utilizó el contenido de filosilicatos con el contenido de limo, también derivado del análisis textural.

Tabla 4.10. Correlaciones entre el RIP_K y variables de suelo relacionadas con las arcillas.

Correlación	r	% varianza
$RIP_K = 92 \cdot$ filosilicatos	0,76	58
$RIP_K = 145 \cdot$ filosilicatos 2:1	0,78	61
$RIP_K = 130 \cdot$ arcilla	0,65	42
$RIP_K = 93 \cdot$ filosilicatos $+ 61 \cdot$ limo $- 1700$	0,86	74

Una vez obtenidas estas correlaciones, es interesante comprobar si pueden ser útiles para predecir los valores experimentales de K_d(Cs). Descartando el uso de los filosilicatos 2:1, la Tabla 4.11 resume las correlaciones obtenidas, en las que los valores de K_d(Cs) predicho se calcularon substituyendo el RIP_K por las correlaciones de la Tabla 4.10. Los resultados mostrados en la Tabla 4.11 muestran que los modelos de predicción empeoraron respecto a los mostrados en la Tabla 4.7. Sin embargo, la calidad de las correlaciones puede ser suficiente para ser usadas en ciertos sistemas de toma de decisión, ya que los errores en la predicción de las K_d(Cs) puede ser del mismo orden de magnitud o inferiores a la estimación de otros parámetros de entrada de estos sistemas. Una correlación basada en el contenido de arcillas del análisis textural, además de explicar un porcentaje alto de varianza, supondría poder predecir la K_d(Cs) en función de parámetros edáficos generales.

Tabla 4.11. Correlaciones entre la K_d(Cs) experimental y la K_d(Cs) predicha.

Modelo predicción RIP_K	Correlación	r	% varianza
Filosilicatos	$\log K_d(Cs)_{exp} = 0,85 \log K_d(Cs)_{pred}$	0,74	55
Arcilla	$\log K_d(Cs)_{exp} = 0,84 \log K_d(Cs)_{pred}$	0,74	55
Filosilicatos + limo	$\log K_d(Cs)_{exp} = 0,86 \log K_d(Cs)_{pred}$	0,62	39

4.3.2. Uso de modelos multivariantes blandos para la predicción de los coeficientes de distribución de radioestroncio y radiocesio

Los modelos multivariantes están basados en técnicas quimiométricas, siendo la regresión de mínimos cuadrados parciales (PLS) el método más extendido. El PLS es un método de correlación multivariante entre una serie de variables de entrada o desctores de las muestras (matriz *X*), que en este caso son las diferentes propiedades edáficas determinadas para cada suelo, y una variable de salida (matriz *y*) que es la variable a predecir, que en nuestro caso es el valor de K_d obtenido experimentalmente.

La construcción del modelo de regresión PLS, $y = XB$, consiste en la creación de un espacio PLS y el cálculo de los coeficientes de regresión (*B*) en este espacio. En este trabajo se utilizó una validación cruzada integral para determinar el número de componentes principales significativos. Este procedimiento se basa en excluir consecutivamente una fila de la matriz *X* y la *y* correspondiente. Para la matriz restante se construye el modelo PLS para varios componentes principales y se usa para predecir el valor de *y* en la muestra excluida. Finalmente se escoge el número de componentes PLS que proporciona un error menor de predicción.

El uso de PLS permite el desarrollo de un estudio cualitativo, basado en la identificación de las variables de suelos que mejor describen/predicen el valor de K_d y también para la construcción de un modelo de regresión multivariante que permite la predicción cuantitativa del valor de K_d en las distintas muestras de suelo.

Así, en una primera etapa se usa el modelo PLS para identificar la importancia de las distintas variable en el valor de K_d y evaluar las diferencias entre las tres bases de datos consideradas: solución de suelo, solución de *wash off* y la conjunta (solución de suelo + solución de *wash-off*). Como esta parte del estudio podía considerarse una interpretación cualitativa de los datos, los modelos se construyeron con todas las muestras correspondientes a cada base de datos. Las diferencias entre modelos y entre relevancia de las variables se evaluó a partir de los parámetros de calidad del modelo y del valor de los coeficientes de regresión (*B*), que contienen información sobre la relevancia de las variables *X* para la predicción de *y*. Cuanto mayor es el valor absoluto del coeficiente, mayor es la relevancia de la variable, y el signo indica, generalmente, la dirección de la correlación. Este razonamiento sólo es válido si las variables son completamente independientes.

En una segunda etapa, considerada de validación, es necesario demostrar que el modelo de predicción es suficientemente válido para predecir el valor de K_d en muestras que no han sido empleadas para la construcción del modelo. Para ello, la matriz de datos se divide en una matriz de calibración para el establecimiento del modelo, y una matriz de predicción, usada para validar externamente la capacidad de predicción del modelo, mediante la comparación de los valores de K_d predichos con los valores obtenidos experimentalmente para cada una de las muestras.

La aplicación de análisis multivariante para la determinación de la K_d, implicó que los datos fueran previamente tratados. El primer paso fue la creación de una matriz de datos, en la cual las filas correspondían a los suelos y las columnas a las propiedades edáficas. La distribución de datos presentaba sesgo para la mayor parte de las variables, por lo que fue necesario la transformación logarítmica excepto para el caso del pH que ya presentaba una distribución normal. Dada la gran diferencia de escala entre variables, los datos también fueron autoescalados (restando la media de todos los valores de la variable y dividiendo por la desviación estándar) previamente a la construcción de los modelos.

4.3.2.1. Identificación de las variables con mayor relevancia en la predicción del valor de K_d.

Para el caso de radioestroncio, se observó que cuando se utilizaban las bases de datos de solución de suelo y solución de *wash-off* por separado el mejor modelo propuesto estaba constituido por 4 componentes PLS, mientras que para el modelo obtenido con la base de datos global sólo eran necesarios 3 componentes PLS para describir más del 80% de varianza acumulada en el valor de K_d.

La Figura 4.11 muestra los coeficientes de regresión obtenidos para los tres conjuntos de datos para el radioestroncio. En los tres casos estudiados, la composición catiónica de la solución de contacto (especialmente las concentraciones de Ca y Mg) la concentración de cationes intercambiables, la CIC y el C_{org} se mostraron como las variables más relevantes en la explicación de la variabilidad de los valores de la K_d(Sr), lo cual está en concordancia con los mecanismos de interacción descritos en la sección anterior para los modelos mecanísticos.

Para el caso del radiocesio, al igual que para los modelos mecanísticos se ha comparado la relevancia de las variables y los parámetros de calidad de los modelos teniendo en cuenta el contenido de filosilicatos obtenido por análisis mineralógico por difracción de rayos X, pero también empleando el contenido de arcilla obtenido por textura que es un parámetro más universal en la caracterización de suelos. Por otra parte, como el parámetro RIP_K puede considerarse un valor de K_d, aunque en las mismas condiciones para todos los suelos, se decidió comparar los modelos obtenidos incluyendo o excluyendo esta variable.

Los mejores modelos obtenidos para radiocesio fueron, en todos los casos, más complejos que para el radioestroncio, es decir, con un mayor número de componentes PLS. Sin embargo, 4 componentes PLS ya proporcionaban una varianza explicada muy elevada para el valor de K_d(Cs) y componentes adicionales no mejoraban sustancialmente el modelo, por lo que las comparaciones se realizaron con 4 componentes PLS. La Figura 4.12 muestra los coeficientes de regresión obtenidos para los tres conjuntos de datos, considerando el contenido en arcilla obtenido por análisis de textura e incluyendo o excluyendo la variable RIP_K.

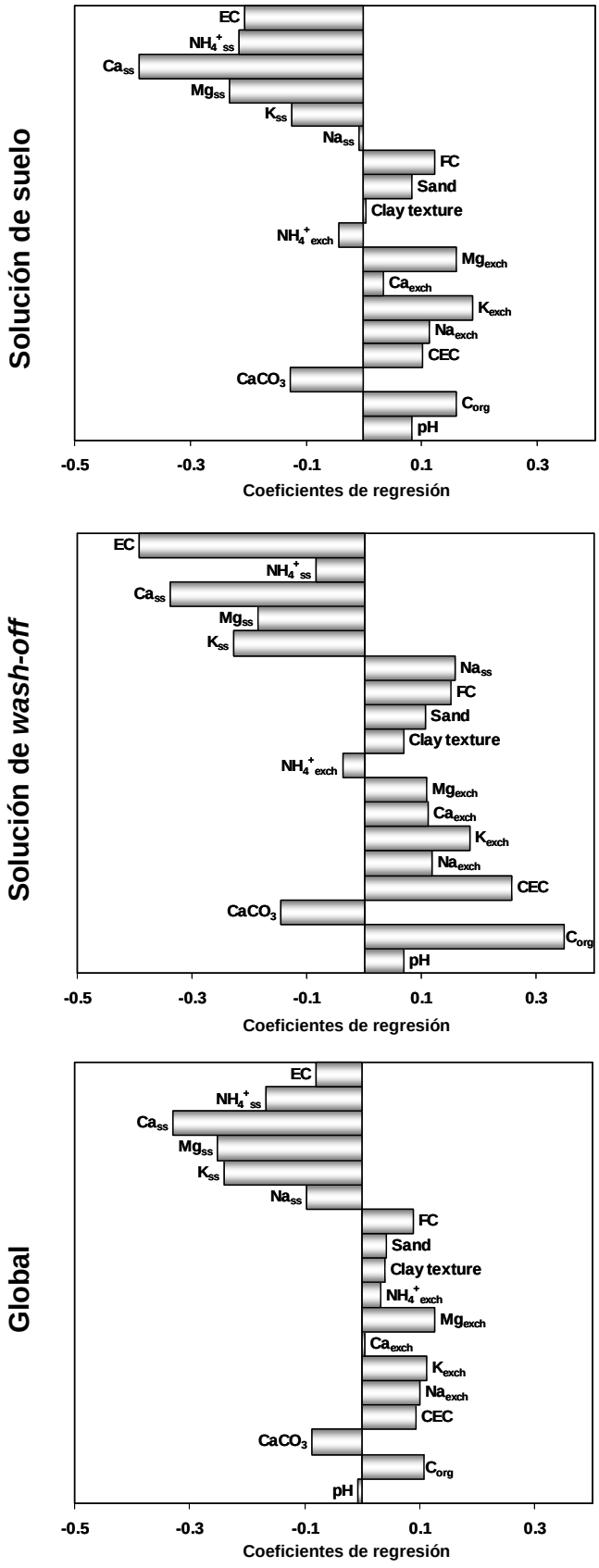

Figura 4.11. Coeficientes de regresión obtenidos para radioestroncio.

Cuando se incluyó la variable RIP_K, ésta fue la variable con más peso dentro de los modelos, lo cual coincide con los mecanismos de interacción de radiocesio destacados en la sección anterior. Además del RIP_K, las variables que también destacaron por su influencia sobre el valor de la K_d(Cs) fueron las concentraciones de NH_4 y K, tanto en la solución de contacto como en el complejo de intercambio, así como el contenido de arcilla. Cuando se excluyó la variable RIP_K todas las variables pasaron a tener una mayor relevancia, pero las que pasaron a tener una mayor importancia en el modelos fueron el contenido en arcillas y en filosilicatos 2:1.

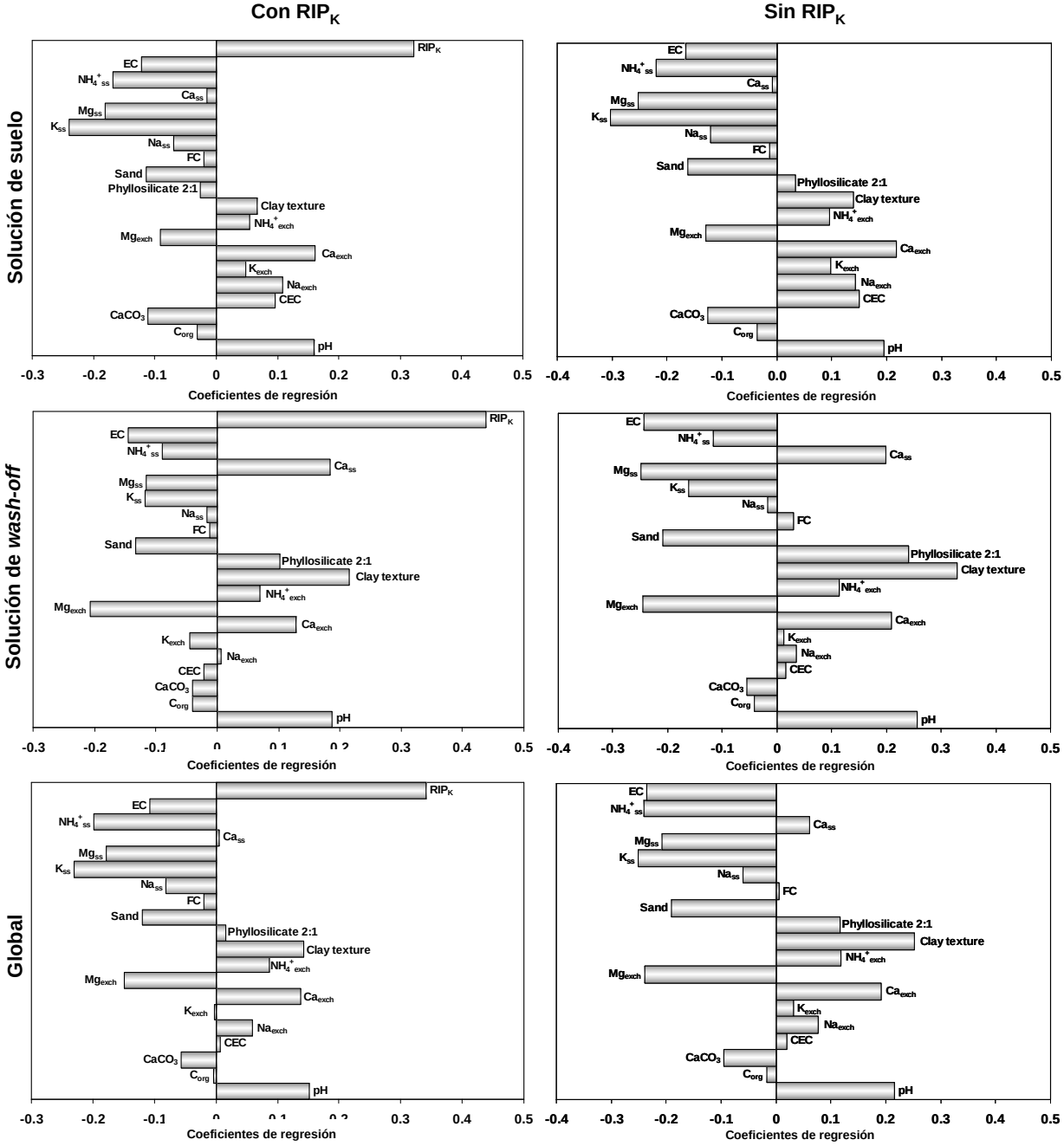

Figura 4.12. Coeficientes de regresión obtenidos para radiocesio.

En esta primera etapa del análisis de los datos, también se examinaron los parámetros de calidad de los modelos obtenidos por validación cruzada de todos los datos para cada una de las bases de datos y, tanto para radioestroncio como para radiocesio. Para los dos radionucleidos, las correlaciones entre los valores K_d experimentales y predichos, cuyos resultados se muestran en las Figuras 4.13 para radioestroncio y 4.14 para radiocesio, presentaron pendientes de 1, confirmando la ausencia de sesgo y, por lo tanto, no hubo ni sobre ni subestimación sistemática de los valores. Además, en todos los casos se obtuvieron coeficientes de regresión superiores a 0,8, lo que indica que es posible correlacionar el valor de la K_d con las propiedades de suelo.

Para los dos radionucleidos las correlaciones fueron algo mejores para la base de datos de solución de suelo que para la de solución de *wash-off*, y siempre sustancialmente mejores utilizando la base de datos global. En el caso de radiocesio, el contenido de arcilla proveniente del análisis de la textura proporcionó resultados muy similares o incluso algo mejores que en el caso del contenido de filosilicatos obtenido por análisis mineralógico. Por otra parte, la inclusión del parámetro RIP_K proporcionó mejores parámetros de calidad de los modelos, aunque también fue posible obtener modelos de mucha calidad sin necesidad de determinar este parámetro.

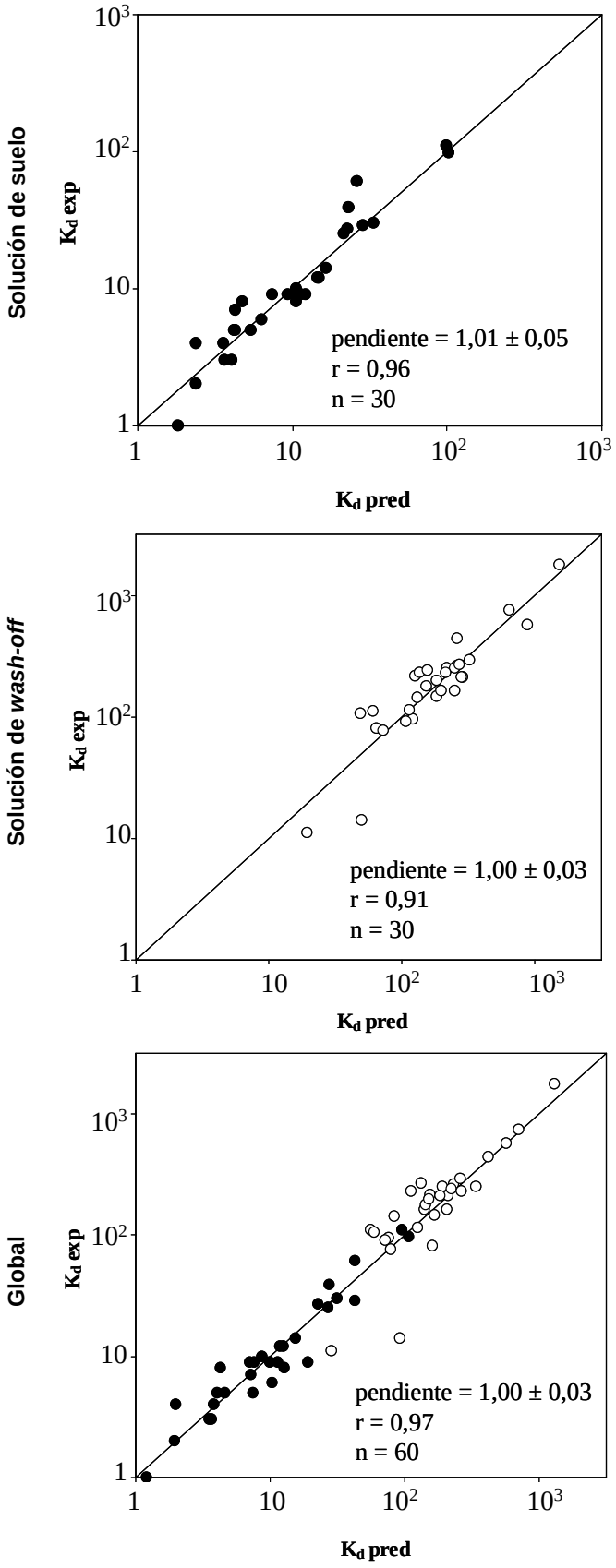

Figura 4.13. Correlaciones obtenidas entre los valores de K_d(Sr) experimentales y predichos utilizando los tres conjuntos de datos para el caso de radioestroncio.

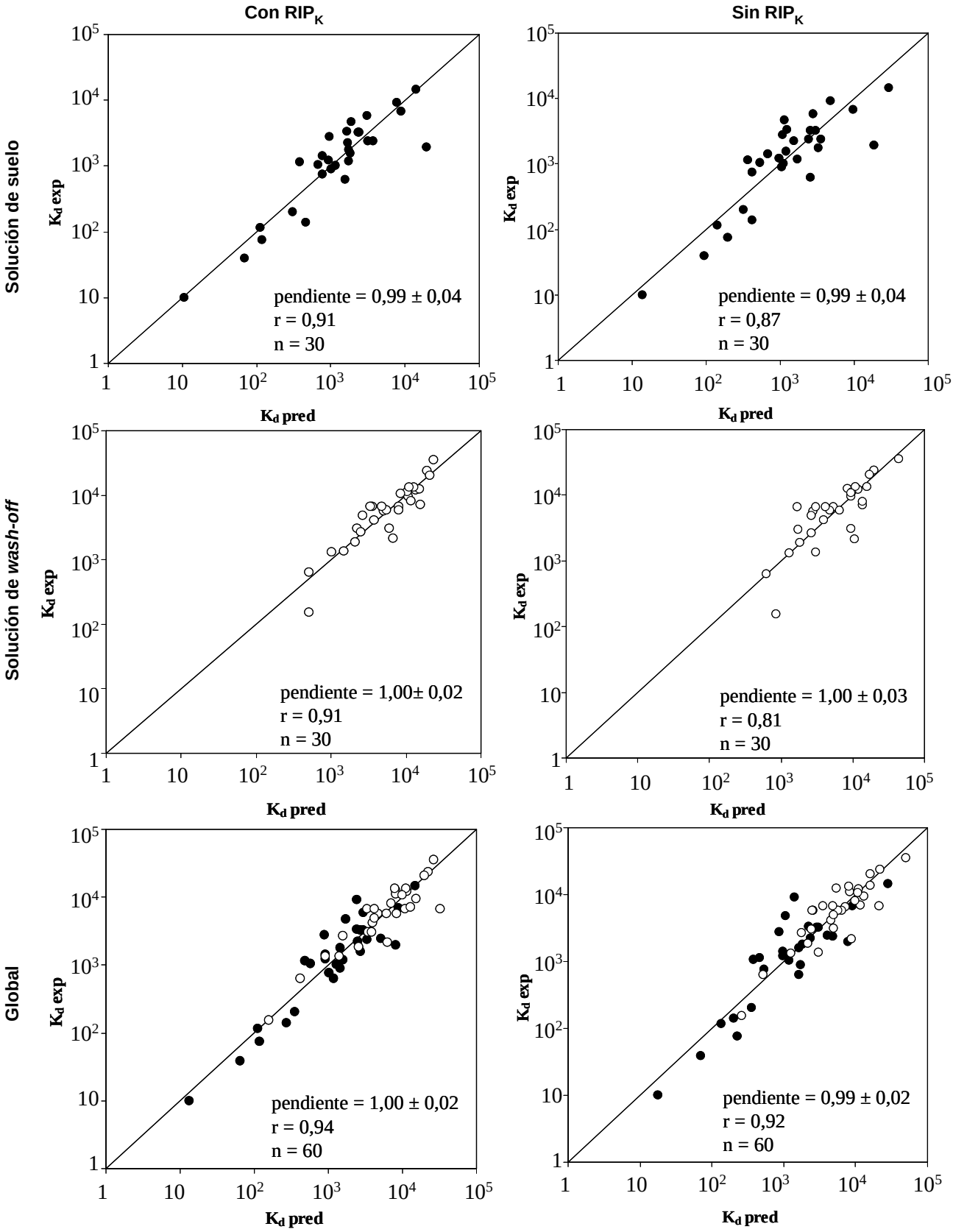

Figura 4.14. Correlaciones obtenidas entre los valores de K_d(Cs) experimentales y predichos utilizando los tres conjuntos de datos, con y sin la variable RIP_K, para el caso de radiocesio.

4.3.2.2. Validación externa de los modelos de predicción

Como última etapa de la evaluación de los modelos multivariantes basados en PLS, se realizó la validación externa mediante la predicción de valores de K_d para un grupo de suelos no utilizados en la calibración. Esta validación se realizó para la matriz de datos global, que permitía una mayor representatividad de distintas situaciones. Así, los modelos para radioestroncio y radiocesio se crearon con un menor número de muestras. La selección de muestras a considerar para la construcción de los modelos se realizó mediante el algoritmo de Kennard-Stone. La Tabla 4.12 muestra los parámetros de calidad del modelo para radioestroncio y para radiocesio, incluyendo o no el parámetro RIP_K, y para 4 componentes PLS. Las pendientes y coeficientes de correlación fueron del mismo orden que en los modelos que utilizaban todos los datos, lo que aseguró la representatividad de las muestras seleccionadas para la construcción de los modelos.

Finalmente, la predicción de los valores de K_d para las muestras de la matriz de predicción fue muy satisfactoria, tanto para radiocesio como para radioestroncio.

Tabla 4.12. Modelos de calibración para la validación externa y correlaciones obtenidas para la matriz de predicción

Radionucleido	Modelo de calibración		Matriz de predicción	
	pendiente	r	pendiente	r
Sr	1,00	0,97	1,07	0,97
Cs (con RIP_K)	0,99	0,94	1,03	0,93
Cs (sin RIP_K)	0,99	0,92	1,01	0,89

5. CONCLUSIONES

En relación con el estudio de los coeficientes de distribución de radioestroncio y radiocesio en suelos del territorio español (primer objetivo específico de la presente Tesis Doctoral, el trabajo realizado permite destacar las siguientes conclusiones:

- Se dispuso de un total de 30 suelos del territorio español, obtenidos en algún caso, tras su toma de muestra directa. Su caracterización permitió comprobar que muchos de estos suelos tenían valores de pH > 8, contenido de $CaCO_3$ > 25%, contenido en arcillas superior al 10% y un bajo contenido en materia orgánica, lo que confirmó que sus propiedades edáficas eran diferentes de las de los suelos de climas templados, que son los suelos más utilizados en el establecimiento de parámetros y mecanismos de interacción de radioestroncio y radiocesio.
- Entre los parámetros cuantificados, se determinó el valor del Potencial de Intercepción de Radiocesio en medio de potasio (RIP_K) en los 30 suelos. Es la primera vez que este parámetro se determina de forma sistemática en un número tan alto de suelos españoles.
- La cuantificación del coeficiente de distribución sólido-líquido (K_d) de los dos radionucleidos en los suelos se llevó a cabo con una metodología en *batch*, en dos soluciones de contacto, una que simulaba la composición catiónica de la solución de suelo, y otra obtenida tras extraer el suelo con agua con una relación sólido-líquido de 1:10 (solución de *wash-off*), lo que permitió evaluar el efecto de la composición catiónica de la solución de contacto en la K_d.
- La K_d(Sr) fue sistemáticamente inferior a la K_d(Cs), y las K_d obtenidas en la solución de contacto que simulaba la solución de suelo fueron también inferiores a las cuantificadas con la solución de *wash-off*, debido a la mayor concentración de las especies competitivas de ambos radionucleidos (Ca y Mg, para Sr, y K y NH_4^+ para Cs). Los intervalos de valores obtenidos para K_d(Sr) fueron 11-1764 L kg^{-1} y 1-110 L kg^{-1}, en la solución de *wash-off* y de solución de suelo, respectivamente, mientras que para K_d(Cs) fueron 153-34945 L kg^{-1} y 10-19437 L kg^{-1}.
- Se recomienda como solución de compromiso llevar a cabo los experimentos de sorción con la aproximación experimental de la solución de *wash-off*, pero con una menor relación líquido/sólido.

- Los estudios sobre la reversibilidad de la sorción (llevados a cabo con un agente extractante basado en intercambio catiónico), tras la aplicación de ciclos de secado-mojado a los suelos procedentes de los experimentos de sorción, mostraron que la sorción de Sr fue mucho más reversible que la de Cs, tanto a corto como a medio plazo. Además, mientras que la reversibilidad en el caso de Sr no varió con la aplicación de los ciclos de secado-mojado, la de Cs disminuyó hasta un total de 5 veces, lo que se explicó por la difusión de Cs a sitios interlaminares en los filosilicatos 2:1, en los que se provocó el colapso de las láminas por desplazamiento del agua interlaminar.
- Los resultados obtenidos sugieren la necesidad de que los modelos de toma de decisiones incluyan datos de la dinámica de interacción para ciertos radionucleidos, que simulen los procesos de atenuación natural.
- Tras agrupar los valores de los parámetros obtenidos (especialmente, K_d(Sr) y K_d(Cs)) en función de diferentes criterios (por ejemplo, en función de clases texturales o de parámetros responsables de la interacción) y compararlos con valores de la literatura agrupados con los mismos criterios, se observó que no habían diferencias estadísticamente significativas entre los valores obtenidos con los suelos del territorio español y los procedentes de climas templados.
- Los resultados obtenidos confirmaron que los mecanismos de interacción eran comunes para suelos de climas temperados y suelos del territorio español a pesar de que los intervalos de valores en los que se encontraban las propiedades edáficas generales en cada caso eran distintos. En consecuencia, los modelos y mecanismos de interacción establecidos a partir de suelos de otros climas son aplicables a suelos del territorio español.

En relación con la evaluación de los criterios adecuados para el agrupamiento de los valores de K_d en función de propiedades edáficas generales y de los factores clave que rigen la interacción-radionucleido en suelos (segundo objetivo específico de esta Tesis Doctoral), se destacan las siguientes conclusiones:

- Se creó una base de datos de sorción en suelos, con más de 2900 entradas para 67 radionucleidos, basada en la aceptación de más de 80 documentos, tras una revisión crítica, incluyendo artículos publicados, tesis doctorales e informes internos de agencias internacionales. La base de datos consta de 22 campos obligatorios (incluyendo valores de propiedades edáficas y detalles de la metodología seguida), más algunos adicionales para ciertos radionucleidos.

- Respecto a bases de datos anteriores (en concreto, la relacionada con el *Handbook of parameter values for the prediction of radionuclide transfer in temperate environments* TRS 364, de la IAEA), se aumentó considerablemente el número de valores de K_d para un número elevado de radionucleidos, mientras que se incluyeron por primera vez valores de K_d para más de veinte radionucleidos no considerados anteriormente.
- Los valores de K_d de cada radionucleido se agruparon en unas clases determinadas en función de criterios prefijados, con el objeto de cuantificar un valor estimado mejor para cada clase de suelo (a partir del cálculo de la media geométrica de todos los valores de la clase) e informar sobre la variabilidad dentro de cada clase.
- En el agrupamiento basado en la textura y contenido de materia orgánica de los suelos se definieron cinco clases: arenoso, franco, arcilloso, orgánico e inespecífico. La aplicación de este criterio de agrupamiento mostró que aunque se mejoraban los valores estimados de las K_d para ciertos radionucleidos respecto a cálculos hechos con bases de datos anteriores, la variabilidad de resultados en cada clase era aún de varios órdenes de magnitud.
- Se definieron nuevos criterios de agrupamiento para ciertos radionucleidos (radioestroncio, radiocesio, uranio, radioisótopos de metales pesados, radioyodo) basados en cofactores, es decir, en propiedades edáficas relacionadas con sus mecanismos de interacción. Los cofactores que se definieron fueron:
    - Cs: RIP_K y concentración de K en la solución de suelo
    - Sr: CIC y concentraciones de Ca y Mg en la solución de suelo
    - Radioisótopos de metales pesados, U y Th: pH
    - I: especiación química y contenido de materia orgánica
- Esta nueva estrategia de agrupamiento permitió cuantificar valores estimados de K_d más representativos para cada clase, así como disminuir significativamente la variabilidad dentro de las clases.
- Las correlaciones entre los valores de K_d y propiedades edáficas basadas principalmente en los cofactores explicaron un porcentaje muy elevado de la varianza para ciertos radionucleidos, en algún caso por encima del 70% (radioestroncio, radiocesio y algún metal pesado).

En relación con la predicción de los valores de K_d de radioestroncio y radiocesio en suelos a partir de modelos mecanísticos y de modelos multivariantes blandos (tercer objetivo específico de esta Tesis Doctoral), los resultados de los experimentos realizados permitieron formular las siguientes conclusiones:

- Se crearon y aplicaron modelos mecanísticos para predecir los valores individuales de K_d(Sr) y K_d(Cs), obtenidos en el contexto del primer objetivo, a partir de valores de propiedades edáficas.

- En el caso de radioestroncio, a partir de la propuesta de un modelo mecanístico más complejo basado en las concentraciones de Ca y Mg en el complejo de intercambio y en la solución de contacto, junto con los respectivos coeficientes de selectividad Sr-Ca-Mg, se propuso un modelo mecanístico más simplificado basado sólo en la CIC y la concentración de Ca y Mg en la solución de suelo. La varianza explicada por estos modelos fue del orden de 75% o superior, con predicciones sin sesgo (pendientes próximas a la unidad), incluso para el caso del modelo más simplificado.

- La aplicación del modelo mecanístico para radiocesio exigió la cuantificación de la $K_C^{FES}(NH_4/K)$. La cuantificación a partir de la relación RIP_K/RIP_{NH4} ($K_C^{FES}(NH_4/K)$: 1,4 - 4,4) mostró valores sistemáticamente inferiores a los obtenidos mediante la cuantificación de este parámetro a partir de cambios de K_d(Cs) con la concentración de NH_4^+ en un medio con Ca y K (escenario mixto) ($K_C^{FES}(NH_4/K)$: 5,6 - 10,2).

- Se propuso un modelo mecanístico para radiocesio basado en el parámetro RIP_K, las concentraciones de Na, K y NH_4^+ en el complejo de intercambio y en la solución de contacto, y las correspondientes $K_C^{FES}(NH_4/K)$ y $K_C^{FES}(Na/K)$. Simplificaciones de este modelo permitieron proponer un modelo mecanístico más sencillo basado únicamente en RIP_K y la concentración de K intercambiable y en la solución de contacto. La varianza explicada por estos modelos fue del orden del 80% o superior, incluso para el caso del modelo más sencillo, con pendientes próximas o superiores a 0,9.

- Se evaluó una simplificación adicional del modelo basada en substituir la variable RIP_K por sus correlaciones con el contenido y el tipo de arcillas. En este caso, la varianza explicada fue superior al 55%, con una pendiente próxima a 0,9, lo que puede ser considerado como un modelo suficientemente bueno para los sistemas de toma de decisión, con la ventaja de no ser necesaria la determinación de parámetros de suelo específicos.

- Se aplicó un modelo multivariante blando, basado en la regresión por mínimos cuadrados parciales (PLS), para predecir los valores individuales de K_d(Sr) y K_d(Cs) al conjunto de datos procedentes de los experimentos realizados con suelos del territorio español. Los modelos de predicción no variaron significativamente en función del conjunto de datos utilizado (solución de suelo; solución de *wash-off*; global). Cuando se utilizó el conjunto de datos global, 3 componentes explicaron el 80% de la varianza acumulada de K_d(Sr), mientras que en el caso de radiocesio fueron necesarios 4.
- La validación externa de los modelos PLS mostró que era posible predecir los valores K_d(Sr) y K_d(Cs) con un porcentaje de varianza explicada de hasta el 85% de la varianza y sin sesgo.
- Los modelos multivariantes blandos se confirman como una potente herramienta para el estudio y posterior predicción de parámetros de interacción de contaminantes en suelos.

BIBLIOGRAFÍA

Absalom, J. P., Young, S. D., Crout, N. M. J. (1995). Radiocaesium fixation dynamics: measurement in six Cumbrian soils. *European Journal Soil Science*, 46, 461-469.

Aldaba, D., Rigol, A., Vidal, M. (2010). Diffusion experiments for estimating radiocesium and radiostrontium sorption in unsaturated soils from Spain: Comparison with batch sorption data. *Journal of Hazardous Materials,* 181, 1072–1079.

ASTM (American Society For Testing And Materials), (2001). Standard test method for distribution ratios by the short-term batch method, ASTM D 4319-93, West Conshohocken, PA, US.

Baham, J., Sposito, G. (1994). Adsorption of dissolved organic carbon extracted from sewage sludge on montmorillonita and kaolinite in the presence of metal ions. *Journal of Environmental Quality*, 23, 147-153.

Bégin, L., Fortin, J., Caron, J. (2003). Evaluation of the fluoride retardation factor in unsaturated and undisturbed soil columns. *Soil Science Society of America Journal*, 67, 1635–1646.

Brady, N. C., Weil, R. R. (2008). En: The nature and properties of soils. Ed. Pearson Prentice Hall. Upper Saddle River, New Yersey 07458. ISBN: 0-13-227938-X.

Canoba, A.C., Gnoni, G. (2006). Informe sobre TENORM: situación nacional e internacional. Memoria técnica de la Autoridad Regulatoria Nuclear Argentina del año 2005.

CIEMAT (Centro de Investigaciones Energéticas, Medioambientales y Tecnológicas), (2000). Techniques and management strategies for environmental restoration and their ecological consequences-TREMAS project. Final report. Colección Docuementos Ciemat. Editorial Ciemat. ISBN: 84-7834-378-4.

Comans, R. N. J.; Middelburg, J. J.; Zonderhuis, J., Woittiez, J. R. W., De Lange, G. J., Das, H. A., Van der Weijden, C. H. (1989). Mobilization of radiocesium in pore water of lake sediments. *Nature*, 339, 367-369.

Cotton, F. A., Wilkinson, G. (1986). Química inorgánica avanzada. Limusa, ISBN: 968-18-1795-8. Méjico.

Cremers, A.; Elsen, A.; De Preter, P.; Maes, A. (1988). Quantitative analysis of radiocesium retention in soils. *Nature*, 335, 247-249.

CSN (Consejo de Seguridad Nuclear), (2008). Comparecencia del 11 de junio de 2008 de la Presidenta del Consejo de Seguridad Nuclear en la Ponencia encargada por la Comisión de Industria, Turismo y Comercio del Congreso de los Diputados para informar sobre el suceso notificado el pasado 4 de abril 2008 en la central nuclear Ascó I (Tarragona), relativo a la detección de partículas radiactivas en el emplazamiento.(www.csn.es/images/stories/actualidad_datos/especiales/asc_i_partculas/comparecenciacmtcongreso110608.pdf)

De Cort, M., Dubois, G., Fridman, Sh. D., Germenchuck, M. G., Izrael, Y. A., Janssens, A., Jones, A. R., Kelly, G. N., Kvasnikova, E. V., Matveenko, I. I., Nazarov, I. M., Pokumeiko, Y. M., Sitak, V. A., Stukin, E. D., Tabachny, L. Y., Tsaturov, Y. S., Audinshin, S. I. (1998). Atlas of caesium deposition on Europe after the Chernobyl accident. Eds. Office for Official Publications of the European Communities. EUR 16733, Luxembourg. ISBN: 92-828-3140-X.

Degryse, F., Smolders, E., Cremers, A. (2004). Enhanced sorption and fixation of radiocaesium in soils amended with K-bentonites, submitted to wetting–drying cycles. *European Journal Soil Science*,55, 513–522.

Di Bonito, M. (2005) Trace Elements in Soil Pore Water: A Comparison of Sampling Methods. Tesis Doctoral. University of Nottingham.

Echevarria, G., Sheppard, M., Morel, J.L. (2001). Effect of pH on the sorption of uranium in soils. *Journal Environmental Radioactivity*, 53, 257–264.

Eisenbud, M., Gessell, T., (1997). Environmental radioactivity: from natural industrial and military sources. Academic Press, San Diego. ISBN: 0-12-235154-1.

ENRESA (Empresa Nacional de Residuos Racioactivos, S.A.). (2010a). El almacén temporal centralizado. (http://www.enresa.es/files/multimedios/dossier_atc.pdf)

ENRESA (Empresa Nacional de Residuos Racioactivos, S.A.). (2010b) Almacén centralizado de residuos radioactivos de baja y media actividad El Cabril. (http://www.enresa.es/actividades_y_proyectos/rbma).

EPA (Enviromnental Protection Agency). (1998). MINTEQA2/PRODEFA2, A geochemical assessment model for environmental systems: User manual supplement for version 4.0. (http://www.epa.gov/ceampubl/mmedia/minteq/).

EPA (Environmental Protection Agency). (1999). Understanding Variation in Partitioning Coefficients, K_d, Values: Volume II: Review of Geochemistry and Available K_d Values for Cadmium, Caesium, Chromium, Lead, Plutonium, Radon, Strontium, Thorium, Tritium and Uranium. US-EPA, Office of Air and Radiation, Washington, USA. EPA 402-R-99-004B.

EPA (Environmental Protection Agency). (2004). Understanding Variation in Partitioning Coefficients, K_d, Values: Volume III: Review of Geochemistry and Available K_d Values for Americium, Arsenic, Curium, Iodine, Neptunium, Radium, and Technetium. US-EPA, Office of Air and Radiation, Washington, USA. EPA 402-R-99-004C.

Evans, David W.; Alberts, James J.; Clark, Roy A., III. (1983). Reversible ion - exchange fixation of cesium-137 leading to mobilization from reservoir sediments. *Geochimica et Cosmochimica Acta*, 47, 1041-1049.

FAO-UNESCO (1994). Soil Map of the World, 1:5,000,000. United Nations Educational, Scientific and Cultural Organization, Paris.

Fernández-Torrent, R., Vidal, M., Rauret, G., Rigol, A., (2005). Laboratory experiments to characterize radionuclide diffusion in soils, paper presentado a *2nd International Conference on Radioactivity in the Environment*, Aix-en-Provence, France.

García-Gutiérrez, M., Cormenzara, J. L., Missana, T., Mingarro, M., (2004). Diffusion coefficient and accessible porosity for HTO and $^{36}Cl^-$ in compacted FEBEX bentonite. *Applied Clay Science*, 26, 65-73.

Gerritse, R. G., Vriesema, R., Dalenberg, J. W, De Roos., H. P. (1982). Effect of Sewage Sludge on Trace Element Mobility in Soils. *Journal of Environmental Quality*, 11, 359-364.

Gesell, T. F., Prichard, H. M. (1975). The technologically enhanced natural radiation environment. *Health Physics*, 28, 361-366.

Gillet, A.G., Crout, N.M.J., Absalom, J.P., Wright, S.M., Young, S.D., Howard, B.J., Barnett, C.L., McGrath, S.P., Beresford, N., Voigt. G. (2001). Temporal and spatial prediction of radiocaesium transfer to food products. *Radiation Environmental Biophysics*, 40, 227–235.

Goody, D.C., Shand, P., Kinnburgh, D.G., Van Riemsdijk, W.H., (1995). Field-based partition coefficients for trace elements in soil solutions. *European Journal of Soil Science*, 46, 265.

Hillel, D. (1998). Environmental soil physics. Ed. Academic Press. ISBN: 0-12-348525-8.

Hilton, J., Comans, R. N. J. (2001). Chemical forms of radionuclides and their quantification in environmental samples. En: Radioecology: Radioactivity & Ecosistems. Van der Stricht, E., Kirchman, R., (Eds.), Fortems, Rue du Charbonnage 22, Lieja, Bélgica. ISBN: 2-9600316-0-1.

Hunter, K. A., D. J. Hawke, and L. K. Choo. (1988). Equilibrium Adsorption of Thorium by Metal Oxides in Marine Electrolytes. *Geochimica et Cosmochimica Acta*, 52, 627-636.

IAEA (International Atomic Energy Agency) (1999). Report on the preliminary fact finding mission following the accident at the nuclear accident at the fuel processing facility in Tokaimura, Japan. Vienna.

IAEA (International Atomic Energy Agency) (2003). Extent of Environmental Contamination by Naturally Occurring Radioactive Material (NORM) and Technological Options for Mitigation, Technical Report Series Nº 419, Vienna, ISBN: 92–0–112503–8.

IAEA, (International Atomic Energy Agency) (2006). Environmental consequences of the Chernobyl accident and their remediation: twenty years of experience. Report of the Chernobyl Forum Expert Group 'Environment', Vienna, ISBN: 92-0-114705-8.

IAEA, (International Atomic Energy Agency) (2006b). *Classification of Soil Systems on the Basis of Transfer Factors of Radionuclides from Soil to Reference Plants*, IAEA TECDOC-1497, Vienna.

IAEA (International Atomic Energy Agency), (2010). Hanbook of Parameter Values for the Prediction of Radionuclide Transfer in Terrestrial and Freshwater Environments, TECHNICAL REPORTS SERIES No. 472, IAEA, Vienna. ISBN: 978-92–0–113009–9.

Iggy Liator, M. (1988). Review of soil solution samplers. *Water Resources Research*, 24, 727-733

Izrael, Y. A., De Cort, M., Jones, A. R., Nazarov, I. M., Fridman, Sh, D., Kvasnikova, E. V., Stukin, E. D., Kelly, G. N., Matveenko, I. I., Pokumeiko, Y. M., Tabatchnyl, L. Y., Tsaturov, Y., (1996). The atlas of caesium-137 contamination of Europe after the Chernobyl accident. In *The Radiological consequences of the Chernobyl accident*. Karaoglou, A., Desmet, G., Kelly, G. N., Menzel, H. G. Eds. European Commission: EUR 16544 EN. Luxembourg. ISBN: 92-827-5248-8.

Jacob, P., Fesenko, S., Bogdevitch, I., Kashparov, V., Sanzharova, N, Grebenshikova, N., Isamov, N., Lazarev, N., Panov, A., Ulanovsky, A., Zhuchenko, Y., Zhurba, M., (2009). Rural areas affected by the Chernobyl accident: Radiation exposure and remediation strategies. *Science of the Total Environment*, 408, 14–25.

Juo, A. S. R., Barber, S. A., (1969). An explanation for the variability in Sr-Ca exchangeable selectivity of soils, clays and humic acid. *Soil Science Society American Proceedings*, 33, 360-363.

Kabata-Pendias, A., Pendias, H. (2001). Trace elements in Soils and Plants. CRC Press, 3ª Edición, Boca Ratón, Florida, Estados Unidos. ISBN : 0-8493-1575-1.

Kaiser, K., Zech, W. (2000). Dissolved organic matter sorption by mineral constituents of subsoil clay fractions. *Journal of Plant Nutrient Soil Science*, 163, 531-535.

Kennedy, V. H., Sanchez, A. L., Oughtin, D. H., Rowlan., A. P. (1997). Use of the single and extractants to assess radionuclide and heavy metal availability from soils for root uptake. *Analyst*, 122, 89R-100R.

Kocher, D. C., (1981). Radioactive decay data tables. A handbook of decay data for application to radiation dosimetry and radiological assessments, U.S. Departament of Energy, ISBN: 0-87079-124-9.

LaFlamme, B. D., Murray, J. W (1987). Solid/Solution Interaction: The Effect of Carbonate Alkalinity on Adsorbed Thorium. *Geochimica et Cosmochimica Acta,* 51, 243-250.

Lawrence, G. B., David, M. B. (1996). Chemical evaluation of soil-solution in acid forest soils. *Soil Science*, 161, 298-313.

Llauradó, M., Torres, J.M., Tent, J., Sahuquillo, A., Muntau, H., Rauret, G. (2001). Preparation of a soil reference material for the determination of radionuclides. *Analytica Chimica Acta*, 445, 99–106.

Martínez, C.E., McBride, M.B. (1998). Solubility of Cd^{2+}, Cu^{2+}, Pb^{2+}, and Zn^{2+} in aged coprecipitates with amorphous iron hydroxides. *Environmental Science and Technology*, 32, 743-748.

Mclaren, R. G., Cameron, K. C. (1996). Soil Science. Oxford University Press. ISBN: 0-19-558345-0.

McDonald, J.A. (2000). Evaluating natural attenuation for groundwater cleanup. *Environmental Science and Technology*, 34, 346A-353A.

Meeussen, J. C. L. (2003). ORCHESTRA: An object-oriented framework for implementing chemical equilibrium models. *Environmental Science and Technology,* 37, 1175-1182.

Moore, D.M., Reynolds, R.C. (1989). X-ray Diffraction and the Identification and Analysis of Clay Minerals. Oxford University Press, Nueva York, Estados Unidos. ISBN: 0-19-508713-5.

NEA (Nuclear Energy Agency). The disposal of high-level radioactive waste. NEA Issue Brief: An analysis of principal nuclear issues, Nº 3, 1989 (www.nea.fr/brief/brief-03.html).

Ochs, M., Boonekamp, M., Wanner, H., Sato, H., Yui, M., (1998) A quantitative model for ion diffusion in compacted bentonite. *Radiochimica Acta*, 82, 437-443.

Ochs, M., Lothenbach, B., Wanner, H., Sato, H., Yui, M., (2001). An integrated sorption-diffusion model for the calculation of consistent distribution and diffusion coefficients in compacted bentonite. *Journal of Contaminant Hydrology*, 47, 283-296.

OECD, (ORGANISATION FOR ECONOMIC COOPERATION AND DEVELOPMENT), (2000). Guideline for the testing of chemicals: Adsorption-desorption using a batch equilibrium method, Guideline 106.

OGP (International Association of Oil & Gas Producer), (2008). Guidelines for the management of Naturally Occurring Radioactive Material (NORM) in the oil & gas industry. Report No. 412. September 2008.

Okamoto, A., Idemitsu, K., Furuya, H., Inagaki, Y., Arima, T., (1999). Distribution coefficients and apparent diffusion coefficients of caesium in compacted bentonites, Materials Research Society Symposia Proceedings. 556, 1091.

Ortega, X., Jorba, J. (1996). Las radiaciones ionizantes. Su utilización y riesgos, Edicions UPC, Barcelona, ISBN: 84-8301-170-0.

Ortega, X, Duch, M., Vargas, López, N. (2008). Dose assessment at a phosphate industry landfill using solid state detectors. *Radiation Measurements*, 43, 664-667.

Porta, J., López-Acevedo, M., Roquero, C. (1994). Edafología para la agricultura y el medio ambiente. Ediciones Mundi-Prensa, Madrid, España.

Quindós Poncela, L. S. (1995). Radón: Un gas radioactivo de origen natural en su casa. Consejo de Seguridad Nuclear. ISBN: 84-87275-59-1.

Rauret, G., Firsakova, S., (1996). The transfer of radionuclides through the terrestrial environment to agricultural products, including the evaluation of agrochemical practices, EUR 16528 EN, European Commission, Luxemburgo.

Rhoads, K., Bjornstad, B. N., Lewis, R. E., Teel, S. S., Cantrell K. J., Serne R. J., Smoot J. L., Kincaid, C. T., Wurstner, S. K., (1992). Estimation of the Release and Migration of Lead Through Soils and Groundwater at the Hanford Site 218-E-12B Burial Ground. Volume 1: Final Report. PNL-8356 Volume 1, Pacific Northwest Laboratory, Richland, Washington.

Rigol, A., Vidal, M., Rauret, G, Shand, C. A.; Cheshire, M. V. (1998). Competition of Organic and Mineral Phases in Radiocesium Partitioning in Organic Soils of Scotland and the Area near Chernobyl. *Environmental Science and Technology*, 32, 663-669.

Roig, M., Vidal, M., Rauret, G. (1998). Estimating the radionuclide available fraction in mineral soils using an extraction technique. *Analyst*, 123**,** 519-526.

Roig, M., Vidal, M., Rauret, G., Rigol, A. (2007). Prediction of radionuclide aging in soils from the Chernobyl and Mediterranean areas. *Journal of Environmental Quality* 36, 943-952.

Sanchez, A.L., Smolders, E., Van den Brande, K., Merckx, R., Wright, S.M., Naylor, C. (2002). Predictions of in situ solid-liquid distribution of radiocaesium in soils. *Jounal of Environmental Radioactivity*. 63, 35- 47.

Sanderson, D.C.W., Cresswell, A.J., Allyson, J.D., McConville, P. (1997). Review of past nuclear accidents: source terms and recorded gamma ray spectra. UK Department of the Environment Report. London. Number DOE/RAS/97.001.

Simon, S. L., Ibrahim, S. A., (1990). Biological uptake of radium by terrestrial plants: a review.The Environmental Behaviour of Radium Vol 1. IAEA, Vienna, 545-599.

Sposito, G. (1986). Distinguishing adsorption from surface precipitation. En: Geochemical Processes at Mineral Surfaces. Davis, J.A., Hayes, K.F. (Eds.). ACS Symposium Series, Washington DC, Estados Unidos, 323 (Geochem. Processes Miner. Surf.), 217-228.

Staunton, S., (2004) Sensitivity of the distribution coefficient, K_d, of nickel to changing soil chemical properties. *Geoderma*, 122, 281-290.

Stevenson, F. J. (1982). Humus chemistry: genesis, composition, reactions. John Willey & Sons, Nueva York. ISBN: 0-471-09299-1.

Stumm, W., Morgan, J.J. (1981). Aquatic Chemistry. Wiley (Interscience), Nueva York, Estados Unidos. ISBN: 0-471-51184-6.

Sweeck, L.; Wauters, J.; Valcke, E.; Cremers, A., (1990) The specific interception potential of soils for radiocesium. En: Tra*nsfer of radionuclides in natural and semi-natural environments*, Desmet , G., Nassibeni, P., Belli, M. Eds. Elsevier Applied Science Publishers: London and New York, pp. 249-258.

Sweeck, L., (1996). Soil chemical availability of radiocesium in mineral soils. Tesis Doctoral. Katholieke Universiteit Leuven, Bélgica.

Sysoeva, A. A., Konopleva, I. V., Sanzharova, N. I. (2005). Bioavailability of radiostrontium in soil: Experimental study and modeling. *Journal of Environmental Radioactivity*, 81(2-3), 269-282.

Thibault, D. H., Sheppard, M. I., Smith, P. A. (1990). A Critical Compilation and Review of Default Soil Solid/Liquid Partition Coefficients, K_d, for Use in Environmental Assessments. AECL-10125, Whiteshell Nuclear research Establishment, Pinawa, Canada.

Vandenhove, H., Van Hees, M., Wouters, K., Wannijn, J., (2007a) Can we predict uranium bioavailability based on soil parameters? Part 1: effect of soil parameters on soil solution uranium concentration. *Environmental Pollution*, 145, 587–595.

Vandenhove, H.; Van Hees, M. (2007b). Predicting radium availability and uptake from soil properties. *Chemosphere*, 69, 664-674.

Valcke, E., (1993) The behaviour dynamics of radioCaesium and radiostrontium in soils rich in organic matter, Tesis Doctoral, Katholieke Universiteit Leuven, Bélgica.

Vidal, M., Roig, M., Rigol, A., Llauradó, M., Rauret, G., Wauters, J., Elsen, A., Cremers, A., (1995). Two approaches to the study of radiocaesium partitioning and mobility in agricultural soils from the Chernobyl area. *Analyst*, 120, 1785-1791.

Vidal, M.; Rigol, A.; Gil-García, C. (2009), Soil-radionuclide interactions. En: Quantification of radionuclide transfer in terrestrial and freshwater environments for radiological assessments; 71-102. IAEA-TECDOC-1616. IAEA, Viena. ISBN: 978-92-0-104509-6)

Wauters, J.; Elsen, A.; Cremers, A.; Konoplev, A. V.; Bulgakov, A. A.; Comans, R. N. J. (1996a). Prediction of solid / liquid distribution coefficients of radiocesium in soils and sediments. Part one: a simplified procedure for the solid phase characterization. *Applied Geochemistry*, 11, 589-594.

Wauters, J.; Elsen, A.; Cremers, A.; Vidal, M. (1996b). Prediction of solid / liquid distribution coefficients of radiocesium in soils and sediments. Part two: a new procedure for solid phase speciation of radiocesium. *Applied Geochemistry*, 11, 595-599.

WNA (World Nuclear Association. Radioactive waste management) (2009) (http://www.world-nuclear.org/info/inf04.html).

ACRÓNIMOS Y ABREVIATURAS

Å	Ångström
AGP	Almacén Geológico Profundo
ATP	Almacén Temporal Centralizado
Bq	Bequerel
Ci	Curie
CIC	Capacidad de intercambio catiónico
CIEMAT	Centro de Investigaciones Energéticas, Medioambientales y Tecnológicas
CSN	Consejo de Seguridad Natural
DOC	*Dissolved Organic Matter*
	Materia organic disuelta
DEG	Desviación Estárdar Geométrica
EPA	*Environmental Protection Agency*
	Agencia de Protección Medioambiental
ENRESA	Empresa Nacional Residuos Radioactivos, S.A.
ENUSA	Empresa Nacional Uranio, S.A.
FAO	*Food and Agriculture Organization*
	Organización de las Naciones unidas para la Agricultura y la Alimentación
FES	*Frayed Edge Sites*
	Sitios específicos de los extremos expandidos de las arcillas
IAEA	*International Atomic Energy Agency*
	Organismo Internacional de la Energía Atómica
ICRP	*International Comission on Radiological Protection*
	Comisión Internacional de la Protección Radiológica
ISSS	*International Society of Soil Science*
	Sociedad Internacional de la Ciencia del Suelo
K_C	Coeficiente de selectividad
K_d	Coeficiente de distribución sólido-líquido
MG	Media geométrica
MO	Materia Orgánica
m_X	Concentración de un ión X en solución de contacto
NORM	*Naturally Occurring Radioactive Material*
	Radionucleidos primordiales
PLS	*Partial Least Squares Regression*
	Regresión por mínimos Cuadrados Parciales

RES *Regular Exchangeable Sites*
Sitios de intercambio regular

RIP *Radiocaesium Interception Potencial*
Potencial de Intercepción de Radiocesio

TENORM *Technologically Enhanced Naturally Occurring Radioactive Material*
Radionucleidos primordiales concentrados por actividades humanas

UNESCO *United Nations Educational, Scientific and Cultural Organization*
Organización de la Naciones Unidas para la Educación la Ciencia y la Cultura

$\mathbf{X_{ss}}$ Concentración de un ión en solución de contacto

$\mathbf{Z_X}$ Proporción relativa de un ión X en el complejo de intercambio

ANEXO

IAEA-TECDOC-1616

Quantification of Radionuclide Transfer in Terrestrial and Freshwater Environments for Radiological Assessments

IAEA
International Atomic Energy Agency

May 2009

The originating Section of this publication in the IAEA was:

Chemistry Unit, Agency's Laboratories, Seibersdorf
International Atomic Energy Agency
Wagramer Strasse 5
P.O. Box 100
A-1400 Vienna, Austria

QUANTIFICATION OF RADIONUCLIDE TRANSFER IN TERRESTRIAL
AND FRESHWATER ENVIRONMENTS FOR RADIOLOGICAL ASSESSMENTS
IAEA, VIENNA, 2009
ISBN 978–92–0–104509–6
ISSN 1011–4289

Printed by the IAEA in Austria
May 2009

SOIL-RADIONUCLIDE INTERACTIONS

M. VIDAL, A. RIGOL, C.J. GIL-GARCÍA.
Analytical Chemistry Department–Universitat de Barcelona, Barcelona, Spain

Abstract

Radionuclide mobility in agricultural systems, and thus in the food chain, is strongly affected by the extension of its sorption in soils, which can be estimated by the quantification of the solid-liquid distribution coefficient (K_d). This parameter may vary within various orders of magnitude depending on the radionuclide and soil combination, but also on the experimental method used for its determination. Here, a new K_d database was built up with around 2900 records of 67 elements, which allows us to calculate the best estimates for the K_d values of a number of radionuclides for various soil types. Best estimates are derived from geometric means calculated from grouping soils by texture and organic matter content and, when possible, also using the main soil cofactors governing soil-radionuclide interaction, concretely for radiocaesium, radiostrontium, uranium, radioiodine, and a few heavy-metal radionuclides. The use of the cofactor approach permits, in most cases, decreasing the variability of the ranges of K_d values associated with a soil type. Additionally, some hints are given in this section on the sorption dynamics of radiostrontium and radiocaesium, based on rate constants values and changes with time in the reversibly sorbed fraction.

1. DISTRIBUTION OF RADIONUCLIDES BETWEEN SOLID AND LIQUID PHASES

1.1. The solid-liquid distribution coefficient concept

The chemical form and speciation of radionuclides strongly affects their movement through environmental media and uptake by biota. Specifically, the way that a radionuclide is bound to solids (soils in the terrestrial environment; sediments in aquatic systems) eventually controls the amount of radionuclide in solution, which directly influences the fraction of radionuclide that may be incorporated by organisms.

Dissolved radionuclide ions can bind to solid surfaces by a number of processes often classified under the broad term of sorption. Although significant progress has been made to describe sorption in heterogeneous solids as a weighted result of sorption on homogeneous surfaces, models for the description of radionuclide sorption are still mostly based on empirical solid-liquid distribution coefficient (K_d) values. This approach is the simplest sorption model available and is the ratio of the concentration of radionuclide sorbed on a specified solid to the radionuclide concentration in a specified liquid phase at equilibrium (K_d, L/kg). The K_d -based model does not assume any knowledge of sorption mechanisms, nor does it contain a term to quantify the capacity and selectivity of the sorption sites or the competition with other ions to fill the sorption sites. Such competitive effects can only be taken into account by the empirical selection of different K_d values applicable in different environmental contexts.

The simple K_d -based model relies on the hypothesis that the radionuclide on the solid phase is in equilibrium with the radionuclide in solution, and thus can exchange with it. However, the elapsed time since the incorporation of the radionuclide is known to affect the quantification of K_d, since a fraction of the incorporated radionuclide may become fixed by the solid phase (an aging effect related to sorption dynamics). Although in most cases no specific comments are made on this issue in published papers, consideration of this process has led to the definition and reporting of various types of K_d in the literature. Whereas the *labile* or *exchangeable* K_d refers to the initial sorption process where the radionuclide is reversibly sorbed, due to an ion-exchange based mechanism for most radionuclides, terms such as *total* K_d are used when there may be radionuclide irreversibly sorbed to the solid phase. Therefore, and as the radionuclide speciation in the solid phase may change with time, an estimation of the changes in the reversibility of the sorption in the short and medium term

is also required in any experimental approach designed to derive information on sorption dynamics.

Most laboratory tests are, in principle, designed to obtain the so-called exchangeable K_d (K_d^{exch}). The additional advantage of using this approach is that the value of K_d^{exch} can be easily predicted on the basis of soil characteristics, such as binding capacity of the soil (number and selectivity of sorption sites), and the composition of the soil solution (concentration of sorption-competitive ions present in the solution). However, a K_d deduced from a laboratory test cannot be unequivocally considered to be a K_d^{exch}, since the nature of the sorption process for a given radionuclide may lead to a *quasi* instantaneous irreversible sorption, and, in other cases, long contact times, for instance, may result in a fraction of the radionuclide activity becoming irreversible sorbed, and thus no longer participating in the soil – soil solution equilibrium. Besides this, the large number of approaches used to quantify K_d values, and the contrasting experimental conditions applied in each case, lead to wide ranges of K_d values being obtained for similar soil and radionuclide combinations. The variation in approaches adopted often makes it difficult to compare among K_d values derived from laboratory experiments.

In this document, generally, the term K_d is utilized to describe the radionuclide distribution coefficient, although other terms are used, as required in specific cases.

1.2. Experimental methods used to estimate the K_d values

Most common approaches derive K_d values from field-contaminated soils, and from sorption and mass transport experiments at a laboratory scale with initially non-contaminated soils.

1.2.1. K_d values from field contaminated soils

The K_d values can be quantified from the radionuclide concentration in the soil solid phase divided by the concentration of the radionuclide in the soil solution obtained from the contaminated soil [1]. This approach is reliable when the level of contamination is high enough to disregard the uncertainty in obtaining and measuring a representative sample of the soil solution.

This approach may lead to K_d values higher than those resulting from a laboratory sorption test, because the radionuclide quantified in the solid phase of the contaminated soil may include sorbed radionuclide not available for exchange with the soil solution due to the time elapsed since the radionuclide incorporation. Therefore, this approach is not recommended for quantification of K_d^{exch}.

1.2.2. Laboratory sorption experiments

Among the laboratory studies, the approach applied most often is to undertake sorption experiments on non-contaminated soils, mainly using batch methods. Experimental conditions may be extremely different from one experiment to another, since a harmonized procedure has not been established, although recommended methods are available from several organizations [2-3].

Sorption experiments are conducted at various radionuclide activity and (more pertinently) mass concentrations, in different hydro chemical and mineralogical contexts. Experimental conditions, such as the composition of the contact solution, contact (shaking) time,

volume/mass ratios, and filtration of the resulting solution, may differ. Regarding filtration, the absence or presence of this step, as well as the pore size of the filter can be of a major significance for those radionuclides exhibiting an association with colloids, since colloids may be mobile and in batch experiments the colloid fraction may either be associated with the solution or solid phase depending on the filtration employed. As the competitive effect of major ions has been widely described, especially when dealing with specific sorption sites, it is recommended that sorption experiments should be performed that simulate as closely as possible field conditions of interest, e.g. by reproducing the pH and ionic composition of the soil solution in the sorption medium [4-5].

Care is needed to avoid undertaking experiments at higher concentrations than could be expected after a radioactive release. In particular, excessively high mass concentrations may arise in simulations of radionuclide sorption using stable or very long-lived isotopes of the element or analogue elements. It is important to ensure that at no time in the experiment do solution concentrations exceed the solubility limit for the radionuclide or stable element being studied.

1.2.3. Laboratory mass transport experiments

Another experimental approach is to derive K_d values from the diffusion pattern of a radionuclide in compacted soils, in column or diffusion cells [6].

In a porous medium like soils, the radionuclide diffusion process differs from diffusion in free water. An effective diffusion coefficient (D_e; m^2/s) must, therefore, be defined. Only the pores that contribute to the transport of the dissolved radionuclide species have to be considered (the diffusion-accessible porosity, Φ), although in most cases (mainly when the relative saturation tends to one and for cationic radionuclides) to use the total porosity (ε) is an adequate approximation. In the case of radionuclides with significant sorption, an apparent diffusion coefficient (D_a; m^2/s) can be calculated from the diffusion profile into the sample. The latter diffusion coefficient takes into account the retardation of the radionuclide due to interactions with the porous material. It can be written:

$$D_a = \frac{D_e}{f_{ret}} \tag{1}$$

where f_{ret} is the Retardation Factor. If we hypothesize a linear sorption pattern, with a constant K_d in the range of concentrations studied, the f_{ret} can be defined as:

$$f_{ret} = 1 + (\frac{\rho}{\varepsilon}) \cdot K_d \tag{2}$$

where ρ is the dry bulk density of the soil.

Scarce data comparing K_d values from batch and diffusion experiments are available to date, and conclusions on whether the batch sorption methods over- or under-estimated K_d values are still contradictory [7-8]. However, overall more cases are described where the K_d values derived from diffusion experiments were lower than those derived from batch experiments than *vice versa* [9-10], mostly due to in the experimental conditions adopted in the batch studies, such as the volume/mass ratio and contact time.

1.3. Mechanistic approach to prediction of K_d values

The increased knowledge of interaction mechanisms between certain radionuclides and solid materials allows review of K_d values in terms of a more fundamental description of underlying processes. In this section, the mechanisms responsible for radionuclide sorption are described for a number of radionuclides, thus introducing the concept of *cofactors* influencing soil-radionuclide interactions. An advantage of using cofactors for grouping soils is that the variability of K_d values may decrease considerably with respect to the variability observed when the classification is based solely on sand, clay, and organic matter contents.

1.3.1. Cofactors for radiostrontium

The solid-liquid partitioning of a number of radionuclides (*RN*), such as radiostrontium, may be better understood by reference to the partitioning of an analogue (sorption competitive) ion (*AN*), characterized by similar sorption behaviour. In this approach:

$$K_d(RN) = K_d(AN) \cdot K_c(\frac{RN}{AN}) \tag{3}$$

where the $K_d(RN)$ is calculated by a linear amplification of the $K_d(AN)$ by a factor equal to the RN-AN selectivity coefficient at the sorption sites $K_c(\frac{RN}{AN})$.

Regarding radiostrontium, $K_d(Sr)$ can be predicted from the ratio of the Ca and Mg in the exchangeable complex in soil solids (in $cmol_c/kg$) to the sum of the concentrations of Ca and Mg in the soil solution (in $cmol_c/L$) [11-12], amplified by the trace selectivity coefficient Sr-to-Ca and Sr-to-Mg, K_c (Sr/Ca-Mg), which corresponds to equation (4):

$$K_d(Sr) = K_c(Sr/Ca-Mg)\frac{Ca_{exch} + Mg_{exch}}{Ca_{ss} + Mg_{ss}} \tag{4}$$

As the K_c (Sr/Ca-Mg) is reported to be close to 1 [13], in most cases similar trace selectivity coefficients Sr-to-Ca and Sr-to-Mg may be assumed to derive a simpler model. Therefore, equation 4 can be simplified to:

$$K_d(Sr) = \frac{Ca_{exch} + Mg_{exch}}{Ca_{ss} + Mg_{ss}} \tag{5}$$

If data on exchangeable cations are not available, the ratio of the cationic exchange capacity (CEC, in $cmol_c/kg$, which is usually quantified in routine soil analyses), to the sum of the concentrations of Ca and Mg in the soil solution can be used as a satisfactory approach to estimate the K_d(Sr), especially when dealing with soils with a saturated exchange complex [11].

Another approach to the prediction of $K_d(Sr)$ is based on correlating the $K_d(Sr)$ to other soil properties that are also easily measured in routine studies. An example of this is to relate the $K_d(Sr)$ to the Cation Distribution Ratio (CDR), defined as the value of the cationic exchange capacity (CEC, $cmol_c/kg$) divided by the electrical conductivity (EC, mS/cm) in the soil solution [14]. This correlation is easily explained by the fact that the electrical conductivity is controlled by the concentrations of major cations in the soil solution, especially Ca and Mg:

$$EC\ (mS\ cm^{-1}) \approx 1000\ [Na_{ss} + K_{ss} + NH_4^+{}_{ss} + Mg_{ss} + Ca_{ss}]\ (cmol_c/L) \quad (6)$$

The resultant regression equation for the set of soils examined is [14]:

$$K_d\ (Sr)\ (L/kg) = 2.1\ CDR\ (L/kg) \quad (7)$$

1.3.2. Cofactors for radiocaesium

One approach to prediction of the value of $K_d(Cs)$ is based on the application of the Radiocaesium Interception Potential (RIP) concept. The RIP value estimates the capacity of a given soil to specifically sorb Cs. The most common protocol to determine the RIP is based on pre-equilibrating the samples with a solution containing 100 mmol/L of Ca and 0.5 mmol/L of K (m_K). After pre-equilibrating the samples, these are equilibrated with the same solution, but labelled with radiocaesium. The distribution coefficients ($K_d(Cs)$) are obtained by measuring the radiocaesium activity in the supernatant, before and after the equilibration. The calculated product $K_d(Cs) \times m_K$ defines the RIP value (in mmol/kg). Details can be found elsewhere [15].

The RIP value relates to the content and selectivity of expandable clays, especially illite and other 2:1 phyllosilicates, in which Frayed Edge Sites (FES), which are specific sites for Cs sorption, are present [16]. Other exchange sites are of little relevance for Cs sorption [17-19], except when dealing with soils with extremely low clay content (*e.g.* organic matter content over 90%; highly sandy podzols), in which Cs may also be sorbed at other, less specific sites [20].

As Cs sorption is controlled by the specific FES, the Cs solid-liquid distribution coefficient at these sites ($K_d^{FES}(Cs)$) accounts for more than 80 % of the total sorption process [19]. The $K_d^{FES}(Cs)$ can be predicted by dividing the RIP value by the sum of K and NH_4^+ concentrations in the soil solution, the latter amplified by the NH_4-to-K trace selectivity coefficient in the FES ($K_c^{FES}(NH_4/K)$) [16]. This parameter, which can be easily quantified by laboratory experiments, ranges from 4 to 8 for soils in which specific sites control Cs sorption quantitatively, and down to 2 in those soils where sorption at regular exchange sites may be significant [20-21].

For a more accurate prediction of the value of K_d (Cs), a second term must be added to account for Cs sorption at regular exchange sites ($K_d^{RES}(Cs)$) by dividing the sum of the exchangeable K and NH_4^+ by the sum of K and NH_4^+ concentrations in the soil solution (in mmol/L), assuming a selectivity coefficient NH_4/K of approximately 1 at these sites. The equation derived may be written as follows:

$$K_d(Cs) = K_d^{FES}(Cs) + K_d^{RES}(Cs) = \frac{RIP}{K_{ss} + K_c^{FES}(NH_4/K)\cdot NH_{4\,ss}^+} + \frac{K_{exch} + NH_{4\,exch}^+}{K_{ss} + NH_{4\,ss}^+} \quad (8)$$

For the case of highly saline soils, near to marshlands, with high Na concentrations in the soil solution, equation 8 may be slightly modified to include the potential competitive role of Na and its effect on the quantification of $K_d{}^{FES}$. The equation may be rewritten as follows:

$$K_d(Cs) = K_d^{FES}(Cs) + K_d^{RES}(Cs) =$$

$$= \frac{RIP}{K_{ss} + K_c^{FES}(NH_4 / K)\cdot NH_{4\,ss}^{+} + K_c^{FES}(Na / K)\cdot Na_{ss}} + \frac{K_{exch} + NH_{4\,exch}^{+}}{K_{ss} + NH_{4\,ss}^{+}} \qquad (9)$$

where the K_c^{FES} (Na/K) term is the Na-to-K trace selectivity coefficient in the FES. As this coefficient takes values of around 0.02 [15], the role of Na will have a significant effect only in those contexts in which an unusually high Na concentration occurs.

Equations (8) and (9) may be simplified by considering that Na and NH_4^+ concentrations are generally much lower than K concentrations, as is the case for most agricultural systems with mineral soils. As the value of K_d^{FES} (Cs) is much larger than the value of K_d^{RES} (Cs), K_d (Cs) is reasonably well predicted by equation 10, except for those soil types (upland, peat soils; soils affected by flooding) in which $NH_4^+{}_{ss}$ can be significant:

$$K_d(Cs) = \frac{RIP}{K_{ss}} \qquad (10)$$

A major limitation of this approach to predicting the value of K_d (Cs) is the fact that a K_d value must be obtained to quantify the *RIP* value. To date, attempts to predict the *RIP* value from soil properties have been only partially successful. Waegeneers et al. showed that the *RIP* value depended not only on the clay content, but also on the type of clay and geological origin of the soil [22]. After performing a stepwise regression analysis, the clay content alone accounted for up to the 71% of the variance of the *RIP* in the most favourable set of soils, whereas for another set of soils it explained only 13% of the variance. Regarding the K_d database compiled for this IAEA-TECDOC (see below), the *RIP* and the clay content had a correlation coefficient near to 0.7.

1.3.3. Cofactors for uranium and radium[1]

Uranium occurs in the valences +3, +4, +5 and +6. In soils, the valences +4 and +6 are the most important. U (IV) dominates at $E_h < 200$ mV [23], which is typical for waterlogged to wet soils. U (IV) tends to strongly bind to organic matter and to precipitate, and it is, therefore, immobile. The most oxidized state for U in nature is U (VI). At pH below 5, U (VI) is present as the uranyl ion, UO_2^{2+}. At a higher pH, the uranyl ion hydrolyzes, forming a number of aqueous hydroxide complexes, according to the general hydrolysis reaction:

$$UO_2^{2+} + yH_20 \Leftrightarrow UO_2(OH)_y + yH^+$$

The hydrolysed species (*e.g.* UO_2OH^+, $UO_2(OH)_2{}^0$ and $(UO_2)_2(OH)_2{}^{2+}$) often dominate U(VI) speciation in the absence of dissolved inorganic ligands (carbonate, fluoride, sulphate and phosphate). In the presence of dissolved carbonates, U(VI) forms strong carbonate complexes, such as $(UO_2)_2CO_3(OH)_3{}^-$, UO_2CO_3, $UO_2(CO_3)^{2-}$, $UO_2(CO_3)_3{}^{4-}$. At the pH range of 6 to 10, uranium is largely partitioned into three stable complexes: the acid biphosphate, bicarbonate and tricarbonate [24]. The oxidized uranyl ion phosphate, sulphate and carbonate complexes are soluble and readily transported.

---

[1] The section was written by H. VANDENHOVE, SCK-CEN, Belgian Nuclear Research Centre, Mol, Belgium.

The above description of the uranium speciation under oxidizing conditions points out the importance of pH on uranium behaviour. EPA [25] performed an extensive review of K_d (U) values for soils, crushed rock material and single-mineral phases, which indicated that pH and dissolved carbonate concentrations are the two most important factors influencing the sorption behaviour of U(VI). Dissolved carbonate species increase uranium availability through the formation of strong anionic carbonate complexes, especially in alkaline conditions. The complexity of these reactions requires application of geochemical reaction codes and surface complexation models as the best approaches to predicting values of K_d (U).

Since so many factors affect K_d (U) (pH, dissolved carbonates, amorphous Fe content, soil mineralogy, CEC, soil organic matter content), K_d (U) exhibits large variability. However, K_d(U) values show a specific trend in relation to the pH. In general, the sorption of uranium by soils is low at pH values less than 3, increases rapidly with increasing pH from 3 to 5, reaching a maximum in the pH range from 5 to 7 and then decreases with increasing pH at pH values greater than 7 [25].

One important source of variability in the relationship between K_d (U) and pH is the heterogeneity in soil mineralogy. Soils containing larger percentages of iron oxide minerals and mineral coatings and/or clay minerals will exhibit higher sorption than soils dominated by quartz and feldspar minerals.

Echevarria et al. explored the effect of pH on the sorption of uranium in French soils [26]. They deduced a linear relationship for soils ranging in pH from 5.8–8.8 [$\log K_d = -1.25 \times \text{pH} + 10.9$, $R^2=0.89$]. When including K_d *(U)*–pH values for Canadian soils in their regression analysis, the same influence on K_d (U) was found [$\log K_d = -1.29 \times \text{pH} + 11.0$, $R^2=0.76$]. Vandenhove et al. [27] explored the effect of soil properties on uranium availability for eighteen soils, and a similar linear decrease of $\log K_d$ with pH was observed for soils with pH ≥6 [$\log K_d = -1.18 \times \text{pH} + 10.8$, $R^2=0.65$], which was explained by the increased amount of soluble uranyl-carbonate complexes at high pH. For soils with pH<6, these latter authors suggested exploring the possibility of relating the K_d(U) to organic matter (OM, %) [K_d(U) = $1963 \times \text{OM} - 5432$, $R^2=0.78$] or to concentration of amorphous iron in soil (mg kg^{-1}) [K_d(U) = $1.02 \times \text{Fe}_{\text{amorphous}} + 1691$, $R^2=0.88$]. Considering all soils (complete pH range), these relationships remained significant [K_d (U) = $1591 \times \text{OM} - 3362$, $R^2=0.70$; K_d (U) = $1.08\ \text{Fe}_{\text{amorphous}} + 2783$, $R^2=0.88$].

Radium occurs in nature as a divalent cation. It has a high affinity for the regular exchange sites of the soil, as shown by the fact that organic matter sorbs about ten times as much radium as clay [28]. It also co-precipitates with barium and strontium to form insoluble sulphates. Due to its alkaline character, it is not easily complexed. There has been limited research on defining K_d (Ra). In geochemical equilibrium models, often data for Ba, which may act as analogue, are recommended for assessing the behaviour of radium. High Ca levels in the soil solution or exchangeable phase and low organic matter and clay content are conducive to higher radium availability. Overall, not enough data have been assembled so far to mathematically relate K_d(Ra) to any of these soil properties. Vandenhove et al., exploring the effect of soil properties on radium availability [29] in a small-scale study covering 8 soils, concluded that K_d(Ra) could be predicted by CEC [K_d(Ra) = $0.71 \times \text{CEC} - 0.64$, $R^2=0.91$] and soil organic matter content (%) [K_d(Ra) = $27 \times \text{OM}–27$, $R^2=0.83$].

1.3.4. Cofactors for other radionuclides

Other soil properties are as significant as mineral and organic matter contents in governing soil-radionuclide interactions for a large number of radionuclides. These other properties,

alone or combined with textural information, can be used as cofactors for classification of soils in order to reduce the variability in the ranges of K_d values.

As for U, pH strongly affects the sorption of heavy metal radionuclides. Chemical speciation may also affect the K_d values of several radionuclides, since different species (*e.g.* oxidized-reduced species; oxyanions) may have contrasting sorption behaviour. As an example of this, a major effect of speciation on K_d values has been observed for selenium. Whereas selenate shows K_d values close to zero, for selenite they are up to a few thousand L kg^{-1} [30]. For iodine, the effect of the speciation (iodide and iodate) on the K_d should also be initially taken into account, as well as the content of organic matter and Fe and Al oxides, microbial activity and the water regime of the soil [31].

1.4. K_d database and ranges of K_d values

Estimates of K_d values for soils grouped on the basis of the texture and organic matter content criterion as well as on cofactors are given in Tables 1-16 and in Figs. 1-3. Data come from field and laboratory experiments, with various contamination sources, considering mainly the scenario of soils contaminated by radionuclides, and from references mostly from 1990 onwards, including the former Technical Reports Series No. 364 and related reports [32-34], reviewed papers, and grey literature (PhD theses; reports). Around 80 references (see Appendix) have been finally accepted to elaborate the K_d database. In most cases, data from experiments using other materials (*e.g.* sediments; pure soil phases such as clays or Fe-Mn-Al oxides; rock materials) or stable elements have not been considered. Data from radioisotopes of the same radioelement have been pooled. From around 2900 records for 67 elements, caesium and strontium have the highest number of observations. A few elements have more than 100 entries each, such as iodine, uranium, cobalt, potassium, antimony and selenium.

Comparing the new database with the former Technical Reports Series No. 364, no new data are available for radionuclides of a few elements (Ac, Br, Ho, Pa, Rb, Si and Sm), and data presented in the tables originate from the former Technical Reports Series No. 364. For a number of elements (Ag, Be, Bi, Hf, Mo, P, Pd, Sn, and Ta) although some new data are available, most originate also from the former Technical Reports Series No. 364. In contrast, data on elements not covered in the former Technical Reports Series No. 364 (As, Ba, Cl, Cu, Dy, Ga, H, Hg, In, Ir, K, La, Lu, Mg, Na, Pm, Pt, Rh, Sc, Tb, Te, Tm, V, and Y) have been included. However, for a few cases, data come from a single reference.

The K_d values, expressed in L kg^{-1}, have been grouped according to the organic matter content and sand and clay percentages of the mineral matter content (texture/OM criterion). This criterion for soil classification is described in earlier.[1]Besides presenting the K_d data according to the texture/OM criterion, the K_d values are also grouped for a limited number of radionuclides according to the cofactor approach, using specific soil properties (radiostrontium and radiocaesium), soil pH (uranium and heavy metal radionuclides with a sufficiently large number of observations) and speciation data and water regime (radioiodine).

Although AM and SD values are given, GM and GSD are preferred to describe K_d data, since the log-transformed K_d values are typically normally distributed. Exploratory analysis, based on box-and-whisker plots, has been applied to exclude potential outliers and thus to decrease

[1] See paper by Fesenko et al. 'Radioecological Definitions, Soil, Plant Classifications and Reference Ecological Data For Radiological Assessments' in this publication.

data variability. A potential outlier is identified when it is beyond three times the interquartile ranges defined by the box-and-whisker plots.

1.4.1. Strontium

Whereas grouping the K_d (Sr) according to soil CEC values is a slightly worse approach than the soil texture/OM criterion (since there is not a consistent relationship between the CEC value and K_d (Sr)), grouping according to the CEC/$(Ca+Mg)_{ss}$ ratio leads to a good estimation of the K_d (Sr) and to the construction of ranges with lower variability (Tables 1 and 2, Fig. 1).

TABLE 1 K_d (Sr) FOR SOILS GROUPED ACCORDING TO THE TEXTURE/OM CRITERION (L kg^{-1})

Soil group	N	GM	GSD	AM	SD	Min	Max	# ref.
All soils	255	5.2×10^1	6	2.0×10^2	5.4×10^2	4.0×10^{-1}	6.5×10^3	28
Sand	65	2.2×10^1	6	1.1×10^2	3.2×10^2	4.0×10^{-1}	2.4×10^3	19
Loam	120	5.7×10^1	5	1.6×10^2	2.9×10^2	2.0	2.5×10^3	12
Clay	19	9.5×10^1	4	1.9×10^2	2.0×10^2	9.0	7.5×10^2	5
Organic	37	1.1×10^2	6	4.9×10^2	1.2×10^3	3.0	6.5×10^3	10
Unspecified	14	7.3×10^1	3	1.1×10^2	9.0×10^1	8.0	2.7×10^2	8

TABLE 2 K_d (Sr) FOR SOILS GROUPED ACCORDING TO THE COFACTOR CRITERION (L kg^{-1})

Soil group	N	GM	GSD	AM	SD	Min	Max
CEC < 10	50	2.1×10^1	4	5.0×10^1	6.0×10^1	4.0×10^{-1}	3.3×10^2
10 < CEC < 20	44	2.0×10^2	2	2.3×10^2	1.0×10^2	3.3×10^1	4.6×10^2
20 < CEC < 50	82	6.2×10^1	6	2.9×10^2	8.6×10^2	1.0	6.5×10^3
CEC > 50	25	9.4×10^1	6	2.9×10^2	4.1×10^2	5.0	1.8×10^3
$CEC/M_{ss} < 15$	25	4.2	2	5.4	3	4.0×10^{-1}	1.5×10^1
$15 < CEC/M_{ss} < 150$	28	2.2×10^1	3	3.3×10^1	3.0×10^1	4.0	1.1×10^2
$150 < CEC/M_{ss} < 500$	18	1.7×10^2	2	1.8×10^2	6.0×10^1	7.7×10^1	2.7×10^2
$CEC/M_{ss} > 500$	25	3.2×10^2	2	4.1×10^2	3.5×10^2	8.1×10^1	1.8×10^3

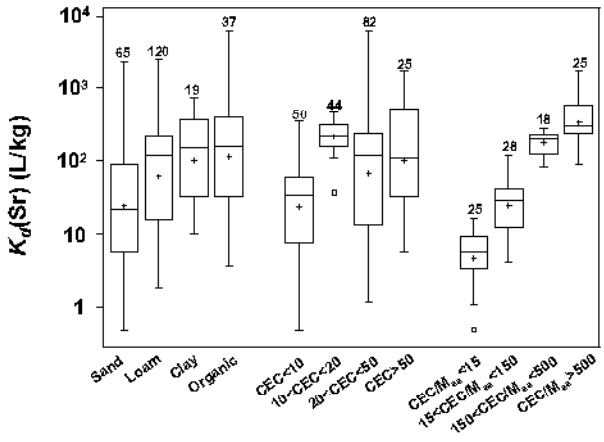

FIG. 1. Box-and-whisker plots of K_d (Sr) for soils grouped according to the texture/OM and cofactor criteria. The box encloses the middle 50% of the distribution of values, and the median is represented as a horizontal line inside the box. Vertical lines extend to the limits of the 1.5 interquartile ranges. Other symbols represent GM (+) and points at >1.5 interquartile ranges (□).

1.4.2. Caesium

As expected, the K_d (Cs) increases consistently with the clay content, and exhibits the lowest GM value in the organic soils. The K_d (Cs) can also be estimated for soils grouped according to their RIP values, and with respect to the ratio RIP/K_{ss}, which leads to a good prediction of the K_d (Cs) and to ranges of values of K_d (Cs) with the lowest variability (Tables 3 and 4, Fig. 2).

TABLE 3 K_d (Cs) FOR SOILS GROUPED ACCORDING TO THE TEXTURE/OM CRITERION (L/kg)

Soil group	N	GM	GSD	AM	SD	Min	Max	# ref.
All soils	469	1.2×10^3	7	6.1×10^3	2.1×10^4	4.3	3.8×10^5	32
Sand	114	5.3×10^2	6	2.2×10^3	5.0×10^3	1.0×10^1	3.5×10^4	19
Loam	191	3.5×10^3	4	7.2×10^3	9.9×10^3	3.9×10^1	5.5×10^4	17
Clay	36	5.5×10^3	4	2.2×10^4	6.7×10^4	5.7×10^2	3.8×10^5	9
Organic	108	2.7×10^2	7	3.0×10^3	1.2×10^4	4.3	9.5×10^4	14
Unspecified	20	1.7×10^3	5	6.7×10^3	1.5×10^4	4.0×10^1	5.5×10^4	8

TABLE 4 K_d (Cs) FOR SOILS GROUPED ACCORDING TO THE COFACTOR CRITERION (L/kg)

Soil group	N	GM	GSD	AM	SD	Min	Max
RIP < 150	47	7.4×10^1	2	1.1×10^2	1.3×10^2	1.0×10^1	7.3×10^2
150 < RIP < 1000	78	3.2×10^2	6	1.8×10^3	5.2×10^3	1.0×10^1	3.4×10^4
1000 < RIP < 2500	72	2.4×10^3	4	7.2×10^3	1.5×10^4	6.2×10^1	9.5×10^4
RIP > 2500	60	7.2×10^3	4	2.1×10^4	5.2×10^4	2.2×10^2	3.8×10^5
RIP/K_{ss} < 100	37	8.5×10^1	3	1.5×10^2	1.6×10^2	1.0×10^1	7.0×10^2
100 < RIP/K_{ss} < 1000	85	2.4×10^2	5	7.9×10^2	1.3×10^3	2.0×10^1	5.8×10^3
1000 < RIP/K_{ss} < 10000	78	2.0×10^3	4	4.5×10^3	6.7×10^3	6.2×10^1	3.4×10^4
RIP/K_{ss} > 10000	57	9.9×10^3	4	2.6×10^4	5.5×10^4	2.2×10^2	3.8×10^5

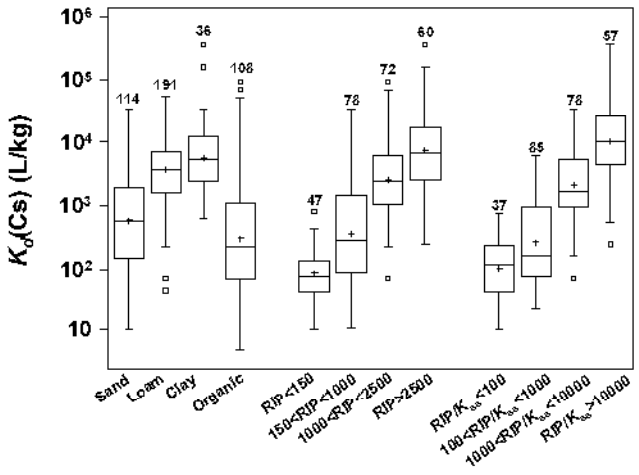

FIG. 2. Box-and-whisker plots of K_d (Cs) for soils grouped according to the texture/OM and cofactor criteria. The box encloses the middle 50% of the distribution of values, and the median is represented as a horizontal line inside the box. Vertical lines extend to the limits of the 1.5 interquartile ranges. Other symbols represent GM (+) and points at >1.5 interquartile ranges (□).

1.4.3. Uranium

Estimates of $K_d(U)$ values for soils grouped based on the texture/organic matter content cretarion and pH are given in Tables 5-6 and in Fig. 3.

Whereas values of K_d (U) do not show any correlation with soil texture, the values of K_d (U) can also be grouped according to the pH of the soil, which leads to ranges of K_d (U) with lower variability and confirms the K_d-pH dependence. A significant 10-fold higher K_d (U) value is observed for the 5-7 pH range.

TABLE 5 K_d (U) FOR SOILS GROUPED ACCORDING TO THE TEXTURE/OM CRITERION (L/kg)

Soil group	N	GM	GSD	AM	SD	Min	Max	# ref.
All soils	178	2.0×10^2	1.2×10^1	2.0×10^2	6.7×10^3	7.0×10^{-1}	6.7×10^4	22
Sand	50	1.1×10^2	1.2×10^1	2.1×10^3	9.5×10^3	7.0×10^{-1}	6.7×10^4	8
Loam	84	3.1×10^2	1.2×10^1	2.5×10^3	6.3×10^3	9.0×10^{-1}	3.9×10^4	12
Clay	12	2.8×10^1	7	1.2×10^2	1.7×10^2	2.6	4.8×10^2	3
Organic	9	1.2×10^3	6	2.9×10^3	2.8×10^3	3.3×10^1	7.6×10^3	7
Unspecified	23	1.7×10^2	6	8.6×10^2	1.7×10^3	1.6×10^1	6.2×10^3	5

TABLE 6 K_d(U) FOR SOILS GROUPED ACCORDING TO THE pH (L/kg)

Soil group	N	GM	GSD	AM	SD	Min	Max
pH < 5	36	7.1×10^1	1.1×10^1	5.4×10^2	1.2×10^3	7.0×10^{-1}	6.7×10^3
5 ≤ pH < 7	78	7.4×10^2	8	4.0×10^3	9.7×10^3	2.6	6.7×10^4
pH ≥7	60	6.5×10^1	8	4.4×10^2	1.1×10^3	9.0×10^{-1}	6.2×10^3

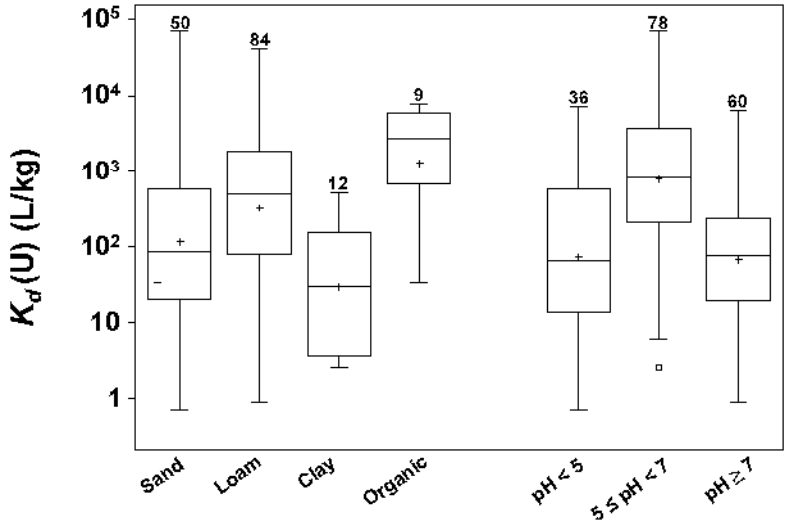

FIG. 3. Box-and-whisker plots of K_d (U) for soils grouped according to the texture/OM and pH criteria. The box encloses the middle 50%, and the median is represented as a horizontal line inside the box. Vertical lines extend to the point within 1.5 interquartile ranges. Other symbols represent GM (+) and points at > 1.5 interquartile ranges (□).

1.4.4. Iodine

K_d (I) values for soils grouped on the basis of the texture and organic matter content criterion as well as data on effect of watter content on K_d values for iodine are presented in Table 7.

The effect of organic matter and water regime can be more significant than the iodine species involved in the sorption, depending on the soil redox potential and factors such as drying temperature and sorption contact time. This indicates a complex dependency of K_d (I) on the organic matter and water content, microbial activity, and oxidizing-reducing conditions.

1.4.5. Heavy metals: Cd, Co, Ni, and Zn

K_d values for some heavy metals (Cd, Co, Ni, Zn) K_d values for soils grouped on the basis of the texture and organic matter content criterion as well as data on effect of pH (excluding organic soils) are given in Tables 8-15.

While there is not a straight relationship between the soil texture and the K_d value for the selected heavy metals, the K_d values of these heavy metal radionuclides in mineral soils show a clear dependence on pH.

2. CHANGES IN SOIL-RADIONUCLIDE INTERACTIONS WITH TIME: SORPTION DYNAMICS

Radionuclide-soil interactions exhibit changes with time. After an extended period since the contamination, radionuclides incorporated in the solid soil phase can occur in exchangeable and non-exchangeable forms. Whereas the exchangeable form includes radionuclide sorbed by the ion-exchange mechanism that is easily transferred to soil solution, the non-exchangeable form refers to radionuclide sorbed by irreversible mechanisms. The significance of the fixation process is controlled by the rate of transition between the mobile and fixed states.

TABLE 7 K_d (I) FOR SOILS GROUPED ACCORDING TO THE TEXTURE/OM CRITERION, SPECIATION, AND ORGANIC MATTER CONTENT (L/kg). ADDITIONAL EFFECT OF WATER CONTENT ON K_d (I)

	Soil group	N	GM	GSD	AM[1]	SD	Min	Max	# ref.
All data	All soils	250	6.9	5	2.5×10^{1}	7.0×10^{1}	1.0×10^{-2}	5.8×10^{2}	9
	Sand	48	4.1	7	1.3×10^{1}	2.0×10^{1}	1.0×10^{-2}	1.3×10^{2}	7
	Loam	129	8.0	4	2.5×10^{1}	7.0×10^{1}	2.0×10^{-1}	5.4×10^{2}	6
	Clay	19	1.1×10^{1}	5	3.1×10^{1}	4.0×10^{1}	1.0	1.8×10^{2}	5
	Organic	11	3.2×10^{1}	3	8.0×10^{1}	1.7×10^{2}	8.5	5.8×10^{2}	4
	Unspecified	43	4.2	6	1.8×10^{1}	6.0×10^{1}	1.0×10^{-1}	3.7×10^{2}	2
I^-	All soils	157	5.4	6	2.5×10^{1}	7.0×10^{1}	1.0×10^{-2}	5.8×10^{2}	6
	Sand	37	3.6	8	1.3×10^{1}	2.0×10^{1}	1.0×10^{-2}	1.3×10^{2}	5
	Loam	74	6.5	5	2.4×10^{1}	7.0×10^{1}	2.0×10^{-1}	5.3×10^{2}	4
	Clay	13	6.8	6	2.1×10^{1}	3.0×10^{1}	1.0	1.2×10^{2}	2
	Organic	9	3.6×10^{1}	4	9.3×10^{1}	1.8×10^{2}	8.5	5.8×10^{2}	3
	Unspecified	24	2.6	6	2.0×10^{1}	7.0×10^{1}	1.0×10^{-1}	3.7×10^{2}	2
IO_3^-	All soils	67	7.9	4	2.3×10^{1}	7.0×10^{1}	4.0×10^{-1}	5.4×10^{2}	2
	Sand	6	3.6	5	1.0×10^{1}	2.0×10^{1}	4.0×10^{-1}	4.1×10^{1}	1
	Loam	41	8.9	4	2.9×10^{1}	8.0×10^{1}	1.0	5.4×10^{2}	2

	Organic	1	-	-	1.3×10^{1}	-	-	-	1
	Unspecified	19	7.7	5	1.6×10^{1}	2.0×10^{1}	4.0×10^{-1}	5.8×10^{1}	2
All data	OM < 2	75	2.3	6	7.3	1.0×10^{1}	1.0×10^{-2}	5.7×10^{1}	
	2 < OM < 5	106	9.1	3	2.0×10^{1}	5.4×10^{1}	6.0×10^{-1}	5.4×10^{2}	
	5 < OM < 10	27	1.8×10^{1}	4	3.8×10^{1}	5.5×10^{1}	2.0	2.6×10^{2}	
	OM > 10	19	3.4×10^{1}	3	8.7×10^{1}	1.7×10^{2}	8.5	5.8×10^{2}	
Effect of water content on the K_d [30, 35-36]									3
I^-	Sand-dry	1	-	-	2.8×10^{1}	-	-	-	
	Sand-wet	1	-	-	3.2×10^{1}	-	-	-	
	Unspecified-dry	9	1.9×10^{1}	6	7.5×10^{1}	1.5×10^{2}	8.0×10^{-1}	4.7×10^{2}	
	Unspecified-wet	9	5.5×10^{2}	6	1.4×10^{3}	2.2×10^{3}	8.0	7.0×10^{3}	
IO_3^-	Sand-dry	1	-	-	2.8×10^{1}	-	-	-	
	Sand-wet	1	-	-	3.5×10^{1}	-	-	-	
	Unspecified-dry	9	1.5×10^{1}	7	8.5×10^{1}	1.8×10^{2}	7.0×10^{-1}	5.5×10^{2}	
	Unspecified-wet	9	6.8×10^{2}	7	1.8×10^{3}	2.3×10^{3}	8.0	7.5×10^{3}	

[1]Single value is given in this column if N=1.

TABLE 8 K_d (Cd) FOR SOILS GROUPED ACCORDING TO THE TEXTURE/OM CRITERION (L/kg)

Soil group	N	GM	GSD	AM	SD	Min	Max	# ref.
All soils	61	1.5×10^{2}	9	7.7×10^{2}	1.3×10^{3}	2.0	7.0×10^{3}	11
Sand	30	1.1×10^{2}	8	4.2×10^{2}	5.3×10^{2}	2.0	1.8×10^{3}	5
Loam	5	1.0×10^{2}	7	4.1×10^{2}	7.3×10^{2}	9.2	1.7×10^{3}	4
Clay	4	1.3×10^{2}	1.5×10^{1}	8.2×10^{2}	1.3×10^{3}	6.9	2.7×10^{3}	3
Organic	13	6.5×10^{2}	6	1.7×10^{3}	2.2×10^{3}	9.6	7.0×10^{3}	6
Unspecified	9	6.8×10^{1}	1.5×10^{1}	7.3×10^{2}	1.4×10^{3}	6.2	4.4×10^{3}	4

TABLE 9 K_d (Cd) FOR SOILS GROUPED ACCORDING TO THE pH (EXCLUDING ORGANIC SOILS; L/kg)

Soil group	N	GM	GSD	AM	SD	Min	Max
pH < 5	8	1.1×10^{1}	3	1.9×10^{1}	2.0×10^{1}	2.0	6.4×10^{1}
5 < pH < 6.5	11	1.8×10^{1}	4	5.4×10^{1}	9.0×10^{1}	6.2	2.5×10^{2}
pH > 6.5	24	3.8×10^{2}	6	9.2×10^{2}	1.0×10^{2}	3.7	4.4×10^{3}

TABLE 10 K_d (Co) FOR SOILS GROUPED ACCORDING TO THE TEXTURE/OM CRITERION (L/kg)

Soil group	N	GM	GSD	AM	SD	Min	Max	# ref.
All soils	118	4.8×10^{2}	1.6×10^{1}	6.3×10^{3}	1.7×10^{4}	2.0	1.0×10^{5}	8
Sand	18	2.6×10^{2}	1.8×10^{1}	4.8×10^{3}	1.1×10^{4}	5.0	3.7×10^{4}	4
Loam	71	8.1×10^{2}	1.5×10^{1}	6.6×10^{3}	1.8×10^{4}	2.0	1.0×10^{5}	5
Clay	10	3.8×10^{3}	6	1.6×10^{4}	3.2×10^{4}	5.4×10^{2}	9.9×10^{4}	3
Organic	17	8.7×10^{1}	9	7.0×10^{2}	1.6×10^{3}	4.0	5.8×10^{3}	4
Unspecified	2	-	-	7.5×10^{3}	-	1.3×10^{2}	1.5×10^{4}	2

TABLE 11 K_d (Co) FOR SOILS GROUPED ACCORDING TO THE pH (EXCLUDING ORGANIC SOILS; L/kg)

Soil group	N	GM	GSD	AM	SD	Min	Max
pH < 5	21	1.2×10^1	5	3.5×10^1	5.0×10^1	2.0	1.5×10^2
5 < pH < 6.5	50	1.9×10^3	5	9.5×10^3	2.0×10^4	2.9×10^1	9.9×10^4
pH > 6.5	26	4.6×10^3	4	1.0×10^4	2.4×10^4	5.5×10^2	1.0×10^5

TABLE 12 K_d (Ni) FOR SOILS GROUPED ACCORDING TO THE TEXTURE/OM CRITERION (L/kg)

Soil group	N	GM	GSD	AM	SD	Min	Max	# ref.
All soils	64	2.8×10^2	7	9.5×10^2	1.4×10^3	3.0	7.2×10^3	12
Sand	26	1.3×10^2	1.0×10^1	9.4×10^2	1.8×10^3	3.0	7.2×10^3	4
Loam	14	1.8×10^2	5	4.1×10^2	4.1×10^2	7.7	1.2×10^3	6
Clay	12	9.3×10^2	2	1.2×10^3	9.4×10^2	2.5×10^2	3.2×10^3	5
Organic	8	1.1×10^3	2	1.4×10^3	1.5×10^3	4.1×10^2	5.0×10^3	3
Unspecified	4	4.8×10^2	8	1.1×10^3	9.6×10^2	2.2×10^1	2.3×10^3	3

TABLE 13 K_d (Ni) FOR SOILS GROUPED ACCORDING TO THE pH (EXCLUDING ORGANIC SOILS; L/kg)

Soil group	N	GM	GSD	AM	SD	Min	Max
pH < 5	10	1.4×10^1	2	1.8×10^1	1.0×10^1	3.0	4.8×10^1
5 < pH < 6.5	11	5.8×10^1	4	1.6×10^2	3.0×10^2	7.0	1.1×10^3
pH > 6.5	30	8.2×10^2	3	1.4×10^3	1.6×10^3	4.0×10^1	7.3×10^3

TABLE 14 K_d (Zn) FOR SOILS GROUPED ACCORDING TO THE TEXTURE/OM CRITERION (L/kg)

Soil group	N	GM	GSD	AM	SD	Min	Max	# ref.
All soils	92	9.5×10^2	1.1×10^1	5.2×10^3	1.6×10^4	9.0×10^{-1}	1.5×10^5	11
Sand	17	1.1×10^2	2.3×10^1	2.6×10^3	6.8×10^3	9.0×10^{-1}	2.8×10^4	6
Loam	48	2.4×10^3	4	7.6×10^3	2.2×10^4	2.1×10^2	1.5×10^5	4
Clay	8	2.4×10^3	2	3.2×10^3	2.4×10^3	4.8×10^2	6.9×10^3	3
Organic	12	5.6×10^2	8	1.9×10^3	2.5×10^3	9.7	7.6×10^3	6
Unspecified	7	2.4×10^2	3.5×10^1	2.6×10^3	2.8×10^3	4.6	6.2×10^3	5

TABLE 15 K_d (Zn) FOR SOILS GROUPED ACCORDING TO THE pH (EXCLUDING ORGANIC SOILS; L/kg)

	N	GM	GSD	AM	SD	Min	Max
pH < 5	9	8.2	8	6.0×10^1	1.1×10^2	0.9×10^{-1}	3.0×10^2
5 < pH < 6.5	49	1.6×10^3	6	4.2×10^3	6.0×10^3	6.2	3.0×10^4
pH > 6.5	17	4.3×10^3	4	1.4×10^4	3.6×10^4	4.4×10^2	1.5×10^5

1.4.6. Miscellany of elements

TABLE 16 K_d FOR SOILS GROUPED ACCORDING TO THE TEXTURE/OM CRITERION (L/kg)

Element	Soil group	N	GM	GSD	AM/Value	SD	Min	Max	# ref.
Ac	All soils	4	1.7×10^{3}	3	2.4×10^{3}	2.0×10^{3}	4.5×10^{2}	5.4×10^{3}	1[a]
	Sand	1	-	-	4.5×10^{2}	-	-	-	1
	Loam	1	-	-	1.5×10^{3}	-	-	-	1
	Clay	1	-	-	2.4×10^{3}	-	-	-	1
	Organic	1	-	-	5.4×10^{3}	-	-	-	1
Ag	All soils	9	3.8×10^{2}	7	2.3×10^{3}	5.0×10^{3}	3.6×10^{1}	1.5×10^{4}	5
	Sand	3	1.3×10^{2}	5	2.7×10^{2}	3.7×10^{2}	3.6×10^{1}	7.0×10^{2}	3
	Loam	1	-	-	1.2×10^{2}	-	-	-	1[a]
	Clay	1	-	-	1.8×10^{2}	-	-	-	1[a]
	Organic	2	-	-	9.7×10^{3}	-	4.4×10^{3}	1.5×10^{4}	2
	Unspecified	2	-	-	2.6×10^{2}	-	1.2×10^{2}	4.0×10^{2}	2
Am	All soils	62	2.6×10^{3}	6	1.0×10^{4}	1.8×10^{4}	5.0×10^{1}	1.1×10^{5}	6
	Sand	17	1.0×10^{3}	7	5.1×10^{3}	1.0×10^{4}	6.7×10^{1}	3.7×10^{4}	4
	Loam	31	4.2×10^{3}	6	1.2×10^{4}	1.6×10^{4}	5.0×10^{1}	4.8×10^{4}	5
	Clay	1	-	-	8.1×10^{3}	-	-	-	1[a]
	Organic	13	2.5×10^{3}	5	1.1×10^{4}	3.0×10^{4}	2.1×10^{2}	1.1×10^{5}	4
As	All soils	7	5.5×10^{2}	5	1.2×10^{3}	1.2×10^{3}	2.5×10^{1}	3.0×10^{3}	3
	Sand	4	2.1×10^{2}	5	4.7×10^{2}	6.0×10^{2}	2.5×10^{1}	1.4×10^{3}	2
	Loam	1	-	-	1.0×10^{3}	-	-	-	1
	Unspecified	2	-	-	2.8×10^{3}	-	2.5×10^{3}	3.0×10^{3}	2
Ba	Loam	1	-	-	4.0×10^{-1}	-	-	-	1
Be	All soils	5	9.9×10^{2}	2	1.3×10^{3}	1.0×10^{3}	2.4×10^{2}	3.0×10^{3}	2
	Sand	1	-	-	2.4×10^{2}	-	-	-	1[a]
	Loam	1	-	-	8.1×10^{2}	-	-	-	1[a]
	Clay	1	-	-	1.3×10^{3}	-	-	-	1[a]
	Organic	1	-	-	3.0×10^{3}	-	-	-	1[a]
	Unspecified	1	-	-	1.3×10^{3}	-	-	-	1
Bi	All soils	6	4.8×10^{2}	2	6.1×10^{2}	4.7×10^{2}	1.2×10^{2}	1.5×10^{3}	2
	Sand	2	-	-	3.0×10^{2}	-	1.2×10^{2}	4.9×10^{2}	2[a,b]
	Loam	1	-	-	4.0×10^{2}	-	-	-	1[a]
	Clay	1	-	-	6.7×10^{2}	-	-	-	1[a]
	Organic	1	-	-	1.5×10^{3}	-	-	-	1[a]
	Unspecified	1	-	-	4.9×10^{2}	-	-	-	1[b]
Br	All soils	4	5.5×10^{1}	3	8.0×10^{1}	7.0×10^{1}	1.5×10^{1}	1.8×10^{2}	1[a]

	Sand	1	-	-	1.5×10^{1}	-	-	-	1
	Loam	1	-	-	4.9×10^{1}	-	-	-	1
	Clay	1	-	-	7.4×10^{1}	-	-	-	1
	Organic	1	-	-	1.8×10^{2}	-	-	-	1
Ca	All soils	34	8.0	3	1.7×10^{1}	4.0×10^{1}	7.0×10^{-1}	1.1×10^{2}	2
	Sand	7	3.0	4	6.6	1.0×10^{1}	7.0×10^{-1}	2.8×10^{1}	2
	Loam	21	8.3	3	1.4×10^{1}	2.0×10^{1}	2.0	8.9×10^{1}	2
	Clay	5	1.6×10^{1}	3	2.3×10^{1}	2.0×10^{1}	6.0	4.9×10^{1}	2
	Organic	1	-	-	1.1×10^{2}	-	-	-	1
Ce	All soils	11	1.2×10^{3}	5	3.7×10^{3}	5.9×10^{3}	1.2×10^{2}	2.0×10^{4}	5
	Sand	3	4.0×10^{2}	1	4.0×10^{2}	9.0×10^{1}	3.2×10^{2}	4.9×10^{2}	3
	Loam	4	3.0×10^{3}	3	4.1×10^{3}	3.1×10^{3}	6.5×10^{2}	8.1×10^{3}	4
	Clay	3	9.1×10^{2}	1.5×10^{1}	6.8×10^{3}	1.1×10^{4}	1.2×10^{2}	2.0×10^{4}	2
	Organic	1	-	-	3.0×10^{3}	-	-	-	1[a]
Cl	All soils	22	3.0×10^{-1}	3	5.0×10^{-1}	4.0×10^{-1}	4.0×10^{-2}	1.2	4
	Sand	3	5.0×10^{-1}	4	7.0×10^{-1}	5.0×10^{-1}	1.0×10^{-1}	1.1	2
	Loam	10	4.0×10^{-1}	3	5.0×10^{-1}	3.0×10^{-1}	4.0×10^{-2}	9.0×10^{-1}	3
	Clay	5	2.0×10^{-1}	3	4.0×10^{-1}	4.0×10^{-1}	6.0×10^{-2}	9.0×10^{-1}	4
	Organic	2	-	-	7.0×10^{-1}	-	1.0×10^{-1}	1.2	2
	Unspecified	2	-	-	2.0×10^{-1}	-	1.0×10^{-1}	2.0×10^{-1}	1
Cm	All soils	18	9.3×10^{3}	4	1.6×10^{4}	1.4×10^{4}	1.9×10^{2}	5.2×10^{4}	2
	Sand	5	3.4×10^{3}	1.4×10^{1}	1.0×10^{4}	1.3×10^{4}	1.9×10^{2}	3.1×10^{4}	2
	Loam	9	1.9×10^{4}	2	2.3×10^{4}	1.5×10^{4}	6.8×10^{3}	5.2×10^{4}	2
	Clay	1	-	-	5.4×10^{3}	-	-	-	1[a]
	Organic	3	7.4×10^{3}	2	7.9×10^{3}	3.6×10^{3}	5.1×10^{3}	1.2×10^{4}	2
Cr	All soils	31	4.0×10^{1}	2.0×10^{1}	7.3×10^{2}	1.7×10^{3}	1.0	7.9×10^{3}	6
	Sand	9	8.4	8	3.5×10^{1}	4.0×10^{1}	1.2	1.0×10^{2}	4
	Loam	9	4.5×10^{1}	2.3×10^{1}	4.2×10^{2}	5.7×10^{2}	1.0	1.6×10^{3}	3
	Clay	5	1.4×10^{1}	2.0×10^{1}	3.1×10^{2}	6.7×10^{2}	1.0	1.5×10^{3}	2
	Organic	6	1.6×10^{2}	1.0×10^{1}	7.2×10^{2}	1.1×10^{3}	8.3	2.9×10^{3}	3
	Unspecified	2	-	-	6.4×10^{3}	-	4.8×10^{3}	7.9×10^{3}	2
Cu	All soils	11	5.3×10^{2}	3	8.7×10^{2}	8.7×10^{2}	7.6×10^{1}	2.7×10^{3}	4
	Sand	2	-	-	2.3×10^{2}	-	1.3×10^{2}	3.3×10^{2}	1
	Loam	1	-	-	4.8×10^{2}	-	-	-	1
	Clay	2	-	-	2.1×10^{3}	-	1.4×10^{3}	2.7×10^{3}	1
	Organic	4	3.2×10^{2}	3	4.6×10^{2}	3.7×10^{2}	7.6×10^{1}	8.8×10^{2}	2
	Unspecified	2	-	-	1.3×10^{3}	-	5.0×10^{2}	2.1×10^{3}	2
Dy	All soils	2	-	-	1.5×10^{3}	-	8.2×10^{2}	2.1×10^{3}	1[b]
	Sand	1	-	-	8.2×10^{2}	-	-	-	1

	Unspecified	1	-	-	2.1×10^{3}	-	-	-	1
Fe	All soils	23	8.8×10^{2}	2	1.2×10^{3}	1.1×10^{3}	2.2×10^{2}	4.9×10^{3}	2
	Sand	4	3.2×10^{2}	1	3.3×10^{2}	9.0×10^{1}	2.2×10^{2}	4.2×10^{2}	2
	Loam	12	8.9×10^{2}	2	1.1×10^{3}	7.2×10^{2}	2.9×10^{2}	2.2×10^{3}	2
	Clay	4	1.6×10^{3}	1	1.7×10^{3}	5.5×10^{2}	1.2×10^{3}	2.2×10^{3}	1
	Organic	3	1.4×10^{3}	3	2.2×10^{3}	2.4×10^{3}	5.2×10^{2}	4.9×10^{3}	2
Ga	All soils	2	-	-	3.0×10^{2}	-	2.8×10^{2}	3.1×10^{2}	1[b]
	Sand	1	-	-	3.1×10^{2}	-	-	-	1
	Unspecified	1	-	-	2.8×10^{2}	-	-	-	1
H	Sand	1	-	-	1.0×10^{-1}	-	-	-	1
Hf	All soils	6	2.5×10^{3}	3	3.6×10^{3}	3.0×10^{3}	4.5×10^{2}	8.5×10^{3}	2
	Sand	2	-	-	1.9×10^{3}	-	4.5×10^{2}	3.3×10^{3}	2[a,b]
	Loam	1	-	-	1.5×10^{3}	-	-	-	1[a]
	Clay	1	-	-	2.4×10^{3}	-	-	-	1[a]
	Organic	1	-	-	5.4×10^{3}	-	-	-	1[a]
	Unspecified	1	-	-	8.5×10^{3}	-	-	-	1[b]
Hg	Unspecified	1	-	-	6.3×10^{3}	-	-	-	1
Ho	All soils	4	9.3×10^{2}	3	1.3×10^{3}	1.2×10^{3}	2.4×10^{2}	3.0×10^{3}	1[a]
	Sand	1	-	-	2.4×10^{2}	-	-	-	1
	Loam	1	-	-	8.1×10^{2}	-	-	-	1
	Clay	1	-	-	1.3×10^{3}	-	-	-	1
	Organic	1	-	-	3.0×10^{3}	-	-	-	1
In	All soils	2	-	-	4.8×10^{2}	-	2.4×10^{2}	7.3×10^{2}	1[b]
	Sand	1	-	-	2.4×10^{2}	-	-	-	1
	Unspecified	1	-	-	7.3×10^{2}	-	-	-	1
Ir	Unspecified	15	3.0	-	-	-	1	1.1×10^{1}	1
K	All soils	237	1.3×10^{1}	4	3.5×10^{1}	7.0×10^{1}	7.0×10^{-1}	9.1×10^{2}	9
	Sand	60	3.4	3	1.4×10^{1}	4.0×10^{1}	7.0×10^{-1}	1.8×10^{2}	8
	Loam	81	2.0×10^{1}	4	5.0×10^{1}	1.1×10^{2}	1.8	9.1×10^{2}	5
	Clay	12	4.3×10^{1}	3	7.7×10^{1}	9.0×10^{1}	9.3	2.9×10^{2}	2
	Organic	76	1.9×10^{1}	3	3.0×10^{1}	3.0×10^{1}	2.5	1.3×10^{2}	5
	Unspecified	8	1.1×10^{1}	3	2.9×10^{1}	6.0×10^{1}	4.3	1.8×10^{2}	2
La	Sand	1	-	-	5.3×10^{3}	-	-	-	1[b]
Lu	Sand	1	-	-	5.1×10^{3}	-	-	-	1[b]
Mg	All soils	30	3.8	3	8.0	1.0×10^{1}	4.0×10^{-1}	4.5×10^{1}	1
	Sand	6	1.3	4	3.5	6	4.0×10^{-1}	1.6×10^{1}	1
	Loam	20	4.8	3	8.8	1.0×10^{1}	9.0×10^{-1}	4.5×10^{1}	1
	Clay	4	6.8	3	1.1×10^{1}	1.0×10^{1}	2.1	2.9×10^{1}	1

Mn	All soils	83	1.2×10^{3}	9	9.8×10^{3}	1.8×10^{4}	3.6×10^{1}	7.9×10^{4}	4
	Sand	13	9.8×10^{2}	1.4×10^{1}	1.2×10^{4}	2.5×10^{4}	4.0×10^{1}	7.9×10^{4}	4
	Loam	56	1.1×10^{3}	8	7.7×10^{3}	1.5×10^{4}	6.0×10^{1}	7.7×10^{4}	3
	Clay	10	4.5×10^{3}	1.3×10^{1}	2.2×10^{4}	2.4×10^{4}	1.4×10^{2}	5.7×10^{4}	3
	Organic	3	1.6×10^{2}	4	2.5×10^{2}	2.3×10^{2}	3.6×10^{1}	4.9×10^{2}	2
	Unspecified	1	-	-	1.0×10^{4}	-	-	-	1
Mo	All soils	9	3.8×10^{1}	3	5.7×10^{1}	5.0×10^{1}	7.4	1.3×10^{2}	5
	Sand	2	-	-	4.5×10^{1}	-	7.4	8.2×10^{1}	2
	Loam	1	-	-	1.3×10^{2}	-	-	-	1[a]
	Clay	1	-	-	9.0×10^{1}	-	-	-	1[a]
	Organic	2	-	-	2.3×10^{1}	-	1.8×10^{1}	2.7×10^{1}	2
	Unspecified	3	3.7×10^{1}	3	5.3×10^{1}	5.0×10^{1}	1.3×10^{1}	1.1×10^{2}	3
Na	All soils	30	3.4	3	5.7	6	2.0×10^{-1}	2.6×10^{1}	1
	Sand	6	2.2	4	5.2	9	4.0×10^{-1}	2.3×10^{1}	1
	Loam	20	4.6	2	6.3	6	3.0×10^{-1}	2.6×10^{1}	1
	Clay	4	1.7	6	3.9	5	2.0×10^{-1}	1.1×10^{1}	1
Nb	All soils	11	1.5×10^{3}	4	2.9×10^{3}	2.7×10^{3}	1.6×10^{2}	8.4×10^{3}	3
	Sand	2	-	-	1.7×10^{2}	-	1.6×10^{2}	1.9×10^{2}	2
	Loam	5	2.5×10^{3}	3	3.6×10^{3}	3.0×10^{3}	5.4×10^{2}	8.4×10^{3}	2
	Clay	3	2.4×10^{3}	2	3.0×10^{3}	1.9×10^{3}	9.0×10^{2}	4.7×10^{3}	2
	Organic	1	-	-	2.0×10^{3}	-	-	-	1[a]
Np	All soils	26	3.6×10^{1}	6	1.6×10^{2}	3.2×10^{2}	1.3	1.2×10^{3}	3
	Sand	8	1.4×10^{1}	4	2.9×10^{1}	4.0×10^{1}	3.0	1.1×10^{2}	3
	Loam	12	2.3×10^{1}	4	4.2×10^{1}	4.0×10^{1}	1.3	1.2×10^{2}	3
	Clay	2	-	-	3.8×10^{1}	-	2.0×10^{1}	5.5×10^{1}	2
	Organic	4	8.1×10^{2}	1	8.5×10^{2}	2.9×10^{2}	5.0×10^{2}	1.2×10^{3}	3
P	All soils	6	8.7×10^{1}	5	2.2×10^{2}	3.0×10^{2}	9.0	7.6×10^{2}	2
	Sand	2	-	-	3.9×10^{2}	-	9.0	7.6×10^{2}	2
	Loam	2	-	-	2.0×10^{2}	-	3.0×10^{1}	3.8×10^{2}	2
	Clay	1	-	-	4.9×10^{1}	-	-	-	1[a]
	Organic	1	-	-	1.1×10^{2}	-	-	-	1[a]
Pa	All soils	4	2.0×10^{3}	3	2.9×10^{3}	2.6×10^{3}	5.4×10^{2}	6.6×10^{3}	1[a]
	Sand	1	-	-	5.4×10^{2}	-	-	-	1
	Loam	1	-	-	1.8×10^{3}	-	-	-	1
	Clay	1	-	-	2.7×10^{3}	-	-	-	1
	Organic	1	-	-	6.6×10^{3}	-	-	-	1
Pb	All soils	23	2.0×10^{3}	1.0×10^{1}	1.5×10^{4}	3.3×10^{4}	2.5×10^{1}	1.3×10^{5}	5
	Sand	9	2.2×10^{2}	4	4.0×10^{2}	4.3×10^{2}	2.5×10^{1}	1.3×10^{3}	2
	Loam	5	1.0×10^{4}	3	1.5×10^{4}	1.6×10^{4}	3.6×10^{3}	4.3×10^{4}	2
	Clay	2	-	-	6.6×10^{4}	-	5.4×10^{3}	1.3×10^{5}	2
	Organic	5	2.5×10^{3}	3	3.7×10^{3}	3.8×10^{3}	8.8×10^{2}	1.0×10^{4}	2

	Unspecified	2	-	-	5.9×10^{4}	-	1.6×10^{4}	1.0×10^{5}	2
Pd	All soils	6	1.8×10^{2}	2	2.4×10^{2}	2.2×10^{2}	5.5×10^{1}	6.7×10^{2}	2
	Sand	2	-	-	9.0×10^{1}	-	5.5×10^{1}	1.3×10^{2}	2[a,b]
	Loam	1	-	-	1.8×10^{2}	-	-	-	1[a]
	Clay	1	-	-	2.7×10^{2}	-	-	-	1[a]
	Organic	1	-	-	6.7×10^{2}	-	-	-	1[a]
	Unspecified	1	-	-	1.7×10^{2}	-	-	-	1[b]
Pm	All soils	2	-	-	4.5×10^{2}	-	4.5×10^{2}	4.5×10^{2}	1[b]
	Sand	1	-	-	4.5×10^{2}	-	-	-	1
	Unspecified	1	-	-	4.5×10^{2}	-	-	-	1
Po	All soils	44	2.1×10^{2}	5	5.6×10^{2}	1.1×10^{3}	1.2×10^{1}	7.0×10^{3}	2
	Sand	14	1.0×10^{2}	6	7.4×10^{2}	1.9×10^{3}	1.7×10^{1}	7.0×10^{3}	1
	Loam	27	2.3×10^{2}	4	4.6×10^{2}	4.6×10^{2}	1.2×10^{1}	1.8×10^{3}	2
	Clay	2	-	-	1.7×10^{3}	-	7.2×10^{2}	2.7×10^{3}	2
	Organic	1	-	-	6.6×10^{3}	-	-	-	1[a]
Pt	Unspecified	15	2.4×10^{1}	-	-	-	1.2×10^{1}	8.3×10^{1}	1
Pu	All soils	62	7.4×10^{2}	4	1.6×10^{3}	2.0×10^{3}	3.2×10^{1}	9.6×10^{3}	7
	Sand	11	4.0×10^{2}	4	1.0×10^{3}	2.0×10^{3}	3.3×10^{1}	6.9×10^{3}	5
	Loam	27	9.5×10^{2}	4	1.9×10^{3}	2.3×10^{3}	1.0×10^{2}	9.6×10^{3}	4
	Clay	10	1.8×10^{3}	2	2.5×10^{3}	2.2×10^{3}	4.3×10^{2}	7.6×10^{3}	4
	Organic	6	7.6×10^{2}	4	1.3×10^{3}	1.1×10^{3}	9.0×10^{1}	3.0×10^{3}	4
	Unspecified	8	2.3×10^{2}	5	6.1×10^{2}	8.5×10^{2}	3.2×10^{1}	2.1×10^{3}	2
Ra	All soils	51	2.5×10^{3}	1.3×10^{1}	3.4×10^{4}	1.3×10^{5}	1.2×10^{1}	9.5×10^{5}	8
	Sand	20	3.1×10^{3}	8	9.6×10^{3}	1.2×10^{4}	4.9×10^{1}	4.0×10^{4}	4
	Loam	19	1.1×10^{3}	1.7×10^{1}	1.5×10^{4}	3.2×10^{4}	1.2×10^{1}	1.2×10^{5}	5
	Clay	6	3.8×10^{4}	1.2×10^{1}	2.0×10^{5}	3.7×10^{4}	7.0×10^{2}	9.5×10^{5}	3
	Organic	2	-	-	1.3×10^{3}	-	2.0×10^{2}	2.4×10^{3}	2
	Unspecified	4	1.2×10^{3}	1	1.3×10^{3}	5.0×10^{2}	7.8×10^{2}	1.9×10^{3}	1
Rb	All soils	4	2.1×10^{2}	3	2.9×10^{2}	2.7×10^{2}	5.5×10^{1}	6.7×10^{2}	1[a]
	Sand	1	-	-	5.5×10^{1}	-	-	-	1
	Loam	1	-	-	1.8×10^{2}	-	-	-	1
	Clay	1	-	-	2.7×10^{2}	-	-	-	1
	Organic	1	-	-	6.7×10^{2}	-	-	-	1
Rh	Unspecified	12	4.0	-	-	-	6.0×10^{-1}	2.9×10^{1}	1
Ru	All soils	15	2.7×10^{2}	8	4.7×10^{3}	1.7×10^{4}	5.0	6.6×10^{4}	5
	Sand	3	3.6×10^{1}	6	7.7×10^{1}	9.0×10^{1}	5.0	1.7×10^{2}	3
	Loam	3	3.0×10^{2}	3	4.7×10^{2}	4.7×10^{2}	8.2×10^{1}	9.9×10^{2}	3
	Clay	4	5.0×10^{2}	2	6.0×10^{2}	3.6×10^{2}	2.0×10^{2}	9.9×10^{2}	3
	Organic	1	-	-	6.6×10^{4}	-	-	-	1[a]
	Unspecified	4	1.4×10^{2}	3	2.3×10^{2}	2.1×10^{2}	3.4×10^{1}	4.9×10^{2}	2
Sb	All soils	152	6.2×10^{1}	4	1.3×10^{2}	2.0×10^{2}	6.0×10^{-1}	2.1×10^{3}	5

	Sand	19	1.7×10^{1}	6	6.4×10^{1}	1.2×10^{2}	6.0×10^{-1}	4.7×10^{2}	4
	Loam	92	6.1×10^{1}	3	1.2×10^{2}	2.3×10^{2}	4.0	2.1×10^{3}	2
	Clay	18	1.4×10^{2}	2	2.0×10^{2}	1.7×10^{2}	3.8×10^{1}	6.1×10^{2}	2
	Organic	3	7.5×10^{1}	8	2.2×10^{2}	2.8×10^{2}	7.8	5.4×10^{2}	2
	Unspecified	20	9.9×10^{1}	4	1.7×10^{2}	1.6×10^{2}	4.0	6.1×10^{2}	2
Sc	All soils	2	-	-	2.1×10^{3}	-	6.7×10^{2}	3.5×10^{3}	1[b]
	Sand	1	-	-	6.7×10^{2}	-	-	-	1
	Unspecified	1	-	-	3.5×10^{3}	-	-	-	1
Se	All soils	172	2.0×10^{2}	3	3.6×10^{2}	3.7×10^{2}	4.0	2.1×10^{3}	10
	Sand	15	5.6×10^{1}	5	2.2×10^{2}	4.6×10^{2}	4.0	1.6×10^{3}	6
	Loam	101	2.2×10^{2}	3	3.7×10^{2}	3.5×10^{2}	1.2×10^{1}	1.6×10^{3}	4
	Clay	33	2.4×10^{2}	3	3.7×10^{2}	4.0×10^{2}	2.2×10^{1}	2.1×10^{3}	6
	Organic	2	-	-	1.0×10^{3}	-	2.3×10^{2}	1.8×10^{3}	2
	Unspecified	21	2.3×10^{2}	2	3.0×10^{2}	1.9×10^{2}	2.0×10^{1}	6.2×10^{2}	3
Si	All soils	4	1.3×10^{2}	3	1.8×10^{2}	1.6×10^{2}	3.3×10^{1}	4.0×10^{2}	1[a]
	Sand	1	-	-	3.3×10^{1}	-	-	-	1
	Loam	1	-	-	1.1×10^{2}	-	-	-	1
	Clay	1	-	-	1.8×10^{2}	-	-	-	1
	Organic	1	-	-	4.0×10^{2}	-	-	-	1
Sm	All soils	4	9.3×10^{2}	3	1.3×10^{3}	1.2×10^{3}	2.4×10^{2}	3.0×10^{3}	1[a]
	Sand	1	-	-	2.4×10^{2}	-	-	-	1
	Loam	1	-	-	8.1×10^{2}	-	-	-	1
	Clay	1	-	-	1.3×10^{3}	-	-	-	1
	Organic	1	-	-	3.0×10^{3}	-	-	-	1
Sn	All soils	12	1.6×10^{3}	6	5.7×10^{3}	9.1×10^{3}	1.3×10^{2}	3.1×10^{4}	4
	Sand	2	-	-	1.5×10^{2}	-	1.3×10^{2}	1.7×10^{2}	2[a,b]
	Loam	1	-	-	4.5×10^{2}	-	-	-	1[a]
	Clay	1	-	-	6.7×10^{2}	-	-	-	1[a]
	Organic	1	-	-	1.6×10^{3}	-	-	-	1[a]
	Unspecified	7	4.1×10^{3}	5	9.4×10^{3}	1.1×10^{4}	3.3×10^{2}	3.1×10^{4}	3
Ta	All soils	5	7.8×10^{2}	3	1.1×10^{3}	1.1×10^{3}	2.4×10^{2}	3.0×10^{3}	2
	Sand	2	-	-	3.1×10^{2}	-	2.4×10^{2}	3.8×10^{2}	2[a,b]
	Loam	1	-	-	8.1×10^{2}	-	-	-	1[a]
	Clay	1	-	-	1.3×10^{3}	-	-	-	1[a]
	Organic	1	-	-	3.0×10^{3}	-	-	-	1[a]
Tb	All soils	2	-	-	6.0×10^{3}	-	5.4×10^{3}	6.6×10^{3}	1[b]
	Sand	1	-	-	5.4×10^{3}	-	-	-	1
	Unspecified	1	-	-	6.6×10^{3}	-	-	-	1
Tc	All soils	33	2.3×10^{-1}	9	2	5	1.0×10^{-2}	1.1×10^{1}	4
	Sand	5	4.0×10^{-2}	3	5.0×10^{-2}	5.0×10^{-2}	1.0×10^{-2}	1.0×10^{-1}	2

	Loam	14	7.0×10^{-2}	3	2.0×10^{-1}	2.0×10^{-1}	1.0×10^{-2}	9.0×10^{-1}	4
	Clay	3	9.0×10^{-2}	1.0×10^{1}	4.0×10^{-1}	7.0×10^{-1}	2.0×10^{-2}	1.2	2
	Organic	11	3.1	3	6	7	9.2×10^{-1}	1.1×10^{1}	2
Te	All soils	2	-	-	4.9×10^{2}	-	1.8×10^{2}	7.9×10^{2}	1[b]
	Sand	1	-	-	1.8×10^{2}	-	-	-	1
	Unspecified	1	-	-	7.9×10^{2}	-	-	-	1
Th	All soils	46	1.9×10^{3}	1.0×10^{1}	1.6×10^{4}	4.2×10^{4}	1.8×10^{1}	2.5×10^{5}	8
	Sand	12	7.0×10^{2}	1.1×10^{1}	1.0×10^{4}	2.8×10^{4}	3.5×10^{1}	1.0×10^{5}	3
	Loam	6	1.8×10^{4}	4	5.3×10^{4}	9.7×10^{4}	5.0×10^{3}	2.5×10^{5}	2
	Clay	7	4.5×10^{3}	3	7.4×10^{3}	8.0×10^{3}	8.0×10^{2}	2.4×10^{4}	2
	Organic	5	7.3×10^{2}	4.4×10^{1}	1.9×10^{4}	3.5×10^{4}	1.8×10^{1}	8.0×10^{4}	3
	Unspecified	16	1.5×10^{3}	5	8.9×10^{3}	2.5×10^{4}	2.1×10^{2}	1.0×10^{5}	3
Tm	Sand	1	-	-	3.3×10^{2}	-	-	-	1[b]
V	All soils	2	-	-	3.0×10^{2}	-	1.8×10^{2}	4.1×10^{2}	1[b]
	Sand	1	-	-	1.8×10^{2}	-	-	-	1
	Unspecified	1	-	-	4.1×10^{2}	-	-	-	1
Y	All soils	7	4.7×10^{1}	4	6.5×10^{1}	1.0×10^{2}	1.0×10^{1}	3.8×10^{2}	1
	Sand	5	2.2×10^{1}	2	2.6×10^{1}	2.0×10^{1}	1.0×10^{1}	4.7×10^{1}	1
	Organic	2	-	-	3.2×10^{2}	-	2.6×10^{2}	3.8×10^{2}	1
Zr	All soils	11	4.1×10^{2}	2.1×10^{1}	3.0×10^{3}	3.8×10^{3}	1.5	1.0×10^{4}	4
	Sand	4	3.2×10^{1}	1.6×10^{1}	2.0×10^{2}	2.8×10^{2}	1.5	6.0×10^{2}	3
	Loam	2	-	-	5.2×10^{3}	-	2.2×10^{3}	8.1×10^{3}	2
	Clay	2	-	-	6.8×10^{3}	-	3.3×10^{3}	1.0×10^{4}	2
	Organic	2	-	-	3.7×10^{3}	-	2.3×10^{1}	7.3×10^{3}	2
	Unspecified	1	-	-	4.8×10^{2}	-	-	-	1[b]

[a] K_d values originate from the Technical Reports Series No. 364 [32].
[b] K_d values originate from experiments using neutron activation analyses [37].

2.1. A kinetic approach to examining sorption dynamics

The form of radionuclides when they are first deposited on the soil is initially governed by their chemical form in the contamination source (*e.g.* fuel particles; water soluble fallout). Regarding soluble contamination sources, water soluble forms of radionuclides are sorbed onto soil particles and undergo a number of reactions in the solid soil phase. The processes underlying transformation between chemical forms of radionuclides in the soil and soil solution can be summarized as shown in Fig. 4 [38-39]. The transformation between chemical forms would eventually lead to changes (mostly, increases) in the K_d values, as a result of the transfer of the radionuclide to sites where it is no longer available to exchange with the radionuclide in solution, thus decreasing the reversibly sorbed radionuclide fraction. This process is often described as aging in the literature.

Kinetics studies have examined the changes in K_d value with time. Various models have been proposed to fit the experimental data. Although for several radionuclides their soluble complexes must be taken into account (RN_2), in most cases to postulate that the radionuclide occurs in the soil solution as a free cation is an adequate approach.

A three-box model is often used to describe the kinetics of radionuclide sorption [13, 38, 40]. This model assumes that the radionuclide in the soil solution may be sorbed either at a labile pool of sites (RN_3), thus defining an exchangeable K_d, or sorbed at non-exchangeable sites (RN_4). This process is estimated through its corresponding rate constants (see k_{14} and k_{41} in the Fig. 4), which describes a pseudo-first order reaction, assuming that forward and backward reactions are independent of the capacity of sorption sites and composition of the soil solution. Other models postulate that additional types of transformation should be considered. For instance, it has been suggested that the radionuclide reaches the non-labile pool after being sorbed in the labile pool [39]. Therefore, the corresponding rate constants (see k_{43} and k_{43} in the Fig. 4) must be quantified.

2.1.1. The case of radiostrontium

In most soil types, radiostrontium does not undergo complexation reactions in soil solution, in contrast to the transition elements. Moreover, the fixation process is almost negligible for this radionuclide [38], although slight decreases in the reversible sorbed fraction have been seen in the short-term after contamination [13, 41]. Besides the ion exchange mechanisms that control radiostrontium sorption in soils, other specific interactions (*e.g.* isomorphic substitutions in Ca-bearing minerals; formation of insoluble inorganic and organic compounds) have been postulated to explain radiostrontium aging processes. In any case, the rate constant k_{41} can be hypothesized to be much larger than k_{14}, resulting in a major part of radiostrontium being in an exchangeable form. Representative values for these rate constants in loam soils are k_{14} = 0.01 – 0.03 d^{-1} and k_{41} = 0.13 – 0.14 d^{-1} [42].

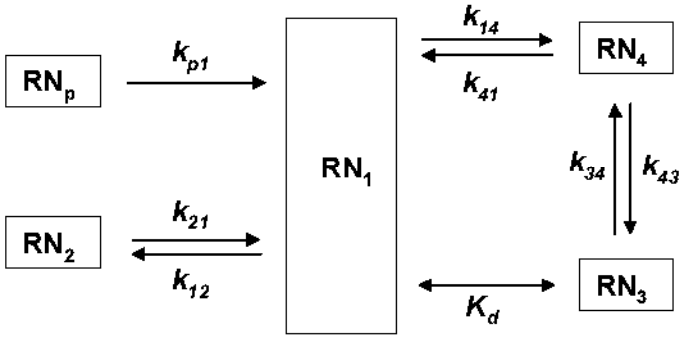

RN_1: Cationic form of a radionuclide in soil solution
RN_2: Radionuclide soluble complex compounds in the soil solution
RN_3: Radionuclide cation sorbed by ion-exchange process (labile pool)
RN_4: Non-exchangeable (strongly-bonded) form of a radionuclide (non-labile pool)
RN_p: Radionuclide in solid particles (fuel particles) as a source-term
K_d: Exchangeable (labile) distribution coefficient
k_{ij}: Rate constant for a given (kinetically controlled) transformation process

FIG. 4. Kinetic steps of radionuclide sorption in the soil solution-soil system.

2.1.2. The case of radiocaesium

As with radiostrontium, radiocaesium does not undergo complexation reactions in solution. For radiocaesium, the three-box kinetic model is the most usually applied approach to describe the kinetics of its sorption [13, 38, 40]. However, for this radionuclide it has been shown that after an initial rapid sorption at the most outer *FES* and on the organic and planar surface sites of the soil particles, there is a second kinetic step in which a moderately fast

sorption on interlayer wedge sites in the *FES* takes place, where the radiocaesium remains fixed by the interlayer core. This process is often described as diffusion in the solid state, especially in the presence of expanded interlayers [43-44], which allows radiocaesium to penetrate into the crystal lattice of clays [45]. Moreover, the labile pool can be subdivided in relation to the types of site involved (regular exchange complex or specific sites at *FES*), while the sorption at the non-labile pool can be characterized as progressive fixation controlled by the solid-phase diffusion into collapsed micaceous interlayers [46]. For soils with a high organic matter content and/or extremely low clay content, this second process may be negligible. Table 17 summarizes some rate constants for ^{137}Cs fixation and release processes in various soils.

TABLE 17 ^{137}Cs RATE CONSTANTS (d^{-1}) FOR SOILS GROUPED ACCORDING TO THE TEXTURE/OM CRITERION

			k_{1d}			k_{d1}			
Source term	Soil group	N	GM/Value	Min	Max	GM/Value	Min	Max	# ref.
Water soluble	Sand	10	1.2×10^{-1}	5.1×10^{-2}	6.9×10^{-1}	6.7×10^{-2}	7.0×10^{-3}	1.9×10^{-1}	
Water soluble	Loam	4	2.6×10^{-1}	9.0×10^{-2}	4.3×10^{-1}	2.2×10^{-2}	7.0×10^{-3}	2.8×10^{-2}	
Water soluble	Clay	1	1.3	-	-	3.5×10^{-2}	-	-	
Water soluble	Organic	5	1.6	1.5×10^{-1}	1.2×10^{1}	2.2×10^{-1}	6.0×10^{-3}	8.7×10^{-1}	5[a]
Water soluble	Unspecified	10	1.5	6.0×10^{-1}	3.8	8.7×10^{-2}	1.9×10^{-2}	6.1×10^{-1}	
Water soluble	All soils	30	5.0×10^{-1}	5.0×10^{-2}	1.2×10^{1}	7.5×10^{-2}	6.0×10^{-3}	8.7×10^{-1}	
Leachate from particles	Unspecified	3	1.4×10^{-2}	1.2×10^{-2}	1.5×10^{-2}	1.4×10^{-3}	9.0×10^{-4}	3.7×10^{-3}	1[b]
			k_{3d}			k_{d3}			
Source term	Soil group	N	GM	Min	Max	GM	Min	Max	# ref.
Water soluble	Organic	5	3.0×10^{-2}	7.0×10^{-3}	2.0×10^{-1}	3.5×10^{-3}	6.0×10^{-4}	1.1×10^{-2}	1[c]

[a] [13, 40, 47-49]; [b] [47]; [c] [39].

2.2. Additional approaches to examining sorption dynamics

Other widespread experimental approaches to examining sorption dynamics are based on the construction of desorption isotherms in the same conditions as in the sorption step [50] or on the use of single and sequential extraction tests to quantify the desorption yields in controlled experimental conditions [51-54]. While the first approach may give some light on the mechanisms involved in sorption reversibility, the second represents a simpler, faster experiment to estimate the percentage of the radionuclide that may be remobilized.

Single and sequential extraction tests have been widely used when dealing with the characterization of field-contaminated soils [41, 55-56]. While single extractions focus on quantifying the reversibly sorbed fraction of a given radionuclide (f_{rev}), sequential extractions allow a better distinction between the exchangeable and non-exchangeable pools, and their changes with time. Some common patterns have been found in these studies, which agree with conclusions derived from the kinetic approach. Although it is extremely difficult to establish a range of f_{rev} values, the f_{rev} (Sr) is usually higher than f_{rev} (Cs) for mineral soils, whereas the opposite trend can be observed in organic soils. Regarding radiocaesium, the f_{rev}

(Cs) in mineral soils usually decreases with the texture sequence sand > loam > clay soils. For actinides, the f_{rev} values reported are much smaller than for radiostrontium and radiocaesium.

Although to date a successful approach to predicting desorption yields from sorption data has not been developed, the quantification of f_{rev} through the use of harmonized laboratory tests has improved radionuclide mobility predictions based solely on radionuclide distribution coefficients.

3. CONCLUSIONS

A significant amount of data has been added to the new K_d database, comparing with the former Technical Reports Series No. 364. However, there are still evident gaps of values of K_d for a substantial number of radionuclides and soil types. In some cases, values originate from a single reference. This fact restricts the possibility of proposing best estimates in many cases, and GM and single values must be considered only as approximate estimates, suitable for screening purposes, but not for specific risk assessments. For these gaps, the use of analogues (data on other elements or media, such as pure soil phases or sediments) is an option, but must be undertaken with care, with due consideration for the distinctions in chemical form and affinity for different types of binding site that may exist between the analogue and the radionuclide of interest.

The large number of experimental approaches used to quantify K_d values is partly responsible for the wide ranges of values that can be found for a given radionuclide-soil type combination. Values derived from mass transport experiments seem to lead to K_d values one-two orders of magnitude lower than those derived from batch experiments. Regarding this latter approach, the ionic composition of the contact solution may affect the K_d value by up to some orders of magnitude.

Finally, it is recommended not to use stable isotopes (at larger concentrations than radioisotopes), to quantify the K_d values of the corresponding radionuclide, since the derived values will often be significantly lower.

The K_d values derived from field-contaminated soils are usually higher than those resulting from a laboratory sorption tests, because the radionuclide quantified in the solid phase of the contaminated soil may include sorbed radionuclide not available for exchange with the soil solution due to a larger time elapsed since radionuclide incorporation, in comparison with laboratory experiments.

There is a need to have information on the reversibility of sorption and how it may change with time. The dynamics of the soil-radionuclide interaction is significant for a limited number of radionuclides, as in the cases of radiostrontium and radiocaesium. For radionuclides with very low or very high sorption, this may be a consideration of minor significance.

Soil-radionuclide interactions are governed by multiple factors that depend on the radionuclide and on various soil properties. As the quality and quantity of the mineral matter is one of the key soil properties, the definition of K_d values for soil groups based on soil texture and organic matter content is a satisfactory approach to establish the estimated values of K_d for a large number of radionuclides. However, it is recommended that consideration and use be made, as much as possible, of additional soil and radionuclide properties (cofactors)

that govern soil-radionuclide interactions, for better prediction of K_d values and to decrease the variability in estimates of those values.

The main soil parameters controlling the interaction should be measured and monitored to improve the prediction of K_d, and they should also be included in models predicting the radionuclide transport in the environment. Clear examples are *RIP* and K and NH_4^+ status for radiocaesium, *CEC* and Ca and Mg concentrations for radiostrontium, and pH for heavy metal radionuclides and uranium. Therefore, modellers can choose to use the best estimates derived from the GM values of K_d for soils arranged according to texture and organic matter or, when available, according to other criteria such as specific properties, pH and speciation. Moreover, modellers and end-users can also consider using existing single and multiple correlations between soil properties and K_d to calculate best estimates from soil properties, especially in those cases where the mechanisms governing radionuclide interactions are well known.

REFERENCES

[1] GOODY, D.C., SHAND, P., KINNIBURGH, D.G., VAN RIEMSDIJK, W.H., Field-based partition coefficients for trace elements in soil solutions, European Journal of Soil Science **46** (1995) 265.

[2] ORGANISATION FOR ECONOMIC COOPERATION AND DEVELOPMENT, Guideline for the testing of chemicals: Adsorption-desorption using a batch equilibrium method, Guideline 106 (2000).

[3] AMERICAN SOCIETY FOR TESTING AND MATERIALS, Standard test method for distribution ratios by the short-term batch method, ASTM D 4319-93, West Conshohocken, PA, US (2001).

[4] STAUNTON, S., Sensitivity of the distribution coefficient, K_d, of nickel to changing soil chemical properties, Geoderma **122** (2004) 281.

[5] GIL-GARCÍA, C.J., RIGOL, A., RAURET, G., VIDAL, M., Radionuclide sorption-desorption pattern in soils from Spain, Applied Radiation and Isotopes (2007), doi:10.1016/j.apradiso.2007.07.032.

[6] GARCÍA-GUTIÉRREZ, M., CORMENZARA, J. L., MISSANA, T., MINGARRO, M., Diffusion coefficient and accessible porosity for HTO and $^{36}Cl^-$ in compacted FEBEX bentonite, Applied Clay Science **26** (2004) 65.

[7] OCHS, M., BOONEKAMP, M., WANNER, H., SATO, H., YUI, M., A quantitative model for ion diffusion in compacted bentonite, Radiochimica Acta **82** (1998) 437.

[8] OCHS, M., LOTHENBACH, B., WANNER, H., SATO, H., YUI, M., An integrated sorption-diffusion model for the calculation of consistent distribution and diffusion coefficients in compacted bentonite, Journal of Contaminant Hydrology **47** (2001) 283.

[9] OKAMOTO, A., IDEMITSU, K., FURUYA, H., INAGAKI, Y., ARIMA, T., Distribution coefficients and apparent diffusion coefficients of caesium in compacted bentonites, Mater. Res. Soc. Symp. Proc. **556** (1999) 1091.

[10] FERNANDEZ-TORRENT, R., VIDAL, M., RAURET, G., RIGOL, A., Laboratory experiments to characterize radionuclide diffusion in soils, paper presented at 2nd International Conference on Radioactivity in the Environment, Aix-en-Provence, France (2005).

[11] RAURET, G., FIRSAKOVA, S., The transfer of radionuclides through the terrestrial environment to agricultural products, including the evaluation of agrochemical practices, EUR 16528 EN, European Commission, Luxembourg (1996).

[12] HILTON, J., COMANS, R. N. J., Chemical forms of radionuclides and their quantification in environmental samples", Radioecology, Radioactivity and Ecosystems (VAN DER STRICHT, E., KIRCHMANN, R. Eds.), Fortemps, Liège (2001) 99-111.

[13] VALCKE, E., The behaviour dynamics of radioCaesium and radiostrontium in soils rich in organic matter, PhD Thesis, Katholieke Universiteit Leuven (1993).

[14] YASUDA, H., UCHIDA, S., Statistical approach for the estimation of strontium distribution coefficient, Environmental Science and Technology **27** (1993) 2462.

[15] WAUTERS, J., ELSEN, A., CREMERS, A., KONOPLEV, A., BULGAKOV, A. A., COMANS, R. N. J., Prediction of solid liquid distribution coefficients of radiocaesium in soils and sediments. Part one: A simplified procedure for the solid phase characterization, Applied Geochemistry **11** (1996) 589.
[16] SWEECK, L., WAUTERS., J., VALCKE., E., CREMERS., A. The specific interception potential of soils for radiocaesium, Transfer of Radionuclides in Natural and Seminatural Environments (DESMET G, NASSIMBENI P, BELLI M. Eds.), EUR 12448, Elsevier Applied Science, London (1990) 249-258.
[17] BROUWER, E., BAEYENS, B., MAES, A., CREMERS, A., Caesium and rubidium ion equilibrium in illite clay, Journal of Physical Chemistry **87** (1983) 1213.
[18] CREMERS, A., ELSEN, A., DE PRETER, P., MAES, A., Quantitative analysis of radiocaesium retention in soils, Nature **335** (1988) 247.
[19] VIDAL, M., ROIG, M., RIGOL, A., LLAURADÓ, M., RAURET, G., WAUTERS, J., ELSEN, A., CREMERS, A., Two approaches to the study of radiocaesium partitioning and mobility in agricultural soils from the Chernobyl area, Analyst **120** (1995) 1785.
[20] RIGOL, A., VIDAL, M., RAURET, G., SHAND, C. A., CHESHIRE, M. V., Competition of organic and mineral phases in radiocaesium partitioning in organic soils of Scotland and the area near Chernobyl, Environmental Science and Technology **32** (1998) 663.
[21] WAUTERS, J., VIDAL, M., ELSEN, A., CREMERS, A., Prediction of solid liquid distribution coefficients of radiocaesium in soils and sediments. Part two: a new procedure for solid phase speciation of radiocaesium, Applied Geochemistry **11** (1996) 595.
[22] WAEGENEERS, N., SMOLDERS, E., MERCKX, R., A statistical approach for estimating the radiocaesium interception potential of soils, Journal of Environmental Quality **28** (1999) 1005.
[23] ALLARD, B., OLOFSSON, U., TORSTENFELT, B., Environmental actinide chemistry, Inorganica Chimica Acta **94** (1984) 205.
[24] LANGMUIR, D., Uranium solution-mineral equilibrium at low temperature with applications to sedimentary ore deposits, Geochimica et Cosmochimica Acta **42** (1978) 547.
[25] ENVIRONMENTAL PROTECTION AGENCY, Understanding Variation in Partitioning Coefficients, K_d, Values: Volume II: Review of Geochemistry and Available K_d Values for Cadmium, Caesium, Chromium, Lead, Plutonium, Radon, Strontium, Thorium, Tritium and Uranium, US-EPA, Office of Air and Radiation EPA 402-R-99-004B, Washington, USA (1999).
[26] ECHEVARRIA, G., SHEPPARD, M., MOREL, J.L., Effect of pH on the sorption of uranium in soils, Journal of Environmental Radioactivity **53** (2001) 257.
[27] VANDENHOVE, H., VAN HEES, M., WANNIJN. J., Can we predict uranium bioavailability based on soil parameters? Part 1: Effect of soil parameters on soil solution uranium concentration, Environmental Pollution **145** (2007) 587.
[28] SIMON, S. L., IBRAHIM, S. A., Biological uptake of radium by terrestrial plants: a review, The Environmental Behaviour of Radium Vol 1. IAEA, Vienna, (1990) 545-599.
[29] VANDENHOVE, H., VAN HEES, M., Predicting radium availability and uptake from soil properties, Chemosphere (2007) (in press).
[30] YLARANTA, T., Sorption of selenite and selenate in the soil, Annales Agriculturae Fenniae **22** (1983) 30.
[31] YOSHIDA, S., MURAMATSU, Y., UCHIDA, S., Adsorption of I^- and IO_3^- onto 63 Japanese soils, Radioisotopes **44** (1995) 837.
[32] INTERNATIONAL ATOMIC ENERGY AGENCY, Handbook of Parameter Values for the Prediction of Radionuclide Transfer in Temperate Environments, Technical Report No 364, IAEA, Vienna (1994).
[33] SHEPPARD, M.I., THIBAULT, D.H., Default soil solid/liquid partition coefficients, K_d s, for four major soil types: a compendium, Health Physics **59** (1990) 471.
[34] THIBAULT, D.H., SHEPPARD, M.I., SMITH, P.A., A critical compilation and review of default soil solid/liquid partition coefficients, K_d, for use in environmental assessments, AECL 10125, Atomic Energy of Canada Limited, Pinawa, Manitoba, Canada (1990).

[35] MURAMATSU, Y., UCHIDA, S., SRIYOTHA, P., SRIYOTHA, K., Some considerations on the sorption and desorption phenomena of iodide and iodate on soil, Water, Air and Soil Pollution **49** (1990) 125.

[36] YOSHIDA, S., MURAMATSU, Y., UCHIDA, S., Soil-solution distribution coefficients, K_d's, of I^- and IO_3^- for 68 Japanese soils, Radiochimica Acta **82** (1998) 293.

[37] ZUYI, T., XIANGKE, W., XIONGXIN, D., JINZHOU, D., Adsorption characteristics of 47 elements on a calcareous soil, a red earth and an alumina: a multitracer study, Applied Radiation and Isotopes **52** (2000) 821.

[38] KONOPLEV A.V., VIKTOROVA, N.V., VIRCHENKO, E.P., POPOV, V.E., BULGAKOV, A.A., DESMET, G.M., Influence of agricultural countermeasures on the ratio of different chemical forms of radionuclides in soil and soil solution, Science of the Total Environment **137** (1993) 147.

[39] ABSALOM, J.P., Radiocaesium lability and fixation in upland soils: measurement and modelling, PhD Thesis, Nottingham Univ. (1995).

[40] SWEECK L., Soil-chemical availability of radiocaesium in mineral soils, PhD Thesis, Katholieke Universiteit Leuven (1996).

[41] RIGOL, A., ROIG, M., VIDAL, M., RAURET, G., Sequential extractions for the study of radiocaesium and radiostrontium dynamics in mineral and organic soil from Western Europe and Chernobyl areas, Environmental Science and Technology **33** (1999) 887.

[42] FRERE, M.H., CHAMPION, D.F., Characterisation of fixed strontium in sesquioxide gel – kaolinite clay systems, Soil Science Society of America, Proceedings **31** (1967) 188.

[43] HIRD, A.B., RIMMER, D.L., Total caesium-fixing potentials of acid organic soils, Journal of Environmental Radioactivity **26** (1995) 103.

[44] ABSALOM, J. P., YOUNG S. D., CROUT N. M., Radio-caesium fixation dynamics: measurement in six Cumbrian soils, European Journal of Soil Science **46** (1995) 461.

[45] KONOPLEV, A.V., BULGAKOV, A.A., POPOV, V.E., BOBOVNIKOVA, Ts.I., Behaviour of long-lived Chernobyl radionuclides in a soil-water system, Analyst **117** (1992) 1041.

[46] ABSALOM, J.P., CROUT, N.M. J., YOUNG, S.D., Modelling radiocaesium fixation in upland organic soils of Northwest England, Environmental Science and Technology **30** (1996) 2735.

[47] KONOPLEV, A.V., BULGAKOV, A.A., SHKURATOVA, V., Migration of certain radioactive products in the soil and surface run off in the Chernobyl NPP Zone (in Russian), Meteorologiya i Gidrologiya **6** (1990) 119.

[48] MOISEEV, U.T., TIKHOMIROV, F.A., RERIKH, L.A., CHIZHIKOVA, N.P., Radionuclide speciation in soils and their transformations (in Russian), Agrokhimiya **1** (1981) 110.

[49] SURKOVA, L.V., POGODIN, P.U., Speciation and occurrence of forms of ^{137}Cs in soil of different areas of accidental Chernobyl release (in Russian), Agrokhimiya **4** (1991) 84.

[50] COMANS, R.N.J., HALLER, M., DE PRETER P., Sorption of caesium on illite: non-equilibrium behaviour and reversibility, Geochimica et Cosmochimica Acta **55** (1991) 433.

[51] WAUTERS, J., SWEECK, L., VALCKE, E., ELSEN, A., CREMERS, A., Availability of radiocaesium in soils: A new methodology, Science of the Total Environment **157** (1994) 239.

[52] FAWARIS, B.H., JOHANSON, K.J., Sorption of ^{137}Cs from undisturbed forest soil in a zeolite trap, Science of the Total Environment **172** (1995) 251.

[53] KENNEDY, V.H., SANCHEZ, A.L., OUGHTON, D. H., ROWLAND, A. P., Use of single and sequential chemical extractants to assess radionuclide and heavy metal availability from soils for root uptake, Analyst **122** (1997) 89R.

[54] ROIG, M., VIDAL, M., RAURET, G., Estimating the radionuclide available fraction in mineral soils using an extraction technique, Analyst **123** (1998) 519.

[55] RIISE, G., BJOERNSTAD, H.E., LIEN, H. N., OUGHTON, D.H., SALBU, B., A study on radionuclide association with soil components using a sequential extraction procedure, Journal of Radioanalytical and Nuclear Chemistry **142** (1990) 531.

[56] SANZHAROVA, N.I., FESENKO, S.V., ALEXAKHIN, R.M., ANISIMOV, V.S., KUZNETSOV, V.K, CHERNYAYEVA, L.G., Changes in the forms of ^{137}Cs and its availability for plants as dependent on properties of fallout after the Chernobyl nuclear power plant accident, Science of the Total Environment **154** (1994) 9.

APPENDIX

List of publications used for K_d data evaluation

ABSALOM, J.P., Radiocaesium liability and fixation in upland soils: measurement and modelling, PhD Thesis, Nottingham Univ. (1995).

AGAPKINA, G.I., TIKHOMIROV, F.A., SHCHEGLOV, A.I., KRACKE, W., BUNZL, K., Association of Chernobyl derived ^{239,240}Pu, ^{241}Am, ^{90}Sr and ^{137}Cs with organic matter in the soil solution, Journal of Environmental Radioactivity **29** (1995) 257.

ASHWORTH, D.J., SHAW, G., Effects of moisture content and redox potential on in situ K_d values for radioiodine in soil, Science of the Total Environment **359** (2006) 244.

BARNETT, M.O., JARDINE, P.M., BROOKS, S. C., SELIM, H.M., Adsorption and transport of Uranium(VI) in subsurface media, Soil Science Society of America Journal **65** (2000) 908.

BACHHUBER, H., BUNZL, K., SCHIMMACK, W., Spatial variability of the distribution coefficients of ^{137}Cs, ^{65}Zn, ^{85}Sr, ^{57}Co, ^{109}Cs, ^{141}Ce, ^{103}Ru, ^{95m}Tc and ^{131}I in a cultivated soil, Nuclear Technology **72** (1985) 359.

BELL, J., BATES, T. H., Distribution coefficients of radionuclides between soils and groundwaters and their dependence on various test parameters, Science of the Total Environment **69** (1988) 297.

BENES, P., STAMBERG, K., STEGMANN, R., Study of the kinetics of the interaction of Cs-137 and Sr-85 with soils using a batch method: methodological problems, Radiochimica Acta **66/67** (1994) 315.

BUNZL, K., SCHIMMACK, W., Kinetics of the sorption of ^{137}Cs, ^{85}Sr, ^{57}Co, ^{65}Zn and ^{109}Cd by the organic horizons of a forest soil, Radiochimica Acta **54** (1991) 97.

CAMPS, M., RIGOL, A., VIDAL, M., RAURET, G., Assessment of the suitability of soil amendments to reduce ^{137}Cs and ^{90}Sr root uptake in meadows, Environmental Science and Technology **37** (2003) 2820.

CAMPS, M., RIGOL, A., HILLIER, S., VIDAL, M., RAURET, G., Quantitative assessment of the effects of agricultural practices designed to reduce ^{137}Cs and ^{90}Sr soil-plant transfer in meadows, Science of the Total Environment **332** (2004) 23.

CHRISTENSEN, T. H., LEHMANN, N., JACKSON, T., HOLM, P. E., Cadmium and nickel distribution coefficients for sandy aquifer minerals, Journal of Contaminant Hydrology **24** (1996) 75.

CHOI, Y. H., LIM, K. M., CHOI, H. J., CHOI, G. S., LEE, H. S., LEE, C. W., Plant uptake and downward migration of ^{85}Sr and ^{137}Cs after their deposition on to flooded rice fields: lysimeter experiments with and without the addition of KCl and lime, Journal of Environmental Radioactivity **78** (2005) 35.

COLLE, C., MAUGER, S., MASSIANI, C., KASHPAROV, A. A., GRASSET, G., Behaviour of chlorine (^{36}Cl) in cultivated terrestrial ecosystems, Radioprotection-Colloques **37** (2002) C18.

CRANÇON, P., VAN DER LEE, J., Speciation and mobility of uranium(VI) in humic-containing soils, Radiochimica Acta **91** (2003) 673.

DE BROUWERE, K., SMOLDERS, E., MERCKX, R., Soil properties affecting solid-liquid distribution of As(V) in soils, European Journal of Soil Science **55** (2004) 165.

DENYS, S., Prédiction de la phytodisponibilité de deux radionucléides (^{63}Ni et ^{99}Tc) dans les sols, PhD Thesis, Sciences Agronomiques, Nancy Univ. (2001).

ECHEVARRIA, G., Contribution à la prévision des transferts sol-plante des radionucléides, PhD Thesis, Sciences Agronomiques, Nancy Univ. (1996).

ECHEVARRIA, G., MOREL, J. L., FLORENTIN, L., LECLERC-CESSAC, E., Influence of climatic conditions, soil type and plant physiology on $^{99}TcO_4^-$ uptake by crops, Journal of Environmental Radioactivity **70** (2003) 85.

ECHEVARRIA, G., MOREL, J. L., LECLERC-CESSAC, E., Retention and phytoavailability of ^{95}Nb in soils, Journal of Environmental Radioactivity **78** (2005) 343.

ELEJALDE, C., HERRANZ, M., LEGARDA, F., ROMERO, F., Determination and analysis of distribution coefficients of ^{137}Cs in soils from Biscay (Spain), Environmental Pollution **110** (2000) 157.

FERRAND, E., Étude de la spéciation en solution, de la rétention dans les sòls et du transfert sol-plante du Zr, PhD Thesis, Paris VI Pierre et Marie Curie Univ. (2005).

FEVRIER, L., MARTIN-GARIN, A., LECLERC E., Variation of the distribution coefficient K_d of selenium in soils under various microbial states, Journal of Environmental Radioactivity **97** (2007) 189-205.

FUKUI, M., FUJIKAWA, Y., SATTA, N., Factors affecting interaction of radioiodide and iodate species with soil, Journal of Environmental Radioactivity **31** (1996) 199.

HAKEM, N., MHAMID, I., APPS, J., MORIDIS, G. J., Sorption of caesium and strontium on Hanford soil, Journal of Radioanalytical and Nuclear Chemistry **246** (2000) 275.

HANSEN, W. R., WATTERS, R. L., Unsupported polonium-210 oxide in soil. Soil absorption and characterization of soil solution species, Soil Science **112** (1971) 145.

JINZHOU, D., WENMING, D., XIANGKE, W., ZUYI, T., Sorption and desorption of radiostrontium on calcareous soils and its solid components, Journal of Radioanalytical and Nuclear Chemistry **203** (1996) 31.

JOHN, M.K., SAUNDERS, W.M.H., WATKINSON, J.H., Selenium adsorption by New Zealand soils. I. Relative adsorption of selenite by representative soils and the relation to soil properties, New Zealand Journal of Agricultural Research **19** (1975) 143.

JOHNSON, W. H., SERKIZ, S. M., JOHNSON, L. M., CLARK, S. B. Uranium partitioning under acidic conditions in a sandy soil aquifer, U.S. Department of Energy Report WSRC-MS-94-0528 (1995).

KONOPLEV, A. V., BULGAKOV, A. A., SHKURATOVA, V., Migration of certain radioactive products in the soil and surface run off in the Chernobyl NPP Zone (in Russian), Meteorologiya i Gidrologiya **6** (1990) 119.

KOTOVA A.Y., A study into the mechanisms of ^{90}Sr, ^{106}Ru, ^{137}Cs, and ^{144}Ce sorption and bioavailability in different soil types, PhD thesis, Obninsk Univ. (1998).

KAMEI-ISHIKAWA N., UCHIDA, S., TAGAMI, K., "Sorption behaviour of ^{137}Cs in Japanese agricultural soils", Proc. International Symposium on Environmental Modeling and Radioecology, Rokkasho, Japan, 2006.

LAKIN, H. W., Selenium accumulation in soils and its absorption by plants and animals, Geological Society of America, Bulletin **83** (1972) 173.

COLLE, C., Transfert de l'iode 129 dans la biosphere – étude bibliographique, IRSN Report for ANDRA, CRPPSTR060007 (2006).

LEGOUX, Y., BLAIN, G., GUILLAUMONT, R., OUZOUNIAN, G., BRILLARD, L., HUSSONNOIS, M., K_d measurements of activation, fission and heavy elements in water/solid phase systems, Radiochimica Acta **58-59** (1992) 211.

MASSOURA, S. T., Fate of ^{36}Cl in the soil-plant system through isotopic exchange processes, ANDRA post-doc report, CRP1INR050001 (2005).

MOISEEV, U.T., TIKHOMIROV, F.A., RERIKH, L.A., CHIZHIKOVA, N.P., Radionuclide speciation in soils and their transformations (in Russian), Agrokhimiya **1** (1981) 110.

MU, D.H., DU, J. Z., LI, D.J., SONG, H.Q., YAN, S. P., GU, Y.J., Sorption/desorption of radiozinc on the surface sediments, Journal of Analytical Chemistry **267** (2006) 585.

NAKAMARU, Y., TAGAMI, K., UCHIDA, S., Distribution coefficient of selenium in Japanese agricultural soils, Chemosphere **58** (2005) 1347.

NAKAMARU, Y., TAGAMI, K., UCHIDA, S., Antimony mobility in Japanese agricultural soils and the factors affecting antimony sorption behaviour, Environmental Pollution **141** (2006) 321.

NAKAMARU, Y., UCHIDA, S., Distribution coefficients of tin in Japanese agricultural soils and the factors affecting tin sorption behaviour, submitted to Journal of Environmental Radioactivity

NATHWANI, J.S., PHILLIPS, C.R., Adsorption of radium-226 by soils, Chemosphere **8** (1979) 285.

NATHWANI, J.S., PHILLIPS, C. R., Adsorption of radium-226 by soils in the presence of Ca^{+2} ions: specific adsorption, Chemosphere **8** (1979) 293.

OHNUKI, T., Sorption characteristics of strontium on sandy soils and their components, Radiochimica Acta **64** (1994) 237.

PAYNE, T.E., HARRIES, J.R., Adsorption of Cs and U(VI) on soils of the Australian arid zone, Radiochimica Acta **88** (2000) 799.

PINEL, F., Chimie de ^{63}Ni et de ^{137}Cs dans le système sol-plante, PhD Thesis, Montpellier Univ. (2002).

PINEL, F., LECLERC-CESSAC, E., STAUNTON, S., Relative contributions of soil chemistry, plant physiology and rhizosphere induced changes in speciation on Ni accumulation in plants shoots, Plant Soil **255** (2003) 619.

RIGOL, A., VIDAL. M., RAURET, G., Effect of the ionic status and drying on radiocesium adsorption and desorption in organic soils, Environmental Science and Technology **33** (1999) 3788.

ROCA, M. C., VALLEJO, V. R., ROIG, M., TENT, J., VIDAL, M., RAURET, G., Prediction of caesium-134 and strontium-85 crop uptake based on soil properties, Journal of Environmental Quality **26** (1997) 1354.

ROUSSEL-DEBET, S., Experimental values for ^{241}Am and $^{239+240}Pu$ K_d's in French agricultural soils, Journal of Environmental Radioactivity **79** (2005) 171.

SANCHEZ, A. L., WRIGHT, S. M., SMOLDERS, E., NAYLOR, C., STEVENS, P. A., KENNEDY, V. H., DODD, B. A., SINGLETON, D. L., BARNETT, C. L., High plant uptake of radiocesium from organic soils due to Cs mobility and low soil K content, Environmental Science and Technology **33** (1999) 2752.

SANCHEZ, A. L., SMOLDERS, E., VAN DEN BRANDE, K., MERCKX, R., WRIGHT, S. M., NAYLOR, C., Predictions of in situ solid/liquid distribution of radiocaesium in soils, Journal of Environmental Radioactivity **63** (2002) 35.

SASTRE, J., RAURET, G., VIDAL, M., Sorption-desorption tests to assess the risk derived from metal contamination in mineral and organic soils, Environment International **33** (2007) 246.

SAURAS, T., WAEGENEERS, N, TENT, J., VALLEJO, V.R., VIDAL, M., Effect of soil water content on radiouclide availability, submitted to Journal of Environmental Quality

SAUVÉ, S., HENDERSHOT, W., ALLEN H., Solid-solution partitioning of metals in contaminated soils: dependence on pH, total metal burden, and organic matter, Environmental Science and Technology **34** (2000) 1125.

SHANG, Z. R., LEUNG, J. K.C., ^{110m}Ag root and foliar uptake in vegetables and its migration in soil, Journal of Environmental Radioactivity **68** (2003) 297.

SHENBER, M. A., ERIKSSON, A., Sorption behaviour of caesium in various soils, Journal of Environmental Radioactivity **19** (1993) 41.

SHEPPARD, M. I., SHEPPARD, S. C., A solute transport model evaluated on two experimental systems, Ecological Modelling **37** (1987) 191.

SHEPPARD, S. C., EVEDEN. W. G., The assumption of linearity in soil and plant concentration ratios: an experimental evaluation, Journal of Environmental Radioactivity **7** (1988) 221.

SHEPPARD, S. C., EVEDEN, W., G., POLLOCK., J. R., Uptake of natural radionuclides by field and garden crops, Canadian Journal of Soil Sciences **69** (1989) 751.

SHEPPARD, M. I., THIBAULT, D. H., Migration of technetium, iodine, neptunium and uranium in the peat of two minerotrophic mires, Journal of Environmental Quality **17** (1988) 644.

SHEPPARD, M. I., THIBAULT, D. H., A four-years mobility study of selected trace elements and heavy metals, Journal of Environmental Quality **20** (1991) 101.

SHEPPARD, S.C., SHEPPARD, M.I., ILIN, M., TAIT, J.C., SANIPELLI, B. L., Primordial radionuclides in Canadian background sites: secular equilibrium and isotopic differences, EcoMatters, Canada (2004).

SHEPPARD, S.C., SHEPPARD, M.I., TAIT, J.C., SANIPELLI, B. L., Revision and meta–analysis of selected biosphere parameter values for chlorine, iodine, neptunium, radium, radon and uranium, Journal of Environmental Radioactivity **89** (2006) 115.

SKIPPERUD, L., OUGHTON, D., SALBU, B., The impact of Pu speciation on distribution coefficients in Mayak soil, Science of the Total Environment **257** (2000) 81.

SMOLDERS, E., BRANS, K., FÖLDI, A., MERCKX, R., Cadmium fixation in soils measured by isotopic dilution, Soil Science Society of America Journal **63** (1999) 78.

SOKOLIK, G.A., IVANOVA, T.G., LEINOVA, S.L., OVSIANNIKOVA, S.V., KIMLENKO I.M., Migration ability of radionuclides in soil-vegetation cover of Belarus after Chernobyl accident, Environment International **26** (2001) 183.

STAUNTON, S., BARTHES, M., LECLERC-CESSAC, E., PINEL, E., Effect of sterilization, incubation time, solution composition and soil: solution ratio on the isotopic exchange of nickel in two contrasting soils, European Journal of Soil Science **53** (2002) 655.

SURKOVA, L.V., POGODIN, P.U., Speciation and occurrence of forms of ^{137}Cs in soil of different areas of accidental Chernobyl release (in Russian), Agrokhimiya **4** (1991) 84.

SWEECK L., Soil-chemical availability of radiocesium in mineral soils, PhD Thesis, Katholieke Universiteit Leuven (1996).

SZENKNECT, S., Transfert de radioéléments en zone non saturée. Étude expérimentale et modélisation appliquées au Site Pilote de Tchernobyl, PhD Thesis, Université Joseph Fourier (2003).

TIANWEI, Q., HONGXIAO, T., JIAJUN, C., SHENG, W. J., CHUNLI, L. GUIBIN, W., Simulation of the migration of ^{85}Sr in Chinese loess under artificial rainfall condition, Radiochimica Acta **89** (2001) 403.

TIPPING, E., WOOF, C., KELLY, M., BRADSHAW, K., ROWE, J. E., Solid-solution distributions of radionuclides in acid soils: application of the Wham Chemical speciation model, Environmental Science and Technology **29** (1995) 1365.

TWINING, J. R., PAYNE, T. E., ITAKURA, T., Soil-water distribution coefficients and plant transfer factors for ^{134}Cs, ^{85}Sr and ^{65}Zn under field conditions in tropical Australia, Journal of Environmental Radioactivity **71** (2004) 71.

TYLER, G., OLSSON, T., Conditions related to solubility of rare and minor elements in forest soils, Journal of Plant Nutrition and Soil Science **165** (2002) 594.

VALCKE, E., The behaviour dynamics of radiocesium and radiostrontium in soils rich in organic matter, PhD Thesis, Katholieke Universiteit Leuven (1993).

VANDENHOVE, H., QUARCH, H., CLERC, J.J., LEJEUNE, J.M., SWEECK, L., SILLEN, X., MALLANTS, D., ZEEVAERT, TH. Remediation of Uranium Mining and Milling Tailing in Mailuu

Suu District Kyrgyzstan, Final report, EC-TACIS Project N° SCRE1/N°38, SCK•CEN R-3721, Mol, Belgium (2003).

VANDENHOVE, H. ANTUNES, K., WANNIJN, J., DUQUÈNE, L., VAN HEES, M., Method of diffusive gradient in thin films (DGT) compared with other testing methods to predict uranium phytoavailability, Science of the Total Environment **373** (2007), 542.

WILLETT, I. R., BOND, W. J., Sorption of manganese, uranium, and radium by highly weathered soils, Journal of Environmental Quality **24** (1995) 834.

YASUDA, H., AMBE, S., UCHIDA, S., Distribution coefficient of platinum group metals between soil solid and liquid phases, Environmental Technology **17** (1996) 1151.

YASUDA, H., UCHIDA, S., MURAMATSU, Y., YOSHIDA, S., Sorption of manganese, cobalt, zinc, strontium and caesium onto agricultural soils: statistical analysis on effects of soil properties, Water, Air and Soil Pollution **83** (1995) 85.

ZHENG, Z., TOKUNAGA, T. K., WAN, J., Influence of calcium carbonate on U (VI) sorption to soils, Environmental Science and Technology **37** (2003) 5603.

ZHENG, Z., WAN, J., Release of contaminant U (VI) from soils, Radiochimica Acta 93 (2005) 211